EPFL

Thèse n° 10 735

Probing and modulating inter-areal coupling in the cortical visual motion processing pathway with non-invasive brain stimulation

Présentée le 21 juin 2024

Faculté des sciences de la vie
Unité du Prof. Hummel
Programme doctoral en neurosciences

pour l'obtention du grade de Docteur ès Sciences

par

Michele BEVILACQUA

Acceptée sur proposition du jury

Prof. S. Micera, président du jury
Prof. F. C. Hummel, directeur de thèse
Prof. A. Valero-Cabré, rapporteur
Prof. L. Battelli, rapporteuse
Dr M. G. Preti, rapporteuse

École polytechnique fédérale de Lausanne

2024

"As our circle of knowledge expands,

so does the circumference of darkness surrounding it."

Acknowledgements

I couldn't start my acknowledgements without deeply thanking Prof. Friedhelm Hummel for the constant support and encouragement throughout my whole PhD. When results were not coming and the mood was low, your precious scientific advices and human support kept me on the right track and helped me reaching the goals. It has been a great pleasure and luck to have the chance to work with you and to be part of this amazing lab.

Surely my most sincere thanks have to be given also to Dr. Estelle Raffin, my direct supervisor during these years. I never felt your support lacking. Thanks to your guidance I grew a lot as a scientist and I learnt to overcome the toughest "troughs" of the scientific life and to exploit the exciting "peaks". It has always been a pleasure to discuss about science and to realize what it really means to be a scientist and to work in a team.

A special thanks to all my lab mates, the past and the present ones. The lab has always felt like home thanks to you. I meet so many incredible people and I think if now I am a better person and scientist compared to when I started it is due to the time spent with all of you, inside and outside the lab's walls. Thank you, Takuya, Roberto, Maeva, Manon, Laurijn, Fabienne, Giorgia, Elena, Pierre, Julia, Andeol, Pablo, Lisa, Pauline, Sarah, Thomas, Beatrice, Simona, Umberto. A particular space in these acknowledgements has to go to Claudia, supporting me since the Bachelor and with whom I had the pleasure to work in our Closed-Loop project, and to "Sylveyn", my "bar business partner", always giving me precious scientific advices and teaching me how to enjoy the PhD life.

An enormous thanks to my "family" in Switzerland: Teo, Cek, Cesare, Ari, Damien, Lampros: without you the darkest moments would have been unbearable. A special thought to Andre, the best flatmate I could have ever desired, and to Kimi and Roquette, for sharing these years always with the best mood.

I also want to thank Laura Sofia, an incredible person that I have not been able to properly thank in previous occasions. If I am now here it is also thanks tou you and to your tracendental support.

I cannot leave a special place to thank my "adopted brother" Ramon. You have been by my side since always, metaphorically and physically, and probably you better than anyone know

what this PhD is about. It is in big part thanks to you and to our neverending discussions about the mysteries of the world while biking in the Italian countryside if I am here now.

No words can describe the gratitude I have for my family. Thank you, Marco, papà Gianni, mamma Sonia. Grazie per avermi fatto diventare chi sono e per supportarmi sempre, anche quando è difficile. Grazie anche a zia Patri, Alida, zio Leo, nonna Bianca, nonna Rita, nonno Lino, nonno Francesco e tutti i membri della famiglia. Questo traguardo parte da lontano e senza di voi non sarebbe stato possibile, con un po' di zucchero.

Last, but definitely not the least, thank you Beatrice. You are my source of inspiration, what gives me the strength to go on when things become hard. Your unconditional support, your strength and your unique view on life allows me to be a better person every day. I feel blessed to be sharing my life with such an incredible person.

Michele Bevilacqua

Abstract

In the last few years, stroke ranked as the second most common cause of death and is the third most significant condition affecting disability-adjusted life years (DALYs) worldwide. Being the most prevalent and quality of life impacting post-stroke symptoms, rehabilitation of motor deficits, such as paresis or speech impairments, have concentrated most of the stroke rehabilitation research. Nonetheless, approximatively 1 stroke survivor out of 4 will have to deal with permanent Homonimous Hemianopia (HH), the loss of half of the visual field due to postchiasmatic lesions.

This Thesis uses non-invasive brain stimulation techniques to unveil the electrophysiological mechanisms underlying healthy human visual motion perception, and applies these new insights for the development of a novel functional plasticity index and a new biologically-inspired visual rehabilitation protocol. One of the clinically relevant pathways to study and promote in this context, is the neural pathway connecting the ipsilesional middle temporal area (MT) to the primary the visual cortex V1 that mediates motion perception and awareness. First, to measure plasticity induction along this pathway, we tested the potential of cortico-cortical paired associative stimulation (ccPAS) in enhancing spike-timing-dependent plasticity (STDP) between MT and V1. By triggering one TMS pulse first on MT followed 20ms after by a second TMS pulse over V1, we observed a significant connectivity increase in the MT-to-V1 inputs, correlated with motion discrimination improvement. A similar relationship was reported in HH stroke patients, but only in patients with sufficient structural or functional integrity between V1 and MT. Next, we focused on the idea that exogenously modulating the well-reported oscillatory interactions between the two areas would boost visual learning. We developed a cross-frequency (Alpha and Gamma) dual-site transcranial alternate current stimulation (tACS) protocol. We observed an increase in motion perception in the blind field after one tACS session associated with an increase in V1-MT coupling in both healthy and HH stroke patients, when tACS delivered Alpha oscillations over V1 and Gamma oscillations over MT. Furthermore, applied repeatedly during 10 daily training sessions in HH patients, this tACS condition enhanced motion discrimination in the blind field to similar extends to long-term training studies. In line with the previous approach, patients who better responded to the intervention were the ones with preserved structural integrity of the cortical motion pathway. Importantly, improvement in motion discrimination was accompanied by an enlargement of

visual field borders assessed with kinetic perimetry, paving the way to a novel intervention for visual field recovery.

In conclusion, this work deepens our understanding of MT-V1 motion discrimination pathway properties and highlights a multimodal marker to index visual system structural and functional integrity potentially predictive of treatment efficacy. Finally, it introduces the first steps towards a promising approach for rehabilitating visual impairments in stroke patients. Further improvements include a novel state-dependent version based on inter-areal coupling, aiming at reducing the variability and increasing the efficacy.

Keywords: Stroke, Homonimous Hemianopia, Visual rehabilitation, Motion perception, cortico-cortical Paired associative Stimulaiton (ccPAS), cross-frequency multisite transcranial Alternate Current Stimulation (tACS), Phase-Amplitude Coupling (PAC).

Sinossi

Negli ultimi anni, l'ictus si è classificato come la seconda causa di morte più comune e come terza condizione in funzione dell'attesa di vita corretta per disabilità in tutto il mondo. Essendo i deficit motori, come la paresi o i disturbi del linguaggio, i sintomi post-ictus più diffusi e che più impattano sulla qualità della vita, la maggior parte delle ricerche sulla riabilitazione dell'ictus si è concentrata su di essi. Tuttavia, circa 1 sopravvissuto su 4 all'ictus dovrà affrontare una permanente emianopsia omonima, ossia la perdita di metà del campo visivo a causa di lesioni postchiasmatiche.

Questa tesi utilizza tecniche di stimolazione cerebrale non invasiva per indagare i meccanismi elettrofisiologici alla base della percezione visiva del movimento negli individui sani e applica queste nuove intuizioni per lo sviluppo di un nuovo indice di plasticità funzionale e di un nuovo protocollo di riabilitazione visiva biologicamente ispirato. Uno dei sistemi cerebrali clinicamente rilevanti da studiare e promuovere in questo contesto, è il sistema neurale che collega l'area temporale media ipsilesionale (MT) alla corteccia visiva primaria V1, il quale media la percezione e la consapevolezza del movimento. Prima di tutto, per misurare l'induzione della plasticità su questo network, abbiamo testato l'efficacia della stimolazione associativa cortico-corticale (ccPAS) nel potenziare la plasticità dipendente dal tempo di attivazione (STDP) tra MT e V1. Scaricando prima un impulso TMS su MT seguito 20ms dopo da un secondo impulso TMS su V1, abbiamo osservato un significativo aumento della connettività negli input da MT a V1, correlato con il miglioramento della discriminazione visiva del movimento. Un effetto simile è stato osservato in pazienti emianopsici con ictus, ma solo in pazienti con sufficiente integrità strutturale o funzionale tra V1 e MT. Successivamente, ci siamo concentrati sull'idea che la modulazione esogena delle ben note interazioni oscillatorie tra le due aree potrebbe potenziare l'apprendimento visivo. Abbiamo sviluppato un protocollo di stimolazione a corrente alternata transcranica (tACS) cross-frequenza (Alpha e Gamma) su due siti. Abbiamo osservato un aumento della percezione del movimento nel campo visivo cieco dopo una sessione di tACS associata a un aumento dell'accoppiamento funzionale tra V1 e MT sia nei pazienti sani che in quelli con ictus, quando il tACS forniva oscillazioni Alpha su V1 e Gamma su MT. Inoltre, applicato ripetutamente durante 10 sessioni di allenamento giornaliere in pazienti emianposici, questa condizione di stimolazione ha migliorato la discriminazione del movimento nel campo visivo cieco in misura simile a studi di allenamento

a lungo termine. In linea con l'approccio precedente, i pazienti che hanno risposto meglio all'intervento erano quelli con integrità strutturale conservata del sistema corticale legato alla percezione del movimento. Importantemente, il miglioramento nella discriminazione del movimento è stato accompagnato da un allargamento dei confini del campo visivo valutato con perimetria cinetica, aprendo la strada a un nuovo tipo di intervento per il recupero del campo visivo.

In conclusione, questo lavoro approfondisce la nostra comprensione delle proprietà del sistema neurale di discriminazione del movimento MT-V1 ed evidenzia una misura multimodale per indicizzare l'integrità strutturale e funzionale del sistema visivo potenzialmente predittiva dell'efficacia del trattamento. Infine, introduce i primi passi verso un promettente approccio verso la riabilitazione delle disabilità visive nei pazienti con ictus. Ulteriori miglioramenti dell'intervento includono una nuova versione del protocollo dipendente dal momentaneo stato cerebrale basata sulla sinronizzazione inter-areale, mirata a ridurre la variabilità dell'effetoo e aumentare l'efficacia della stimolazione.

Parole chiave: Ictus, Emianopsia Omonima, Riabilitazione Visiva, Percezione del Movimento, Stimolazione Associativa Cortico-Corticale (ccPAS), Stimolazione a Corrente Alternata Transcranica Multisito Cross-Frequenza (tACS), Accoppiamento Fase-Amplitude (PAC).

Contents

List of figures

List of tables

Chapter 1 - Introduction

Stroke, also known as cerebrovascular accident (CVA), arises when the blood supply to part of the brain is either interrupted or occluded, depriving brain tissue of essential oxygen and nutrients. This event often leads to the death of brain cells and can result in permanent neurological impairments. The majority of strokes are ischemic, caused by blockages often due to blood clots, while hemorrhagic strokes occur from ruptured blood vessels (Kuriakose and Xiao, 2020).

The damage caused by a stroke varies greatly, depending on its type, severity, and location within the brain. Stroke can in fact lead to a wide range of disabilities, the most frequent being motor deficits, affecting around 80% of stroke survivors. It's also common for patients to experience multiple deficits simultaneously, which can hinder recovery and lead to prolonged impairments well beyond hospital discharge. The impact of a stroke is thus profound, not just in its immediate effects but also in the long-term health and quality of life of survivors (Tsao et al., 2023).

1.1 The burden of stroke

The most recent report from the World Stroke Organization indicates that stroke ranks as the second most common cause of death and is the third most significant condition affecting disability-adjusted life years (DALYs) (Feigin et al., 2022; GBD 2019 Stroke Collaborators, 2021).

Over the 1990-2019 period, there was a significant increase in the absolute number of incidents, survivors and in stroke-related DALYs. To report some epidemiologic numbers, in 2019, 63% of stroke occurred in people younger than 70 years old, 12 million new stroke every year were reported (1 every 3 seconds) and 101 million of stroke survivors were reported worldwide (GBD 2019 Stroke Collaborators, 2021). Projections predict that 1 out of 4 living human being will unfortunately experience stroke in the course of their life (GBD 2019 Stroke Collaborators, 2021). The developing countries are the most hit by the burden of stroke (75% of the worldwide deaths from stroke and 81% of stroke-related DALYs). In the analyzed time period, the contribution of stroke-related DALYs in proportion to all diseases has increased of ~1% and

the contribution of the deaths of ~2%, also with a more significant trend in the developing countries (Feigin et al., 2022).

Because of the high impact of stroke is linked to a slight general decrease in mortality, especially in the high-income countries where the development and improvement of acute stroke treatment interventions such as thrombolysis and thrombectomy (Winstein et al., 2016) has been shown to be precious life-saving progresses, a huge increasing number of survivors will experience serious life-changing deficits, even beyond the acute phase. Furthermore, the societal impact of stroke is profoundly significant as well in economic terms: it amounts to 891 billion USD, which equates to 1.2% of the world's GDP (Anwer et al., 2022; Feigin et al., 2022). For this reason, facing the challenge of improving and refining the knowledge and the techniques of stroke neurorehabilitation is becoming of priority importance for the world health system and, most importantly, for the quality of life of thousands of people.

As previously mentioned, more than 80% of stroke survivors presents with some form of paresis, most often of the upper extremities (75.5%), although a majority reported paresis of the face (54.6%) and legs (68.6%) (Rathore et al., 2002). This is followed by deficits in the somatosensory domain (40-50%), attention (25-30%), language (20-25%), memory (15-25%), and, importantly for the scope of this Thesis, visual impairments (15-20%) (Appelros, 2002; Buxbaum et al., 2004; Nys et al., 2007; Ramsey et al., 2017). Furthermore, often not only one domain but several are affected concomitantly. Being considered one of the most prevalent and life-impairing consequences, scientific and medical research has been focused mainly on the study, rehabilitation and restoration of the motor-related issues, such as hemiparesis and other motor impairments.

Nevertheless, three quarters of stroke patients presents visual deficits: 56% with impaired central vision, 40% eye movement abnormalities, 28% visual field loss, 27% visual inattention, 5% visual perceptual disorders (Rowe, 2017). One of the most common stroke signs on presentation is hemianopia (Rathore et al., 2002). About 20% of patients admitted to the hospital with complete Homonymous Hemianopia (HH) after focal stroke present chronic persisting complete HH, while about the 20% recovered with partial HH (e.g., quadrantopia and scotoma) still present a partial HH one month after the stroke. Furthermore, approximately 8-10% of the total stroke patients present permanent HH (Goodwin, 2014; Zhang et al., 2006).

1.1.1 Damages to the visual field

Homonymous Hemianopia implies loss of vision on the same side of the visual field of both eyes. This specific type of visual field deficit indicates a lesion that affects the postchiasmatic visual pathway (Figure 1.1). Consult Section 1.3 for a more detailed description of the anatomo-functional features of the structures involved.

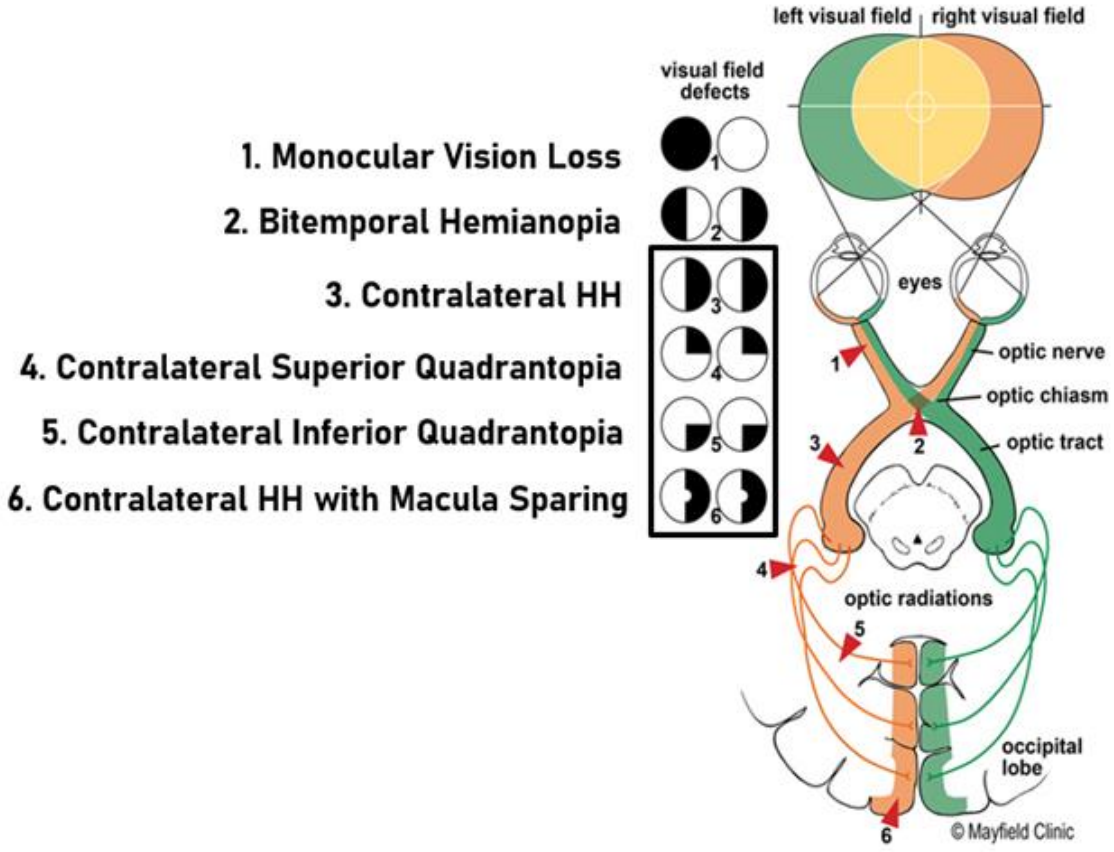

Figure 1.1*: Graphical representation of the visual retino-geniculate-striatal pathway, with the different visual field deficits presented on the left according to the location of the damage on the visual pathway. The stroke patients considered for this Thesis are presenting a postchiasmatic lesion of the visual pathway, with corresponding visual field deficits showed in 3-6. Image adapted from UC Neuroscience Institute at University Hospital of Cincinnati (https://www.uchealth.com/wp-content/uploads/2013/01/PE-VisualFieldTest_UCNI.pdf).*

Between 52% and 70% of hemianopia cases are caused by stroke (Goodwin, 2014). HH can severely impair the ability to read, walk in crowded areas, drive and perform basic daily life tasks and may result in injuries due to falls or to the inability to avoid obstacles (Choi et al.,

2022). Worryingly, a large number of these HH stroke patients are not even completely aware of their visual field defect and most are still driving (de Haan et al., 2015) representing a danger for themselves and for the community. Despite the high occurrence of homonymous hemianopia in stroke patients and its profound impact on their quality of life, it often goes undiagnosed and untreated (Sand et al., 2012). This oversight is partly due to the focus on concurring neuropsychological disorders socially considered as more disabling, such as motor or speech impairments (Sand et al., 2013). Additionally, the extent of spontaneous visual recovery is generally limited, with most patients regaining only a small portion of their visual field. Complete recovery is rare, occurring in only about 5.3% of the patients (Zhang et al., 2006) (See subchapter 1.3 for a more detailed overview on HH rehabilitation). Also for this reason, most health professionals assume that complete recovery from this type of visual field loss is close to impossible (Perez and Chokron, 2014).

However, these assumptions are not always accurate (Howard and Rowe, 2018). In the coming years, the medical and scientific communities are required to recognize the need for effective rehabilitation strategies for HH resulting from strokes to provide efficient rehabilitation approaches for these patients. Understanding, identifying, managing and intervening on the visual deficits caused by stroke's HH can have a significant and tangible effect on patient's quality of life. Moreover, because of the actual size of the phenomena and its increasing trend, discoveries in the field and novel therapeutic approaches will indirectly benefit the whole worldwide healthcare system.

Before exploring more in detail where we stand in the understanding and in the application of clinical care for HH, in the next sub-chapter I will introduce the human visual system from the anatomical and functional point of view. I will focus specifically on the motion discrimination network, crucial for the scope of the studies discussed in this Thesis.

1.2 The visual system

The brain requires an enormous amount of computational effort to process visual stimuli, requiring highly hierarchically organized networks and extremely efficient neural communication. Primates use more than half of their brain's cortex for visual processing (55%), compared to a smaller part for feeling touch (11%) and even less for hearing (3%) (Felleman and Van Essen, 1991). The different visual pathways have to receive, relay, and ultimately process visual information. The structures involved in visual processing include the eye, optic nerves, chiasm, tracts, lateral geniculate nucleus (LGN) of the thalamus, radiations, the primary

visual cortex (or striate cortex), and the secondary visual cortex (extrastriate cortex). Within these structures, different receptors and cell types play crucial and function-specific roles.

First, in the retina, photoreceptors (rods and cones) are responsible for light detection, with rods being more sensitive to low light and cones to colour and fine detail (Kolb, 2003). Bipolar cells convey signals from photoreceptors to retinal ganglion cells, which travel until they reach the optic chiasm, where they input from the eye on the opposite side. Beyond the chiasm, the visual signal is transmitted along a pathway leading to the LGN in the Thalamus. From the LGN, a direct pathway extends to the primary visual cortex (V1) (v. Monakow, 1895). The LGN plays a crucial role in refining the topographical mapping initially conducted in the retina, ensuring precise visual representation (Weyand, 2016). The visual system incorporates additional pathways and structures beyond the primary and secondary visual cortex. One such pathway involves the superior colliculus, a structure in the midbrain that plays a role in orienting movements of the eyes, through saccades, and head towards visual stimuli. This pathway is particularly important for processing motion and spatial orientation, and it integrates visual information with auditory and somatosensory inputs driving reflexive behaviours (King, 1993).

Mishkin and Ungerleider, (1982) identified two main functional parallel streams in the brain for processing visual information. These streams are composed of multiple extrastriate visual areas, each specialized in detecting specific visual features. The ventral stream is known for its role in recognizing visual features to identify objects, often referred to as the "what" pathway. Meanwhile, the dorsal stream focuses on understanding the spatial features of objects, named the "where" pathway. Beyond visuospatial processing, the dorsal stream also plays a crucial role in coordinating vision and movement, such as in actions like grasping and manipulating objects (Goodale et al., 1991). The concepts of “what” and “where” pathways were significantly advanced through lesion studies on macaques. These studies specifically focused on observing the effects of targeted lesions in different areas of the brain on visual processing abilities. For example, lesions in the inferior temporal cortex of macaques were found to cause severe deficits in visual discrimination tasks. This included an impaired ability to identify objects, colours, patterns, or shapes, which underscored the role of this area in object recognition and categorization (Desimone and Ungerleider, 1989). Notably, these impairments were observed without significant effects on the animals' visuospatial processing abilities, which indicated a distinct neural pathway responsible for spatial processing. Similarly, lesions

in areas corresponding to the dorsal stream, particularly the posterior parietal cortex, resulted in difficulties with spatial awareness and coordination. Macaques with such lesions exhibited problems in assessing the spatial relationship between objects and their environment, affecting their ability to navigate and interact physically with objects. However, their ability to recognize and discriminate between these objects remained largely intact (Colby and Goldberg, 1999). These lesion studies in macaques were important in demonstrating the functional dissociation between the ventral and dorsal streams in the brain. They provided a foundation for understanding how visual information is processed and segregated into different pathways for object recognition and spatial localization.

Notably, this double processing stream (the “what” and the “where” processing streams) have also been extended directly to the initial sensory input processing through the identification of parvocellular cells (P-cells) and magnocellular cells (M-cells) in both the retina and the LGN (Livingstone and Hubel, 1984). P-cells, which relay information from the bipolar cells in the retina to layers III, IV, V and VI of the LGN and finally to layer IVCβ of the primary visual cortex, are characterized by their small receptive fields, sensitivity to colour (i.e., different wavelengths), the ability to process high-spatial frequencies, medium conductance velocity, and responses that last only as long as the stimulus is present. In contrast, M-cells, projecting from the retina to layers I and II of the LGN to layer IVCα of V1, show larger receptive fields, lack colour sensitivity, and demonstrate rapid conductance and transient responses, making them integral to motion perception. Further primate research by Van Essen and Gallant revealed a continuous interplay between these two streams. When attempting to isolate the precortical path, they found evidence of significant interactions between the two routes, suggesting an intricate network of connections (Van Essen and Gallant, 1994).

The present work focuses on the dorsal stream, which emerges in motion-sensitive components of layer IVCα in area V1. From here, projections reach areas V2 and V3 (Shipp and Zeki, 1985). Subsequently, neurons in these regions project to the medial temporal area (MT or V5), and finally these inputs reach higher-level brain areas (e.g., intraparietal cortex) and prefrontal cortex and even in high-level cognitive areas encoding task rules and decision strategies (Gold and Shadlen, 2007). Dorsal stream processes visual information faster than the ventral stream (Schmolesky et al., 1998). This led to the concept of the "fast brain" associated with the dorsal stream. This quicker processing is partly due to the fact that the axons in the dorsal stream have more myelin, a type of insulation, compared to those in the ventral stream (Nowak and Bullier,

1997). From an evolutionary perspective, the distinction between the dorsal and ventral streams can be seen as an adaptation to different environmental and survival needs. The dorsal stream, or "fast brain," is crucial for rapid and efficient processing of spatial information and motion, enabling quick responses to environmental changes. This rapid processing capability would have been essential for survival tasks such as navigating through complex environments, avoiding predators, and capturing prey. The increased myelination in this pathway is an evolutionary adaptation that supports these time-critical functions by enabling faster neural conduction (Goodale and Milner, 1992).

On the other hand, the ventral stream, characterized by a slower processing speed, is adapted for tasks that require more detailed analysis, such as recognizing objects, faces, and colours. This pathway supports fundamental evolutionary functions like identifying food sources, recognizing individuals, and navigating social interactions, which may not require the same immediacy as the spatial and motion processing of the dorsal stream but demand more detailed visual analysis (Milner and Goodale, 2008).

See Figure 1.2 for a detailed schematic overview of the human visual system and of the two pathways.

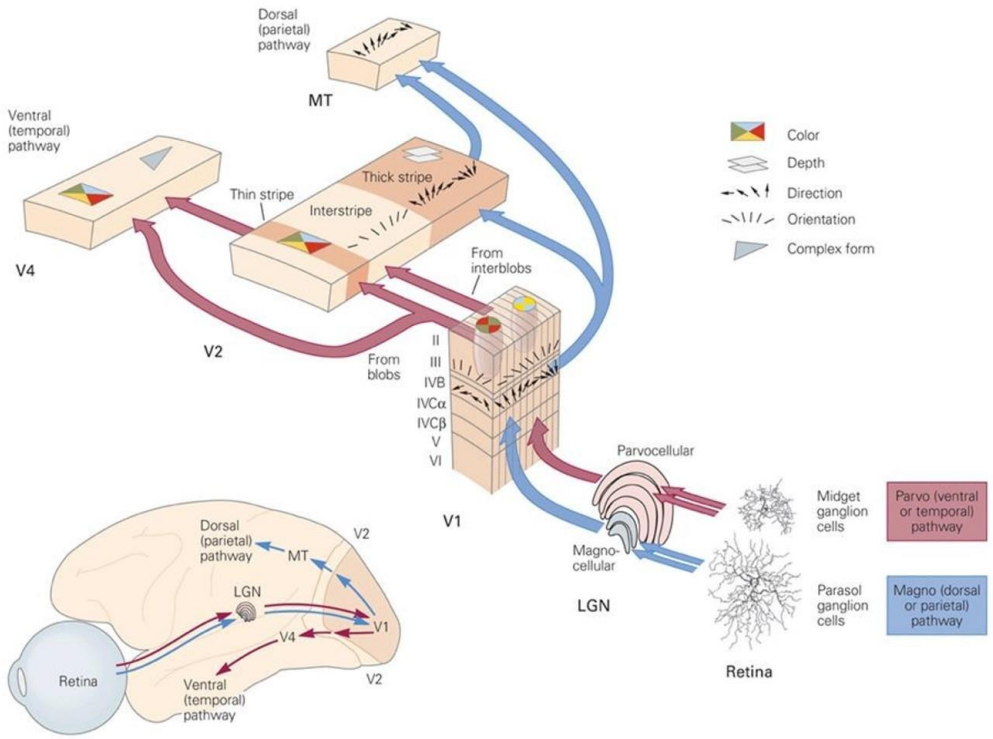

***Figure 1.2**: Schematic model of human visual system. Taken from Kandel, (2014)*

The evolutionary development of these distinct pathways reflects the different survival strategies that primates, including humans, have had the need to adapt to. While the dorsal stream evolved to prioritize speed for immediate environmental interaction, the ventral stream developed to handle complex perceptual analyses essential for more intricate tasks (Kravitz et al., 2011).

1.2.1 Visual Motion Perception

Historically, research on motion perception has been significantly advanced through studies on cats. Initial work by Hubel and Wiesel, (1962) revealed that cats' primary visual cortex contain neurons grouped, according to the topographical sensitivity, in cortical columns or “blobs” specifically responsive to certain spatial motion features, such as direction, orientation and position (Hubel and Wiesel, 1962; Livingstone and Hubel, 1984). It was then reported that specific neurons in cats’ primary visual cortex were sensitive not only to the direction of motion but also to the speed of moving stimuli, integrating the temporal component of motion perception to the mere spatial one (DeAngelis et al., 1995, 1994). This neural feature provides an essential mechanism for the cat's ability to track and respond to moving objects in its environment. Furthermore, neurons in the cat's medial suprasylvian cortex activate to different types of motion and showed to be particularly responsive to moving visual texture patterns (Merabet et al., 2000), highlighting a complex and specialized motion processing system involving the point of convergence between the geniculostriate and extrageniculostriate visual pathways.

Motion perception in humans is a complex process that begins at the earliest stages of visual processing. As described in the previous subchapter, before reaching V1 motion signals are initially detected by the photoreceptors, rods and cones, in the retina. These signals are then processed by retinal ganglion cells, which already play a crucial role in transmitting visual information to the brain, setting the stage for more complex motion processing (Kim et al., 2021; Rodieck, 1965). Motion perception process is thus initiated by the detection of movement through changes in luminance or intensity patterns (first-order motion) and characteristics beyond luminance, like texture, contrast or flicker (second-order motion) (Chubb and Sperling, 1989). First-order motion is directly linked to the activity of photoreceptors responding to varying light intensities (Cavanagh and Mather, 1989). Second-order motion, instead, allows

us to detect movements even in the absence of clear luminance differences, through the processing of more complex spatio-temporal features.

In the context of human studies, understanding how the visual system distinguishes and integrates these motion features is important in the selection of a potential therapeutic substrate for visual recovery. Initially, these visual signals are processed in parallel streams, and this early-stage processing is essential for the accurate perception of motion in our dynamic visual environment (Ledgeway and Smith, 1994). The neural substrates for first and second-order motion detection involve different regions and mechanisms in the brain. First-order motion is predominantly processed in the primary visual cortex and MT (Smith et al., 1998). Second-order motion, sensitive to contrast changes, is represented in visual areas such as V3 (or VP, ventral posterior area), with MT also contributing to this second-order motion processing. This differentiation in processing mechanisms is supported by studies on brain lesions, functional magnetic resonance imaging (fMRI), and neuronal recordings (Ashida et al., 2007). Further along the visual processing hierarchy, these parallel streams converge, allowing for the integration of first- and second-order motion information. Research has shown that both MT and MST (medial superior temporal) areas exhibit responses to both first-order and second-order motion, even if with different spatial/temporal tuning (Mareschal and Baker, 1998). This integration is essential for the formation of a coherent motion perception (Albright, 1992; Geesaman et al., 1997). Additionally, fMRI studies have also revealed varying degrees of specialization and overlap in cortical responses to first- and second-order motion (Smith et al., 1998).

Furthermore, the visual system's ability to process motion is closely linked to various sensory inputs. This interplay involves not just the processing of visual stimuli but also the integration of information from other sensory modalities, such as auditory somatosensory and tactile inputs (Hagen et al., 2002; Zihl et al., 1983). Multisensory integration is also involved in the creation of a comprehensive and accurate representation of the motion in the environment (Soto-Faraco and Väljamäe, 2012; Stein and Stanford, 2008).

As seen, the primary visual cortex plays a foundational role in processing visual motion, but it is the higher-order areas, like MT and MST, that are crucial for interpreting complex motion patterns. These higher cortical areas are tuned to complex motion cues, including global expansion, rotation, and contraction. These motion types are particularly noteworthy as they arise from the interplay between an observer and their surroundings. For instance, radial motion

patterns like expansion and contraction are observed on the retina in response to objects moving towards or away from the observer, respectively. Such motion can stem from the object itself, the observer's head and body movements, or a combination of both. Similarly, rotational motion patterns can result from either the observer's head tilt or the actual rotation of an object in the environment. Neurons that are sensitive to these specific motion patterns are potentially key for the navigation and interaction with the world around us (Gibson, 1950). MT and MST are also responsible for integrating the motion information from V1 and projecting it to other brain regions involved in perception and decision-making (Ilg, 2008; Saproo and Serences, 2014). Between these areas, it is important to note the Intraparietal Sulcus (IPS), involved in the integration of visual feaures supporting visual short-term memory of stimuli presenting several complex attributes (Xu, 2007), in spatial attention (Chica et al., 2011), in eye saccadic movements (Bourgeois et al., 2013) and in visual decision-making processes (Colby and Goldberg, 1999; Grefkes and Fink, 2005). Moreover, the Frontal Eye Fields (FEF) is involved in eye movement control, crucial for decision-making processes that guide eye movements in response to visual stimuli (Hsu et al., 2021), and in conscious visuo-spatial attention (Chanes et al., 2012). Another high order area crucial for coherent motion perception is the Inferior Temporal Cortex (IT), involved in object recognition and in the higher-level processing and interpretation of visual information, also contributing to complex decision-making tasks (Christiansen, 2002; Desimone et al., 1984). Furthermore, some higher order visual areas' functional activity, such as FEF and IPS (Bourgeois et al., 2013), has been reported to be hemispheric-specific. In the FEF case, it is the area in the right hemisphere to be the one typically associated with conscious visual perception (Chanes et al., 2012). Nonetheless, it has been shown by modulating the left FEF through arryhmic non-frequeny-specific transcranial magnetic stimulation that also this area could contribute to conscious visual perception sensitivity but with different coding mechanisms compared to its contrahemispheric equivalent (Chanes et al., 2015). See Vernet *et al.* (2014) for a comprehensive review on the role of FEF in visual perception.

The evolutionary development of specialized motion perception mechanisms, such as first-and second-order motion, is also relevant for understating the role of motion perception and discrimination pathway in the attempt of defining a potential substrate for a visual rehabilitation intervention. In fact, motion detection skills are believed to have evolved to meet specific environmental and survival needs and the visual motion processing system, through its

evolution, demonstrates a great degree of adaptation, observable in its ability to handle complex and varied motion cues (Aaen-Stockdale et al., 2012; Price and Khan, 2017).

This evolutionary perspective is crucial for understanding the inherent flexibility and plasticity of the visual motion processing system. In fact, global motion perception is usually not persistently impaired by focal brain lesions. Large part of the injured patients still can perform specific motion perception task (Huxlin, 2008) and they might show residual activity in the visual motion network also soon after the lesion (Saionz et al., 2020). For what concerns this Thesis, these concepts and findings are at the core of the rationale behind the decision of targeting the MT-V1 motion discrimination pathway in the attempt of enhancing plasticity, synchronize neural activation and partially restore visual abilities. See sub-chapter 1.3 for a more detailed overview of existent clinical approaches and of how our approach relates to them.

1.2.2 Role of MT-V1 feedback pathway

Information processing relies not only on feedforward connections to higher visual areas (see section 1.2) but also on reciprocal connections that drive the communication in the opposite direction. These feedback connections, which are much more numerous than the feedforward inputs coming from the LGN (Catani et al., 2003) , are thought to adjust, regulate and improve the processing of incoming stimuli (Felleman and Van Essen, 1991; Salin and Bullier, 1995). Even in V1, the neural responses do not exactly replicate retinal inputs; instead, they are modulated by inputs from higher brain areas to form a unified and coherent visual perception.

Feedback mechanisms within the visual system also allow for the refinement and adjustment of motion processing, contributing to the system's plasticity (Briggs, 2020; Kafaligonul et al., 2015). They enable the brain to modify its responses based on past experiences and contextual information, enhancing the accuracy and efficiency of motion detection and interpretation (Gilbert and Li, 2013; Kveraga et al., 2007). Indeed, the neural correlates of motion adaptation highlight the visual system's capacity for change and learning, evident in the brain's response to sustained exposure to motion stimuli, where changes in neural activity can lead to alterations in motion perception (Merabet et al., 1998; Villeneuve et al., 2005). The complete understanding of these adaptation processes is also important for developing strategies to enhance visual plasticity, particularly in rehabilitation contexts.

The anatomical and functional connection, synchronization and the interaction between visual areas V1 and MT has been thoroughly investigated in the past years (Bressler, 1996; Bullier, 2003; Hinds et al., 2009; Thomas Yeo et al., 2011). These first studies showed that the synchronization between the areas depends on the integrity of the cortico-cortical connections and that the onset and offset of the synchrony between group of neurons is related to fast synaptic changes occurring in reentrant fibres from area MT to area V1, highlighting thus the role of higher inputs in the coherent signal processing of the visual area.

One of the first computer model for the simulation of dynamic integration in the visual system and the important role of feedback connections between the visual areas in motion perception processing was proposed by Tononi et al., (1992). The model reported that the main function of the system of reentrant connections in the visual cortex is to generate integrative function within and between functionally segregated areas, and that such cooperative effects between areas are the basis for information categorization and integration. Thus, neural responses related to the detection of motion coherence may be depending on the re-entrant projections from area MT to area V1.

A study on an animal model performed by Marcar and Cowey, (1992), in which nine macaques were trained with a behavioural task to discriminate between randomly moving dots and a proportion of dots moving coherently either towards the right or towards the left, confirmed the importance of the feedback and integrative mechanisms between areas MT and V1 in the ability to discriminate motion coherence. Indeed, after MT area was surgically removed from two macaques, the latter lost their ability to discriminate coherently moving dots, while their performance was in line with the control group before the surgery. Positron Emission Topography (PET) combined with Magnetic Resonance Imaging (MRI) study performed on human, confirmed the role of area MT in motion discrimination tasks (Watson et al., 1993).

In Transcranial Magnetic Stimulation (TMS), a brief (around 100 µs (Toft et al., 1990)) but intense electrical current is sent through a coil. This creates a magnetic field around the coil, which, when positioned on a person's scalp, induces electrical currents in the brain's cortical neurons, primarily affecting fibres aligned perpendicularly to the magnetic field. See Valero-Cabré *et al.* (2017) for a review on TMS mechanism and applications. For instance, when TMS is applied to the visual cortex, the rapid fluctuation of the magnetic field generates electrical gradients, triggering action potentials in the underlying neurons (Goetz and Deng, 2017). A human study of Pascual-Leone and Walsh, (2001), using TMS to probe the timing and feedback

from visual areas MT to V1, confirmed the rapid and crucial role of the feedback back-projections for the awareness of visual motion. In this study indeed, moving phosphenes (quick flashes of light that might appear in the visual field after stimulating visual areas with TMS (Cowey and Walsh, 2000)), usually perceived in response to a suprathreshold TMS pulse over MT, were not perceived by the subjects, or perceived but just as a static phosphene, in case the pulse over MT was followed by a 10 to 40ms later subthreshold TMS pulse over V1. This result showed how masking with a precisely timed TMS pulse the visual feedback inputs coming from MT to V1 back-projections might disrupt a coherent perceptual interpretation of motion. Another human study performed by Silvanto *et al.* (2009) showed that back-projections from extrastriate cortex influence information content in V1, but it is V1 that determines whether that information reaches awareness.

After this introduction on the visual system, visual motion processing and the importance of the feedback connections in a healthy brain, I will present the idea behind our approach to the problem of rehabilitation of the visual field in HH after a stroke.

1.3 Rehabilitation strategies to treat Homonymous Hemianopia (HH)

Spontaneous recovery from HH is possible, but the probability of this event to happen is proportional to the time passed since the stroke event. Recovery rate has been reported in a range from 7% to 86% (Sabel and Kasten, 2000). Spontaneous recovery in HH patients has been analyzed by Zhang *et al.* (2006) in a 15-years longitudinal study: in a period of 6 months after the lesion (after which the HH is considered chronic), spontaneous recovery was observed in about the 38.4% of the patients. Recovery in most cases is very limited, only few degrees of the visual field have been regained in most of the patients, while only 5.3% of all patients showed a complete recovery.

Because of the poor rate of spontaneous recovery from HH, three categories of rehabilitation programs have been proposed and classified according to their goals and approaches to the visual field deficit: substitution, compensation and restoration (Perez and Chokron, 2014).

Substitution rehabilitation programs are based on the use of optic and prosthetic devices, or environmental redesign techniques, to present objects and stimuli presented in the blind

hemifield to the intact ipsilesional visual hemifield (Grunda et al., 2013). One of the first substitution techniques, nowadays considered obsolete, involved the use of optical aids as mirrors or Fresnel prisms (Véronneau-Troutman, 1978) to translate the visual information from the blind to the intact visual hemifield. Anyway, not only this approach gave scarce and not reliable results, but such devices were reported in some cases to cause diminished acuity, confusion and diplopia (Apfelbaum and Peli, 2015; Apfelbaum et al., 2013).

Compensation techniques are based on the idea that often complete recovery from a very severe visual deficit can be difficult or impossible to obtain. Thus, they aim to exploit the residual capacities of the patient to bypass the impairment or to make it less burdening. They involve the use of the ipsilesional visual hemifield (or central visual field) to compensate for the blind hemifield. One type of compensation techniques is based on a top-down mechanism, since they aim to train the patient to focus their attention on the blind hemifield, for example by researching a visual stimulus presented in the latter one and responding to it as quick as possible (Zihl and Werth, 1984). Conversely, a second category of compensation techniques is based on a bottom-up strategy, involving multisensory stimulation and integration. This approach allows to bypass the attention level of the patient, that could be impaired by the lesion, and exploit the capacity of a fully functioning sense (e.g. hearing) to be transferred and integrated to the impaired one (e.g. vision) (Bolognini et al., 2005).

Although compensation techniques have reported overall good results in improving patients' quality of life, their efficacy is still moderated. They still do not restore the damaged pathways or reorganize the impaired network; thus, they cannot induce any significant reversal of visual deficits caused by the cortical damage. For this reason, compensation techniques need to be considered as a valid second step for hemianopia treatment when restoration therapies are not available.

Restoration techniques are therefore based on the direct retraining of impaired functions, in order to restore part of the lost functions. This last category is based on intensive visual training aiming at strengthening residual visual structures by repetitively activating them through the repetition of a customized precise visual protocol, leading to the enhancement of synaptic transmission (Dundon et al., 2015), similarly to long term potentiation (LTP) mechanisms.

Today, behavioral training effects in patient with primary visual pathway lesion are obtained either by strengthening the function of partially damaged regions located at the visual field border or by training pathways left intact after the damage which project directly or indirectly

to higher cortical regions (for example the one involved in blindsight (Sanders et al., 1974), the phenomenon describing the ability of some patients with striate lesions to unconsciously perceive and discriminate moving stimuli presented in the scotoma (Huxlin, 2008, 2004)).

Visual perceptual learning is the general term describing the improvement in visual task performance with practice or training (Sagi, 2011) and triggers plasticity in the visual system (Huxlin et al., 2009b). Substantial improvements in visual task performance can usually occur in adults whose cortical organization and function are developmentally mature, defining a stable architecture of the visual system and in absence of major injuries and reorganization (Wandell and Smirnakis, 2009). Nevertheless, a few studies reported spared perceptual relearning of complex visual abilities also in brains presenting damage primary visual network. For example, studies training patients to direct saccades towards the borders of their blind visual field in order to increase the size of the isolated patches of residual vision in the blind hemifield, reported slight increase in the visual stimuli detection (3.8%) (Kasten et al., 2006). From a different perspective, Huxlin, (2004) trained animals (cats) and patients (Huxlin, 2008) at a motion detection task, through the repeated presentation of an array of moving dots in the blind hemifield. While mainly targeting extrastriate pathways that connect directly to the MT area, either through the LGN or via the tectal/pulvinar route, they discovered that both in animals and in HH patients presenting V1 lesions there was still potential for enhancement in movement percetpion. Additionally, in a subsequent human study, Das *et al.* (2014) found that with consistent and targeted double training with moving and static stimuli, patients could improve their motion perception in the blind fields and, importantly, that the visual system in cases of cortical blindness is capable of relearning a broader range of visual tasks than what is typically suggested by the phenomenon of blindsight.

Following these insights, more recent studies have paved the way towards the possibility that restoration techniques involving visual training could benefit beyond the sole recruitment of intact extrageniculate pathways, which exploit the blindsight phenomenon. For example, Barbot *et al.* (2021) showed through an fMRI visual training study on cortical blind stroke patients that spared V1 activity is directly related to the amount of training-induced recovery of luminance detection sensitivity. Their training protocol induced also an enlargement of population receptive fields in perilesional V1, which increases blind-field restoration. Furthermore, Cavanaugh and Huxlin, (2017) highlighted the plastic potential of the blind field border in adults with chronic cortical visual impairment. The recruitment of the blind border

by the mean of gaze-controlled visual discrimination training showed the potential to directly expand the visible field. It has also been recently assessed the importance of intervening with visual training techniques already in the early acute post-stroke phase, since this initial period seems to be characterized by gradual loss of visual processing, and the visual training can stop the degradation (Saionz et al., 2020).

Thus, perceptual relearning of complex visual motion processing is possible without an intact V1 but only when specific behavioral training is administered in the blind field. However, the efficacy of these approaches involving only visual task training is moderate, and cannot be considered by its own satisfying in respect to their goal of restoring lost visual functions (Grunda et al., 2013). Furthermore, these strategies present several shortcomings impacting not only their efficacy but also the involvement level of the patients: they are usually very long (lasting months), training is very intensive (at least 1 hour every day), it requires an high level of resilience (sometimes even impaired by the stroke) and strictness on the protocol setup. In consequence, a better understanding of brain correlates of visual processing and plasticity mechanisms underlying recovery is critical to better consider the burden of HH and build innovative treatments.

1.4 Properties of the intact and lesioned visual system

1.4.1 Oscillatory activity

The brain's spontaneous electrical activity is characterized by rhythmic patterns reflecting the periodic oscillatory behavior underlying the local neural processing and the interactions among different interconnected and communicating brain regions (Singer, 2018). Neural oscillations can in fact be seen as the product of synchronized inter-membrane cellular ion exchanges (Llinás and Yarom, 1986) or rhythmic action potentials activity (Azouz and Gray, 2000), occurring at both local and wider brain network levels and representing the intrinsic electrophysiological signature of the specific networks' activity in the frequency domain (Buzsáki, 2006; Buzsáki and Draguhn, 2004). This oscillatory-tuned nature, influenced by networks of neurons synchronously engaging in excitatory and inhibitory dynamics, is at the base of the processing, inter-areal transmission and -very importantly- coherent integration of neural information. It has also been shown to be directly related to behavioral outcomes

involving cognitive (Fries, 2005; Wang, 2010) and perceptual functions (Cabral-Calderin and Wilke, 2020; Chanes et al., 2013).

As introduced in subchapter 1.2, Hubel and Wiesel's pioneering studies on cats revealed oscillatory activities in the visual cortex, observing synchronized neural firing patterns correlated to specific orientation and speed of moving visual stimuli (Hubel and Wiesel, 1962). Further research by Gray and Singer, (1989) showed the importance of synchronized oscillations in encoding visual information. Neurons in different cortical columns communicate through synchronized firing, influenced by stimulus features such as orientation and direction (Gray and Singer, 1989; Singer, 1999). Two primary mechanisms have initially been proposed for this inter-areal synchronized oscillations: neural coherence (Fries, 2005), where neuronal clusters activate in unison, and gating by inhibition, which utilizes lower frequency oscillations to regulate irrelevant brain regions (Jensen and Mazaheri, 2010). Specifically, neural coherence is achieved when neuronal pools belonging to two different interconnected areas oscillate at a similar frequency and maintain a consistent phase difference. This synchronization enables the neurons in the receiving area to be targeted by synaptic input from the connected one during their simultaneous excitable phase, allowing inter-areal communication. Conversely, if neurons in the network's clusters are out of phase, communication can be disrupted by the desynchronization in excitability level, reducing the synaptic influence of the first area on the second one. Fries (2009) further explored this concept, suggesting that oscillations in one neuronal pool can entrain those in another to synchronize at a higher gamma (>30 Hz) frequency. This entrainment strengthens the functional connectivity between the synchronized areas while diminishing the influence of other connected areas not involved in that specific moment in communication and information binding. The gating by inhibition hypothesis, instead, suggests that the control of information flow between different brain regions is achieved by selectively suppressing pathways that are not necessary for the current task. This model proposes that alpha brainwave activity (8-12 Hz) is indicative of targeted regional inhibition: higher levels of alpha activity are associated with more intense inhibition. This idea is corroborated by numerous studies that have found elevated alpha activity in areas of the brain not engaged in the task at hand (Capilla et al., 2014; Haegens et al., 2010; Snyder and Foxe, 2010), as well as in specific groups of neurons within a non-task relevant brain region (van Kerkoerle et al., 2014). Additionally, a decrease in alpha power in connected brain regions correlates with an increase in gamma power within these areas, facilitating the transmission of information. A third more recent model proposed a unified

framework based on nested oscillations (Bonnefond et al., 2017), trying to merge the basic concepts of neural coherence and gating by inhibition. In this updated model, the alpha-band synchronization creates a functional link between two connected regions, facilitating the flow of gamma band activity, representing neuronal firing related specific information transmission. Communication blockage between non-communicating but connected region is accomplished through elevated alpha power in the suppressed area, coupled with a lack of synchrony between clusters. Thus, both the modulation of alpha-band power, as seen in gating by inhibition, and the phase synchronization across regions, as observed in the communication through coherence model, play crucial roles in directing the flow of information between different brain regions. It's important to note that the synchronization is hypothesized to occur in the alpha band, while the actual transfer of specific information is represented by activity in the gamma band.

Focusing on the visual activity, to understand the intricate properties observed in a moving visual stimulus the brain relies on a process of binding and synchronizing neural columns that each process different visual features (Gray et al., 1989). This concept involves the coordination of neural activities across different cortical areas, allowing for the integration of diverse pieces of visual information. The perceptual binding process, when examined over time, serves as a mechanism for combining information from different stages of cortical processing, leading to a comprehensive understanding of the visual input (Engel et al., 1997; Singer and Gray, 1995). As seen, the coherent oscillatory activity of neurons is key in this process, providing a quick and efficient mean to encode the perception of motion. This is because various aspects of motion perception, such as orientation, direction and speed, are associated with distinct resonant frequencies (ranging from 35-85 Hz) within the organized neural columns (Eckhorn et al., 1988; Fries et al., 2001). Specifically, alpha and gamma rhythms are the most prominent in terms of local feature processing and inter-areal information coherent exchange. Alpha rhythms not only consistently emerge in response to visual stimuli characteristics like flicker and direction (Childers and Perry, 1971; Varela et al., 1981), but, together with beta (14-30 Hz), are also implicated in different aspects of perceptual binding. Beta oscillations are mainly associated to temporal binding, integral for memory retrieval and retaining event continuity (Hanslmayr et al., 2012; Waldhauser et al., 2012), while alpha oscillations are usually more linked to spatial attention and selection, crucial for navigation and environmental interaction (Foster and Awh, 2019; Waldhauser et al., 2012). Furhtermore, in a TMS study, high-beta oscillatory activity in the FEF has been reported to be causally related to conscious visual detection (Vernet et al., 2019). Gamma rhythms (35-55 Hz) are instead

essential in encoding the different visual stimulus features and ensuring synchronization between neuron clusters in the visual cortex (Eckhorn et al., 1988; Fries, 2009). Moreover, intracortical studies on the visual cortex illustrated how feedforward and feedback communications occur at different frequency ranges. Feedforward communication happens predominantly in the gamma range, while feedback occurs in the beta or alpha ranges (Bastos et al., 2015; Michalareas et al., 2016; van Kerkoerle et al., 2014). Researches on motion discrimination showed specific low-frequency delta (0.5-4 Hz) and alpha oscillations in brain areas V1 and MT correlate with movement characteristics and timings (Händel et al., 2007). Additionally, experiments on primates demonstrated precise timings in cross-frequency interactions between feedforward and feedback signals (Richter et al., 2017).

In the context of this Thesis, it is important to point out that a stroke can disrupt visual neural pathways, causing significant impairments in network's oscillatory activity synchronization and mutual cross-frequency information exchange and integration (Guggisberg et al., 2019; Rowe et al., 2022). Interestingly, as exposed in section 1.3, patients with stroke-induced visual field defects often retain some motion discrimination abilities, making this a promising target for new treatment strategies. Bifocal non-invasive stimulation can be effective in enhancing long-range cortico-cortical connectivity (Vosskuhl et al., 2018), particularly through the potentiation of cross-frequency interactions in the visual system, which can help in re-establishing functional communication between V1 and MT, crucial for motion perception. This idea supports the potential of a bifocal non-invasive electrical stimulation protocols, like transcranial alternating current stimulation (tACS) (See subchapters 1.6.2 and 1.7.2), which can mimic the network's natural endogenous brain oscillations, to facilitate inter-areal information processing in healthy individuals and motion perception recovery and network reorganization in stroke HH patient.

1.4.2 Plasticity

A recent study on human of Fahrenthold *et al.* (2021), showed that the process of trans-synaptic retrograde degeneration caused by V1 damages becomes detectable with MRI as optic tract shrinkage index by 7 months poststroke. In adult mammals, when neurons in the visual cortex lose their input from the retinas, they have the ability to develop new receptive fields by altering the efficiency of the aready existing intrinsic connections, a mechanism at the foundation of topographic map reorganization. In addition, early studies on adult cats whose striate cortex

was silenced in correspondence of precise retinal lesions have shown that the affected cortex became responsive again, thanks to the intrinsic cortical connections' reorganization with adjacent visual area immediately outside the scotoma's area. This finding supports the idea that intracortical axonal sprouting mediates long-term reorganization of cortical functional architecture (Darian-Smith and Gilbert, 1994).

To understand which specific brain regions contribute to recovery from damage to the visual cortex, additional research was conducted using animal models. In one of the early studies involving cats, Baumann and Spear (1977) first let the animals heal from a lesion in the visual cortex and then they removed additional brain areas. They found that when the lateral parts of the suprasylvian gyrus were removed, the animals completely lost their ability to recover, emphasiing the critical role of this brain area in the recovery process. Other studies on animal models reported that other brain areas, such as pretectum, might be crucial for recovery after a postchiasmatic focal lesion (Fischman and Meikle, 1965). Furthermore, it was shown that recovery was no longer possible only in the case of simultaneous damage to all alternative pathways of the visual system. After these initial observations, more recent studies on animals have focused on two key aspects: the electrophysiological indicators of cortical reorganization and the behavioral aspects of vision restoration and reorganization after cortical deafferentation. These include investigations into both total and partial spontaneous recovery of vision following damage to the cortex (Weerd et al., 1993), or to the optic tract (Jacobson et al., 1979).

Recent scientific works have reported the potential of exploiting residual neuroplasticity to increase the outcomes of rehabilitation protocols, although with significant constraints. (Maniglia et al., 2016), one of those being the time passed from the stroke event. For example, a functional imaging study performed on a single subject with cortical blindness showed hyperactivation in V1/V2, V3, and hMT+ of the intact hemisphere before visual training, with no measurable activity on the damaged side. After intensive global direction discrimination training of the blind field, this hyperactivation was reduced toward control levels, while a recovered activation pattern was seen in regions of on the lesioned side, including perilesional tissue (V1/V2), V3a and hMT+ (Martin et al., 2009).

In sum, while postchiasmatic injuries were traditionally considered to result in complete and permanent visual loss in the topographically related area of the visual field (Holmes, 1918), there are often intact alternative pathways supporting recovery of visual functions. The residual

visual function associated with spared, perilesional V1 regions, such as MT, might thus enable some plastic changes supporting partial recovery of vision. This effect might even be boosted when combined with non-invasive brain stimulation.

1.5 Non-invasive brain stimulation approaches of the lesioned visual network

Only a few non-invasive brain stimulation (NIBS) protocols have been tested on stroke patients in the context of visual field defects and consist largely in transcranial electrical stimulation (tES) studies (Alber et al., 2017; Kraft et al., 2010; Olma et al., 2013).

As one of these cases, transorbital alternate current stimulation has been shown in a 7-Tesla MRI to have the potential to increase BOLD activity, potentially explained by more coherent activation and lower variability in the activation or by direct increase of neural activity (Sabel et al., 2020).

Furthermore, the study of Matteo *et al.* (2017) reports one of the first attempts to integrate tDCS (transcranial Direct Current Stimulation) over the parieto-occipital cortex with blindsight behavioural training treatment in the rehabilitation of the HH. In their two-subjects case report study, tDCS stimulation with anode placed over the parieto-occipital cortex of the affected hemisphere and the cathode placed in the contralateral supraorbital position showed a modulation of the effects induced by blindsight hemianopia training treatment alone. In the session with tDCS, patients showed better scores in clinical-instrumental, functional and ecological assessments. In another study on two patients with hemianopia after occipital stroke performed by Plow *et al.* (2011), occipital cortical tDCS was performed only on one of the two patients in combination with traditional VRT (Vision Restoration Therapy), while the other underwent only the traditional VRT rehabilitation protocol. High-resolution perimetry revealed a greater shift in visual field border for the patient that underwent both VRT and tDCS protocol. The same patient also showed greater recovery of function in activities of daily living. This visual function recovery was associated with functional magnetic resonance imaging activity in surviving peri-lesional and bilateral higher-order visual areas. Also, this study reported that occipital cortical tDCS may enhance recovery of visual function associated with concurrent VRT through visual cortical reorganization.

Transcranial Random Noise Stimulation (tRNS) has also shown effects combined with visual training techniques, both in healthy and in cortical blind subjects. In fact, in the study of Herpich *et al.* (2019), tRNS applied over visual areas paired with visual training enhanced visual learning twice faster and significantly longer in a healthy cohort compared to control. Furthermore, when applied to chronic cortical blind patients, this intervention led to visual motion perception improvements after only 10 days, a notably short period compared to studies using only VRT, without electrical stimulation (Das et al., 2014; Huxlin et al., 2009b).

These first proof of principle studies suggests that NIBS, might be a promising add-on approach for neurorehabilitation of visual field deficits (see Raffin et al., 2020, for a review). However, the mechanisms of these transcranial electrical stimulation studies appear to be not specific. The neural bases of motion discrimination have been extensively studied. Therefore, more specific protocols targeting in a physiology-inspired way on the pathway of interest might provide more efficient results.

1.6 Other opportunities to modulate the cortical motion network

1.6.1 ccPAS

Although it had never been applied to the lesioned visual system, a potential tool to enhance synaptic plasticity between two cortical areas is cortico-cortical Paired Associative Stimulation (ccPAS) (Chiappini et al., 2018). From Hebbian Learning theory, it is known that pairing of subthreshold synaptic stimulation and action potential trains can induce LTP (Long-Term Potentiation): if the presynaptic spike occurs before the postsynaptic spike ("pre-before-post"), the synapse is strengthened (Magee, 1997). In vivo whole-cell recording from developing frog tectal neurons shows that convergent retinotectal synapses undergo activity-dependent cooperation and competition following correlated pre- and postsynaptic spiking within a narrow time window (Zhang et al., 1998). Also, human studies showed that two minutes of 5 Hz repetitive PAS with a delay of 25ms between motor cortex and medial nerve produce a long-lasting and somatotopically specific increase in corticospinal excitability because of sensorimotor disinhibition (Quartarone et al., 2006). Thus, PAS can induce spike-timing-dependent plasticity (STPD) synapses are strengthened or weakened according to the temporal

order and precise millisecond-scale interval between presynaptic and postsynaptic spiking activity (Caporale and Dan, 2008).

These Hebbian principles extend beyond early sensory and motor processing, revealing the intricate nature of sensorimotor and crossmodal networks. PAS-induced changes consistently exhibit timing dependence, input specificity, persistence, and reversibility, suggesting a shared neurophysiological basis underlying diverse PAS protocols (Carson and Kennedy, 2013; Suppa et al., 2017).

The timing of stimuli and the structural and functional connectivity within cortical networks form the basis of PAS protocols. Timing precision is needed, with the Inter-Stimulus Interval (ISI) as an essential determinant of PAS efficacy. Within-system PAS, such as S1-PAS and M1-PAS, capitalize on well-understood sensory pathway conduction times to select optimal ISIs (Allison et al., 1989; Stefan, 2000). Cross-systems PAS, particularly those targeting long-range connectivity, has to face the challenge of determining effective ISIs (Gavaret et al., 2018; Guidali et al., 2021; Suppa et al., 2013). Temporal windows, reflecting the asymmetrical STDP window, are prevalent in most within-system PAS and cortico-cortical PAS studies (Koch et al., 2013; Wolters et al., 2005). However, only selected cross-systems PAS protocols have achieved both LTP and LTD induction, hinting at variations in STDP-like mechanisms in complex brain systems.

Also metaplasticity, shaped by prior neural activity, influences PAS outcomes. PAS studies have delved into homeostatic and non-homeostatic properties of sensorimotor systems, highlighting the dynamic nature of plasticity during PAS interventions (Bliem et al., 2008; Pötter-Nerger et al., 2009; Suppa et al., 2015). Brain state-dependency additionally affects PAS effects, with disparate outcomes when protocols are administered during different brain states (Buch et al., 2011; Chiappini et al., 2018). The study conducted by Buch *et al.* (2011) focused on how cortical excitability and the phase of neural oscillatory activity at the time of PAS application could alter its effects. When PAS was applied during a phase of high cortical excitability and specific oscillatory activity phases, it resulted in a more pronounced induction of synaptic plasticity compared to when applied during low excitability phases.

Furthermore, high variability in PAS outcomes among individuals showed the need for the identification of "PAS responders" to mitigate this inconsistency (Klöppel et al., 2015; López-Alonso et al., 2014). Individual factors, including attention, age, and gender, contribute to this

variability. For this reason, precision in being consistent to PAS protocols is essential, as even slight modifications to stimulation parameters can impact efficacy (Gorgoni et al., 2015; Tamura et al., 2009).

1.6.1.1 ccPAS on the motion discrimination network

The rationale behind the idea of performing ccPAS to enhance MT-V1 back-projections is that a first TMS pulse over MT will activate the functionally connected V1 region, that will be stimulated at the exact same moment of the activation by a V1 pulse in that same region. These repeated paired stimulations should then strengthen MT-V1 back-projections thanks to LTP mechanisms. In support of this idea, recently Romei *et al.* (2016) performed a study on healthy subjects using TMS in a MT-V1 ccPAS protocol to target reentrant connectivity from MT to V1 and to assess the effect of the intervention on the synaptic plasticity between the two areas and on the motion discrimination performance by mean of a motion coherence discrimination task. They found that only ccPAS aimed at strengthening reentrant connectivity from MT to V1, thus with the first pulse delivered over MT and the second one over V1, and with an optimal time delay of 20ms between the first and the second pulse, enhanced the human ability to perceive coherent visual motion. No significant changes in the motion discrimination performance was observable in the control groups in which the paired pulses were delivered in the opposite sequence (first V1, then MT) o the two pulses were delivered synchronously over the two areas instead of with the optimal time delay of 20ms between the pulses. This perceptual enhancement followed the temporal profile of Hebbian plasticity (Caporale and Dan, 2008). Furthermore, the highest changes in motion coherence discrimination performance were seen between 30 and 60 minutes after the ccPAS intervention, following the temporal effect of LTP. The experiment of Romei *et al.* (2016) on healthy subjects thus showed not only the importance and the role of MT-V1 back-projections in the visual discrimination network, but also that plastic connectivity changes in the network may be triggered and enhanced by ccPAS intervention performed with the correct timing and direction, resulting in LTP increasing motion coherence discrimination.

Based on these concepts and findings, in the first part of this Thesis (Chapter 2 and 3) we exploited the potential of MT-V1 ccPAS paired with EEG recording, in order not only to replicate the behavioural results reported in literature (e.g. Romei, 2016), but also to gain insights on the electrophysiological mechanisms underlying ccPAS intervention on the motion perception network.

1.6.2 tACS

Transcranial alternating current stimulation (tACS) modulates brain activity and elicits electrophysiological responses linked to changes in cortical excitability, neural plasticity, and specific behavioral changes. This technique works by emitting low-power sinusoidal current at specific frequencies to replicate natural endogenous brain activity, offering a versatile tool for research in areas like motion perception (Antal and Paulus, 2013; Castellano et al., 2017).

tACS provides a novel approach to study oscillatory activities and their causal role in perceptual binding (Antal and Paulus, 2013). For instance, applying tACS at alpha frequencies has been shown to alter temporal integration and segregation, suggesting a causal link between alpha oscillations and temporal binding (Battaglini et al., 2020a; Ronconi et al., 2020). Multimodal brain stimulation and imaging techniques such as combined tACS and electroencephalography (EEG) demonstrate how tACS-induced modulations in one frequency band can affect other frequencies (Bergmann et al., 2016). tACS shows varying effects on visual perception across different behavioral tasks. In a two-flash fusion task, alpha tACS over extrastriate areas decreased the ability to distinguish between two flashes, suggesting that alpha tACS can modulate (and possibly hinder) visual perception (Battaglini et al., 2020a). In contrast, applying 4Hz tACS to the parietal cortex improved visual working memory, but stimulating the prefrontal cortex did not produce the same effect (Bender et al., 2019). Furthermore, some studies found no significant influence of individualized alpha tACS on accuracy in segregation and integration tasks, emphasizing the importance of precise tACS placement on the scalp (Brignani et al., 2013).

In relation to motion perception, Helfrich *et al.* (2014) applied bilateral tACS over the occipital cortex in two different phase synchronization conditions. They discovered that In-Phase stimulation enhanced interhemispheric connectivity and altered motion perception, accompanied by a reduction in Alpha oscillations and an increase in Gamma patterns. Another study of Kar and Krekelberg, (2014) showed that 10 Hz tACS over the MT area increased motion direction sensitivity and reduced motion adaptation during stimulus presentation. Furthermore, 60 Hz Gamma tACS over the primary visual cortex influenced attention in a contrast discrimination task, indicating specific frequencies' roles related to distinct perceptual processes (Laczó et al., 2012).

These studies collectively suggest that tACS has the potential to modulate brain oscillatory activity and, consequently, visual-related behavioral performance. Successful modulation depends on precise targeting, specific frequencies, and phase relationships between brain areas (Bender et al., 2019; Helfrich et al., 2014; Laczó et al., 2012).

Thus, tACS, and specifically multi-site cross-frequency tACS, emerges as a promising tool for externally stimulating the V1-MT pathway in order to influence the processing and integration of moving stimuli, with potentially a strong impact on visual rehabilitation strategies for HH stroke patients. Still, arguments remain about the optimal parameters for tACS, such as, for example, which is the most effective inter-areal frequency coupling for cross-frequency stimulation. We will give an answer to this question in Chapter 4 and Chapter 5.

1.7 Aim of the work

1.7.1 Part I

Motivated by the findings described in the previous chapters (see specifically subchapter 1.6.1), the first part of this Thesis (Chapter 2 and 3) is based on the use of a cortico-cortical Paired Associative Stimulation protocol between the visual areas V1 and MT, combined with EEG recordings and a motion coherence discrimination task as readouts to determine the electrophysiological and behavioural effect of ccPAS on healthy participants and stroke patients. Furthermore, we investigate the potential of this technique as a tool to extract indexes of the network's integrity.

Specifically, the first study on healthy participants (Chapter 2), "**Pathway and directional specificity of Hebbian plasticity in the cortical visual motion processing network**", aimed to investigate the STDP inducing effect of the paired associative stimulation intervention (MT-to-V1 versus V1-to-MT, controlled for directionality) on an integer visual network, in order to assess potential benefits on the motion discrimination ability and electrophysiological correlates of the behavioural effect. This allowed us to have a better mechanistic understanding of the effect of ccPAS on the healthy visual network and specifically on the MT-V1 back-projections. The same protocol has then been applied to stroke patients suffering from HH (Chapter 3), "**Hebbian plasticity induction indexes the integrity of cortical motion processing in stroke patients**", in order to define and extract measures that could index the

integrity of the lesioned visual system according to individual responsiveness to ccPAS. These new insights into ccPAS effects on the visual motion network and its translation into motion discrimination ability changes have the potential to be used as a personalized biomarker of the integrity state of each patient's visual network, towards an accurate prognostic tool of recovery. Furthermore, this information could be essential for a future definition of more personalized subject-specific therapies.

1.7.2 Part II

Inspired by the results and concepts exposed in Subchapters 1.4.1 and 1.6.2, in the second part of this Thesis (Chapter 4 and 5) we developed a novel bifocal cross frequency tACS (cf-tACS) interventional strategy that allows to modulate interregional oscillatory activity. It has been illustrated indeed how the endogenous cross-frequency synchronization between clusters has an essential role in inter-areal information transmission and integration. We aimed through bio-inspired exogenous cross-frequency modulation to boost motion discrimination pathway's efficient information exchange during motion discrimination visual training, with the goal of increasing behavioural performance and proposing a novel more effective rehabilitation protocol for HH stroke patients.

cf-tACS was applied over V1 and MT ($V1_{alpha}$-MT_{gamma} versus $V1_{gamma}$-MT_{alpha}) and EEG, structural (sMRI) and functional MRI (fMRI) recordings were used as readouts of the modulatory and connectivity-inducing potential of cf-tACS. Cf-tACS was applied concurrently to the same motion direction discrimination task. Static and dynamic perimetries in HH stroke patients (the same cohort as of Chapter 3) were recorded to assess if our intervention on the motion discrimination pathway MT-V1 will affect the size of the visual field deficit.

Specifically, in the first study (Chapter 4), "**Single session cross-frequency bifocal tACS modulates visual motion network activity in young healthy and stroke patients**", we targeted healthy and HH stroke participants undergoing only one session of tACS stimulation, to study the acute, short-term, effect of our intervention and compare its efficacy between young health subjects (considered by us as "benchmark" population for functional and structural integrity) and on older stroke patients. In the second study (Chapter 5), "**Re-orchestrating cross-frequency visual oscillatory activity to enhance visual training efficacy in occipital stroke patients**", we instead focused only on the HH patient cohort (the

same of study reported in Chapter 4) to assess the neurophysiological, behavioural and visual field recovery effect of a long-term (10 days) daily treatment composed by specific bifocal cross frequency tACS simulation and visual motion discrimination training. The results of these studies will broaden our understanding on the effects of cross-frequency bifocal tACS on motion discrimination processing, whether it can boost the ability to detect motion in young healthy participants and in stroke patients and on the possibility to use this specialized motion network as a target to enhance visual field recovery. These studies are also an important step to pave the way towards a more personalized, home based, patient-specific visual rehabilitation therapy.

Chapter 2 - Pathway and directional specificity of Hebbian plasticity in the cortical visual motion processing network

Michele BEVILACQUA[1,2], Krystel R. HUXLIN[3], Friedhelm C. HUMMEL[1,2,4*], Estelle RAFFIN[1,2*]

[1] Defitech Chair in Clinical Neuroengineering, Center for Neuroprosthetics and Brain Mind Institute, EPFL, Geneva, Switzerland.

[2] Defitech Chair in Clinical Neuroengineering, Center for Neuroprosthetics and Brain Mind Institute, Clinique Romande de Readaptation (CRR), EPFL Valais, Sion, Switzerland.

[3] The Flaum Eye Institute and Center for Visual Science, University of Rochester, Rochester, NY, USA.

[4] Clinical Neuroscience, University of Geneva Medical School, Geneva, Switzerland.

** contributed equally*

Status: Published. Michele Bevilacqua, Krystel R. Huxlin, Friedhelm C. Hummel, Estelle Raffin, "Pathway and directional specificity of Hebbian plasticity in the cortical visual motion processing network", iScience, Volume 26, Issue 7, 2023, 107064, ISSN 2589-0042, https://doi.org/10.1016/j.isci.2023.107064.

Personal contribution: Study design, data acquisition, data analysis, results interpretation, writing, and editing of the manuscript.

Keywords:

- Visual motion processing
- TMS-EEG
- Cortico-cortical Paired Associative Stimulation
- Granger Causality

Abbreviations:

BOLD, Blood oxygenation level dependent;

ccPAS, Cortico-cortical paired associative stimulation;

EEG, Electroencephalography;

FEF, Frontal eye fields;

fMRI, Functional magnetic resonance imaging;

IPS, Intraparietal sulcus;

LTP, Long term potentiation

TMS, Transcranial magnetic stimulation;

V1, Primary visual cortex;

MT, Medio-temporal cortex;

2.1 Abstract

Cortico-cortical paired associative stimulation (ccPAS), which repeatedly pairs single pulse transcranial Magnetic Stimulation (TMS) over two distant brain regions, is thought to modulate synaptic plasticity. We explored its spatial selectivity (pathway and direction specificity) and its nature (oscillatory signature and perceptual consequences) when applied along the ascending (*Forward*) and descending (*Backward*) motion discrimination pathway. We found unspecific connectivity increases in bottom-up inputs in the low Gamma band, probably reflecting visual task exposure. A clear distinction in information transfer occurred in the re-entrant Alpha signals, which were only modulated by Backward ccPAS, and predictive of visual improvements in healthy participants. These results suggest a causal involvement of the re-entrant MT to V1 low frequency inputs in motion discrimination and integration in healthy participants. Modulating re-entrant input activity could provide single-subject prediction scenarios for visual recovery. Visual recovery might indeed partly rely on these residual inputs projecting to spared V1 neurons.

2.2 Introduction

Visual processing represents a massive computational task for the brain, requiring highly organized and efficient neural systems to achieve accurate perception. In primates, approximately 55% of the cortex contributes to visual processing (compared to 11% for somatosensory processing or 3% for auditory processing) (Felleman and Van Essen, 1991). Multiple components of the visual system receive, relay, and ultimately process visual information. These structures include the eye, retina, optic nerves, chiasm, tracts, lateral geniculate nucleus (LGN) of the thalamus, the superior colliculus, optic radiations, the primary visual (or striate, V1) cortex, and multiple extrastriate visual cortical areas. Information processing relies not only on forward connections from lower to higher-level visual areas, but also on connections that transfer information in the opposite direction. These backward connections, which are much more numerous than the forward inputs coming from the LGN (Catani et al., 2003) and from the lower-level visual areas V1 and V2, are thought to adjust, regulate and improve the processing of incoming stimuli (Antal et al., 2004; Bressler et al., 2008; Reynolds and Desimone, 2003). Therefore, neural responses in V1 do not mirror retinal inputs precisely, but are modified by higher inputs to support a coherent perceptual interpretation.

One of the most studied cortical visual processing pathways is the one specialized in decoding motion stimuli (Mikami et al., 1986). The very early stage involves the primary visual cortex (V1). Early single unit recordings in macaque and cats showed that a subset of cells in V1 are highly direction selective (Gizzi et al., 1990; Hubel and Wiesel, 1968; Maunsell and Van Essen, 1983). These direction sensitive cells then project onto the medial temporal area (MT [10]), where all neurons appear to be directionally selective (Albright et al., 1984; Maunsell and Van, 1983; Mikami et al., 1986), with activity well-correlated with behavioral performance on motion tasks (Britten et al., 1996). The information reaches the higher motion areas (MT, MST and V6) also through indirect projection through V2 and V3a areas (Gamberini et al., 2016; Pitzalis et al., 2010). More precisely, MT neurons are capable of coding the direction and speed of the image motion (Felleman and Van Essen, 1987; Lagae et al., 1993; Perrone and Thiele, 2001; Rodman and Albright, 1987). As such, lesions to primate V1 (Das et al., 2014; Huxlin et al., 2009b; Pasternak and Merigan, 1994) or MT (Marcar and Cowey, 1992; Newsome and Pare, 1988; Pasternak and Merigan, 1994; Rudolph, 1999) will both cause deficits in visual motion

perception. Transcranial magnetic stimulation (TMS) studies in humans provide further evidence supporting the role of both areas in motion discrimination (Cowey and Walsh, 2001; Ellison et al., 2003). The majority of humans and macaques' studies have concentrated on the capacity of MT cells to register motion in the fronto-parallel plane and on their directional properties and speed preferences (Krug et al., 2013; Maunsell and Van Essen, 1983; Newsome and Pare, 1988; Rodman and Albright, 1987). In this regard, Ruzzoli and colleagues (Ruzzoli et al., 2010) studied the effect of a TMS perturbation on the shape of the psychometric function in a visual motion discrimination task, showing a decrement in motion discrimination performance when TMS was applied over MT concomitantly with the motion stimulus. Furthermore, the authors found that TMS specifically affected the perceptual ability to discriminate motion direction rather than higher cognitive processes such as perceptual consciousness, decision-making, or response selection and execution.

The interaction and synchronization between visual areas have been previously modelled. One of the first computational models that simulated dynamic integration in the visual system and the pivotal role of backward connections between visual areas in motion perception processing was proposed by Tononi *et al.* (1992). The model suggested that re-entrant connections in the visual cortex are mostly integrative, i.e., they facilitate the coordination of neuronal firing in anatomically and functionally segregated cortical areas. Thus, neural responses related to the detection of motion coherence may depend on re-entrant projections from area MT to area V1, which have been found to be mostly excitatory (Pan et al., 2021). The timing of the backward inputs from MT to V1 has been studied in humans using visual masking stimuli , visually-evoked potentials (Wibral et al., 2009) or by TMS perturbation (Laycock et al., 2007; Pascual-Leone and Walsh, 2001; Silvanto, 2015). TMS studies targeting MT have consistently shown two periods of disruption, suggestive of forward/backward processes (Laycock et al., 2007). Furthermore, paired-pulse TMS protocols can estimate the time delay for information transfer along the pathway. For instance, Pascual-Leone and Walsh, (2001) showed significant impairments of coherent perceptual interpretation of motion when a MT pulse was given 10 to 30 ms before a V1 pulse. Importantly, this processing channel possesses characteristic oscillatory activity that has been linked to the transfer of specific stimulus features or endogenous variables within the pathway. Indeed, backward projections have been found to be mediated by low frequency Alpha/Beta oscillations while forward connections are thought to be supported by high frequency Gamma oscillations, in both monkeys (Bastos et al., 2015; van Kerkoerle et al., 2014) and humans (Michalareas et al., 2016).

A more direct approach to non-invasively test the role of backward projections in motion discrimination is to causally manipulate the synaptic strength of top-down MT-to-V1 connections. This is possible through the use of cortico-cortical Paired Associative Stimulation (ccPAS) (Casarotto et al., 2022; Chiappini et al., 2018; Di Luzio et al., 2022; Fiori et al., 2018; Rizzo et al., 2009; Turrini et al., 2022), an approach that relies on Hebbian Learning theory, which states that the pairing of subthreshold synaptic stimulation and action potential trains can induce Long-Term Potentiation (LTP) (Magee, 1997). More precisely, the induction of LTP requires activation of the presynaptic input milliseconds before the backpropagating action potential in the postsynaptic dendrite. The first human applications performed by Stefan et al. (Stefan, 2000) showed that low-frequency TMS over the primary motor cortex following peripheral stimulation of the median nerve induced plastic changes in the human motor system when using timings relevant for spike-timing-dependent plasticity (STPD) (Caporale and Dan, 2008).

This concept has been applied to cortico-cortical connections – e.g., between frontal and parietal areas (Koch, 2020), or between the cerebellum and M1 (Spampinato et al., 2017). ccPAS has also been applied to the V1-MT pathway (Romei et al., 2016). These authors compared different versions of ccPAS between V1 and MT in healthy subjects and found that only ccPAS targeting the re-entrant connection from MT to V1 with an optimal time delay of 20ms was effective in boosting motion discrimination capacities up to 90 minutes.

In the present study, we applied ccPAS to the V1-MT pathway to compare the effects of enhancing forward or ascending versus backward or descending projections on motion discrimination and visual network activity (Forward-ccPAS versus Backward-ccPAS). We used EEG, and spectral Granger Causality-based network analyses to investigate pathway specificity and directional specificity of ccPAS, as well as the spectral content of the induced changes. The combination of spectral Granger Causality and single pulse TMS over V1 and MT allowed us to distinguish output connectivity from re-entrant connectivity (Keil et al., 2009). In line with the prior study by Romei *et al.* (2016), we hypothesized that enhancing backward projections would induce larger behavioural improvements and would be associated with a specific increase in connectivity restricted to the re-entrant backward MT to V1 inputs, especially in the Alpha band. Conversely, we hypothesized that enhancing forward inputs would induce non-specific changes in bottom-up direct output connections, not necessarily relevant for motion perception.

2.3 Methods

Experimental model and subject details

16 healthy subjects (9 F, 7M, mean ± SD age: 27±4 years) participated in the study. All participants provided informed, written consent prior the experiment and none of them met the MRI or TMS exclusion criteria (Rossi et al., 2021). This study was approved by the local Swiss Ethics Committee (2017-01761) and performed in accordance with the Declaration of Helsinki.

General procedures

This double-blinded and cross-over study involved two sessions of 3 hours each, only differing by the type of ccPAS intervention applied to the participants. The two sessions were performed at least one month apart and the order was randomized and counter-balanced between participants. Each session comprised a familiarization phase including 3 blocks of 20 trials each, to ensure that the subjects understood the visual discrimination task and reached stable performance. After EEG cap preparation, TMS sites and intensities were defined (see below for more details). Task performances and EEG responses to single pulses over V1 and MT were measured at baseline, followed by one of the two ccPAS interventions. Ten minutes after the end of the ccPAS, task performances and single pulse TMS-EEG over V1 and MT were measured again. During the whole experiment, the participants sat on a chair, with the head leaning on the chinrest, in front of a computer screen, centred 47 cm far from the eyes. Every subject was asked to fill in a short questionnaire related to eventual issues and inconveniences caused by the single pulse TMS or ccPAS intervention at the end of both sessions.

Single pulse TMS

For single-pulse TMS over V1 and MT, biphasic TMS pulses inducing an antero-posterior followed by postero-anterior current in the brain (AP-PA) were sent through a MC-B65-HO butterfly coil (MagVenture A/S, Denmark) plugged in a MagPro XP TMS stimulator (MagVenture A/S, Denmark). Pulses duration was 200 μs for MagPro 100 and 300 μs for the MagPro XP, delivered through continuous neuronavigation monitoring using the Localite neuronavigation software (Localite GmbH, Germany).

To determine stimulation intensities, we evaluated the phosphene threshold (Gerwig et al., 2003) on both V1 and MT. If the participants reported phosphenes (9/16 for V1 and 5/16 for MT), we set the stimulation intensity at 90% of the phosphene's threshold. If no phosphenes could be evoked, we used 65 % of the maximal stimulator's output (MSO) in all participants to maximize signal-to-noise ratio and comfort during the exam. Because of discomfort related to the fact that MT is located close to the ear, we decreased the intensity to 60% MSO. The mean stimulation intensity for V1 was 66±6 % MSO and for MT 61±4 % MSO. On each area, 90 TMS pulses were performed with an inter-pulse interval of 4±1s. Stimulation intensities were re-evaluated at the beginning of the second session and adjusted if needed.

To precisely target individual V1 and MT areas, we used a standard fMRI MT localizer task performed prior the TMS-EEG session (Figure 2.1A). During the functional localizer, the screen displayed radially moving dots alternating with stationary dots (see e.g. Sack *et al.*, 2007). A block design alternated six 15 s blocks of radial motion with six blocks featuring stationary white dots in a circular region on a black background. This region subtended 25° visual angle, with 0.5 dots per square degree. Each dot was 0.36° diameter. In the motion condition the dots repeatedly moved radially inward for 2.5 s and outward for 2.5 s, with 100% coherence, at 20°/s measured at 15° from the center. Participants were passively looking at the screen and were asked to focus on a fixation point located in the middle of the screen. The resulting activation map and the individual T1 image were entered into the neuro-navigation software to define the coil positions (Figure 2.1A). The mean coil positions for V1 were -16±9, -86±8, -5±22 and for MT were 66±9, -55±9, -7±17 (coordinates x, y z, MNI space). The coil was held tangentially to the scalp with the handle pointing upwards and laterally at 45° angle to the sagittal plane.

ccPAS interventions

ccPAS was delivered via two independent TMS stimulators externally triggered with Signal (Digitimer, Cambridge Electronic Design, Cambridge, UK). MT was stimulated using the same stimulator/coil combination than for single pulse TMS-EEG recordings, i.e., with a MagVenture MagPro XP stimulator (MagVenture A/S, Denmark) connected to a MC-B65-HO coil. The right MT area was stimulated with a MagVenture MagPro X100 stimulator connected to a smaller coil to allow precise anatomical targeting, i.e., the MC-B35 coil. The same coil positions used for single TMS were applied for the ccPAS procedure, with both coils being neuronavigated (Figure 2.1A). The same intensities were used for MT. For V1, since we used

a different coil, we recalibrated the stimulation intensity to match the single pulse TMS condition. 90 pairs of biphasic stimuli were continuously delivered at a rate of 0.1 Hz for 15 min. The coil handle for MT was held tangentially to the scalp and pointed downwards at an angle of 120°±5 clockwise.

Because our goal was to explore direction-specificity effects of ccPAS in the motion processing network, we compared two types of ccPAS, differing by the order of the two pulses. In the backward MT-V1 ccPAS condition *(Backward-ccPAS*), the first TMS pulse was applied to MT followed by a pulse to V1. In the forward V1-MT ccPAS condition *(Forward-ccPAS)*, the TMS pulses order was reversed; the first pulse was administered to V1 and the second to MT. The inter-stimulus interval (ISI) was set at 20ms for both ccPAS conditions, because it corresponds to the time delays of MT-V1 back projections (Pascual-Leone and Walsh, 2001; Silvanto et al., 2005a). This timing is critical to create sequential presynaptic and postsynaptic activity in the network, and to generate the occurrence of STDP (Caporale and Dan, 2008; Jackson et al., 2006).

Behavioural task

We used a well-established 2-alternative, forced-choice, left-right, global direction discrimination and integration task (150 trials in total), as previously described (Huxlin et al., 2009b; Martin et al., 2010; Raffin et al., 2021; Saionz et al., 2020; Salamanca-Giron et al., 2021). Subjects were asked to discriminate the left–right direction of motion of random-dot stimuli. They performed 150 trials, with each trial initiated by fixation of a small spot of light within an electronic window 2 × 2° in size. Steady fixation of this target for 1000 ms resulted in a tone signaling the onset of stimulus presentation during which subjects were required to maintain fixation. A break in fixation during stimulus presentation produced a loud, 1 s tone and the termination of the trial. After 500 ms, the stimulus and fixation spot disappeared, and the subjects were required to indicate whether they perceived the global direction of motion of the stimulus to be toward the right or the left by pressing the right or left arrow key on a computer keyboard placed in front of them. Correct and incorrect responses were signaled by different computer-generated tones, so that the subjects instantly knew whether they performed correctly or not. The sequence of presentation of rightward and leftward drifting stimuli was randomized. The degree of difficulty or direction range was increased with task performance by increasing the range of dot directions within the stimulus using a 3:1 staircase design. For

every 3 consecutive correct trials, direction range increased by 40˚, while for every incorrect response, it decreased by 40˚.

Stimuli consisted of a group of black dots moving globally left- or rightwards, with a density of 2.6 dots/deg^2 in a 5˚-diameter circular aperture centred at cartesian coordinates [-5°, 5°] (i.e., the bottom left quadrant of the visual field, relative to central fixation. The dots moved at a speed of 10 °/s for a lifetime of 250 ms (half the stimulus duration). Self-confidence was rated (low/medium/high) after each trial. After each trial, auditory feedback indicated whether the response was correct or incorrect.

The task was implemented in Matlab 2019b (Version 1.8, The MathWorks Inc., USA) coupled with an EyeLink 1000 Plus Eye Tracking System (SR Research Ltd., Canada) sampling at a frequency of 1000 Hz to control gaze and pupil movements in real time. The task was projected onto a mid-grey background LCD projector (1024 x 768 Hz, 144 Hz). Participants used the left-right arrows of the keyboard to respond with their right hand; they pressed “a”, “s” or “d” to indicate low/medium/high confidence respectively, on a trial-by-trial basis.

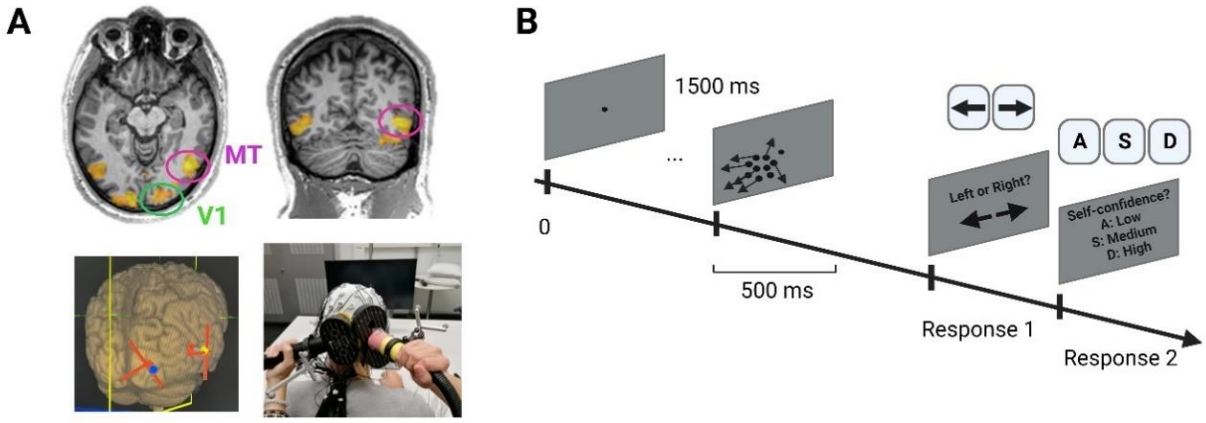

Fig.2.1: A*: Example of an individual functional localizer, online neuronavigation and coil positioning;* ***B:*** *The motion direction discrimination and integration task used before and after the ccPAS interventions.*

EEG recordings

EEG was recorded using a 64-channels, TMS-compatible system (BrainAmp DC amplifiers and BrainCap EEG cap, Brain Products GmbH, Germany) with the ground electrode at Fpz,

the reference electrode at Cz, and the Iz electrode added to the international standard 10-20 layout. Electrode impedances were adjusted and kept under 5 kOhms using conduction gel. The impedance levels were checked throughout the experiment and corrected if needed during breaks between the recordings. The signal was recorded using DC mode, filtered with an 500 Hz anti-aliasing low-pass filter, and digitalized at 5 kHz sampling frequency. Channel coordinates were individually assessed using the neuro-navigation software at the end of the experiment. We used active noise cancellation intra-auricular earphones (Bose QC 20, USA) to mask the TMS click susceptible to evoked auditory responses on the ongoing EEG activity. The sound level was adjusted for each subject, so that the TMS click delivered became barely audible without any discomfort for the participant. A thin layer of soft plastic was placed on the coil surface to dampen both sensory and auditory feedback to the subjects.

TMS-EEG pre-processing

EEG analysis was performed on the EEG recordings of the 90 single pulses sessions over V1 and MT. Pre-processing was computed in MATLAB, using the EEGLAB toolbox, the open source TMS-EEG Signal Analyser (TESA) plugin (Rogasch et al., 2017) and the Brainstorm plugin (Tadel et al., 2011).

Detection of bad channels was performed using the EEGLAB built-in function. Then, the raw EEG signal was epoched in a window of [-0.2, 0.8]s around the stimulation pulse onset, and demeaned. Afterwards, a window of [-5, 25]ms around the pulse onset was removed, to remove the TMS artefact, and the missing data was interpolated using a cubic function by considering the data 5ms before and after the removed TMS artefact window. EEG data were then down-sampled from 5000Hz to 1000Hz, and bad epochs (huge rubbing artefacts or undefined, significant noise) were removed by visual inspection. On average, 13 epochs out of 90 were removed per recording. Interpolated data in the TMS artefact window were removed gain, in order to compute the first round of Independent Component Analysis (ICA), aiming at eliminating components of the pulse artefact. This first ICA was computed by first performing a PCA compression using the TESA built-in function, and by then performing a symmetric fast-ICA with hyperbolic tangent as contrast function. The artefact components were removed manually by visual inspection. On average, 7 (±3) components out of 64 were removed. The EEG signal was re-interpolated in the removed window as described previously, and frequency filtered with a bandpass filter between 1 and 80Hz, with a 4th degree Butterworth notch filter

between 48 and 52Hz to remove the power line noise. Data belonging to the artefact window were removed once more as described earlier, and a second round of fast-ICA was computed to remove other types of artefacts, such as eye movement, blinking, acoustic artefacts and small head movement (Rogasch et al., 2017). On average, 4 (±1) components out of 64 were removed. Finally, the EEG signal was spatially filtered using a Common Average Reference (CAR) filter.

TMS-EEG Local/Remote Source Activity (L/RSA)

Source reconstruction for each TEP was performed following the default procedure proposed in the Brainstorm (version 23-Mar-2022) software (Tadel et al., 2011) together with the OpenMEEG Boundary Element Method (BEM) plugins. First, to each individual was assigned a default head model (ICBM152), with cortex and head meshes (15,000 and 10,000 vertices respectively). The forward model was then computed using the symmetric BEM developed in the OpenMEEG freeware, using default values for conductivity and layer thickness (Gramfort et al., 2010). The locations of the electrodes were individually co-registered on the head model. For each of the single pulse TMS selected epochs, the source level activation was computed using a minimum norm imaging linear method with sLORETA as the inverse model. The dipole orientation of the source model was defined as unconstrained to the cortex surface. Source orientation was kept orthogonal to the cortical surface and source amplitude was estimated using the default values of the Brainstorm implementation of the whitened and depth-weighted linear L2-minimum norm solution.

In order to extract local and remote source activity (L/RSA) power, two ROIs were created on each individual anatomy using the individual TMS coordinates for V1 and MT (see above, section “Single-pulse TMS”), covering about 195 vertices of cortical mesh for V1 and 320 for MT. LSA and RSA power was then computed for each cortical target by averaging the absolute, smoothed (using a spatial smoothing filter with full width at half maximum of 5 mm) and normalized (z-score against baseline) source activity within its corresponding ROI. LSA consisted in the matched condition where local source activity was extracted. RSA consisted in the same procedure but extracting source activity of the non-stimulated area (unmatched condition). Grand average L/RSA power was finally calculated for each stimulation site and ccPAS condition by averaging L/RSA power across subjects. Note that LSA refers to the matched condition (source activity extracted locally) and RSA refers to the unmatched

condition (source activity extracted from the other region). The focus of the study was on LSA and RSA early components (<200ms after the onset).

TMS-EEG Connectivity Analysis

We explored effective connectivity at different frequency ranges using spectral Granger Causality, which is a metric of directed interareal influence (Friston et al., 2014) in a broader visual network known to be involved in motion direction discrimination (Pascual-Leone and Walsh, 2001). Local source activity was extracted from two areas in addition to V1 and MT: the inferior parietal sulcus (IPS, ~120 vertices) and the Frontal Eye Field (FEF, ~140 vertices).

Granger causality is a measure of linear dependence, which tests whether the variance of error for a linear auto-regressive (AR) model estimation of a signal *x(t)* can be reduced when adding a linear model estimation of a second signal *y(t)*. If this is true, signal *y(t)* has a Granger causal effect on the first signal *x(t)*, i.e., independent information of the past of $y(t)$ improves the prediction of *x(t)* above and beyond the information contained in the past of *x(t)* alone. The term independent is emphasized because it creates some interesting properties for Granger Causality, such as that it is invariant under rescaling of the signals, as well as the addition of a multiple of *x(t)* to *y(t)*. The measure of Granger Causality is non-negative, and zero when there is no Granger causality. According to the original formulation of Granger Causality, the measure of Granger Causality from *y(t)* to *x(t)* is defined as:

$$F_{y\to x} = \ln\left(\frac{\mathrm{Var}(e_1)}{\mathrm{Var}(e_2)}\right)$$

Which is 0 for Var(e_1) = Var(e_2) and a non-negative value for Var(e_1) > Var(e_2). Note that Var(e_1) ≥ Var(e_2) always holds, as the model can only improve when adding new information. Under fairly general conditions, $F_{y\to x}$ can be decomposed by frequency if the two AR models in time domain are specified as:

$$\mathrm{x(t)} = \sum_{k=1}^{p}\left[A_{k_{xx}}x(t-k) + A_{k_{xy}}y(t-k)\right] + \sigma_{xy}$$

$$\mathrm{y(t)} = \sum_{k=1}^{p}\left[A_{k_{yy}}y(t-k) + A_{k_{yx}}y(t-k)\right] + \sigma_{yx}$$

In each equation the reduced model can be defined when each signal is an AR model of only its own past, with error terms σ_{xx} and σ_{yy}. We can then define the variance-covariance matrix of the whole system as:

$$\sum = \begin{bmatrix} \sum_{xx} & \sum_{xy} \\ \sum_{yx} & \sum_{yy} \end{bmatrix}$$

Where $\sum_{xx} = Var(\sigma_{xx})$, etc. Applying a Fourier transform to these equations, they can be expressed as:

$$\begin{pmatrix} A_{xx}(\omega) & A_{xy}(\omega) \\ A_{yx}(\omega) & A_{yy}(\omega) \end{pmatrix} \begin{pmatrix} x(\omega) \\ y(\omega) \end{pmatrix} = \begin{pmatrix} \varepsilon_1(\omega) \\ \varepsilon_2(\omega) \end{pmatrix}$$

Rewriting this as:

$$\begin{pmatrix} x(\omega) \\ y(\omega) \end{pmatrix} = \begin{pmatrix} H_{xx}(\omega) & H_{xy}(\omega) \\ H_{yx}(\omega) & H_{yy}(\omega) \end{pmatrix} \begin{pmatrix} \varepsilon_1(\omega) \\ \varepsilon_2(\omega) \end{pmatrix}$$

Where $\mathrm{H}(\omega)$ is the transfer matrix, the spectral matrix is then defined as:

$$S(\omega) = H(\omega) \sum H^*(\omega)$$

Finally, assuming independence of the signals $x$and y, and $\Sigma_{xy} = \Sigma_{yx} = 0$, we can define the spectral Granger Causality as:

$$F_{y \to x}(\omega) = \ln \left(\frac{S_{xx}(\omega)}{H_{xx}(\omega) \sum_{xx} H^*_{xx}(\omega)} \right)$$

Granger Causality was then computed between the four clusters (V1, MT, IPS and FEF), in a frequency range of 1-45 Hz and with a definition of 3 Hz, in order to explore the role of different rhythms in the causal connectivity between brain regions. Note that the use of Granger causality on source-projected EEG data reduces the problem of signal mixing and volume conduction, probably because Granger causality reflects causal, i.e. time-delayed, interactions,

and explicitly discards instantaneous interactions resulting from signal mixing (Bastos et al., 2015; Michalareas et al., 2016; West, 2020). Importantly, we computed Granger Causality on the EEG signals in response to single pulse TMS. This combination allowed us to distinguish direct output signals from re-entrant signals. In the manuscript, we used the term "*output connectivity*" to refer to the condition where single-pulse TMS was applied to the first area (e.g., TMS over V1, Granger Causality from V1 to MT). In contrast, we refer to "*re-entrant connectivity*" for the condition when TMS was applied to the second area (e.g., TMS over MT and Granger Causality from V1 to MT).

Quantification and statistical analysis

Behavioural data:

We computed direction range thresholds by fitting a Weibull function to the percentage correct resulting in 75% correct performance. This criterion was selected because it lays halfway between chance (50% correct) and 100% correct on this two-alternative task (Huxlin et al., 2009b). Direction range thresholds were then normalized by the maximum range (360) to produce the Normalized Direction Ratio (NDR) (e.g., Sailonz et al., 2010) using the following formula:

$$NDRthreshold(\%) = \left[\frac{(360° - WeibullfittedDR)}{360}°\right] * 100$$

NDR values were entered into a mixed ANOVA that included Time (Pre vs Post) and ccPAS type (Forward versus Backward) as within-subject factor and ccPAS order (first Forward versus first Backward) as between-subject factor. Post hoc t-tests were performed when appropriate and significance was defined for p values <0.05.

EEG data: Significant differences in L/RSA curves as well as in connectivity strength/frequency-resolved Granger Causality were evaluated within-subjects through a non-parametric, cluster-based, corrected, permutation testing, excluding frequency-wise outliers (>2SD) (Agustín Lage-Castellanos et al., 2009).

Behavior and EEG: Individual NDR values were then computed as a ratio expressing the change between pre- and post-tests, and entered into forward stepwise regressions to determine which neural pathway modulation(s) (V1-to-MT or MT-to-V1) and which frequencies best predicted changes in motion direction discrimination.

2.4 Results

16 healthy subjects participated in a double-blinded and cross-over study, involving two sessions of 3 hours each, only differing by the type of ccPAS intervention applied to the participants (Forward-ccPAS, strengthening V1-to-MT connexion or Backward-ccPAS, strengthening MT-to-V1 connexion, Figure 2.2A). The two sessions were performed at least one month apart and the order was randomized and counter-balanced between participants. Each session comprised a familiarization phase to ensure that subjects understood the visual discrimination task and reached stable performance. After EEG cap preparation, TMS sites and intensities were defined (see methods details). Task performances were extracted at baseline, and after ccPAS using normalized direction range thresholds (NDR) as classically used in signal theory (Huxlin et al., 2009b). EEG responses to single-pulse TMS over V1 and MT were also recorded at baseline and after ccPAS. During the whole experiment, the participants sat on a chair, with the head leaning on the chinrest, in front of a computer screen, centred 47 cm far from the eyes. The two sessions were equally rated in terms of discomfort and sensations. One participant dropped out, resulting in 16 datasets for Forward-ccPAS and 15 datasets for Backward-ccPAS.

Local and Remote Source activity (LSA & RSA) from single pulse TMS

We used the local EEG source activity to measure the local responses to single pulse TMS and the remote EEG source activity to infer about long-range effects (Figure 2.2B). On the local source activity, we observed a decrease over V1 (from 15ms to 100ms), only significant for the Backward-ccPAS (Figure 2.2C, left column). In contrast, Forward-ccPAS induced an increase in local MT activity (30-150ms). Note that a significant decrease was also found in the late components (> 200ms) in local V1 after Forward ccPAS When source activity was extracted from the opposite area, Forward ccPAS decreased remote MT activity in response to TMS over V1 (from 45ms to 100ms) (Figure 2.2C, second box) while Backward ccPAS showed the opposite effects (from 45ms to 60ms and from 110ms to 130ms). When TMS was applied to V1, Forward ccPAS showed a transient decrease in MT (80-100ms) while Backward-ccPAS showed a decrease (60-75ms).

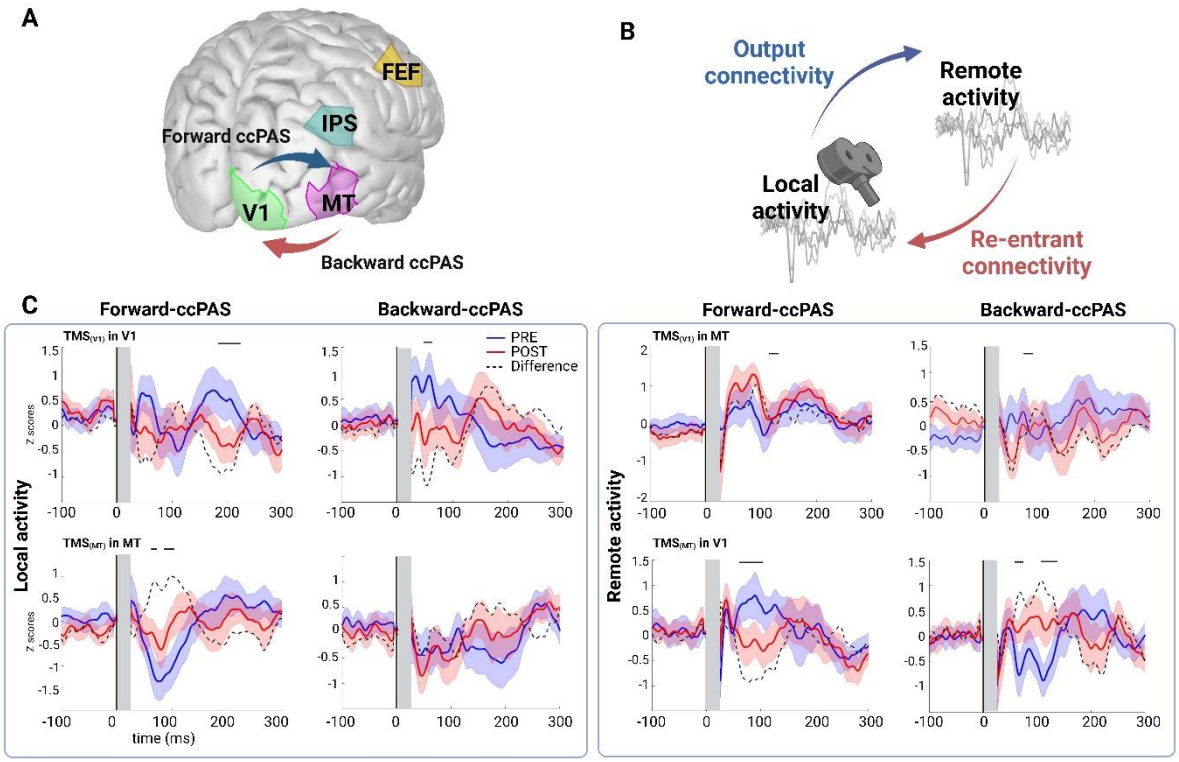

Figure 2.2: Local and Remote Source Activity in the regions of interest. ***A****: Illustration of the Backward and Forward ccPAS interventions as well as the four regions of interest;* ***B****: Illustration of the main EEG outcomes, local and remote source activity (LSA and RSA), output and re-entrant Granger Causality connectivity between V1 and MT;* ***C:*** *Right panel: LSA profiles in response to single pulse TMS over V1 (top) and TMS over MT (bottom) for Forward-ccPAS (left) and Backward-ccPAS (right). Left panel: RSA profiles in response to single pulse TMS over V1 (top) and TMS over MT (bottom) for Forward-ccPAS (left) and Backward-ccPAS (right). The blue and red lines and shaded areas represent mean and standard error of the mean of LSA power z-scored against baseline. Black bars indicate periods of significant difference between PRE and POST using non-parametric, cluster-based, corrected, permutation tests.*

Connectivity changes in response to single pulse TMS

We explored effective connectivity at different frequency ranges using spectral Granger Causality, which reflects directed interareal influence (Friston et al., 2014) in a broader visual network known to be involved in motion direction discrimination (Pascual-Leone and Walsh, 2001). Combining single pulse TMS with Granger Causality, we dissociated *Output*

Connectivity from *Re-entrant Connectivity* (Figure 2.2B). The results showed that Forward-ccPAS (Figure 2.3, left column) caused a significant increase in the bottom-up V1-to-IPS connectivity in the gamma band (35-45 Hz), when V1 was stimulated. When MT was stimulated, the V1-to-IPS connectivity was also upregulated in the theta-alpha band (5-12 Hz), while the top-down MT-to-V1 inputs were significantly inhibited in the alpha and gamma bands.

Backward-ccPAS (Figure 2.3, right column) also significantly increased direct bottom-up inputs (V1-to-MT and V1-to-IPS) in the alpha band when V1 was stimulated. Interestingly the re-entrant MT-to-V1 pathway was also increased in the alpha range (MT-to-V1). When MT was stimulated, the re-entrant V1-to-MT inputs significantly decreased in the alpha band.

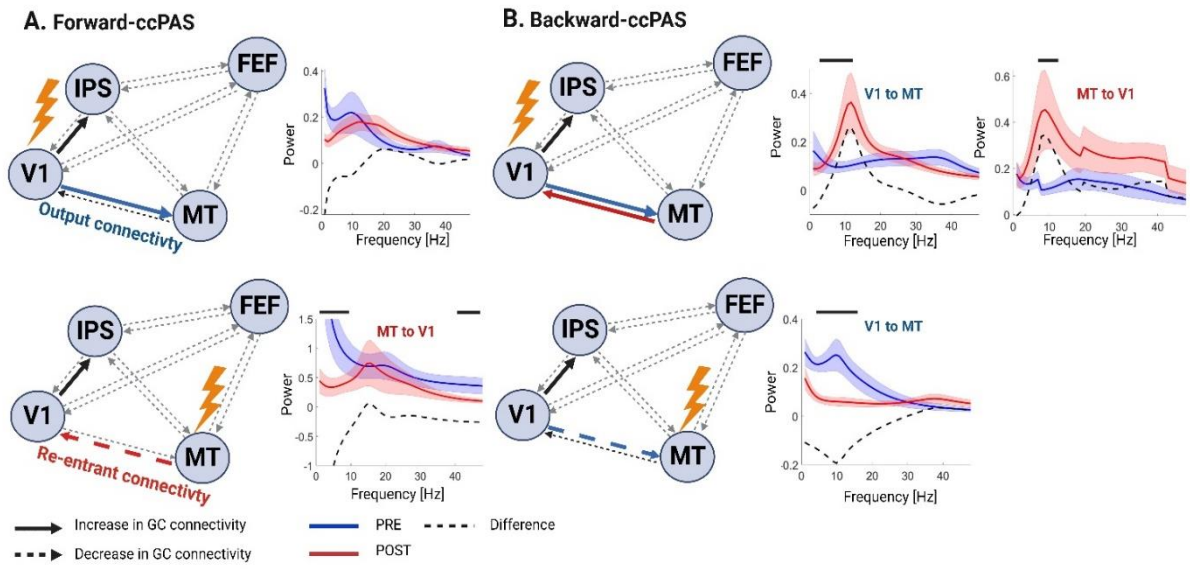

Figure 2.3: Changes in functional connectivity patterns. A*: Spectral Granger Causality of the visual network after single pulse TMS on V1 (upper row) and MT (bottom row) for Forward-ccPAS;* ***B****: Spectral Granger Causality of the visual network after single pulse TMS on V1 (upper row) and MT (bottom row) for Backward-ccPAS condition. Spectral plots displaying significant changes in Granger Causality in the frequency domain are displayed for the V1-MT pathway on the right. The blue and red lines and shaded areas represent the mean and the standard error of the mean PRE and POST ccPAS respectively. Black bars indicate periods of significant differences between PRE and POST using non-parametric, cluster-based, corrected, permutation tests.*

Behavioral results

To examine whether the changes in EEG activity and inter-areal connectivity translated into perceptual changes, we used a 2-alternative, forced-choice, left-right, global direction discrimination and integration task, as previously described (Huxlin et al., 2009b; Martin et al., 2010; Raffin et al., 2021; Saionz et al., 2020; Salamanca-Giron et al., 2021). Subjects were asked to discriminate the left–right direction of motion of random-dot stimuli centred at cartesian coordinates [-5°, 5°] (i.e., the bottom left quadrant of the visual field, relative to central fixation). Self-confidence was rated (low/medium/high) after each trial. Auditory feedback indicated whether the response was correct or incorrect. To measure changes in performance, we computed direction range thresholds by fitting a Weibull function to the percentage correct performance at each stimulus level and computed the stimulus value (i.e., direction range), resulting in 75% correct performance. Direction range thresholds were then normalized by the maximum range (360) to produce the Normalized Direction Ratio (NDR) (Das et al., 2014) (see the 2.3 Method section for more details).

A mixed ANOVA on the NDR values showed a main effect of Time ($F_{(1,11)}$=13.3, p=0.004) and a significant ccPAS type x Time ($F_{(1,11)}$=5.37, p=0.04). The post-hoc comparisons showed that the pre-post difference was only significant in the Backward-ccPAS condition (Backward-ccPAS: t_{13}=3.95, p=0.002, Forward-ccPAS: t_{14}=1.43, p=0.17, paired t tests) (see Figure 2.4A for group results and Figure 2.4B and 2.4C for individual data related to Forward-ccPAS and Backward-ccPAS, respectively). The order effect was not significant ($F_{(1,11)}$=1.21, p=0.29). Confidence ratings also showed a significant Time x ccPAS type interaction ($F_{(1,14)}$=4390, p<0.001), reflecting the specific increase in ratings for the Backward-ccPAS group (Backward-ccPAS: t_{14}=1.6, p=0.783; Forward-ccPAS: t_{15}=22, p<0.001, post hoc within group comparisons).

In order to relate the EEG changes described above (local source activity and Granger Causality connectivity strength involving V1 and MT) to these differences in motion direction discrimination after the two interventions, we designed two forward stepwise regression models, the first one with baseline-corrected NDR values belonging to the Forward-ccPAS session and the second with baseline-corrected NDR values belonging to the Backward-ccPAS session as dependent variables. The results showed that the first model (Forward-ccPAS) was not significant, suggesting that none of the connectivity changes could explain changes in NDR in this ccPAS condition. For the second model (Backward-ccPAS), the model was significant

and the retained variable was the re-entrant MT-to-V1 pathway (see Table 2.1 and Figure 2.4D). These results showed that the significant improvement in behaviour found after Backward-ccPAS could be explained by the increase in top-down inputs from MT-to-V1. All the results are summarized in Figure 2.4E.

Models					**Significant Predictors**		
	Adj. r2	**F**	**Df**	**p**	**Variable**	**Beta**	**p**
Model 1: FW ccPAS	0.0	2.05.	1	0.17	-	-	-
Model 2: BW ccPAS	0.28	5.68.	1	0.036	Re-entrant MT-V1 (TMS over V1)	0.58 (SD = 0.24)	0.036

Table 2.1: Multiple regression analyses

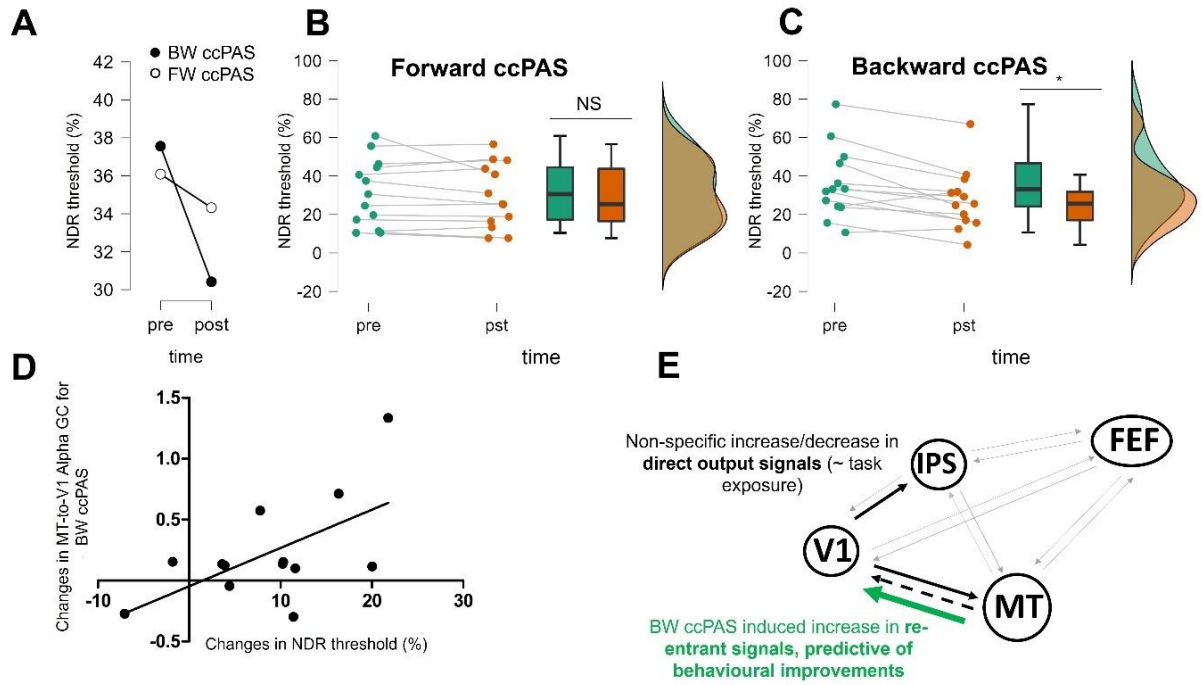

Figure 2.4: Behavioural results. ***A****: Group-level changes in NDR thresholds for the two ccPAS conditions;* ***B****: Individual data and post hoc within group comparison for Forward-ccPAS;* ***C****: Individual data and post hoc within group comparison for Backward-ccPAS;* ***D****: Correlational plot between the changes in MT-V1 connectivity strength and the changes in NDR threshold for the Backward-ccPAS illustrating the results of the forward stepward regression model;* ***E:*** *Summary of the connectivity and behavioural results.*

2.5 Discussion

In the present study, we used a combined TMS-EEG-behavioral paradigm to investigate whether cortico-cortical paired associative stimulation (ccPAS) between V1 and MT can modulate direction-specific network plasticity and improve motion direction discrimination in young, healthy participants.

Strengthening MT-to-V1 feedback inputs improves global motion processing and awareness

The intervention of interest tested in this study aimed at strengthening synaptic plasticity of MT to V1 feedback projections. V1 receives inputs from neighbouring area V2 and from a number of higher-level cortical areas (including MT, IPS and FEF), transmitting the outcomes of many cognitive operations such as attention, expectation or imagination. As a matter of fact, V1 receives considerably more feedback and lateral inputs than forward thalamic afferents (Budd, 1998). V1 is therefore a processing and integrative centre and part of a complex cortical processing cascade. Those modulatory, backward projections from higher visual areas or associative areas are thought to control the gain of thalamocortical inputs to V1 through the activation of glutamatergic receptors, among others (Ekstrom et al., 2008; Hupé et al., 2001; Muckli and Petro, 2013).

Evidence from macaques (Lamme et al., 1998) and humans (Pascual-Leone and Walsh, 2001; Silvanto et al., 2005a) has shown that back-projections from extrastriate areas to V1 are crucial for motion discrimination. In an earlier study, Romei and colleagues (2016) applied MT-V1 ccPAS (Backward-ccPAS) in healthy subjects and found improved motion coherence discrimination, suggesting plastic changes within this pathway. We provided further evidence for this finding, with a significant enhancement of motion direction discrimination only after Backward-ccPAS and not Forward-ccPAS. Furthermore, Backward-ccPAS significantly improved motion awareness, as evidenced by increased, metacognitive confidence rating, confirming the role of this pathway for motion awareness (Pascual-Leone and Walsh, 2001; Silvanto et al., 2005a). Of note, confidence ratings have been shown to influence visual discrimination (Bonder and Gopher, 2019). Therefore, we cannot infer whether ccPAS exerted its effects directly on motion perception, which then impacted confidence ratings or the opposite. Interestingly, previous research has found that the macaque lateral intraparietal area

(LIP), homologue of the human intraparietal sulcus (IPS) plays a crucial role in forming confidence in perceptual decision-making (Di Luzio et al., 2022; Huk et al., 2017; Pasternak and Tadin, 2020). Granger Causality results did reveal an increase in V1-to-IPS connectivity for both conditions, therefore strengthening the MT-V1 pathway might also support the neural circuitry of metacognitive judgements of perceptual decision-making, but future studies should be performed to understand how these two brain functions interact with each other (Di Luzio et al., 2022).

However, modulating the reciprocal forward projections did not further boost motion direction discrimination or motion awareness. The Forward-ccPAS only showed a small, non-significant improvement that might be related to a well-reported gradual improvement through practice at motion direction discrimination (Gibson, 1963; Sagi, 2011). Importantly, the absence of significant improvements justifies the absence of a Sham comparison in this study, and is partly supported by anatomical studies, showing a mixing of early parallel pathways within V1 that result in an apparent lack of compartmentalization in outputs from V1 to extrastriate cortical areas (Sincich et al., 2004; Xiao and Felleman, 2004). Some researchers have even provided evidence against parallel-processing models of the primate visual system. Furthermore, the fact that the ccPAS protocol was applied at rest might prevent the possibility of a functional routing through specific cortical circuits relevant to motion processing. Finally, neurons projecting directly from V1 to MT are located within layer 4B, closer to the layer 4Cα border, deeper than neurons projecting to other visual areas such as V2 or V3 (Nassi and Callaway, 2007) and deeper than MT-projecting neurons to V1, which are mostly located within layer 1 (Blasdel and Lund, 1983). This combination of factors (fibres' density and cortical depth) could explain why the forward inputs are less sensitive to TMS.

Neural correlates of ccPAS

The network-based interventions showed slight local changes in early EEG source activity in response to single pulse TMS, especially when measured remotely from the stimulation site. We interpret these results as reflecting changes in signal propagation from the stimulated region to the recorded region. In line with the directionality of ccPAS, Forward-ccPAS increased source activity in MT when V1 was stimulated and decreased V1 source activity when MT was stimulated. Similarly, Backward-ccPAS increased source activity in V1 when MT was stimulated, and induced a short window of inhibition of MT source activity in response to single pulse over V1. The Granger Causality results provided additional insights on synaptic

transmission and information flow within the cortical motion network. While the source activity profiles are computed from a mixture of signals from all frequency bands, we used spectrally resolved Granger Causality (Chicharro, 2011) to test hypotheses on specific oscillatory channels mediating backward and forward inputs (Bastos et al., 2015; van Kerkoerle et al., 2014). Crucially, the combination of Granger Causality measures with single pulse TMS allowed us to distinguish between direct output signal diffusion from re-entering signal transmission (Winkler et al., 2015). This distinction was particularly relevant to Backward-ccPAS, where the re-entrant top-down MT-to-V1 connection was significantly increased in the Alpha range (8-12Hz), in proportion with enhanced motion direction discrimination. In turn, the bottom-up, re-entrant V1-to-MT pathway was decreased in Alpha, suggesting that the Backward-ccPAS protocol is highly sensitive to and primarily acts on re-entrant fibers. These findings are in accordance with animal and human electrophysiological studies: Alpha oscillations in the visual cortex have been shown to characterize backward processing while Gamma waves are thought to mediate forward connectivity (Michalareas et al., 2016; Richter et al., 2018; van Kerkoerle et al., 2014). The changes in inter-areal coupling we report in the present study might support the hypothesis of a better local and specialized processing after the Backward-ccPAS protocol. Note that the connectivity analysis also revealed a slight but significant decrease in connectivity between MT and V1 after Forward ccPAS and between V1 and MT in the Backward ccPAS, suggesting that there might be an associated LTD-like effect that occurs concomitantly to the LTP-like effect on the other direction. Interestingly, this was more prominent when the networks were probed with TMS over MT. We can speculate that V1 is more roust to plastic changes while MT shows more flexible patterns of activity as demonstrated earlier (Raffin et al., 2021).

Limitations of the study

A limitation of our study is the small sample size. While we have addressed this limitation by ensuring the features of interest (NDR and GC based connectivity) have very good test-ret-test sensitivity levels (Franciotti and Falasca, 2018; Krit et al., 2021). There is an increasing awareness of the importance of both reliability and reproducibility in brain stimulation studies (Bikson et al., 2018; Héroux et al., 2017). Therefore, future work should use an independently collected and larger sample to validate our findings. Another limitation is the absence of direct comparison of our bifocal ccPAS stimulation with monofocal V1 or MT stimulation. While we think that this condition was not as relevant for pathway-specific neuromodulation, a few studies have found a modulation of motion discrimination with monofocal stimulation

(Thompson et al., 2016);·(Waterston and Pack, 2010) but no studies reported any changes in functional connectivity. A last bifocal condition could have been simultaneous V1 and MT stimulation. This control condition has been tested previously and has been shown to have no effect on performances (Romei et al., 2016). Finally, it is likely that the effect and magnitude of ccPAS over the MT-to-V1 back projections, potentially mediated by STDP, might be subject to state-dependent shifts in neocortical excitability (Chao et al., 2015; Fehér et al., 2017; Koch et al., 2013). These different excitability states could be indexed or indirectly read out using EEG-derived phases of neocortical oscillations, in particular during the Alpha cycle (Fehér et al., 2017). Therefore, to further improve the effects of the Backward-ccPAS intervention, one could implement it in a neocortical-excitability state-dependent framework. Future studies should test whether phase information extracted through online EEG recordings could be used to trigger the paired pulse TMS over MT and V1, either to control the onset of the paired pulse or the time delay between the conditioning and test pulse (MT and V1 pulse) to ultimately boost its effects.

2.6 Conclusion

This study reports the first evidence of pathway specific plasticity modulation in humans using a causal probe of effective connectivity via the combination of single pulse TMS and EEG derived Granger Causality. Fundamentally, these results provide evidence that such focality can be achieved non-invasively in humans. Additionally, these results pave the way to new applications in patients. Manipulating top-down signals in the visual system through Backward-ccPAS, could be used to quantify the acute capacity of the visual system to reorganize and from this index, extract a predictor for visual recovery potential in pathological states. The "amount" of induced plasticity in hemianopic stroke patients for instance, could reveal precious information about the functional state of their visual system, and predict whether an individual's brain is able to recruit backward projecting neurons to the spared V1 population to support recovery (Barbot et al., 2021).

Acknowledgments

We would like to thank the EEG and neuromodulation facilities of the Human Neuroscience Platform of the Fondation Campus Biotech Geneva, for technical advice. This study was supported by the Bertarelli Foundation (Catalyst BC77O7 to FCH & ER), by the Swiss

National Science Foundation (PRIMA PR00P3_179867 to ER), and by the Defitech Foundation (to FCH).

Declaration of Interests

The authors declare no competing interests.

Chapter 3 - Hebbian plasticity induction indexes the integrity of cortical motion processing in stroke patients

Running title: Visual motion plasticity in stroke patients

Michele BEVILACQUA[1,2], Fabienne WINDEL[1,2], Elena BENEATO[1,2], Pauline MENOUD[2], Sarah ZANDVLIET[2], Nicola RAMDASS[1,2], Lisa FLEURY[1,2], Julie HERVÉ[1,2], Krystel R. HUXLIN[3], Friedhelm C. HUMMEL[1,2,4], Estelle RAFFIN[1,2]

[1] Defitech Chair of Clinical Neuroengineering, Neuro-X Institute (INX), École Polytechnique Fédérale de Lausanne (EPFL), 1202 Geneva, Switzerland.

[2] Defitech Chair of Clinical Neuroengineering, INX, EPFL Valais, Clinique Romande de Réadaptation,1951 Sion, Switzerland.

[3] The Flaum Eye Institute and Center for Visual Science, University of Rochester, Rochester, NY, USA.

[4] Clinical Neuroscience, University of Geneva Medical School, Geneva, Switzerland.

Status: In preparation for submission

Personal contribution: Study design, data acquisition, EEG data analysis, results interpretation, writing, and editing of the manuscript.

Keywords:

- Hemianopia
- Direction discrimination
- Transcranial Magnetic Stimulation-ElectroEncephaloGraphy (TMS-EEG)
- Cortico-cortical Paired Associative Stimulation (ccPAS)
- Granger causality

3.1 Abstract

Homonymous Hemianopia (HH), a common visual deficit resulting from occipital lobe lesions, affects approximately 30% of stroke survivors. Intensive perceptual training can promote recovery, possibly by enhancing surviving visual pathways. This study used bi-directional cortico-cortical paired associative stimulation (ccPAS) to test associative plasticity induction in the residual, bottom-up or top-down V1-MT fibres in stroke patients. To determine its efficacy, we applied Hebbian principles of spike-timing-dependent plasticity in the cortical motion processing pathway in order to enhance visual motion discrimination through increased ipsilesional re-entrant MT-to-V1 inputs. 16 stroke patients exhibiting an occipital damage were recruited in a double-blinded, cross-over study comparing bidirectional ccPAS effects (V1-to-MT or MT-to-V1) on motion discrimination and EEG-Granger Causality. Additionally, we examined potential multimodal sources of inter-individual variability. Results demonstrated that promoting the re-entrant MT-to-V1 connectivity (Backward-ccPAS), significantly improved motion direction discrimination. However, the expected increase in top-down MT-to-V1 inputs was only visible in responders and in the high-beta band. These good-responders also displayed enhanced whole-brain functional coupling and ipsilesional V1-MT structural integrity. More precisely, larger increases in motion discrimination in the blind field were associated with stronger high-beta MT-to-V1 connectivity and preserved V1-MT structural integrity. These findings suggest that targeted ccPAS can effectively engage residual visual pathways in stroke-affected brains, potentially offering new avenues for patients' stratification and even for visual recovery strategies.

3.2 Introduction

Stroke is the second-leading cause of death and the third-leading cause of death and disability combined (as expressed by disability-adjusted life-years lost – DALYs) in the world (Feigin et al., 2022). Among the survivors, 30% of them will suffer from a visual deficit. The most common form, Homonymous Hemianopia (HH), implies loss of vision on the same side of the visual field of both eyes, secondary to occipital lobe lesions (45% of the patients). Spontaneous recovery from HH is possible in the first 3 to 6 months, but only 15% of stroke survivors will fully recover their initial visual field (Zhang et al., 2006; Zihl, 2010).

Although most of the clinical options are compensatory, some degrees of recovery can be obtained using intensive perceptual training (Bergsma and van der Wildt, 2010; Bergsma and Van der Wildt, 2008; Das et al., 2014; Huxlin et al., 2009b; Poggel et al., 2004). This restorative approach is thought to rely on 1) the function of surviving islands in the primary visual cortex (V1), having their receptive fields located close to the visual field border or/and 2) in alternative pathways left intact after the stroke, which project directly or indirectly to higher cortical visual regions (Bergsma et al., 2012; Elshout et al., 2016; Papageorgiou et al., 2014). These alternative pathways explain why despite the absence of conscious visual perception, humans and monkeys with V1 lesions remain able to respond to moving or to flickering visual stimuli within the scotomas (Barbur et al., 1993; Klüver, 1941, 1937; Pöppel et al., 1973; Riddoch, 1917; Sanders et al., 1974; Weiskrantz, 1996). The likely candidate of the residual ability is the extra-striate medio-temporal (MT) area, which in intact brains, receives most of its input from V1 (Palmer and Rosa, 2006), but also from the the lateral geniculate nucleus (LGN) (Kaas and Lyon, 2007; Sincich et al., 2004; Stepniewska et al., 2000; Warner et al., 2010) and other cortical areas (Palmer and Rosa, 2006; Schmid et al., 2013; Weller et al., 1984). Some weeks after V1 lesions, animal and human studies have shown that MT neurons still respond in a direction selective way to oriented gratings and bars located inside the scotoma (Azzopardi et al., 2003; Cowey et al., 2008; Rodman et al., 1989; Rosa et al., 2000).

Many neurons of the LGN that belong to the lesion projection zone, degenerate in the first months after V1 lesions (Atapour et al., 2017). However, LGN projections to MT appear to be preserved (Ajina et al., 2015; Bridge et al., 2008). Robust responses have been recorded from all layers of the LGN after V1 lesion (Yu et al., 2018), suggesting that this archaic direct pathway might be involved in residual vision, but only when specific behavioural stimuli are

administered in the blind field (i.e., involving stimuli with specific spatio-temporal features, see Das *et al.* (2012)). Some authors have hypothesized that blindsight capacities could be improved through training (Sahraie et al., 2006) and that unconscious vision might translate into conscious vision (Ro and Rafal, 2006). In contrast, we rather posit that the residual visual function enabled by spared, perilesional V1 islands might enable some plastic changes supporting partial recovery of vision through cortico-cortical pathways, for several reasons. First, the lateral excitatory projections in MT that initially received afferent connections from the lesioned V1 have been found to dramatically increase in density after a V1 lesion (Barnes et al., 2017). This local reorganization mechanism occurring in MT is thought to cause the receptive fields of cells inside the lesion projection zone to shift outwards, toward the border of the scotoma (Yamahachi et al., 2009). This suggests that although fewer, the residual connections between V1 and MT might be more excitable. In line with this, Hagan and colleagues (Hagan et al., 2020) found changes in the strength of connectivity units in MT, probably contributing to reinforcing the weight of the residual inputs from V1 to MT and of the feedback drives from MT to residual neurons in V1. Additionally, long-term potentiation appears to be strengthened near the lesion border after V1 lesions (Barmashenko et al., 2003; Mittmann and Eysel, 2001), suggesting that cortico-cortical connections are prone to reorganize (Guzzetta et al., 2010; Klinge et al., 2010). In contrast, the capacity to develop new thalamo-cortical connections able to bypass the lesion is very limited in adults (Guzzetta et al., 2010; Seghier et al., 2005). Finally, from a psychophysics point of view, the V1-MT pathway covers a larger spectrum of visual stimuli whereas the extrastriate pathway only processes a very limited portion of the spatiotemporal range exhibited by normal (intact) vision (Das et al., 2014).

For all these reasons, we investigated the possibility of triggering plasticity in the V1-MT pathway to transiently modulate direction discrimination performance in the blind field of stroke patients. To do so, we employed cortico-cortical paired associative stimulation (ccPAS) to promote associative plasticity between V1 and MT, exploiting the Hebbian principle of spike-timing-dependent plasticity (STDP). The ccPAS technique, involving the repeated administration of transcranial magnetic stimulation (TMS) pulse pairs to two interconnected cerebral regions, utilizes an optimal interstimulus interval (ISI) between pulses (Hernandez-Pavon et al., 2023). This protocol aims to synchronize the activation of pre-synaptic neurons in one site with the stimulation of post-synaptic neurons in the other, enhancing or diminishing the neural pathway's strength between these areas (Sjöström et al., 2008). This approach is

grounded in the Hebbian principle, where the associative coupling of pre- and post-synaptic activity is crucial for STDP, contributing to the modification of functional and effective connectivity within the targeted networks (Caporale and Dan, 2008; Turrini et al., 2022). Applied to the cortical motion processing pathway, participants receive Forward-ccPAS (a first TMS pulse is administered over V1, second over MT) or Backward-ccPAS (the first TMS pulse is administered over MT, the second over V1). Results on healthy participants consistently showed that only Backward-ccPAS boosts performances (Romei et al., 2016), in proportion with increased top-down MT to V1 connectivity (Bevilacqua et al., 2023). In this study, we investigated whether the same applies to patients with lesions affecting V1. We measured motion direction discrimination of stimuli individually located in the blind field of patients and recorded EEG activity in response to TMS over V1 and MT before and after the two ccPAS protocols. Because of the crucial role of feedbacker-entrant MT-to-V1 projections, we anticipated beneficial effects of Backward-ccPAS on motion performances and that the strength of the effect would scale with the functional reactivity of the MT-to-V1 inputs to Backward-ccPAS. Additionally, we investigated whether the level of residual structural connectivity between V1 and MT would be associated to the induced effects. The individual response to Backward-ccPAS has the potential to index the capacity for pathway-specific cortical reorganization in each individual patient, enabling to distinguish patients who would likely benefit from long-term visual retraining paradigms from the ones who won't.

3.3 Methods

General procedures

This double-blinded and cross-over study involved two sessions of 3 hours each, only differing by the type of ccPAS intervention applied to the patients. Seven patients were tested at Biotech Campus (Geneva, Switzerland) and another subgroup of nine patients were tested at the Clinique Romande de Réadaptation (Sion, Switzerland) using exactly the same setup. Prior the first experimental session, patients were familiarized and tested at the motion direction discrimination task to ensure that the subjects understood the task and reached stable performances at baseline. Additionally, patients underwent an MRI session encompassing a

functional MT localizer, the motion direction and discrimination task and some structural scans (T1 weighted image and diffusion weighted imaging).

The two experimental sessions were performed at least one month apart and the order was randomized and counter-balanced between patients. After EEG cap preparation, TMS sites and intensities were defined (see below for more details). Task performances and EEG responses to single pulse TMS over V1 and MT were measured at baseline, followed by one of the two ccPAS interventions. Ten minutes after the end of the ccPAS, task performances and single pulse TMS-EEG over V1 and MT were measured again. During the whole experiment, the participants sat on a chair, with the head leaning on the chinrest, in front of a computer screen, centred 47 cm far from the eyes. Every patient was asked to fill in a short questionnaire related to eventual issues and inconveniences caused by the single pulse TMS or by the ccPAS intervention at the end of both sessions. After the ccPAS experiment, these patients were enrolled in a long-term visual training protocol involving other brain stimulation modalities. These data will be reported in a separate manuscript.

Patients

Sixteen adult patients were enrolled at least one week after a stroke-induced occipital damage (verified using structural MRIs), with reliable 24-2 Humphrey Visual Field (HVF) perimetry. Mean time since stroke was 12.5 months (range: 1-60 months). Exclusion criteria were unreliable HVFs, neglect, neurologic disease unrelated to occipital stroke, use of neuroactive drugs, and any contra-indication to MRI or to TMS (Rossi et al., 2021). Mean (SD) age was 59.93 (11.2) years, range (34–74); 18.75% were female, 81.25% male. Seven patients had left-sided homonymous visual field loss and nine right-sided homonymous visual field loss (see Table 3.1 for patients' characteristics and demographics).

ID	AGE (years)	SEX	LESION	LESION SIDE	TIME SINCE STROKE (months)	MMSE
P101	34	f	cort	left	12	27
P102	62	m	cort	right	12	28
P103	74	m	cort	left	60	25
P104	62	m	cort	right	12	27
P105	66	m	cort + subcort	right	30	27
P106	68	m	cort	right	8	29
P107	53	m	cort	left	2	30
P201	69	m	cort + subcort	left	28	25
P202	40	f	cort	left	11	28
P203	59	m	cort	right	4	28
P204	63	m	cort	right	4	29
P205	51	m	cort	left	3	30
P206	56	m	cort	right	11	30
A201	55	m	cort	right	1	29
A203	66	m	cort	left	1.5	29

Table 3.1: *Patients' characteristics and demographics*

All patients provided informed, written consent prior the experiment. This study belongs to a registered trial (ClinicalTrials.gov: NCT05220449) and was approved by the local Swiss Ethics Committee (2017-01761) and performed in accordance with the Declaration of Helsinki.

Behavioural task

We used a well-established 2-alternative, forced-choice, global direction discrimination and integration task (150 trials in total), as previously described (Huxlin et al., 2009b; Martin et al., 2010; Raffin et al., 2021; Saionz et al., 2020; Salamanca-Giron et al., 2021). Subjects were asked to discriminate the left–right direction of the motion of random-dot stimuli (Figure 3.1C). They performed 150 trials, with each trial initiated by fixation of a small spot of light within an electronic window 2 × 2° in size. Steady fixation of this target for 1000 ms resulted

in a tone signaling the onset of stimulus presentation during which subjects were required to maintain fixation. A break in fixation during stimulus presentation produced a loud, 1 s tone and the termination of the trial. After 500 ms, the stimulus and fixation spot disappeared, and the subjects were required to indicate whether they perceived the global direction of motion of the stimulus to be toward the right or the left by pressing the right or left arrow key on a computer keyboard placed in front of them. Correct and incorrect responses were signaled by different computer-generated tones, so that the subjects instantly knew whether they performed correctly or not. The sequence of presentation of rightward and leftward drifting stimuli was randomized. The degree of difficulty or direction range was increased with task performance by increasing the range of dot directions within the stimulus using a 3:1 staircase design. For every 3 consecutive correct trials, direction range increased by 40˚, while for every incorrect response, it decreased by 40˚.

Stimuli consisted of a group of black dots with a density of 2.6 dots/deg2 in a 5˚-diameter circular aperture, moving at a speed of 10 °/s for a lifetime of 250 ms (half the stimulus duration). Self-confidence was rated (low/medium/high) after each trial. The stimuli were individually placed at the border of the scotoma (see Figure 3.1D) so that performances dropped close to chance level initially (approx. 60% (+/-5.6) accuracy). We ensured stable performance by comparing their behavioral score measured on the actual day of the experiment to the score measured one day before.

The task was implemented in Matlab 2019b (Version 1.8, The MathWorks Inc., USA) coupled with an EyeLink 1000 Plus Eye Tracking System (SR Research Ltd., Canada) sampling at a frequency of 1000 Hz to control gaze and pupil movements in real time. The task was projected onto a mid-grey background LCD projector (1024 x 768 Hz, 144 Hz).

Behavioural analyses

We computed direction range thresholds by fitting a Weibull function to the percentage correct performance at each stimulus level and computed the stimulus value (i.e., direction range), resulting in 75% correct performance. This criterion was selected because it lays halfway between chance (50% correct) and 100% correct on this two-alternative task (Huxlin et al., 2009b). Direction range thresholds were then normalized by the maximum range (360) to

produce the Normalized Direction Ratio (NDR) (e.g., (Saionz et al., 2020) using the following formula:

$$NDRthreshold(\%) = \left[\frac{(360° - WeibullfittedDR)}{360}°\right] * 100$$

Single pulse Transcranial Magnetic Stimulation (TMS)

Biphasic single-pulse TMS over V1 and MT were sent with an antero-posterior followed by postero-anterior current in the brain (AP-PA) through a MC-B65-HO butterfly coil (MagVenture A/S, Denmark) plugged in a MagPro XP TMS stimulator (MagVenture A/S, Denmark). Pulses duration was 300 μs, delivered through continuous neuronavigation monitoring using the Localite neuronavigation software (Localite GmbH, Germany). At both sites the set-up was identical.

To determine stimulation intensities, we evaluated the phosphene threshold (Gerwig et al., 2003) on both V1 and MT. If the participants reported phosphenes (4/16 for V1 and 2/16 for MT), we set the stimulation intensity at 90% of the phosphene's threshold. If no phosphenes could be evoked, we used 65 % of the maximal stimulator's output (MSO) in all participants to maximize signal-to-noise ratio and comfort during the exam. Because of discomfort related to the fact that MT is located close to the ear, we decreased the intensity to 60% MSO. The mean stimulation intensity for V1 was 67±8 % MSO and for MT 59±6 % MSO. On each area, 90 TMS pulses were performed with an inter-pulse interval of 4±1s. Stimulation intensities were re-evaluated at the beginning of the second session and adjusted if needed.

To precisely target individual V1 and MT areas, we used a standard fMRI MT localizer task performed prior the TMS-EEG session (Figure 3.1A). During the functional localizer, the screen displayed radially moving dots alternating with stationary dots (see e.g. Sack et al., 2007). A block design alternated six 15 s blocks of radial motion with six blocks featuring stationary white dots in a circular region on a black background. This region subtended 25° visual angle, with 0.5 dots per square degree. Each dot was 0.36° diameter. In the motion condition the dots repeatedly moved radially inward for 2.5 s and outward for 2.5 s, with 100% coherence, at 20°/s measured at 15° from the center. Participants were passively looking at the screen and were asked to focus on a fixation point located in the middle of the screen. The resulting activation map and the individual T1 image were entered into the neuro-navigation

software to define the coil positions (Figure 3.1A, bottom left panel). The mean coil positions for V1 were -16±9, -86±8, -5±22 and for MT were 66±9, -55±9, -7±17 (coordinates x, y z, MNI space). The coil was held tangentially to the scalp with the handle pointing upwards and laterally at 45° angle to the sagittal plane.

ccPAS interventions

ccPAS was delivered via two independent TMS stimulators externally triggered with Signal (Digitimer, Cambridge Electronic Design, Cambridge, UK). V1 was stimulated using the same stimulator/coil combination of single pulse TMS-EEG recordings, i.e., with a MagVenture MagPro XP stimulator (MagVenture A/S, Denmark) connected to a MC-B65-HO coil. The ipsilesional MT area was stimulated with a MagVenture MagPro X100 stimulator (MagVenture A/S, Denmark), pulse duration 400 μs, biphasic, connected to a smaller coil to allow precise anatomical targeting, i.e., the MC-B35 coil. In Sion, the TMS stimulator used to target MT during ccPAS was a Magstim Rapid^2 (The Magstim Company Ltd, Whitland, UK), pulse duration 400 μs, biphasic. The rest of the setup was exactly the same between the two sites.

The same coil positions used for single TMS were applied for the ccPAS procedure, with both coils being neuronavigated (Figure 3.1C, bottom left panel). The same intensities were used for MT. For V1, since we used a different coil, we recalibrated the stimulation intensity to match the single pulse TMS condition. 90 pairs of biphasic stimuli were continuously delivered at a rate of 0.1 Hz for 15 min. The coil handle for MT was held tangentially to the scalp and pointed downwards at an angle of 120°±5 clockwise.

Because one of our main goals was to explore direction-specificity effects of ccPAS in the motion processing network, we compared two types of ccPAS, differing by the order of the two pulses. In the backward MT-V1 ccPAS condition *(Backward-ccPAS*), the first TMS pulse was applied to MT followed by a pulse to V1. In the forward V1-MT ccPAS condition *(Forward-ccPAS),* the TMS pulses order was reversed; the first pulse was administered to V1 and the second to MT (Figure 3.1B). The inter-stimulus interval (ISI) was set at 20ms for both ccPAS conditions, because it corresponds to the time delays of MT-V1 back projections (Pascual-Leone and Walsh, 2001; Silvanto et al., 2005a). This timing is critical to create sequential presynaptic and postsynaptic activity in the network, and to generate the occurrence of STDP (Caporale and Dan, 2008; Jackson et al., 2006).

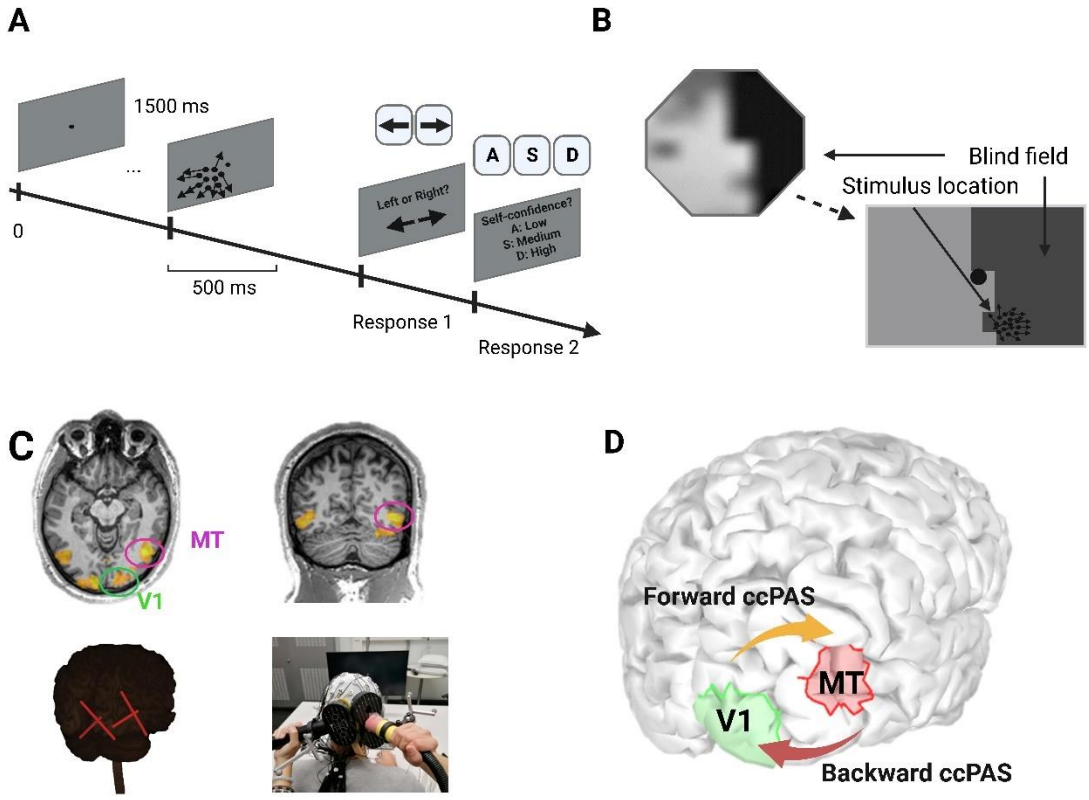

Fig.3.1: ***A****: Activation maps obtained from the individual MT functional localizer, online neuronavigation and coil positioning;* ***B:*** *Forward-tACS and Backward-ccPAS and V1, MT, IPS, FEF scouts on one exemplary patients* ***C:*** *The motion direction discrimination and integration task used before and after the ccPAS interventions;* ***D:*** *Example of stimulus location based on individual each individual's visual field maps.*

EEG recordings

EEG was recorded using a 64-channels, TMS-compatible system (BrainAmp DC amplifiers and BrainCap EEG cap, Brain Products GmbH, Germany) with the ground electrode at Fpz, the reference electrode at Cz, and the Iz electrode added to the international standard 10-20 layout. Electrode impedances were adjusted and kept under 5 kOhms using conduction gel. The impedance levels were checked throughout the experiment and corrected if needed during breaks between the recordings. The signal was recorded using DC mode, filtered with a 500 Hz anti-aliasing low-pass filter, and digitalized at 5 kHz sampling frequency. We used active noise cancellation intra-auricular earphones (Bose QC 20, USA) to mask the TMS click susceptible to evoked auditory responses on the ongoing EEG activity. The sound level was

adjusted for each subject, so that the TMS click delivered became barely audible without any discomfort for the participant. A thin layer of soft plastic was placed on the coil surface to dampen both sensory and auditory feedback to the patients.

TMS-EEG pre-processing

EEG analyses were performed on the EEG recordings of the 90 single pulses sessions over V1 and MT. Pre-processing was computed in MATLAB, using the EEGLAB toolbox, the open source TMS-EEG Signal Analyser (TESA) plugin (Rogasch et al., 2017) and the Brainstorm plugin (Tadel et al., 2011).

Detection of bad channels was performed using the EEGLAB built-in function. Then, the raw EEG signal was epoched in a window of [-0.5, 1] s around the stimulation pulse onset, and demeaned. Afterwards, a window of [-5, 25] ms around the pulse onset was removed, to remove the TMS artefact, and the missing data was interpolated using a cubic function by considering the data 5ms before and after the removed TMS artefact window. EEG data were then down-sampled from 5000Hz to 1000Hz, and bad epochs (huge rubbing artefacts or undefined, significant noise) were removed by visual inspection. On average, 8 epochs out of 90 were removed per recording. Interpolated data in the TMS artefact window were removed again, in order to compute the first round of Independent Component Analysis (ICA), aiming at eliminating components of the pulse artefact. This first ICA was computed by first performing a PCA compression using the TESA built-in function, and by then performing a symmetric fast-ICA with hyperbolic tangent as contrast function. The artefact components were removed manually by visual inspection. On average, 9 components (±5) out of 64 were removed. The EEG signal was re-interpolated in the removed window as described previously, and frequency filtered with a bandpass filter between 1 and 80Hz, with a 4th degree Butterworth notch filter between 48 and 52Hz to remove the power line noise. Data belonging to the artefact window were removed once more as described earlier, and a second round of fast-ICA was computed to remove other types of artefacts, such as eye movement, blinking, acoustic artefacts and small head movement (Rogasch et al., 2017). On average, 8 (±3) components out of 64 were removed. Finally, the EEG signal was spatially filtered using a Common Average Reference (CAR) filter.

TMS-EEG Local/Remote Source Activity (L/RSA)

Source reconstruction for each TEP was performed following the default procedure proposed in the Brainstorm (version 23-Mar-2022) software (Tadel et al., 2011) together with the OpenMEEG Boundary Element Method (BEM) plugins. First, to each individual was assigned their personal head model obtained by segmentation of T1 MRI, with cortex and head meshes (15,000 and 10,000 vertices respectively). The forward model was then computed using the symmetric BEM developed in the OpenMEEG freeware, using default values for conductivity and layer thickness (Gramfort et al., 2010). The locations of the electrodes were individually co-registered on the head model using the default 10-20 layout electrode location. For each of the single pulse TMS selected epochs, the source level activation was computed using a minimum norm imaging linear method with sLORETA as the inverse model. The dipole orientation of the source model was defined as unconstrained to the cortex surface. Source orientation was kept orthogonal to the cortical surface and source amplitude was estimated using the default values of the Brainstorm implementation of the whitened and depth-weighted linear L2-minimum norm solution.

In order to extract local source activity (LSA) power, ROIs were created on each individual anatomy using the individual TMS coordinates for V1 and MT (see above, section "Single-pulse TMS"), covering about 200 vertices of cortical mesh for V1 and 200 for MT. LSA power was then computed for each cortical target by averaging the absolute, smoothed (using a spatial smoothing filter with full width at half maximum of 5 mm) and normalized (z-score against baseline) source activity within its corresponding ROI. Grand average LSA power was finally calculated for each stimulation site and ccPAS condition by averaging LSA power across subjects. The focus of the study was on LSA early components (<200ms after the onset).

TMS-EEG Connectivity Analysis

We explored effective connectivity at different frequency ranges using spectral Granger Causality, which is a metric of directed interareal influence (Friston et al., 2014) in a broader visual network known to be involved in motion direction discrimination (Pascual-Leone and Walsh, 2001). Local source activity was extracted from two areas in addition to V1 and MT: the inferior parietal sulcus (IPS, ~120 vertices) and the Frontal Eye Field (FEF, ~140 vertices), extracted at the subject level as done for the V1 and MT scouts in the previous paragraph.

Granger causality is a measure of linear dependence, which tests whether the variance of error for a linear auto-regressive (AR) model estimation of a signal $x(t)$ can be reduced when adding a linear model estimation of a second signal $y(t)$. If this is true, signal $y(t)$ has a Granger causal

effect on the first signal *x(t)*, i.e., independent information of the past of *y(t)* improves the prediction of *x(t)* above and beyond the information contained in the past of *x(t)* alone. The term independent is emphasized because it creates some interesting properties for Granger Causality, such as that it is invariant under rescaling of the signals, as well as the addition of a multiple of *x(t)* to *y(t)*. The measure of Granger Causality is non-negative, and zero when there is no Granger causality. According to the original formulation of Granger Causality, the measure of Granger Causality from *y(t)* to *x(t)* is defined as:

$$F_{y\to x} = \ln\left(\frac{\mathrm{Var}(e_1)}{\mathrm{Var}(e_2)}\right)$$

Which is 0 for Var(e_1) = Var(e_2) and a non-negative value for Var(e_1) > Var(e_2). Note that Var(e_1) ≥ Var(e_2) always holds, as the model can only improve when adding new information. Under fairly general conditions, $F_{y\to x}$ can be decomposed by frequency if the two AR models in time domain are specified as:

$$\mathrm{x(t)} = \sum_{k=1}^{p}\left[A_{k_{xx}}x(t-k) + A_{k_{xy}}y(t-k)\right] + \sigma_{xy}$$

$$\mathrm{y(t)} = \sum_{k=1}^{p}\left[A_{k_{yy}}y(t-k) + A_{k_{yx}}y(t-k)\right] + \sigma_{yx}$$

In each equation the reduced model can be defined when each signal is an AR model of only its own past, with error terms σ_{xx} and σ_{yy} . We can then define the variance-covariance matrix of the whole system as:

$$\begin{bmatrix}\sum_{xx} & \sum_{xy}\\ \sum_{yx} & \sum_{yy}\end{bmatrix}$$

Where $\sum_{xx} = Var(\sigma_{xx})$, etc. Applying a Fourier transform to these equations, they can be expressed as:

$$\begin{pmatrix}A_{xx}(\omega) & A_{xy}(\omega)\\ A_{yx}(\omega) & A_{yy}(\omega)\end{pmatrix}\begin{pmatrix}x(\omega)\\ y(\omega)\end{pmatrix} = \begin{pmatrix}\varepsilon_1(\omega)\\ \varepsilon_2(\omega)\end{pmatrix}$$

Rewriting this as:

$$\begin{pmatrix} x(\omega) \\ y(\omega) \end{pmatrix} = \begin{pmatrix} H_{xx}(\omega) & H_{xy}(\omega) \\ H_{yx}(\omega) & H_{yy}(\omega) \end{pmatrix} \begin{pmatrix} \varepsilon_1(\omega) \\ \varepsilon_2(\omega) \end{pmatrix}$$

Where $H(\omega)$ is the transfer matrix, the spectral matrix is then defined as:

$$S(\omega) = H(\omega) \sum H^*(\omega)$$

Finally, assuming independence of the signals *x* and *y*, and $\sum_{xy} = \sum_{yx} = 0$, we can define the spectral Granger Causality as:

$$F_{y \to x}(\omega) = \ln \left(\frac{S_{xx}(\omega)}{H_{xx}(\omega) \sum_{xx} H^*_{xx}(\omega)} \right)$$

Granger Causality was then computed between the four clusters (V1, MT, IPS and FEF), in a frequency range of 1-45 Hz and with a definition of 3 Hz, in order to explore the role of different rhythms in the causal connectivity between brain regions. Note that the use of Granger causality on source-projected EEG data reduces the problem of signal mixing and volume conduction, probably because Granger causality reflects causal, i.e. time-delayed, interactions, and explicitly discards instantaneous interactions resulting from signal mixing (Bastos et al., 2015; Michalareas et al., 2016; West, 2020).

Magnetic Resonance Imaging recordings

Whole-brain MR imaging was done on a 3-Tesla Siemens scanner available at Fondation Campus Biotech Genève (FCBG), Geneva, Switzerland or on the exact same scanner at Hopital du Valais, Sion, Switzerland. High-resolution anatomical images were acquired for anatomical references using an MPRAGE inversion time=900ms, voxel size=1 x 1 x 1 mm^3. Task-related activity was measured with one run of approximatively 700 scans using T2*-weighted blood-oxygenation level dependent (BOLD) effect, a gradient echo-planar imaging protocol and the following parameters: echo time (TE)=30ms, repetition time (TR)= 1000ms, flip angle=90, voxel size=3 x 3 x 2 mm^3, field of view =204mm x 204 mm, matrix size=68 x 68 and 37 axial slices each of 2 mm thickness.

DW-MRI data were acquired using a pulsed gradient spin echo sequence with the following parameters: TR = 5000 ms; TE = 77 ms; slices = 84; field of view = 234 × 234 mm2; voxel

resolution = 1.6 × 1.6 × 1.6 mm3; slice thickness of 1.6 mm; readout bandwidth = 1630 Hz/pixels; 64-channel head coil; GRAPPA acceleration factor =3. Seven T2-weighted images without diffusion weighting (b0; b = 0 s/mm2) were acquired, including one in opposite phase encoding direction. A total of 101 images with noncollinear diffusion gradient directions distributed equidistantly over the half-sphere and covering 5 diffusion-weighting gradient strengths were obtained (b-values = [300, 700, 1000, 2000, 3000] s/mm2; shell-samples = [3, 7, 16, 29, 46]).

FMRI-based functional connectivity analyses

Data were analysed using the Statistical Parametric Mapping toolbox (SPM12b, Wellcome Trust Center, London, UK, http://www.fil.ion.ucl.ac.uk/spm), implemented in Matlab 2019b (The Mathworks Inc., Massachusetts, USA). The preprocessing steps included correction for field inhomogeneity, slice timing correction, motion correction and unwarping. Then, the structural image of each patients was co-registered to the mean realigned EPI volume. The co-registered T1 image was then normalized to the Montreal Neurological Institute (MNI) reference space using the unified segmentation approach (Ashburner and Friston, 2005). The resulting deformation parameters were applied to the individual EPI volumes which were then smoothed using an isotropic 4 mm full-width half-maximum (FWHM) Gaussian kernel.

For all datasets, we modelled a GLM using two regressors based on the patients's trial by trial accuracy in line with our staircase procedure (correct (74.63 (+/- 9.6) trials/incorrect (25.99 (+/- 9.7) trials)). Regressors were modelled as series of events (representing individual epochs) convolved with a canonical hemodynamic reference waveform. Low-frequency confounds were controlled by high-pass filtering at 1/128 Hz and head-movement estimates derived from the realignment procedure served as additional covariates of non-interest. Voxel-wise parameter estimates for all conditions and each covariate resulting from the least mean squares fit of the model to the data were computed. For the group analysis, left-side lesions were mirrored to the right hemisphere.

To test the hypothesis that functional coupling between the ipsilesional V1-MT would show different patterns of whole brain interactions in good and bad responders to ccPAS, we conducted a Physio-physiological interaction (PhPI) analysis (Di and Biswal 2013). The PhPI approach (Di and Biswal 2013) applies a linear-regression framework to identify regions in the

whole brain that are correlated with an interaction between two predefined regions, which reflects a modulation of connectivity between two regions by a third region (Di and Biswal 2013). To do this, we determined the seed brain regions on the basis of the individual V1 and MT clusters from the earlier GLM analysis, and the MR signal from each seed region was extracted as an eigenvariate time series. The extracted MR signal was deconvolved with the canonical hemodynamic response function (HRF). Then, the neural time series of the two seed regions were detrended and multiplied (dot product) so that the resulting timeseries represented the interaction of neural activity between the two seed regions (V1 and MT). Finally, the interaction time series was convolved with the HRF, representing an interaction variable at the hemodynamic level (PhPI term). Significant clusters survived false discovery rate FDR (cluster) corrections at $p<0.05$.

MRI-based structural connectivity analyses

Structural diffusion images were pre-processed by means of FSL (Jenkinson et al., 2012) and MRtrix (Tournier et al., 2019) software. A denoising step was firstly applied via the dwidenoise function (MRtrix), followed by correction of Gibbs ringing artefact via mrdegibbs (MRtrix) (Veraart et al., 2016). Images were then corrected for motion, susceptibility induced fields, eddy-current induced distortions, and bias field via the FSL functions topup (Andersson et al., 2003), eddy_openmp (Andersson and Sotiropoulos, 2016; Smith et al., 2004) and fast (Zhang et al., 2001). Probability maps for CSF, grey and white matter were estimated from the T1-weighted image via the fast function (FSL) and then registered to the average b0 image using ANTs (Avants et al., 2014). Fibres orientation distribution function was derived at the voxel level from multi-shell multi-tissue constrained spherical deconvolution and then used to compute whole-brain probabilistic tractography via second-order integration over fibre orientation distribution (iFOD2) (Tournier, 2019). The algorithm stopped once 10 million streamlines were generated. Each streamline was then weighted based on spherical-deconvolution informed filtering of tractograms (SIFT2, MRtrix) (Smith et al., 2015). To extract streamlines information between V1, V5 and the thalamus, two main techniques were used. V1 and V5 were derived from the functional localizer, using the individual thresholded activation in the ipsi- and contralesional hemisphere. The thalamus was extracted from the Destrieux atlas parcellation, output of the recon-all function of Freesurfer on the T1-weighted image (Yendiki et al., 2011). All masks were registered to the average b0 image using ANTs.

The function tckedit (Tournier et al., 2019) from MRtrix was finally used to extract specific streamlines passing through either V1 and V5, V1 and the thalamus or V5 and the thalamus. The sum of the weights or the average FA along these tracts were used as indicators of cross-sectional area and integrity respectively.

Statistics

NDR thresholds were entered into a mixed ANOVA that included Time (Pre vs Post) and ccPAS type (Forward versus Backward) as within-subject factor and ccPAS order (first Forward versus first Backward) as between-subject factor. Post hoc t-tests (Tukey's corrected for multiple comparisons) were performed when appropriate and significance was defined for p values <0.05. A median split was applied to the NDR changes in order to classify patients into good or bad responders to the condition of interest, i.e., Backward-ccPAS. Significant differences in LSA curves as well as in connectivity strength/frequency-resolved Granger Causality were evaluated within-subjects through a non-parametric, cluster-based, permutation testing, excluding frequency-wise outliers (data > 90 percentile) (Agustín Lage-Castellanos et al., 2009). Individual MT-to-V1 effective connectivity derived from Granger Causality and the fractional anisotropy (FA) value in the same tract derived from diffusion weighted imaging were finally entered into a stepwise regression model to explain the variability in behavioural changes after Backward-ccPAS (p value for entry: 0.05, for removal: 0.1).

3.4 Results

16 stroke patients participated in this triple-blinded cross-over study (patient, experimenter and analyser), involving two sessions of 3 hours each, only differing by the type of ccPAS intervention applied to the participants (Forward-ccPAS, targeting specifically V1-to-MT connection or Backward-ccPAS, acting reciprocally on the MT-to-V1 connection, Figure 3.1B). EEG signals in response to single pulse TMS over V1 and MT and Task performances were extracted at baseline and after ccPAS. One participant dropped out after the first session, resulting in 16 datasets for Forward-ccPAS and 15 datasets for Backward-ccPAS.

Backward-ccPAS improves motion direction discrimination in the blind field

The repeated measure ANOVA analysis on the NDR thresholds revealed a significant ccPAS type by Time interaction ($F_{(1,13)} = 6.7$, $p = 0.022$) (Figure 3.2A). Post hoc comparisons showed that only Backward ccPAS had a significant Pre/Post difference (Backward: $t_{(14)} = 3.3$, $p = 0.006$, Forward: $t_{(15)} = -0.24$, $p = 0.81$) (Figure 3.2B and 3.2C). There was no main effect of ccPAS ($F_{(1,13)} = 3.6$, $p = 0.08$), Time ($F_{(1,13)} = 4.01$, $p = 0.07$), or ccPAS order ($F_{(1,13)} = 6.3x10^{-4}$, $p = 0.98$). Importantly, the baseline level was stable as revealed by the absence of difference between the performances measured the day before and on the actual first day of experiment ($t(15) = -1.54$, $p = 0.14$) (Supplementary Figure S3.1). Additionally, we looked at changes in reaction times and confidence levels. No significant differences were found between the two types of ccPAS intervention (Supplementary Figure S3.2).

To understand the neural correlates of Backward-ccPAS induced improvements at the group level, we explored changes in effective connectivity using spectral Granger Causality, which reflects frequency-resolved directed interareal influences, focusing on the bi-directional V1-MT connections after single pulse TMS of V1 and MT (Figure 3.2D, group-level GC results for Forward-ccPAS can be found in Supplementary Figure S3.3).

Results showed a significant decrease in re-entrant V1-MT effective connectivity in the High Beta frequency range (27-36 Hz) after MT single pulse stimulation. No significant changes were observed in connectivity strength with the other stimulated area/direction combinations.

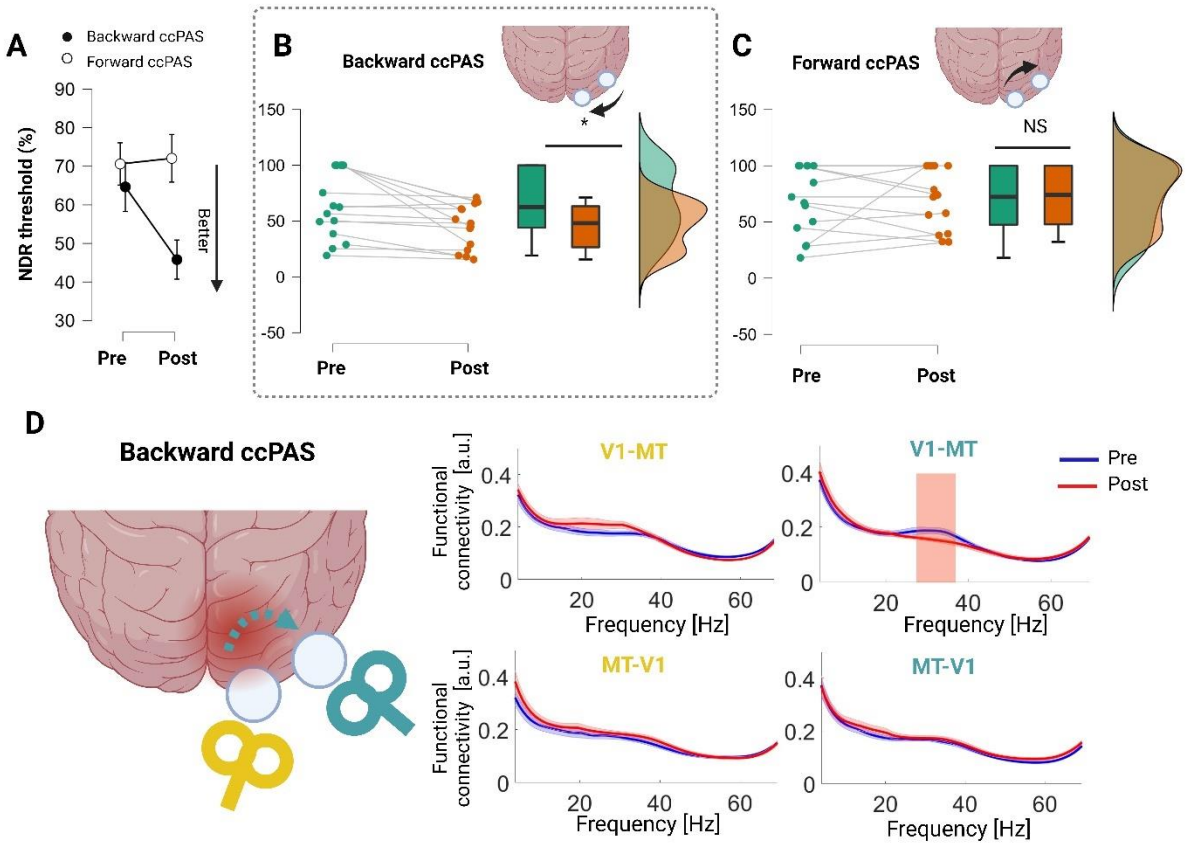

Fig.3.2: A: *Group-level changes in NDR threshold for the two ccPAS conditions (rmANOVA: significant ccPAS type by Time interaction, F(1,13) = 6.7, p = 0.022);* ***B****: Individual subjects changes in NDR threshold for Forward-ccPAS (Post-hoc Pre vs Post: t(15) = -0.24, p = 0.81).;* ***C****: Individual subjects changes in NDR thresholds for Backward-ccPAS (Post-hoc Pre vs Post: t(14) = 3.3, p = 0.006).* ***D****: Group-level Spectral Granger Causality of MT-to-V1 when TMS was given to V1 (in yellow) or to MT (in green). Green dotted arrow indicates direction and type of effective connectivity showing significant changes. Shaded areas indicate periods of significant differences between PRE and POST using non-parametric, cluster-based, permutation tests (10000 permutations, p<0.05), excluding frequency-wise outliers (>90th percentile).*

Differences between Good-Responders and Bad-Responders to Backward-ccPAS

Given the high inter-individual variability in the behavioural responses to Backward-ccPAS and our strong hypothesis on the involvement of the targeted re-entrant MT-to-V1 inputs, we conducted some sub-group analyses based on a median split of the changes in NDR thresholds after Backward-ccPAS. This resulted in 7 “good-responders” and 8 “bad-responders” (Figure 3.3A). We compared the changes in GC of MT-to-V1 and local EEG source activity in response

to single pulse TMS of the perilesional V1. Additionally, we compared to which extent the V1-MT pathway was coupled to other brain regions using whole brain fMRI PhysioPhysiological Interaction (PhPI) analyses as well as the V1-MT pathway's structural integrity based on DWI at baseline, in these two sub-groups of patients.

First, the GC results was significantly enhanced in the High Beta frequency range (19-35 Hz) in good-responders only (frequencywise permutation test, 10000 permutations, $p<0.05$). Contrariwise, no significant changes were observed in the bad-responders group (Figure 3.3B, top left). Additionally, Local Source Activity (LSA) over V1 in response to a TMS single pulse was significantly inhibited in an early time-window (between 40 and 60 ms) in the bad-responders group, while a trend for an increase was observed in the good-responders group (Figure 3.3B, bottom left).

Besides these EEG changes, we aimed to find functional and structural predictors of Backward-ccPAS effects. Because we expected that the ipsilesional V1-MT pathway would differently interact with the rest of the brain in good and bad responders, we computed a PhPI analysis on BOLD data recorded during motion direction discrimination. The results showed that the V1-MT pathway was significantly co-varying with the bilateral LGN, the ipsilateral medial superior temporal (MST) area and the ipsilesional superior parietal lobule (SPL) (Figure 3.3B, top right and Supplementary Table S3.1). In contrast, the pathway appeared to be functionally disconnected to the rest of the brain in the bad-responders group (Figure 3.3B, top right).

This study deals with lesioned brains in which parts of the tract connecting V1 to MT might have been damaged by the ictal event. To index structural integrity of the V1-MT pathway, we computed the mean fractional anisotropy (FA) in the MT-V1 tracts in the lesioned hemisphere. The results expressed significantly higher Fractional Anisotropy (FA) in good-responders compared to bad-responders ($t_{(6)} = 6.16$. $p < 0.001$) (Figure 3.3B, bottom right).

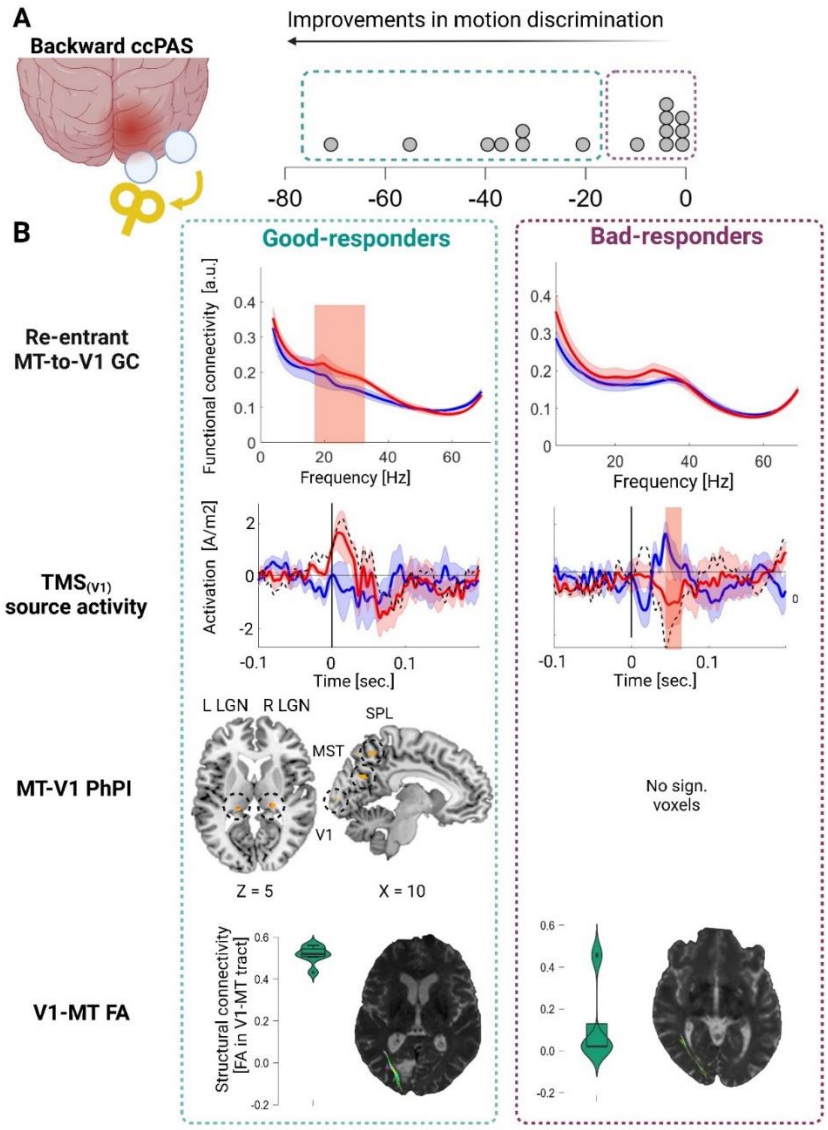

Fig. 3.3: A: *Median split of the pre/post changes in NDR threshold after Backward ccPAS into good-responders (green) and bad-responders (purple);* ***B****: Electrophysiological and neuroimaging characterization of good-responders (left) and bad-responders (right). Top left: Spectral Granger Causality of MT-to-V1 pathway after single pulse TMS on V1. The blue/red lines and shaded areas represent the mean and the standard error of the mean Pre and Post Backward ccPAS, respectively. Red vertically shaded areas indicate periods of significant differences between PRE and POST using frequencywise non-parametric permutation tests (10000 permutations, p<0.05); top right: PhPI results highlighting brain regions that significantly interact with the V1-MT functional coupling (p<0.05 with FDR(cluster) corrections); Bottom left: ipsilesional V1 LSA after single pulse TMS over V1 (pulse at t=0). As above, the blue/red lines and shaded areas represent the mean and the standard error of the mean Pre and Post Backward ccPAS, respectively. Red vertically shaded areas indicate periods of significant differences between Pre and Post using timewise non-parametric permutation tests (10000 permutations, p<0.05); Bottom right: Diffusion Weighted Imaging derived mean fractional anisotropy (FA) in the ipsilesional V1-MT tract and one representative patient.*

Predictors of Backward-ccPAS effects

To understand the weights of each of these variables in the inter-individual variability of the response to Backward-ccPAS, we conducted a stepwise regression model with the following predictors which appeared to distinguish bad from good responders: the changes in GC of the re-entrant MT-to-V1 connection, the changes in local perilesional source activity in response to TMS and the beta-weights extracted from the PhPI analyses in the ipsilesional LGN. Additionally, we added the individual V1-MT FA values into the model.

The stepwise regression model was significant ($F_{(2,13)} = 11.44$, $p = 0.002$) and explained a relevant amount of the variance ($R^2=0.62$). The MT-to-V1 GC and the FA were retained as significant predictors (GC: $t_{(13)} = -2.85$, $p = 0.016$, FA: $t_{(13)} = -3.37$, $p = 0.006$). Importantly, the two predictors were not correlated with each other ($r = 0.15$, $p = 0.61$). Figure 3.4A shows the partial plots of the linear fit between the GC residuals (left panel) or the FA residuals (right panel) and the residuals of the changes in NDR thresholds, illustrating the quality of the linear fit for the two significant predictors.

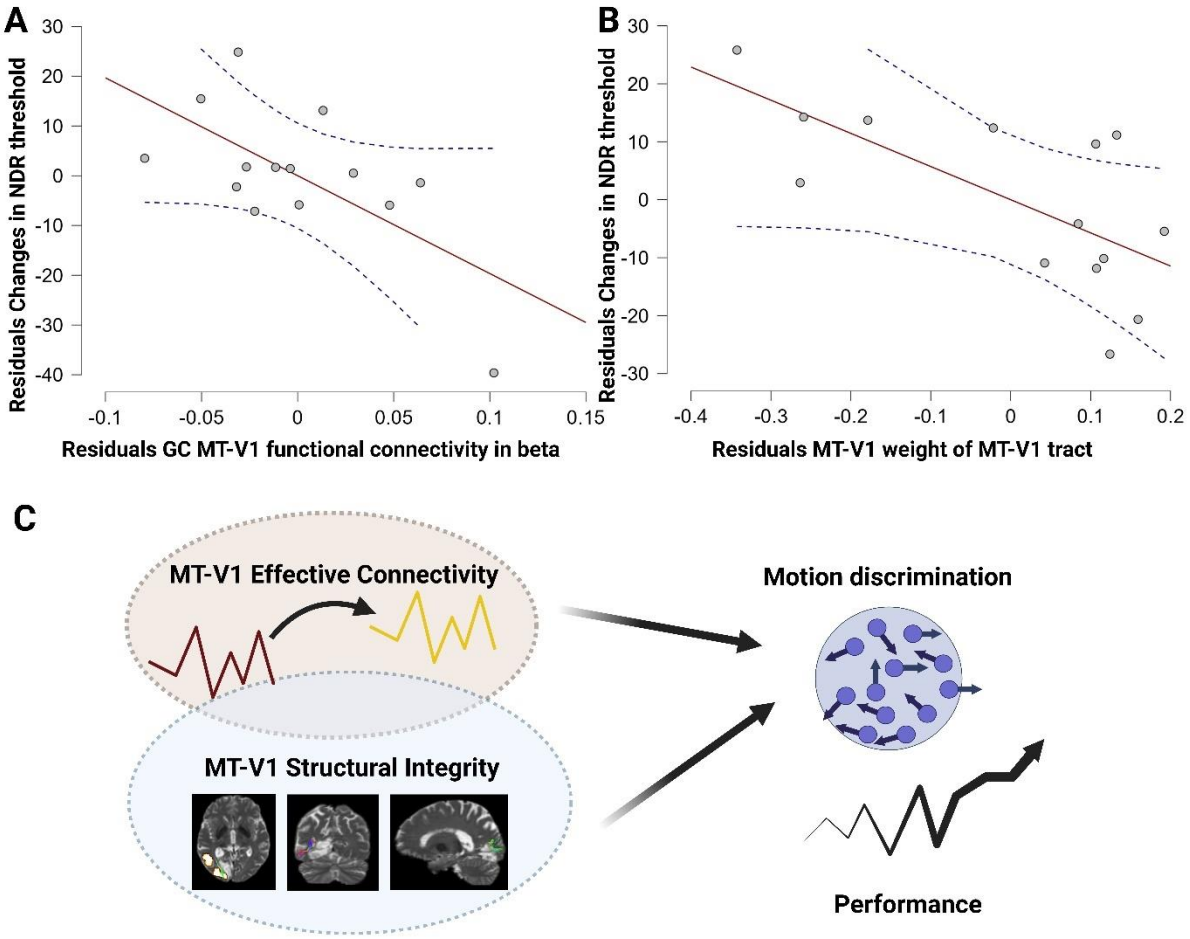

Fig.3.4: Stepwise regression A: *Partial plots and confidence intervals of the linear fit between the GC residuals (left panel) or the FA residuals (right panel) against the residuals of the changes in NDR thresholds, illustrating the quality of the linear regression;* ***B****: Illustration of the two predictors of Backward-ccPAS efficacity. Both functional connectivity changes elicited by single pulse TMS over V1 (represented as changes in beta band spectral Granger Causality MT-to-V1) and residual structural integrity of the pathway of interest are able to predict the change in visual motion discrimination performance at the edge of the scotoma.*

3.5 Discussion

In the present study, we used a combined MRI, TMS-EEG and behavioural paradigm to investigate whether the residual re-entrant MT-to-V1 pathway in V1 lesioned patients, can be purposively modulated to enhance motion discrimination in the border of their visual field. Additionally, we aimed to test whether residual structural connectivity or functional reactivity of the task-relevant pathway can accurately predict how much a single patient will benefit from the cortico-cortical paired associative stimulation (ccPAS) intervention.

Evidence from macaques and humans has shown that back-projections from extrastriate areas to V1 are crucial for motion discrimination (Lamme et al., 1998; Pascual-Leone and Walsh, 2001; Silvanto et al., 2005a). In an earlier study, Romei and colleagues (Romei et al., 2016) applied MT-V1 ccPAS (Backward-ccPAS) in healthy subjects and found improved motion coherence discrimination, suggesting plastic changes within this pathway. We provided additional support for this finding, and revealed for the first time, an associated increase in top-down MT-to-V1 connectivity only after Backward-ccPAS in patients. In this study, we investigated whether Backward-ccPAS would trigger the same mechanisms in the lesioned brain of stroke patients, potentially in proportion with the remaining structural fibers. Our results at the group level suggested that despite the absence of a large portion of V1, Hebbian rules of plasticity appears to apply in patients, with significant improvements in motion discrimination. Beyond our current findings on ccPAS in visual motion discrimination, this technique has demonstrated its potential in other neurological areas. For instance, a study by (Quartarone et al., 2006) showcased the utility of ccPAS in enhancing motor performance in healthy individuals, suggesting potential applications in motor rehabilitation. Furthermore, a study by (Pellicciari et al., 2009) explored the application of ccPAS in cognitive enhancement, revealing its potential to modulate working memory performance in healthy individuals. Such researches underscore the broad utility of ccPAS in diverse neurological applications, extending from motor rehabilitation to cognitive therapy.

Notably, inter-individual variability in the response to Backward-ccPAS was pretty high compared to healthy participants. To understand the bases of this variability, we compared spectral Granger Causality connectivity of the targeted pathway (i.e., the re-entrant MT-to-V1 connection) in the group of patients who had the largest improvements at the task after Backward-ccPAS to the other half-group. While the bad-responders did not show any significant change in the MT-to-V1 inputs, the responders showed the expected increase in the re-entrant top-down MT-V1 connections in the beta band.

This enhanced high beta connectivity highlights the potential of this frequency band as a mediator and biomarker of synaptic plasticity. The beta band's role in cognitive and motor functions is well-documented, with increases in beta connectivity associated with maintaining the status quo and in particular feedback sensorimotor processing (Baker, 2007; Engel and Fries, 2010). Our results suggest that similar mechanisms might be at play within the visual system, particularly in top-down processing (Buschman and Miller, 2007). Note that the

Forward-ccPAS condition led to task-irrelevant changes in direct bottom-up tracts that were also previously reported in healthy participants (Bevilacqua et al., 2023) (see Supplementary Figure S3.3).

The modulation of beta oscillations in the V1-to-MT pathway is reported being crucial for top-down control of motion perception. A study of Richter et al. (2018) revealed that top-down beta-band influences from higher visual areas enhance bottom-up gamma-band processes in V1, suggesting a mechanism where beta oscillations modulate motion perception through cross-frequency interaction. Furthermore, beta oscillations in early visual cortex convey behavioural context, affecting the processing of motion stimuli (Richter et al., 2017). The beta band's role, particularly its alterations post-ccPAS, is a noteworthy finding given its association with cortical excitability and functional connectivity in motor (Pineda, 2005) and visual systems (Siegel et al., 2012). The changes in beta Granger Causality following TMS, therefore, may reflect a state of heightened readiness in the visual cortex to engage in the processes of reorganization required for visual field recovery.

Interestingly, in our study on healthy subjects (Bevilacqua et al., 2023), changes were observed in the alpha frequency band. This shift towards beta in patients can be attributed to the post-stroke neural dynamics, where functional reorganization in cerebral networks leads to changes in oscillatory patterns. This reorganization often results in an altered excitatory-inhibitory balance within neural networks, influencing oscillatory activity in both alpha and beta bands (Ulanov and Shtyrov, 2022). Beta oscillations in particular have been shown to be significant in post-stroke functional recovery (Hordacre et al., 2020; Thibaut et al., 2017). Specifically, Thibaut et al. (2017) found that increased high-beta power in the affected hemisphere correlates with improved motor performance, suggesting a compensatory mechanism due to the lesion-induced excitability imbalance. This shift from alpha to beta band in lesioned environments could signify the brain's adaptive response to injury, emphasizing the role of beta oscillations as a potential biomarker in chronic stroke recovery (Ulanov and Shtyrov, 2022).

This result suggests that when Backward-ccPAS was efficient in patients, it did induce the expected neuronal change. As a matter of fact, we found that Backward-ccPAS effects were predicted by these changes in the re-entrant MT-to-V1 Beta inputs, but also by the residual structural connectivity between the ipsilesional MT and V1 measured with diffusion-weighted imaging (DWI). Fractional anisotropy (FA) within the MT-V1 tract can be seen as a marker of structural integrity, which is essential for efficient signal transmission and is likely critical for

the effectiveness of ccPAS (Reijmer et al., 2013). The presence of intact fiber tracts may facilitate the induction of plastic changes in response to associative stimulation protocols. The bad-responders had lower FA values in the MT-V1 pathway, which was also functionally disconnected to the rest of the brain during motion discrimination as shown in the fMRI data. Conversely, this pathway was coupled to other relevant visual areas in the good-responders such as the LGN or the MST. Altogether, these results provide strong evidence that Backward-ccPAS directly recruits the remaining MT-to-V1 synaptic connections in lesioned brains and that these two measures especially, residual FA and directed connectivity changes could be used more globally as predictors of efficacy when an intervention targets a specific pathway.

Intriguingly, these two variables were statistically independent. When combined together in the multiple regression model, they accounted for significantly more variance in behavioural changes, suggesting that they capture distinct dimensions of the brain's response to injury and potential for recovery. The fact that some patients successfully enhanced functional connectivity despite having low fractional anisotropy (FA), while others with high FA did not show improved functional connectivity, can be explained by the complex coupling between brain microstructure and functional connectivity. Microstructural alterations do not necessarily go along with impaired functional connectivity and reciprocally (Preti and Van De Ville, 2019; Reijmer et al., 2015). This discrepancy could be due to various factors such as the compensatory reorganization of neural networks or differences in the integrity of specific other indirect white matter tracts between the areas (Kim et al., 2023). This suggests that in some stroke patients, despite compromised structural integrity (low FA), there might be compensatory mechanisms at play enabling enhanced functional connectivity. Conversely, patients with relatively preserved structural integrity (high FA) might not exhibit improved connectivity due to other limiting factors in the brain's adaptive response to injury or recovery mechanisms. Our results align with the literature emphasizing the interplay, but not exact coupling between structural integrity and functional connectivity in the context of neural repair and rehabilitation. For instance, evidence suggests that the presence of certain biomarkers of white matter integrity can guide the use of non-invasive brain stimulation techniques such as transcranial magnetic stimulation (TMS) or transcranial direct current stimulation (tDCS), potentially enhancing their efficacy (Buma et al., 2013). However, in our case, a potential biomarker of structural integrity such as residual FA would not be enough to satisfyingly predict the outcome of Backward-ccPAS. The dynamic nature of functional connectivity in response to interventions highlights the relevance of considering both structural and functional

aspects in a complementary fashion (Figure 3.4C). Previous studies suggest that functional connectivity may offer insights into the brain's compensatory mechanisms, which can be leveraged to facilitate recovery (Carter et al., 2010). Here we postulate that both functional and structural connectivity should be considered to optimally design rehabilitation protocols.

Extrapolating these results to any other pathway-specific plasticity inducing interventions, we argue that residual FA and connectivity changes could be efficient predictors of intervention's outcomes and more generally of stroke recovery.

In conclusion, our study lends substantial support to the adoption of a multimodal index that synergistically exploit both structural and functional metrics for enhancing the predictive accuracy of rehabilitation outcomes following Backward ccPAS intervention in stroke patients. Such innovative approach is directly related to the field of precision medicine (Cramer, 2008), which aims at tailoring treatments to each individual characteristics in particular, in the field of post stroke visual recovery (Collins and Varmus, 2015) (Howard and Rowe, 2018). By establishing a precise neural and behavioural profiling of each individuals, it might be possible to accurately predict treatment efficacy on an individual basis (Ramsey et al., 2017).

Complementarily, the dynamic nature of brain activity and its modulation by therapeutic interventions calls for adaptive strategies that can respond to ongoing, real-time changes. This is where the potential need for a state-dependent EEG ccPAS setup becomes apparent. Parts of the variability we measured in response to Backward-ccPAS might not only come from the residual white matter tracts or from the capacity to modulate effective connectivity, but also on the trial-by-trial difference in brain state surrounding ccPAS paired pulses. State-dependent systems are designed to adjust the stimulation parameters (onsets, intensities, location, etc…) automatically in response to EEG signals, thereby providing an individualized therapeutic experience (Bauer et al., 2015; Karabanov et al., 2016). One parameter that can be modulated without disturbing timings for STDP induction is the repetition rate of the pairs of TMS pulses, which are classically repeated at 0.1 Hz in a rigid manner. For instance, based on the pulsed alpha inhibition theory (Jensen et al., 2010), MT-to-V1 ccPAS effects could be strengthened by triggering each paired pulse stimulation at the optimal phase of the on-going alpha activity.

In conclusion, this study provides encouraging results, showing that STDP can be triggered in lesioned visual systems and can result in behaviourally relevant effects, in proportion to enhanced functional connectivity and residual structural integrity of the pathway. To validate

the prognostic values of these results, future research must longitudinally assess these multimodal indexes in various cohorts and different stages of stroke recovery. The possibility to apply such markers for state-dependent ccPAS in clinical settings on a much larger and heterogenous cohort will also necessitate thorough examination (Di Lazzaro et al., 2018).

Acknowledgments

We would like to thank the EEG and neuromodulation facilities of the Human Neuroscience Platform of the Foundation Campus Biotech Geneva, for technical advice.

Fundings

This study was supported by the Bertarelli Foundation (Catalyst BC77O7 to FCH & ER), by the Swiss National Science Foundation (PRIMA PR00P3_179867 to ER), and by the Defitech Foundation (to FCH).

Competing Interests

The authors declare no competing interests.

3.6 Supplementary Materials

Regions	F values	Z max	Cluster extent	MNI coordinates (x;y;z)
R Lateral Geniculate Nucleus	13.4	3.35	31	4;-76;-3
L Lateral Geniculate Nucleus	12.7	3.26	19	3;46;3
R Superior Parietal Lobe	11.7	3.39	17	-29;46;28
R Medial Superior Temporal				
R Primary Visual Cortex				

Supplementary Table S3.1: *Significant clusters in the PhPI analyses with the V1-MT pathway as seed*

Supplementary Figure S3.1: Baseline stability of motion discrimination performance

At the group level, no difference was observed between the performances measured on the day before and on the actual first day of experiment ($t_{(15)}$ = -1.54, p = 0.14), ensuring stable performance at baseline.

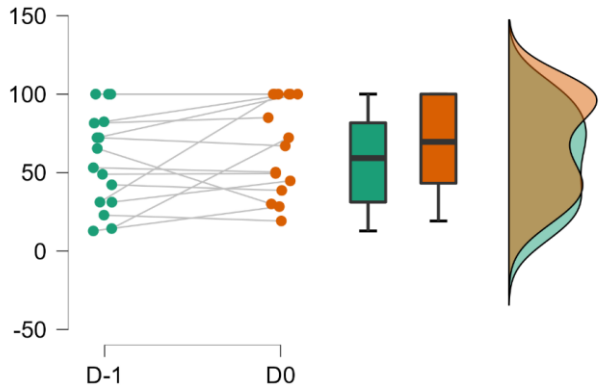

Supplementary Figure S3.1: *A paired t-test revealed no significant difference between NDR thresholds measured the day before the first session of the experiment and the first "Pre" ccPAS measurement (t(15) = -1.54, p = 0.14).*

Supplementary Figure S3.2: Motion awareness and reaction time

For exploratory purposes, we inspected potential changes in motion awareness and in reaction times. Supplementary Figure 3.2A shows the group distribution of the Pre/Post difference in motion awareness for the trials correct trials only, for the two ccPAS conditions. The rmANOVA did not show any significant main effects or interaction (Time effect: $F(1,8) = 1.8$, $p = 0.21$; ccPAS effect: $F(1,8) = 0.07$, $p = 0.8$; Time by ccPAS interaction: $F(1,8) = 3.3$, $p = 0.1$). Supplementary Figure 3.2B reports the group distribution of the Pre/Post difference in response times for the correct trials of the two ccPAS conditions. While we observe a general Time effect ($F(1,8) = 12.7$, $p = 0.007$), no significant ccPAS type by Time interaction was found ($F(1,8) = 0.48$, $p = 0.51$).

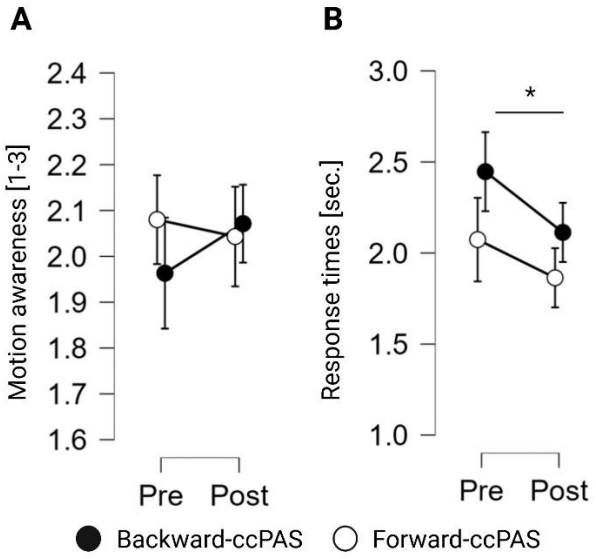

Supplementary Figure S3.2: A: *Distribution of the Pre/Post difference in motion awareness for the correct trials;* ***B****: Distribution of the Pre/Post difference in reaction time for the correct trials.*

Supplementary Figure S3.3: Changes in effective connectivity for Forward ccPAS

Granger Causality analysis at Forward ccPAS group level showed a task-irrelevant significant increase of direct V1-to-MT effective connectivity in the Alpha/Beta frequency range (7-21 Hz) after V1 single pulse stimulation, an a increase of direct MT-

to-V1 effective connectivity in the High Beta frequency band (27-35 Hz) after MT single pulse stimulation. No significant changes were observed elsewhere.

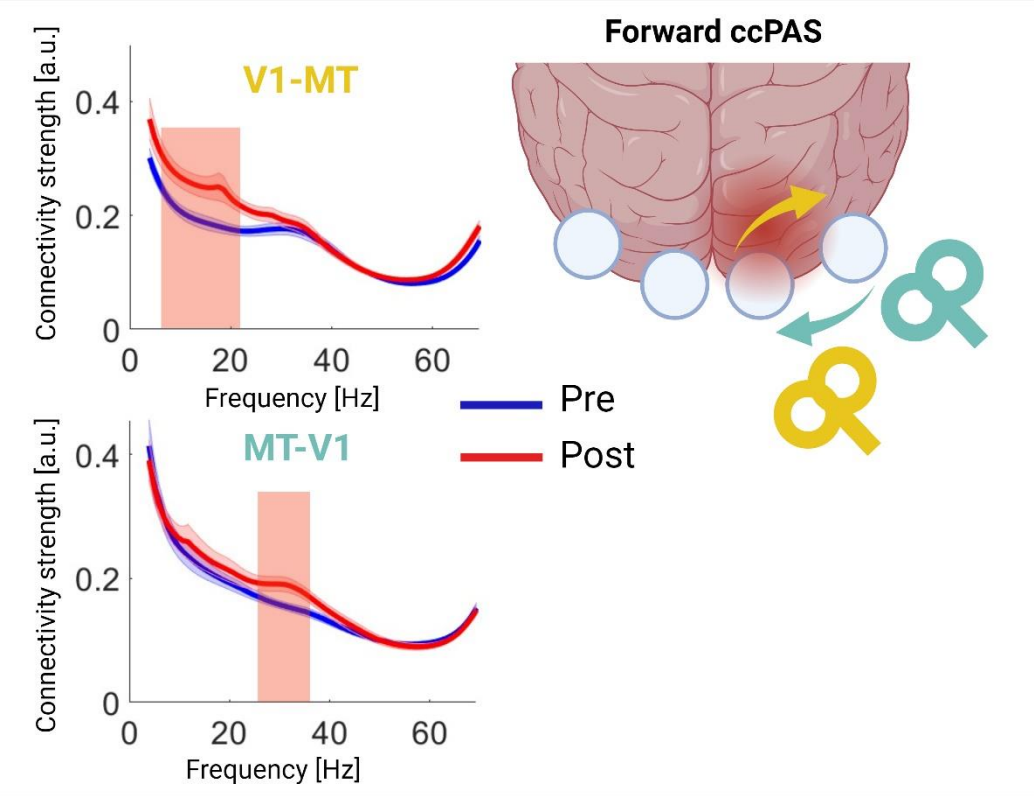

Supplementary Figure S3.3: *Forward ccPAS group-level Spectral Granger Causality of V1-MT network when TMS was given to V1 (in yellow) or to MT (in green). On the left, the significant frequency band for the 2 pathways that showed a significant change in any configuration: significant increase in the alfa/beta (7-21 Hz) band in V1-to-MT after V1 was stimulated with single pulse TMS, significant increase in high beta (27-35 Hz) in MT-to-V1after MT was stimulated with single pulse TMS. Shaded areas indicate periods of significant differences between PRE and POST using non-parametric, cluster-based, permutation tests (10000 permutations, $p<0.05$), excluding frequency-wise outliers (>90th percentile).*

Chapter 4 - Single session cross-frequency bifocal tACS modulates visual motion network activity in young healthy and stroke patients

Michele BEVILACQUA[1,2*], Sarah FEROLDI[1,3*] Fabienne WINDEL[1,2], Pauline MENOUD[1,2], Roberto F. SALAMANCA-GIRON[1,2], Sarah B. ZANDVLIET[1,2], Lisa FLEURY[1,2], Friedhelm C. HUMMEL[1,2,4], Estelle RAFFIN[1,2]

[1] Defitech Chair of Clinical Neuroengineering, Neuro-X Institute (INX), École Polytechnique Fédérale de Lausanne (EPFL), 1202 Geneva, Switzerland.

[2] Defitech Chair of Clinical Neuroengineering, INX, EPFL Valais, Clinique Romande de Réadaptation,1951 Sion, Switzerland.

[3] School of Medicine and Surgery, University of Milano-Bicocca, 20854 Monza, Italy

[4] Clinical Neuroscience, University of Geneva Medical School, Geneva, Switzerland

** contributed equally*

Status: Under review in *Brain Stimulation*

Personal contribution: Patients' data acquisition, patients' EEG data preprocessing, EEG data analysis, results interpretation, writing, and editing of the manuscript.

Keywords: cross-frequency interactions; phase-amplitude coupling; bifocal transcranial alternating current stimulation; motion direction discrimination; visual stroke.

Highlights:

- Single session bifocal Forward-tACS (V1α-MTɣ) increases bottom-up information flow in intact and lesioned brains
- These changes in inter-areal coupling did not translate into meaningful behavioral improvement after one session
- The opposite Backward-tACS condition (V1ɣ-MTα) slightly decreased early bottom-up connectivity in patients while not producing any effect in healthy participants

4.1 Abstract

Objective: This study investigates the impact of single-session, cross-frequency (Alpha-Gamma) bifocal transcranial alternating current stimulation (cf-tACS) to the cortical visual motion network on inter-areal coupling between the primary visual cortex (V1) and the medio-temporal area (MT) and on motion direction discrimination.

Methods: Based on the well-established phase-amplitude coupling (PAC) mechanism driving information processing in the visual system, we designed a novel directionally-tuned cf-tACS protocol. Directionality of information flow was inferred from the area receiving low-frequency tACS (e.g., V1) projecting onto the area receiving high-frequency tACS (e.g., MT), in this case, promoting bottom-up information flow (Forward-tACS). The control condition promoted the opposite top-down connection (from MT to V1, called Backward-tACS), both compared to a Sham-tACS condition. Task performance and EEG activity were recorded from 45 young healthy subjects. An additional cohort of 16 stroke patients with occipital lesions and impairing visual processing was measured to assess the influence of a V1 lesion on the modulation of V1-MT coupling.

Results: The results indicate that Forward cf-tACS successfully modulated bottom-up PAC (V1 $\alpha_{\text{-phase}}$-MT $\gamma_{\text{-amplitude}}$) in both cohorts, while producing opposite effects on the reverse MT-to-V1 connection. Backward-tACS did not change V1-MT PAC in either direction in healthy participants but induced a slight decrease in bottom-up PAC in stroke patients. However, these changes in inter-areal coupling did not translate into cf-tACS-specific behavioural improvements.

Conclusions: Single session cf-tACS can alter inter-areal coupling in intact and lesioned brains but is probably not enough to induce longer-lasting behavioural effects in these cohorts. This might suggest that a longer daily-based visual training protocol paired with tACS is needed in order to unveil the relationship between externally applied oscillatory activity and behaviourally relevant brain processing.

4.2 Introduction

Neural oscillations have been shown to play an essential role in orchestrating communication within and across brain regions. Central to this concept is the interaction between distinct neural oscillations, with a particular focus on the dynamic coupling between the phase of low-frequency oscillations and the amplitude of high-frequency oscillations, known as phase-amplitude coupling (PAC) (Bonnefond and Jensen, 2015; Seymour et al., 2017). This phenomenon is especially evident in the synchronization of alpha (8-13 Hz) and gamma (>40 Hz) oscillations, which has been consistently observed in both human and animal studies (Spaak et al., 2012; van Kerkoerle et al., 2014; von Stein and Sarnthein, 2000; Voytek et al., 2010). This coupling is crucial for facilitating effective neural processing and has important implications for understanding brain motor, sensory, and cognitive function and dysfunction, particularly in stroke patients (Helfrich et al., 2014; Pichiorri et al., 2018).

In the visual system, these oscillatory interactions are fundamental for communication between the primary visual cortex (V1) and the medio-temporal area (MT), encoding motion discrimination (Chey et al., 1998). In this framework, alpha phase has been shown to be critical for motion perception, serving as a temporal reference for encoding features (Han et al., 2023; He et al., 2023; Salamanca-Giron et al., 2021; Varela et al., 1981; Varela et al., 2001). This influence, initially observed locally, has also been identified in broader cortical visual networks (Palva et al., 2010). Animal and human studies have shown that V1 and MT areas are co-activated in a complementary manner, with phase synchronization at lower frequencies temporally driving high-frequency activities (Blakemore and Campbell, 1969; Lamme and Roelfsema, 2000; Newsome and Pare, 1988; Simoncelli and Heeger, 1998). Phase synchronization over long distances underlies inter-areal communication and importantly, modulates the flow of information processing to adjust to cognitive demands. In support of this, phase coherence between different brain areas has been linked to a variety of cognitive and behavioral functions (e.g.,Buschman and Miller, 2007; Colgin et al., 2009; Fries, 2015; Grothe et al., 2012; Salazar et al., 2012). For example, the enhancement of alpha band occipitotemporal coherence improved performance in tasks that require visuotactile integration (Hummel and Gerloff, 2005), the high-alpha band phase synchronization in frontal, parietal, and occipital cortices decreased reaction times in a stimulus discrimination task (Lobier et al., 2018), and the theta coupling between frontal and parietal areas induced faster reaction times during a visual memory matching task (Polanía et al., 2012)

Stroke often disrupts neural pathways, leading to large-scale deficits, for instance, impairing processing of motion information (Guggisberg et al., 2019; Raffin et al., 2020; Rowe et al., 2022). To regain lost brain functions, it is important to develop rehabilitation strategies that restore disconnected inter-areal patterns of communication. Transcranial alternating current stimulation (tACS) emerges as a promising tool in this context. By emitting low-power sinusoidal currents at specific frequencies, tACS can mimic natural brain oscillatory activities, offering a non-invasive method to study and potentially modulate these visual neural processes not only in healthy subjects (He et al., 2023; Salamanca-Giron et al., 2021; Singer, 2018; Thut et al., 2011) but also in stroke patients, presenting a disrupted visual discrimination network. The application of monofocal tACS at alpha or gamma frequencies has shown promise in modulating spatial and motion perception, which are often impaired in stroke patients (He et al., 2023; Helfrich et al., 2014; Kar and Krekelberg, 2014). However, bifocal stimulation has been shown to be an effective tool to increase long-range cortico-cortical connectivity (Vosskuhl et al., 2018), in particular in the context of long-distance cross-frequency interactions in the visual system. Such bifocal modulation has the potential to re-establish effective communication and cross-frequency communication flow between V1 and MT, thus facilitating the recovery of visual functions.

To probe the optimal directionality of rhythmic neural transmission between V1 and MT in optimally functioning brains, we first compared two versions of the bifocal cross-frequency transcranial alternating current stimulation (cf-tACS) protocol in a cohort of young healthy participants undertaking a motion coherence discrimination task. One cf-tACS condition consisted in promoting bottom-up direction of information flow by injecting synchronized V1-alpha signals onto MT-gamma signals. This assumes that low-frequency neural populations project into high frequency populations (Jacques et al., 2022). The other cf-tACS condition rather promoted top-down direction of information flow by injecting synchronized MT-alpha signals onto V1-gamma signals. These two experimental cf-tACS conditions were compared to Sham tACS in another sample of healthy participants.

Furthermore, to assess the neurorehabilitation potential of this approach, we applied these two experimental cf-tACS conditions in a cross-over design, to visual stroke survivors, in whom the bottom-up information flow is necessarily impaired by the lesion involving V1. To summarize, each healthy participant received a single session of sustained electrical flow of personalized alpha and gamma rhythms in one of the two distinct conditions (i.e., Forward cf-

tACS, V1α-MTγ vs. Backward cf-tACS, V1γ-MTα) or sham stimulation to the V1-MT network. Stroke patients received the two single session conditions (i.e., Forward cf-tACS, V1α-MTγ vs. Backward cf-tACS, V1γ-MTα) in a random order, separated by at least one month. Motion discrimination performances and EEG-based V1-MT phase-amplitude coupling (PAC) changes before and after the tACS protocols were compared as a measure of long-distance, cross-frequency neuronal communication. We expected that both active tACS conditions would modulate phase-amplitude coupling in a direction-dependent manner, but that strengthening feedforward information flow from the residual V1 neurons to the higher-level MT area in patients, would more efficiently modulate inter-areal communication and improve motion discrimination. This study can provide a proof of concept that endogenous frequencies can be re-orchestrated through directionally-tuned bifocal cf-tACS over V1 and MT. Furthermore, it might shed light on the oscillatory dynamics underlying visual motion discrimination, highlight potential differences between integer and lesioned brain networks, and finally potentially pave the way towards new interventional strategies to enhance motion discrimination abilities in healthy individuals or boost motion discrimination recovery in patients.

4.3 Methods

Participants

Sixteen stroke patients were enrolled at least one week after stroke-induced occipital damage (verified using structural MRIs), with reliable 24-2 Humphrey Visual Field (HVF) perimetry (<20% fixation losses, false-positive and false-negative errors) in both eyes and ability to fixate precisely (error smaller than ±1 degree relative to fixation spot) during psychophysical testing. Mean time since stroke was 12.5 months (range: 1-60 months). Exclusion criteria were unreliable HVFs, neglect, neurologic disease unrelated to occipital stroke, use of neuroactive drugs, and any contra-indication to MRI or Non-Invasive Brain Stimulation. Seven patients had left-sided homonymous visual field loss and nine right-sided homonymous visual field loss. Mean (SD) age was 59.93 (11.2) years, range (34–74); 18.75% were female, 81.25% male; twelve patients had a homonymous hemianopia and four had homonymous quadranopia. In all patients but one, an etiology of brain injury, as verified by cranial CT and/or MRI, was an infarction in the territory of the posterior cerebral artery causing a lesion to the occipital cortex; one patient had a carotid artery rupture. None of the patients had received any treatment for

their visual field defect. All patients were native French speakers except one German patient and had at least 5 years of education (see Table 4.1 for patients' characteristics and demographics).

ID	AGE (years)	SEX	LESION	LESION SIDE	TIME SINCE STROKE (months)	MMSE
P101	34	f	cort	left	12	27
P102	62	m	cort	right	12	28
P103	74	m	cort	left	60	25
P104	62	m	cort	right	12	27
P105	66	m	cort + subcort	right	30	27
P106	68	m	cort	right	8	29
P107	53	m	cort	left	2	30
P201	69	m	cort + subcort	left	28	25
P202	40	f	cort	left	11	28
P203	59	m	cort	right	4	28
P204	63	m	cort	right	4	29
P205	51	m	cort	left	3	30
P206	56	m	cort	right	11	30
A201	55	m	cort	right	1	29
A203	66	m	cort	left	1.5	29

Table 4.1. *Patients' characteristics and demographics*

Additionally, a total of 45 young healthy participants took part in the study (18 to 40 years old, 25 females), all right-handed with normal or corrected to normal vision. None of them reported cognitive or neurological dysfunction. Written informed consent was obtained from all participants and the study was approved by the local Swiss Ethics Committee (2017-01761) and performed within of the guidelines of the Declaration of Helsinki.

Study design

Patients were randomly allocated into one of the two treatment groups. Group A (n = 8) first received Forward tACS (V1α-MTγ) followed by Backward tACS (V1γ-MTα). Group B (n = 8) did the opposite and received Backward tACS first, followed by Forward tACS in a cross-over

design. The two blocks were performed at least one month apart in order to avoid carry-over effects. Each block started with a familiarization phase, composed of 150 practice trials, followed by the actual experiment. During the familiarization phase, we ensured that the subject understood the visual discrimination task and reached stable performance. After EEG acquisition was prepared, a baseline block ("Pre"), which consisted of a task-related EEG recording without tACS was started. After a few minutes of rest, electrodes were placed over the occipital and temporal cortex, and electrical stimulation was started, remaining on for the entire duration of the block (i.e., approximately 15 minutes for healthy and 25 for patients). Thereafter, the stimulation electrodes were removed and after a few minutes of rest, a post stimulation evaluation ("Post": 10 min after stimulation) was measured using the same task-related EEG setup, without concurring tACS (Figure 4.1A).

Because of the relative ease of recruitment compared to patients, a parallel design was preferred for the healthy cohort, to avoid carry-over effects in this population. They were randomly and evenly (n= 15, n = 15) allocated into one of the experimental tACS conditions described for stroke patients. In addition, results were compared to an additional group on which Sham tACS (n = 15) was applied. Data from the Sham group are already published but were acquired concurrently to the other tACS conditions and in the exact conditions (Salamanca-Giron et al., 2021). The Sham stimulation corresponded to a ramp up and ramp down stimulation lasting in total the equivalent of an individualized Alpha cycle.

This study belongs to a registered trial (ClinicalTrials.gov: NCT05220449). The study was approved by the local Swiss Ethics Committee (2017-01761) and performed within of the guidelines of the Declaration of Helsinki.

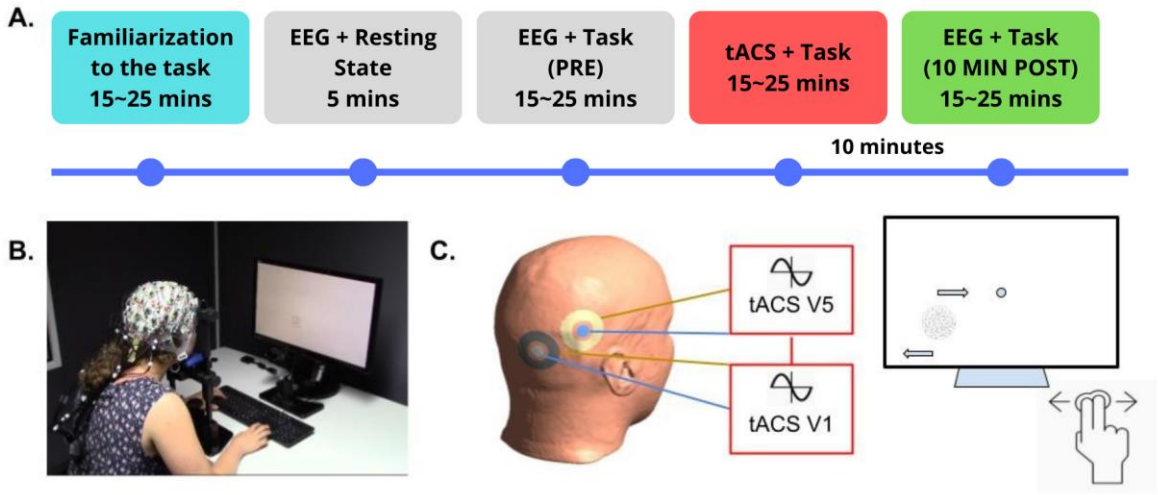

Figure 4.1. A. *Study design consisting of 5 blocks, with approximate duration of each block and waiting time between tACS and POST session.* ***B.*** *Experimental setup showing the EEG headset and the montage for performing the visual task* ***C.*** *Scheme representing the location of the concentric tACS electrodes over PO8 and O2 and an indication of the way the motion takes places in the task.*

tACS Intervention

Electrodes design and electrical stimulation devices: Two customized center-surround electrodes (outer and inner diameters: 5 and 1.5 cm respectively) were connected to two Neuroconn DC Plus stimulators (Neurocare, Germany), which are triggered repetitively and at the same time to ensure no time lag between the two signals.

Electrodes placement: The International 10/20 system was used for the location of V1 (O2 or O1 for the left or right hemisphere respectively) and MT (PO8 or PO7 for the right and left hemisphere respectively) on the lesioned hemisphere. On healthy participants, always the right side (O2 for V1 and PO8 for MT) was considered.

tACS Intensity: A constant current intensity of 3 mA was applied in both stimulators creating a current density of 0.18 mA/cm2.

Frequencies: A priori defined individual α [8-12 Hz] and γ [30-45 Hz] peak frequencies were used to apply tACS. The peak frequencies were extracted from a 5 minutes-resting state EEG prior the intervention.

Stimulation duration: Each tACS session lasted approximately 15 minutes for healthy participants and 25 minutes for patients depending on the individual time to complete the training session, including 150 trials for healthy and 255 trials for patients. The inter-individual variability in the stimulation duration is explained by the fact that participants were told to be as accurate as possible without having any time pressure to complete the task.

Direction discrimination and integration task:

While undergoing tACS, participants engaged in a task designed for coarse direction discrimination and integration (CDDI), where they observed a random dot stimulus. This stimulus, lasting for 500 milliseconds, was displayed within a circular aperture with a 5° diameter on a computer screen (resolution: 1024 x 768 Hz, frame rate: 144 Hz) as shown in Figure 4.1C. The visual presented black dots moving against a mid-grey backdrop. These dots had a lifespan of 250 milliseconds, travelled at a speed of 5 degrees per second, and were spread at a density of 3.5 dots per square degree. The overall motion of the dots was uniformly distributed around either leftward or rightward vectors, creating a range of motion directions (Das et al., 2014; Huxlin et al., 2009a; Salamanca-Giron et al., 2021). Participants were required to identify and report the predominant direction of the dots' movement, either leftward or rightward. To modulate the challenge of the task, a 3:1 staircase method was employed, which varied the range of dot directions from 0° to 360° in increments of 40°.

For the stroke patients participants, the visual stimulus location was individually defined as followed: after Humphrey perimetry, each subject would undergo an extensive psychophysical mapping of the blind field border as previously described (Das et al., 2014; Huxlin et al., 2009a).

All experiments took place inside the same, shielded Faraday cage designed for EEG recordings, and under the same light conditions. Participants' heads were placed over a chin-rest at a distance of 60 cm from the presentation screen, assuring a fixed position across all trials. The task ran on a Windows OS machine, based on a custom Matlab (The MathWorks Inc., USA) script, using the Psychophysics Toolbox. Gaze and pupils' movements were controlled in real time with an EyeLink 1000 Plus Eye Tracking System (SR Research Ltd., Canada) sampling at a frequency of 1000 Hz. The task required the subject to fixate a target at the center of the screen for every trial, with a maximal tolerance for eye deviation from this

fixation target of about 1°. If the participant broke fixation during stimulus presentation, the moving stimulus froze and then disappeared; the trial was discarded, and an auditory tone (at 400 Hz) was presented. Once the participant repositioned their gaze correctly, a novel trial was started.

Direction range threshold:

The performance at the task was fitted using a Weibull psychometric function on single trial data with a threshold criterion of 72% correct to calculate direction range thresholds (where percent correct = 1-(1-chance) * exp(-(k*x/threshold) slope), and k = (-196 log((1-0.72)/(1-chance))) $^{(1/slope)}$.

These direction range thresholds were then normalized to the maximum range of directions in which dots could move (360°) and expressed as a percentage using the following formula: Normalized Direction Range (NDR) threshold (%) = [360° − direction range threshold] / 360° × 100. For ease of analysis, when participants performed at chance (50–60% correct for a given session), the CDDI threshold was set to 100%. Thus, a lower score stands for better performance.

EEG recording and analyses

Resting-state EEG and task-EEG activity (using the CDDI task) was recorded using a 64 channels active system (BrainAmp DC amplifiers and BrainCap EEG cap, Brain Products GmbH, Germany) for stroke patients and using a passive system with 64 electrodes (Brain Products GMBH, Germany) for healthy participants.

The EEG cap set up was done following the 10-20 standard system. Electrode impedances were adjusted and kept under 10 kOhms using conduction gel. The impedance levels were checked throughout the experiment and corrected if needed during breaks between conditions. The signal was recorded using DC mode, filtered at 500 Hz anti-aliasing low-pass filter, and digitalized at 5 kHz sampling frequency. During the experiment, the ground electrode was in Fpz, and the reference electrodes in Cz.

All preprocessing of EEG data was performed on periods without tACS (at Baseline and TP10) using MNE-Python (Gramfort et al., 2013), MATLAB, with the EEGLAB toolbox (Delorme and Makeig, 2004) and customized MATLAB scripts.

For the healthy participants preprocessing, data were re-referenced to the average of signals, filtered through a Finite Response Filter of order 1, between 0.5 and 45 Hz, epoched in 3 s blocks, corresponding to −1.5 s before and +1.5 s after the stimulus onset. Every epoch corresponded to the time interval of a trial from the behavioral task. They were visually inspected to clear up noisy channels or unreadable trials. Bad channels were interpolated, and data was re-sampled to 250 Hz. Independent component analysis was used to remove physiological artifacts (i.e., eyeblinks, muscle torches).

The preprocessing of stroke patients' EEG datasets went through an equivalent pipeline: data were re-referenced to the average of all channels, band-passed filtered between 1 Hz and 80 Hz, notch filtered between 48 and 52 Hz, and divided in epochs of 1.5 s length [-0.5 1 s] around the trial stimulus onset. Visual inspection was used to remove explicit artifacts among channels and trials, followed by the reconstruction of dropped channels and epochs. Ultimately, an Independent Component Analysis was applied to down-sample data (1000 Hz) to remove electrophysiological interferences, such as eyeblinks or muscle artifacts. For both healthy participants and stroke patients, Brainstorm software (Tadel et al., 2011) together with OpenMEEG BEM plugins were used to perform source level reconstruction of EEG data. For stroke patients, first the individual cortex and head mesh (15,000 and 10,000 vertices respectively), based on previously acquired T1 MRI scan, were generated using the automated MRI segmentation routine of FreeSurfer (Fischl, 2012). For healthy participants, instead, a default head model (ICBM152), with cortex and head meshes (15,000 and 10,000 vertices respectively), was assigned to each individual.

For both populations, the forward model was then computed using the symmetric Boundary Element Method developed in the open OpenMEEG freeware, using default values for conductivity and layer thickness (Gramfort et al., 2010). The covariance noise matrix was computed from the concatenated epoch's baselines, e. g. the recorded activity before the onset of each trial [-0.5 -0.005 s]. Source level activation was computed using a minimum norm imaging linear method with sLORETA as the inverse model. The dipole orientation of the source model was defined as unconstrained to the cortex surface. Source orientation was kept orthogonal to the cortical surface and source amplitude was estimated using the default values

of the Brainstorm implementation of the whitened and depth-weighted linear L2-minimum norm solution. All metrics involving a frequency domain decomposition were calculated through Morlet wavelets between 2 and 60 Hz. The source points belonging to specific areas of interest (i.e. V1, MT), were defined manually and ipsilesionally for each stroke patient according to the fMRI localizer recordings performed before the EEG acquisitions (for V1 were 16±9, -86±8, -5±22 and for MT were 66±9, -55±9, -7±17 -coordinates x, y z, MNI space), covering about 200 vertices of cortical mesh for V1 and 200 for MT. For healthy subjects, default ROIs were manually commonly defined on the right hemisphere according to brain atlas (V1: 14.7, -103, -2; MT: 49.3, -74.5, 14.9 - x, y z coordinates in MNI space), covering the same number of vertices as the patients' ones.

In more details, Phase Amplitude coupling (PAC) (Canolty et al., 2006) was obtained through:

$$PAC = n{-}1n\sum t{=}1at\ (f) \cdot ei\theta t \vee$$

Where a corresponds to the amplitude of the instant t among n intervals multiplied by the imaginary component of the phase angle θ. Cross-frequency interactions were computed from the EEG data recorded before and after tACS in phase-amplitude coupling of α-Ɣ between V1 and MT. From a signal processing point of view, directionality arises from the fact that the low frequency Alpha wave that holds the information, must travel and be imposed over the amplitude of the local, high frequency Gamma that turns into the carrier wave (Roder, 1931).

Statistical analyses

To compare the EEG metrics (Phase-Amplitude Coupling and Time-Frequency values) before and after the interventions, we used cluster-based time-wise (in the case of PAC, referring to the maximal PAC for each specific phase and frequency value considered) and time and frequency-wise (in the case of Time-Frequency) non-parametric permutation tests (Alejandro Lage-Castellanos et al., 2009).

To evaluate differences in threshold performance for the CDDI task between interventions and across timepoints ("Pre" – before stimulation, "tACS" – during stimulation, and "Post" – 10 minutes after the intervention), two different Repeated Measures ANOVAs models, one for patients and one for healthy participants, were performed. Timepoint and condition (stimulation type) were considered as parameters for the healthy participants' model, while

timepoint, condition and order, due to the within-subject nature of the paradigm, were considered as parameters for the stroke patients' model. A probability of type I error of $P < 0.05$ was considered statistically significant.

4.4 Results

Changes in PAC in Healthy participants

Electrophysiological analysis on healthy participants (Figure 4.2) revealed an early increase in V1 $\alpha_{\text{-phase}}$-MT $\gamma_{\text{-amp.}}$ PAC between 100-150 ms post stimulus onset for Forward-tACS. The reversed direction, V1 $\gamma_{\text{-amp.}}$-MT $\alpha_{\text{-phase}}$ PAC showed two late time windows of significant decrease around 300 ms and 400 ms post stimulus onset. None of the two PAC was significant for Backward-tACS nor for the Sham condition (Figure 4.2).

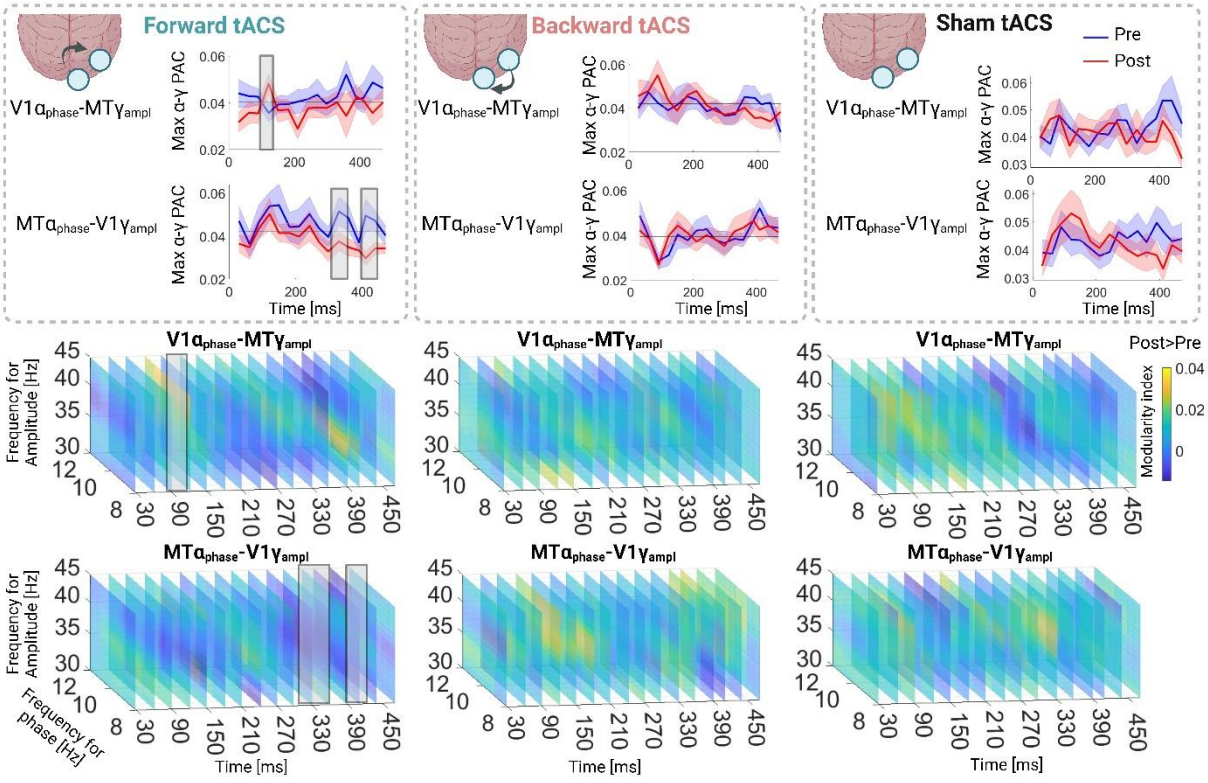

Figure 4.2: *Healthy participants cohort's maximal Phase-Amplitude Coupling (PAC) between $V1\alpha_{\text{-phase}}$-$MT\gamma_{\text{-amplitude}}$ and the opposite $V1\gamma_{\text{-amplitude}}$-$MT\alpha_{\text{-phase}}$ for the three tACS group (upper row) and the associated comodulograms (bottom row). Significant differences in the PAC time-windows are indicated with grey rectangles.*

Changes in PAC in stroke patients

As done in the previous paragraph for healthy participants, we compared the maximal PAC values in the time domain during motion processing before and after Forward-tACS and Backward-tACS (Figure 4.3 upper panels, the associated comodulograms are provided on the bottom panels).

Similar to the healthy cohort, this analysis revealed an early increase in V1 $\alpha_{\text{-phase}}$-MT $\gamma_{\text{-amp.}}$ PAC around 100ms post stimulus onset for Forward-tACS. This was followed by a significant decrease around 250 ms and 350 ms post stimulus onset. The reversed direction, V1 $\gamma_{\text{-amp.}}$-MT $\alpha_{\text{-phase}}$ PAC, showed in this case a very early increase of coupling strength (40-70 ms post stimulus onset). For what concerns Backward-tACS condition, contrariwise to what observed in healthy participants, V1 $\alpha_{\text{-phase}}$-MT $\gamma_{\text{-amp.}}$ PAC revealed an opposite behavior in the early moments after the trial stimulus onset compared to the Forward tACS condition, showing a decrease at around 100 ms after the stimulus onset. The reversed direction showed no changes in this condition.

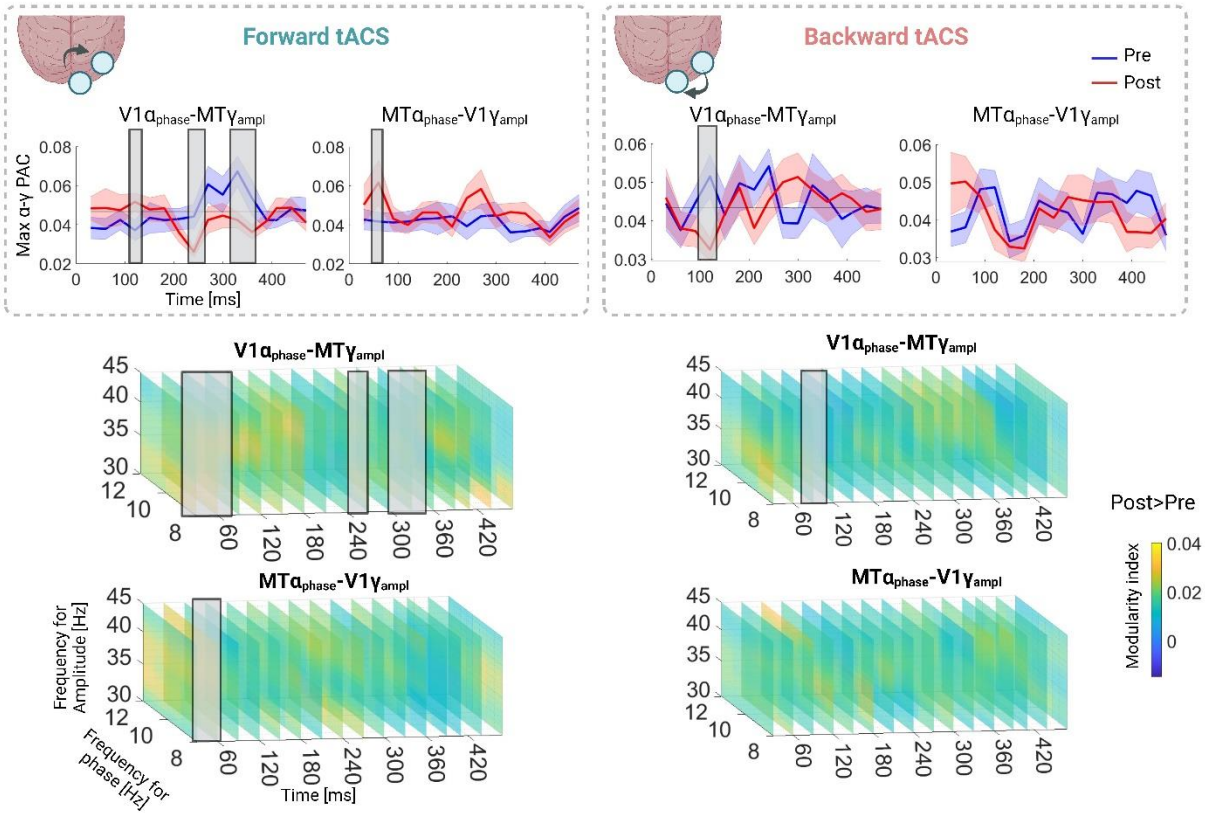

Figure 4.3: *Stroke patients' cohort Maximal Phase-Amplitude Coupling (PAC) between V1α-phase-MTγ-amplitude and the opposite V1γ-amplitude-MTα-phase for the two tACS group (upper row) and the associated comodulograms (bottom row). Significant differences in the PAC time-windows are indicated with grey rectangles.*

Changes in motion discrimination

Figure 4.4 shows the baseline corrected NDR values across timepoints relative to the healthy participants (left panel) and the stroke patients (right panel). The mixed model ANOVA showed a main effect of Time ($F_{(2,24)}$=10.958, p<0.001), but no tACS condition effect ($F_{(2,24)}$=2.694, p=0.088) nor Time by tACS condition interaction ($F_{(4,48)}$=1.314, p=0.278). Baseline values were not different in the three healthy groups (V1α-MTɣ vs V1ɣ-MTα: t = 1.475, p = 0.160, p cor = 1.0, V1α-MTɣ vs Sham: t = 1.225, p = 0.232, p cor = 1.0, V1ɣ-MTα vs Sham: t = -0.057, p = 0.954, p cor = 1.0). For the stroke cohort, the repeated measures ANOVA showed no main effect of Time ($F_{(2,30)}$=1.11, p=0.34), nor tACS condition effect

($F(_{1,15})$=2.9e-4, p=0.98) or Time by tACS condition interaction ($F(_{2,30})$=0.415, p=0.66). Again, baseline performance was similar (t(15) = 1.67, p = 0.12).

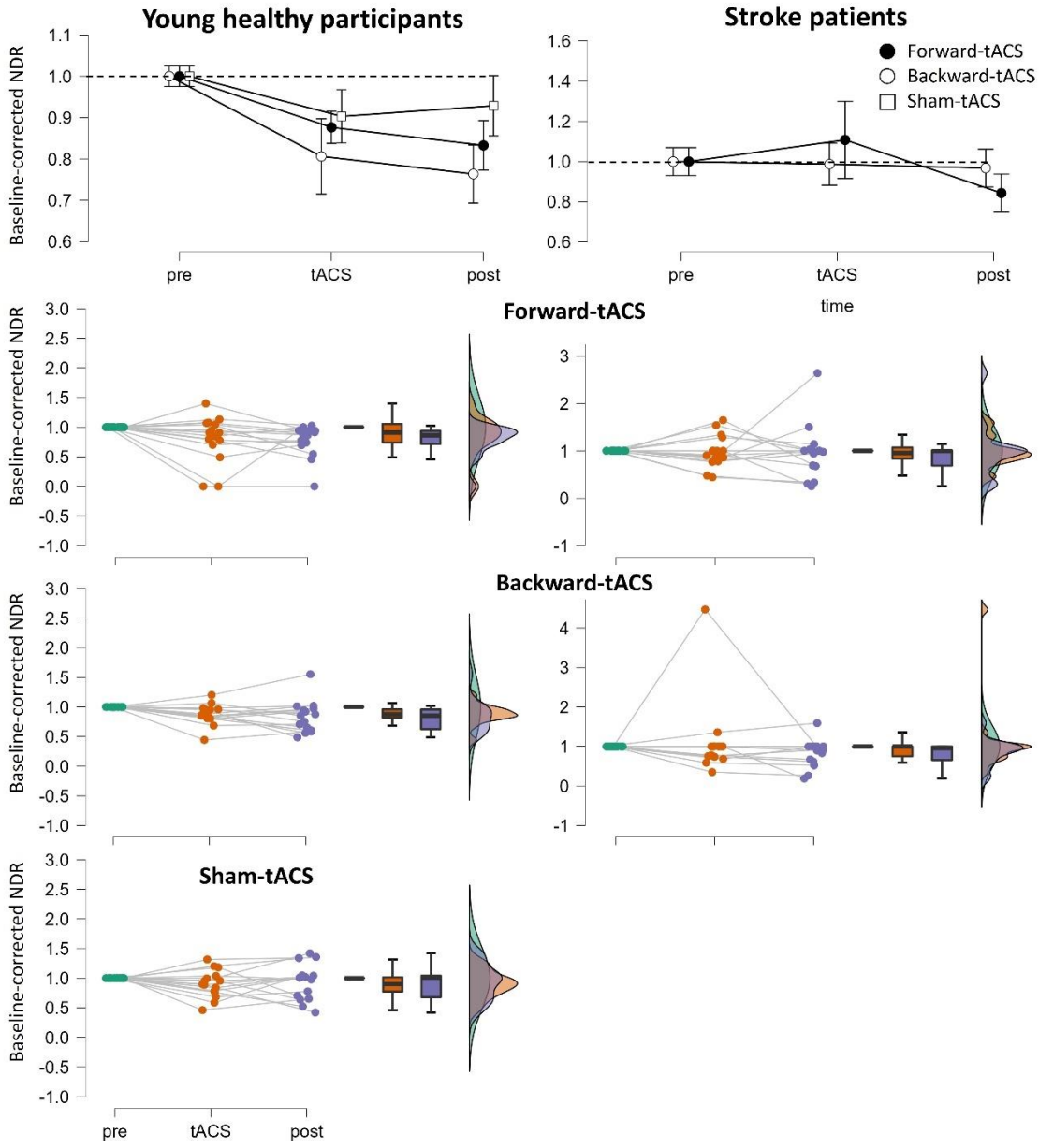

Figure 4.4: *Averaged evolution of the baseline-corrected NDR across all time points for the young healthy cohort (upper left panel) and for the stroke cohort (upper right panel). Individual data for the different tACS condition and time points are shown below.*

4.5 Discussion

The current study examined the effects of bifocal cross frequency (i.e., V1α-MTɣ vs. V1ɣ-MTα) single session tACS applied to two different cohorts, young healthy (compared to a Sham-tACScondition) and occipital stroke patients, undertaking a visual motion discrimination and integration task. Our primary objective focused on the possibility to alter inter-areal cross-frequency coupling between V1 and MT 10 minutes after the stimulation period, in the two different cohorts. The oscillatory activity along the V1-MT pathway at the source level was analysed through phase-amplitude coupling (PAC). A second objective was to gather information about potential similarities or differences in oscillatory re-orchestration in healthy optimally functioning visual networks versus networks disrupted by a lesion affecting V1. Finally, we aimed to determine if any of these exogenous non-invasive modulations of neural oscillatory activity could affect behavioral performance at a motion coherence discrimination visual task.

The main results were threefold: 1) a single session of bifocal cross-frequency Forward tACS (V1α-MTɣ) proved to have the potential to modulate inter-areal synchronization both in healthy and in stroke patients; 2) Forward tACS seemed to increase bottom-up PAC (i.e., V1 $\alpha_{\text{-phase}}$-MT $\gamma_{\text{-amp.}}$) in early latencies in both patients and healthy participants, which cannot be sustained in patients, with a significant decrease in the late time window of motion processing. In parallel, healthy participants show an associated decrease in the opposite direction (top-down MT-to-V1 pathway) while patients show a non-specific increase in the top-down connectivity as well; 3) the induced electrophysiological changes did not translate into a significant group-level behavioural difference in any of the cohorts.

Our data show an early increase in bottom-up V1 $\alpha_{\text{-phase}}$-MT $\gamma_{\text{-amp.}}$ coupling induced by Forward-tACS, occurring about 100ms post stimulus appearance. This timing corresponds to the first feedforward inputs reaching V1, suggesting that in both cohorts, the early feedforward synchronization to MT got promoted by the intervention. The same communication channel in patients became significantly down-regulated in the second half of motion processing. This can be due to several reasons, including, the incapacity of the residual V1 neurons to sustain such enhanced processing. It can also be explained by an over-exaggerated homeostatic response of these same residual V1 neurons, probably functioning sub-optimally, in the aim of preventing the lesioned system to saturate (Chacko et al., 2018).

In addition, the opposite direction of PAC, MT $\alpha_{\text{-phase}}$-V1 $\gamma_{\text{-amp}}$, was associated with a decrease in the late latencies for the healthy cohort. This finding could reflect an optimal visual processing from an intact visual system, where phasic late decoupling in the information flowing through the feedback pathway allows other functional feedback pathways to synchronize. Patients instead, showed a non-direction specific effect as seen in the early increase in the opposite direction. This opposite effect could represent an initial plastic functional reorganization of the perilesional areas, in which, in absence of optimally functional feedforward connectivity, spared higher order visual area initially drive the information flow through the feedback pathway. Of note, Backward-tACS and Sham tACS in healthy participants did not result in any change in PAC. In contrast, Backward-tACS led to a brief decrease in bottom-up V1 $\alpha_{\text{-phase}}$-MT $\gamma_{\text{-amp.}}$ coupling around 100ms post stimulus.

Although slightly different between the two groups, these results overall suggest that bifocal cf-tACS applied to the cortical motion discrimination pathway can modulate inter-areal communication. Several human, animal and computational modeling studies have reported the causal relation between alpha-modulated gamma oscillations and the probability of neurons to respond to specific stimuli, not only in the visual domain (Bahramisharif et al., 2013; Bonnefond and Jensen, 2015; Osipova et al., 2008; Palva et al., 2011; van Kerkoerle et al., 2014) but also in perception and sensory processing network (Palva and Palva, 2011, 2007; Siebenhühner et al., 2016) and in the language network (Wang et al., 2012).

The general mechanism underlying inter-areal alpha-gamma coupling in a network as a way to synchronize selective neural activity and prioritize information gating has been well conceptualized by Bonnefond et al. (2017). According to this concept, when neurons from different nodes of the same network are engaged in information transfer, they exhibit synchronized oscillation in the alpha frequency band, accompanied by a reduction in alpha power. This reduction in alpha power leads to extended periods of neuronal excitability within each cycle, increasing the duty-cycles (Jensen and Mazaheri, 2010). This corresponds to the time window in which gamma activity of the nodes can synchronize to increase information exchange (Gielen et al., 2010). Specifically, gamma oscillations will be integrated within these alpha oscillations, meaning they will primarily occur during the alpha oscillations' excitability phase, the cycle’s through. Since the excitability phases of the alpha oscillations are synchronized, gamma activity originating in one node can significantly influence neuronal activity in remote nodes. The rapid activity coupling is expected to profoundly affect the

receiver region's activity due to the synaptic accumulation within the gamma cycle's timeframe (Salinas and Sejnowski, 2001).

According to this concept, the magnitude of the interplay between the alpha oscillation phase and the intensity of gamma oscillations, measured in our study through inter-areal alpha-gamma PAC, could represent the temporal synchronization of information transfer across V1 and MT and by consequence reflect the network's potential to enhance visual motion discrimination ability. However, our findings showed that the causal manipulation of phase synchrony between V1 and MT reported above, did not translate into significant group-level difference between tACS conditions. While healthy participants showed a significant improvement with task repetition, it was regardless of the tACS condition. In contrast, there was no significant effect of time nor tACS condition in the patients' group. In patients, the absence of overall improvement after a few task repetitions only has been reported elsewhere (Herpich et al., 2019; Huxlin et al., 2009b). It could be due to stroke-related or age-related impaired visual processing. Furthermore, visual re-learning studies suggest that patients might require several dozens of practice sessions before showing some improvements in motion direction discrimination in their blind field (Cavanaugh et al., 2017; Huxlin et al., 2009b). A protocol involving multiple sessions of cf-tACS paired with motion discrimination visual training over weeks/months might be needed in order to observe relevant improvement at the behavioural level.

Finally, the absence of difference between tACS conditions in the two cohorts might point towards more complex relationships between externally applied oscillatory activity and its interaction with behaviorally relevant brain processing. One may argue that the continuous application of cross-frequency tACS (i.e. during the entire visual task) may prevent the optimal synaptic asymmetries between V1 and MT to happen (Anderson et al., 1998; Rockland, 2015). Consequently, future development of the present approach could be to adapt the tACS dosage and timing either to the online state of the brain, towards individualized closed loop applications (Raffin et al., 2020) or to precisely time lock the bursts of cross-frequency tACS to the visual stimulus (e.g., Stonkus et al., 2016). Further experiments systematically varying the timing and dose of cross-frequency tACS potentially towards closed-loop applications might be required to better adjust the externally provided oscillatory activity to the ongoing, endogenous oscillatory activity to effectively modulate motion discrimination.

4.6 Conclusion

This study showed that a single session of bifocal cross-frequency tACS can modulate inter-areal synchronization in both healthy individuals and stroke patients. Specifically, Forward tACS (V1α-MTγ) induced changes in early bottom-up coupling in both cohorts. Despite these electrophysiological changes, no significant behavioral improvements were noted in motion discrimination tasks. This result might point towards two possible explanations: 1) The need for longer-term interventions in healthy participants and in particular in patients; 2) The more complex interaction between externally applied oscillatory activity and behaviourally relevant brain processing, which warrants future research to focus on adjusting tACS dosage and timing to align with the brain's ongoing oscillatory activity. This can be done through state-dependent or closed-loop applications to efficiently enhance motion discrimination abilities.

Competing interests

The authors declare that they have no competing interests.

Funding

Funding was obtained from the Defitech Foundation (to FCH), Bertarelli Foundation (Catalyst BC77O7 to FCH & ER), by the Swiss National Science Foundation (PRIMA PR00P3_179867 to ER)

Acknowledgements

We would like to thank the EEG and neuromodulation facilities of the Human Neuroscience Platform of the Foundation Campus Biotech Geneva, for technical advice.

Chapter 5 - Re-orchestrating cross-frequency visual oscillatory activity to enhance visual training efficacy in occipital stroke patients

Estelle RAFFIN[1,2*], Michele BEVILACQUA[1,2*], Fabienne WINDEL[1,2], Pauline MENOUD[1,2], Roberto F. SALAMANCA-GIRON[1,2], Sarah FEROLDI[1,3] Sarah B. ZANDVLIET[1,2], Nicola RAMDASS[1], Laurijn DRAAISMA[1,2], Patrik VUILLEUMIER[4], Adrian G. GUGGISBERG[5,6], Christophe BONVIN[7], Lisa FLEURY[1,2], Krystel R. HUXLIN[8], Elena BENEATO[1,2], Friedhelm C. HUMMEL[1,2,9]

[1], Swiss Federal Institute of Technology (EPFL), Geneva, Switzerland

[2], Swiss Federal Institute of Technology (EPFL Valais), Sion, Switzerland

[3], School of Medicine and Surgery, University of Milano-Bicocca, Monza, Italy

[4], Laboratory of Neurology and Imaging of Cognition, Department of Fundamental Neurosciences, University Geneva, Geneva, Switzerland

[6], Department of Neurology, University Hospital of Berne, Inselspital, Berne, Switzerland

[7], Stroke Unit Valais, Hôpital du Valais, Sion, Switzerland

[8], The Flaum Eye Institute and Center for Visual Science, University of Rochester, Rochester, NY, USA

[9], Department of Clinical Neuroscience, University of Geneva Medical School, Geneva, Switzerland

** contributed equally*

Status: In preparation for submission

Personal contribution: Data acquisition, EEG data analysis, results interpretation, writing of sections related to EEG results and editing of the manuscript.

Keywords: visual recovery; cross-frequency interactions; interareal synchronization; bifocal transcranial alternating current stimulation; motion direction discrimination.

Highlights:

- Synchronized ipsilesional Alpha tACS(V1) and Gamma tACS(MT) re-orchestrate oscillatory interactions and improve motion discrimination of stroke patients.
- The cross-frequency tACS intervention induces a localized extension of visual field borders.
- Motion discrimination improvements scale with initial perilesional V1 reactivity and residual structural fibers between the ipsilesional V1 and MT.

5.1 Abstract

Visual field loss is a common consequence of stroke and manifests in approximatively one third of patients in the chronic stage. Such loss can significantly impact daily life activities, compromising tasks like reading, navigating surroundings, or driving. Despite the absence of established therapy, sparse evidence suggest that early intervention and tailored rehabilitation programs may play a pivotal role in maximizing visual recovery and improving quality of life in stroke survivors. To enhance the effects of such rehabilitation programs, we designed a novel non-invasive, orchestrated, pathway-specific, physiology-inspired cross-frequency brain stimulation paradigm, where complex oscillatory signal integration was inferred from phase-amplitude coupling (PAC) of oscillatory signals between the primary visual cortex (V1) and the motion-sensitive medio-temporal area (MT). Sixteen stroke patients were enrolled in a double-blinded randomized cross-over trial during which they performed two blocks of ten daily training sessions of a direction discrimination task training, combined with one of the two cross-frequency transcranial alternative brain stimulation (cf-tACS vs. control cf-tACS) conditions. We found that the cf-tACS condition promoting feedforward visual inputs to MT significantly enhanced motion discrimination and visual field borders (i.e., through localized enlargement of isopters). Behavioral improvements were associated with a change in oscillatory activity within the motion processing pathway were proportional to the amount of residual structural fibers along the pathway and perilesional V1 activity. This novel non-invasive orchestrated pathway-specific physiology-inspired brain stimulation approach applied for the first time opens new perspectives to reduce the severity of visual impairments in stroke patients.

5.2 Introduction

Visual field loss manifests in about one-third of stroke patients (Hepworth et al., 2015; Rowe et al., 2013). Among the various forms of visual field defects, homonymous hemianopia (HH) is the most common form. It involves the loss of vision in the same half of the visual field for both eyes after unilateral retrochiasmal lesions (i.e. lesions of the optic tract, the lateral geniculate nucleus, the optic radiations, and/or the occipital cortex) (Liu et al., 2001). Visual field deficits are associated with a myriad of functional impairments in i.e., reading, navigating, or driving a car (Peli et al., 2016; Ungewiss et al., 2018), which significantly alter the quality of life in patients (Chen et al., 2009; Papageorgiou et al., 2007). Despite the increasing demand arising from an aging population, there is currently no accepted therapeutic approach for this condition. The main clinical options are of compensatory nature rather than restorative, implying that they do not induce any significant reversal or restitution of visual deficits induced by the stroke (Bowers et al., 2014; O'Neill et al., 2011; Sahraie et al., 2020).

One main factor that contributes to the lack of established treatment for HH comes from early descriptive studies that show limited spontaneous recovery in the early-stage post stroke, with stabilization of visual field deficits after 6 months post-stroke (And and Kolmel, 1991; Gray et al., 1989). This led to the postulate that the visual system had poor capacities of functional recovery, especially in the chronic phase after stroke (i.e., > 6 months). However, there is encouraging evidence to indicate that very intensive visual-attentional training paradigms presented within the parametrically defined scotoma or blind field might lead to localized improvements in vision (Cavanaugh et al., 2015; Cavanaugh and Huxlin, 2017; Huxlin et al., 2009a; Raninen et al., 2007; Sahraie et al., 2006; Saionz et al., 2020). Nevertheless, these protocols typically require months of training with intensive patient commitment and they seem to provide only a moderate amount of improvement that is transferable to everyday life (Cavanaugh et al., 2015; Das et al., 2014; Huxlin et al., 2009a; Melnick et al., 2016). Targeted interventions inspired from circuit-level synchronization of neuronal oscillations within the visual pathways might enhance visual training effects and recovery after stroke.

A strong dynamic coupling between alpha phase (8–13 Hz) and gamma amplitude (>40 Hz) has been consistently reported in the visual cortex of cats, monkeys (Stein et al., 2000; van Kerkoerle et al., 2014) and humans (Bonnefond and Jensen, 2015; Spaak et al., 2012; Voytek et al., 2010). Precisely, these studies have documented temporally segmented ongoing gamma-band activity, synchronized with distinct phases of alpha-band activity. This synchronization

mode represents a very efficient communication machinery in the visual system: High-frequency activity, mediating local excitatory-inhibitory interactions (Buzsáki and Wang, 2012; Singer and Gray, 1995), is coupled with long-range patterns of low-frequency phase synchrony, reflecting pulses of cortical inhibition (Bonnefond et al., 2017). Inspired by physiology, we designed a non-invasive pathway-specific cross-frequency brain stimulation paradigm, where directionality of information flow is inferred from the low frequency neuronal population projecting to the high-frequency population. Hence, artificial, noninvasive injection of synchronized alpha signals in the primary visual cortex (V1) onto gamma signals in the motion-sensitive medio-temporal area (MT) (Nandi et al., 2019) by means of cross-frequency transcranial alternating current stimulation (cf-tACS), provides an experimental condition that can promote bottom-up direction of information flow. Combined with an established visual re-training protocol based on the presentation of moving dots in the border area of the scotoma (Das et al., 2014; Huxlin et al., 2009a; Saionz et al., 2020), we expect that strengthening specific coordinated oscillatory motifs that are disturbed by the stroke lesion will reinstate more physiological interareal interactions with a respective improvement of motion direction perception in the visual field border area. This approach should translate into improved luminance detection in this specific location. A unique multimodal dataset that included EEG recordings, functional and structural MRI, behavioral and visual field tests was acquired to decipher the underlying mechanisms of pathway-specific cross-frequency tACS for visual field recovery, with a special focus on the integrity and efficiency of the V1-MT pathway.

5.3 Methods

Patients

Sixteen adult patients were enrolled at least one week after stroke-induced occipital damage (verified using structural MRIs), with reliable 24-2 Humphrey Visual Field (HVF) perimetry (<20% fixation losses, false-positive and false-negative errors) in both eyes and ability to fixate precisely (error smaller than ±1 degree relative to fixation spot) during psychophysical testing. Mean time since stroke was 12.5 months (range: 1-60 months). Exclusion criteria were unreliable HVFs, neglect, neurologic disease unrelated to occipital stroke, use of neuroactive drugs, and any contra-indication to MRI or Non-Invasive Brain Stimulation. Seven patients had left-sided homonymous visual field loss and nine right-sided homonymous visual field

loss. Mean (SD) age was 59.93 (11.2) years, range (34–74); 18.75% were female, 81.25% male; Twelve patients had a homonymous hemianopia and four had homonymous quadranopia. In all patients but one, an etiology of brain injury, as verified by cranial CT and/or MRI, was an infarction in the territory of the posterior cerebral artery causing a lesion to the occipital cortex; one patient had a carotid artery rupture. None of the patients had received any treatment for their visual field defect. All patients were native French speakers except one German patient and had at least 5 years of education (see Table 5.1 for patients' characteristics and demographics).

ID	AGE (years)	SEX	LESION	LESION SIDE	TIME SINCE STROKE (months)	MMSE
P101	34	f	cort	left	12	27
P102	62	m	cort	right	12	28
P103	74	m	cort	left	60	25
P104	62	m	cort	right	12	27
P105	66	m	cort + subcort	right	30	27
P106	68	m	cort	right	8	29
P107	53	m	cort	left	2	30
P201	69	m	cort + subcort	left	28	25
P202	40	f	cort	left	11	28
P203	59	m	cort	right	4	28
P204	63	m	cort	right	4	29
P205	51	m	cort	left	3	30
P206	56	m	cort	right	11	30
A201	55	m	cort	right	1	29
A203	66	m	cort	left	1.5	29

Table 5.1. *Patients' characteristics and demographics*

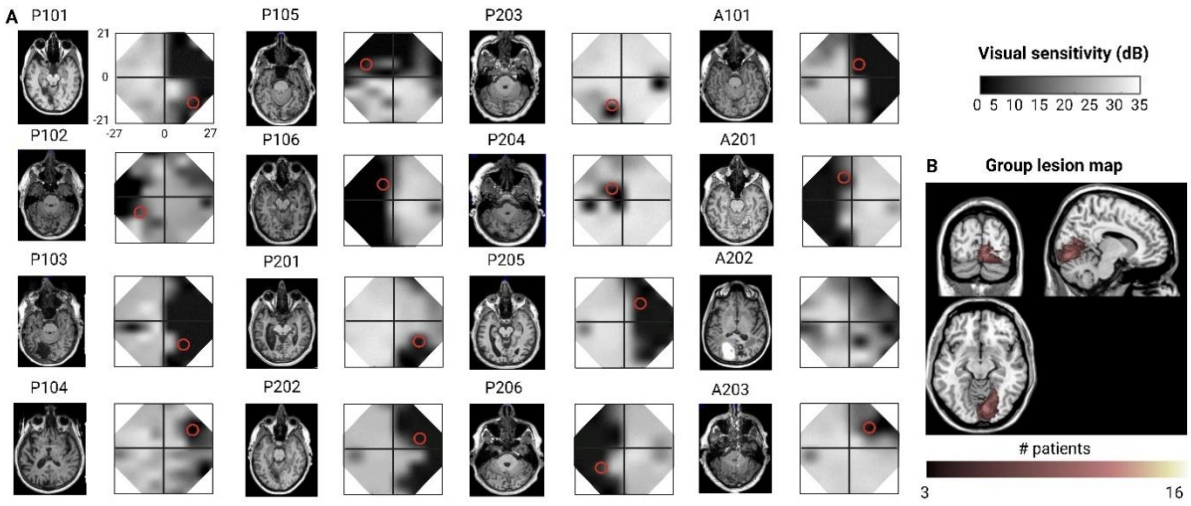

Figure 5.1A: *Visual field maps derived from Humphrey perimetry showing the initial loss of conscious luminance detection sensitivity and T1 MPRAGE images of all individual patients. The red circle on the visual field maps indicates the location of the visual stimuli used for training.* ***B:*** *Lesion overlay maps mirrored to the right hemisphere when needed.*

Study design

Sixteen patients were randomly allocated into one of the two treatment groups. Group A first received Forward tACS (n = 8) followed by Backward tACS. Group B (n = 8) did the opposite and received Backward tACS first followed by Forward tACS in a cross-over design (Figure 5.3). Each block consisted in ten consecutive sessions (excluding weekends) of Backward or Forward tACS over 15 days concurrently applied to a coarse direction discrimination and integration (CDDI) task. The two blocks were performed at least one month apart. Before and after each block, patients performed a 24-2 HVF perimetry test, clinical scales, EEG and MRI recordings. This study belongs to a registered trial (ClinicalTrials.gov: NCT05220449). The study was approved by the local Swiss Ethics Committee (2017-01761) and performed within of the guidelines of the Declaration of Helsinki.

Backward and Forward tACS

Electrodes design and electrical stimulation devices: Two customized center-surround electrodes (outer and inner diameters: 5 and 1.5 cm respectively) were connected to two

Neuroconn DC Plus stimulators (Neurocare, Germany), which are triggered repetitively and at the same time to ensure no time lag between the two signals.

Electrodes placement: The International 10/20 system was used for the location of V1 (O2 or O1 for the left or right hemisphere respectively) and MT (PO8 or PO7 for the right and left hemisphere respectively) on the lesioned hemisphere.

tACS Intensity: A constant current intensity of 3 mA was applied in both stimulators creating a current density of 0.18 mA/cm2.

Frequencies: A priori defined individual α [8-12 Hz] and γ [30-45 Hz] peak frequencies were used to apply tACS. The peak frequencies were extracted from a 5 minutes-resting state EEG prior the intervention. Forward tACS refers to V1α-MTγ tACS and Backward tACS corresponds to V1γ-MTα tACS (Figure 5.4A).

Stimulation duration: Each tACS session lasted approximately 30 min depending on the individual time to complete the 255 trials of a training session and was administered at the same hour every day except on weekends.

Training task

During tACS, patients were practicing a coarse direction discrimination and integration (CDDI) task involving a random dot stimulus appearing for 500 ms in a 5° diameter circular aperture displayed on a computer screen (1024 x 768 Hz at 144 Hz frame rate) (Figure 5.2B). The stimulus consisted of black dots moving on a mid-grey background (dot lifetime: 250 ms, speed: 5 deg/s, density: 3.5 dots/deg^2). Dots moved globally in a range of directions distributed uniformly around the leftward or rightward vectors (Huxlin et al., 2009a; Das et al., 2014; Salamanca-Giron et al., 2021). Participants had to respond whether the global direction of motion was left- or rightward. Task difficulty was adjusted using a 3:1 staircase, increasing dot direction range from 0° to 360° in 40° steps. Training sessions consisted of 255 trials. The visual stimulus location was individually defined as followed: After Humphrey perimetry, each subject would undergo an extensive psychophysical mapping of the blind field border as previously described (Huxlin et al., 2009a) (Das et al., 2014). Training location was selected as the location where performances on the CDDI task declined to chance level (50–60% correct) (Figure 5.1). The training sessions were performed inside a shielded EEG room equipped with a Windows machine running Matlab (Mathworks Inc., USA) and Psychtoolbox,

an EyeLink 1000 Plus Eye Tracking System (SR Research Ltd., Canada) and a chin rest. All individuals sat at 60 cm from the computer's screen supporting their heads with the chin rest, while all the trials were controlled with the eye tracker system. If the gaze fixation was lost for more than 1°, the trial was discarded and replaced, until the person would re center his eyes at the fixation dot.

Direction range threshold

Daily performance at the task was fitted using a Weibull psychometric function on single trial data with a threshold criterion of 72% correct to calculate direction range thresholds (where percent correct = 1-(1-chance) * exp(-(k*x/threshold) slope), and k = (-196 log((1-0.72)/(1-chance))) $^{(1/slope)}$. Figure 5.2B shows the quality of the fits for Training 1 and Training 10 of an example subject.

These direction range thresholds were then normalized to the maximum range of directions in which dots could move (360°), and expressed as a percentage using the following formula: Normalized Direction Range (NDR) threshold (%) = [360° − direction range threshold] / 360° × 100. For ease of analysis, when participants performed at chance (50–60% correct for a given session), the CDDI threshold was set to 100%.

Perimetric mapping of visual field defects

Perimetry was conducted using a Humphrey Field Analyzer II-i750 (Zeiss Humphrey Systems, Carl Zeiss Meditec) and MonCvONE-SAP (Metrovision) collected by a scientist, blinded to each participant's group allocation. The static 30-2 testing patterns were collected for each eye, repeated twice with a break in between. Sensitivity thresholds are determined at a specified number of test locations. To refine scotomas' boundaries, we performed kinetic perimetry, twice on each eye as well. With kinetic perimetry, sensitivity thresholds are determined by moving stimuli of various size and light intensities along a vector from a blind region to a seen region. These measures concentric constriction of the isopter. Measurements were performed either at the Centre Medico-Universitaire (CMU) in Geneva or at the Clinique Romande de Réadaptation in Sion, by the same operators, with fixation controlled using the system's eye

tracker and gaze/blind spot automated controls, visual acuity corrected to 20/20, a white size III stimulus, and a background luminance of 11.3 cd/m2.

Luminance detection thresholds obtained from the four static test patterns were averaged from locations identical in the two eyes to produce a unique visual map and interpolated in MATLAB (Mathworks) to create one composite static visual field map for each patient, as previously described (Cavanaugh and Huxlin, 2017). In brief, natural-neighbour interpolation with 0.1 deg^2 resolution was applied between non-overlapping test points across the four tests, creating composite visual fields of 121 tested locations and 161 398 interpolated datapoints, subtending an area of 1616 deg^2. For the kinetic perimetry, stopping radial positions for each meridian were averaged and displayed on a polar plot. To determine changes induced by the two interventions, difference maps were generated; significant areas that improved on the static perimetry were defined as visual field locations that differed by at least 6 dB (conservative standard of change at twice the measurement error of the Humphrey test (Zeiss Humphrey Systems, Carl Zeiss Meditec) (Cavanaugh and Huxlin, 2017). For the kinetic perimetry, a minimum increase of 10° localized offset compared with the normal isopter is considered as significant (Ma et al., 2021).

EEG recording and analyses

Resting-state EEG and task-EEG activity (using the CDDI task) was recorded before the first session and after the last training session of each block using a 64 channels TMS compatible active system (BrainAmp DC amplifiers and BrainCap EEG cap, Brain Products GmbH, Germany). The EEG cap set up was done following the 10-20 standard system. Electrode impedances were adjusted and kept under 10 kOhms using conduction gel. The impedance levels were checked throughout the experiment and corrected if needed during breaks between conditions. The signal was recorded using DC mode, filtered at 500 Hz anti-aliasing low-pass filter and digitalized at 5 kHz sampling frequency. During the experiment, the ground electrode was in Fpz, and reference electrode in Cz.

All the preprocessing steps have been run on MATLAB, using the EEGLAB toolbox (Delorme and Makeig, 2004). The preprocessing of all EEG datasets went through the same pipeline: data was re-referenced to the average of all channels, band-passed filtered between 1 Hz and 80 Hz, notch filtered between 48 and 52 Hz, and divided in epochs of 1.5 s length. Visual

inspection was used to remove explicit artifacts among channels and trials, followed by the reconstruction of dropped channels and epochs. Ultimately, an Independent Component Analysis was applied to down-sample data (1000 Hz) to remove electrophysiological interferences, such as eyeblinks or muscle artifacts. Brainstorm software (Tadel et al., 2011) together with OpenMEEG BEM plugins were used to perform source level reconstruction of EEG data. First, the cortex and head mesh (15,000 and 10,000 vertices respectively) of the patient were generated using the automated MRI segmentation routine of FreeSurfer (Reuter et al., 2012). The forward model was then computed using the symmetric Boundary Element Method developed in the open OpenMEEG freeware, using default values for conductivity and layer thickness (Gramfort et al., 2010). The covariance matrix was computed from the concatenated epoch's baselines, e. g. the recorded activity before the onset of each trial [-0.5 -0.005] s. All metrics involving a frequency domain decomposition were calculated through Morlet wavelets between 2 and 60 Hz. The source points belonging to specific areas of interest (i.e. V1, MT, IPS, FEF), were defined manually for each subject according to the fMRI localizer recordings performed before the EEG acquisitions.

We first examined the time-frequency content of the V1-MT pathway during the CDDI task at the source level. Since our tACS interventions were based on V1-MT phase amplitude relationship, we computed the two directions of sources-based Phase-Amplitude coupling (Canolty et al., 2006) between V1 and MT (i.e., α_{phase} V1-γ_{amp} MT and γ_{amp} V1-α_{phase} MT). Phase-amplitude coupling was computed using the spectral source activity with phase data frequency ranging from 8 to 12 Hz and amplitude data ranging from 30 to 45 Hz by means of the EEGLAB plug-in Event Related PACTools (PACTools) (Martinez-Cancino et al., 2019). In a more explorative perspective, we computed spectrally resolved Granger causality (Friston et al., 2014) in a broader visual network including the individual sources encompassing the ipsilesional and contralesional V1 and MT.

In more details, Phase Amplitude coupling (PAC) was obtained through:

$$PAC = n-1n\sum t=1at\ (f\ ) \cdot ei\theta t \vee$$

Where t corresponds to a certain time point, a denotes the power at a certain specific frequency for this specific time point, i is the imaginary variable, θ the phase angle and n the number of time points.

The measure of Granger Causality is non-negative, and zero when there is no Granger causality. According to the original formulation of Granger Causality, the measure of Granger Causality from *y(t)* to *x(t)* is defined as:

$$F_{y\to x} = \ln\left(\frac{\mathrm{Var}(e_1)}{\mathrm{Var}(e_2)}\right)$$

Which is 0 for Var(e_1) = Var(e_2) and a non-negative value for Var(e_1) > Var(e_2). Note that Var(e_1) ≥ Var(e_2) always holds, as the model can only improve when adding new information. Under fairly general conditions, $F_{y\to x}$ can be decomposed by frequency if the two AR models in time domain are specified as:

$$\mathrm{x(t)} = \sum_{k=1}^{p}\left[A_{k_{xx}}x(t-k) + A_{k_{xy}}y(t-k)\right] + \sigma_{xy}$$

$$\mathrm{y(t)} = \sum_{k=1}^{p}\left[A_{k_{yy}}y(t-k) + A_{k_{yx}}y(t-k)\right] + \sigma_{yx}$$

In each equation the reduced model can be defined when each signal is an AR model of only its own past, with error terms σ_{xx} and σ_{yy} . We can then define the variance-covariance matrix of the whole system as:

$$\begin{bmatrix}\sum_{xx} & \sum_{xy}\\ \sum_{yx} & \sum_{yy}\end{bmatrix}$$

Where $\sum_{xx} = Var(\sigma_{xx})$, etc. Applying a Fourier transform to these equations, they can be expressed as:

$$\begin{pmatrix}A_{xx}(\omega) & A_{xy}(\omega)\\ A_{yx}(\omega) & A_{yy}(\omega)\end{pmatrix}\begin{pmatrix}x(\omega)\\ y(\omega)\end{pmatrix} = \begin{pmatrix}\varepsilon_1(\omega)\\ \varepsilon_2(\omega)\end{pmatrix}$$

Rewriting this as:

$$\begin{pmatrix}x(\omega)\\ y(\omega)\end{pmatrix} = \begin{pmatrix}H_{xx}(\omega) & H_{xy}(\omega)\\ H_{yx}(\omega) & H_{yy}(\omega)\end{pmatrix}\begin{pmatrix}\varepsilon_1(\omega)\\ \varepsilon_2(\omega)\end{pmatrix}$$

Where $\mathrm{H}(\omega)$ is the transfer matrix, the spectral matrix is then defined as:

$$S(\omega) = H(\omega)\sum H^*(\omega)$$

Finally, assuming independence of the signals *x* and *y*, and $\sum_{xy} = \sum_{yx} = 0$, we can define the spectral Granger Causality as:

$$F_{y\to x}(\omega) = \ln\left(\frac{S_{xx}(\omega)}{H_{xx}(\omega)\sum_{xx}H^*_{xx}(\omega)}\right)$$

Magnetic resonance imaging recording and analyses

Whole-brain MR imaging was done on a 3-Tesla Siemens scanner available at *Fondation Campus Biotech Genève (FCBG)*, Geneva, Switzerland or on the exact same scanner at Hopital du Valais, Sion, Switzerland. High-resolution anatomical images were acquired for anatomical references using an MPRAGE inversion time=900ms, voxel size=1 x 1 x 1 mm^3. One run of 657 scans with the measurement of the T2*-weighted blood-oxygenation level dependent (BOLD) effect was acquired with a gradient echo-planar imaging protocol and these parameters: echo time (TE)=30ms, repetition time (TR)= 1000ms, flip angle=90, voxel size=3 x 3 x 2 mm^3, field of view =204mm x 204 mm, matrix size=68 x 68 and 37 axial slices each of 2 mm thickness. Finally, DW-MRI data were acquired using a pulsed gradient spin echo sequence with the following parameters: TR = 5000 ms; TE = 77 ms; slices = 84; field of view = 234 × 234 mm2; voxel resolution = 1.6 × 1.6 × 1.6 mm3; slice thickness of 1.6 mm; readout bandwidth = 1630 Hz/pixels; 64-channel head coil; GRAPPA acceleration factor =3. Seven T2-weighted images without diffusion weighting (b0; b = 0 s/mm2) were acquired, including one in opposite phase encoding direction. A total of 101 images with noncollinear diffusion gradient directions distributed equidistantly over the half-sphere and covering 5 diffusion-weighting gradient strengths were obtained (b-values = [300, 700, 1000, 2000, 3000] s/mm2; shell-samples = [3, 7, 16, 29, 46]).

Functional MRI: Data was analysed using the Statistical Parametric Mapping toolbox (SPM12b, Wellcome Trust Center, London, UK, http://www.fil.ion.ucl.ac.uk/spm), implemented in Matlab 2019b (The Mathworks Inc., Massachusetts, USA). The preprocessing steps included correction for field inhomogeneity, slice timing correction, motion correction and unwarping. Then, the structural image of each participants was co-registered to the mean realigned EPI volume. The co-registered T1 image was then normalized to the Montreal

Neurological Institute (MNI) reference space using the unified segmentation approach (Ashburner and Friston, 2005). The resulting deformation parameters were applied to the individual EPI volumes which were then smoothed using an isotropic 4 mm full-width half-maximum (FWHM) Gaussian kernel.

For all datasets, we modelled a GLM using two regressors based on the subject's trial by trial accuracy in line with our staircase procedure (correct (74.63 (+/- 9.6) trials/incorrect (25.99 (+/- 9.7) trials)). Regressors were modelled as series of events (representing individual epochs) convolved with a canonical hemodynamic reference waveform. Low-frequency confounds were controlled by high-pass filtering at 1/128 Hz and head-movement estimates derived from the realignment procedure served as additional covariates of non-interest. Voxel-wise parameter estimates for all conditions and each covariate resulting from the least mean squares fit of the model to the data were computed.

For the group analysis, left-side lesions were mirrored to the right hemisphere. A full factorial design was used with the factors Time (*Pre, Post*) and tACS condition (Forward-tACS, Backward-tACS). Post-hoc comparisons were performed by extracting beta weights in the significant group-level cluster at the individual level, when significance was reached. The statistical significance threshold was set to a height threshold of $p < 0.001$ uncorrected, at the voxel level and to that of $p < 0.05$ at the cluster level after false-discovery rate (FDR) correction.

Additionally, to test the hypothesis that the interventions would change how remote visual areas interact with the ipsilesional V1-MT coupling, we conducted a Physio-physiological interaction (PhPI) analysis (Di and Biswal 2013). The PhPI approach applies a linear-regression framework to identify regions in the whole brain that are correlated with an interaction between two predefined regions, which reflects a modulation of connectivity between two regions by a third region (Di and Biswal 2013). To do this, we determined the seed brain regions on the basis of the individual V1 and MT clusters from the earlier GLM analyses, and the MR signal from each seed region was extracted as an eigenvariate time series. The extracted MR signal was deconvolved with the canonical hemodynamic response function (HRF). Then, the neural time series of the two seed regions were detrended and multiplied (dot product) so that the resulting timeseries represented the interaction of neural activity between the two seed regions (V1 and MT). Finally, the interaction time series was convolved with the

HRF, representing an interaction variable at the hemodynamic level (PPI term). Contrasts were computed between Pre and Post interventions for all patients.

Diffusion weighted imaging: Structural diffusion images were pre-processed by means of FSL (Jenkinson et al., 2012) and MRtrix (Tournier et al., 2019) software. A denoising step was firstly applied via the dwidenoise function (MRtrix), followed by correction of Gibbs ringing artefact via mrdegibbs (MRtrix) (Veraart et al., 2016). Images were then corrected for motion, susceptibility induced fields, eddy-current induced distortions, and bias field via the FSL functions topup (Andersson et al., 2003), eddy_openmp (Andersson and Sotiropoulos, 2016; Smith et al., 2004) and fast (Zhang et al., 2001). Probability maps for CSF, grey and white matter were estimated from the T1-weighted image via the fast function (FSL) and then registered to the average b0 image using ANTs (Avants et al., 2014). Fibres orientation distribution function was derived at the voxel level from multi-shell multi-tissue constrained spherical deconvolution and then used to compute whole-brain probabilistic tractography via second-order integration over fibre orientation distribution (iFOD2) (Tournier, 2019). The algorithm stopped once 10 million streamlines were generated. Each streamline was then weighted based on spherical-deconvolution informed filtering of tractograms (SIFT2, MRtrix) (Smith et al., 2015). To extract streamlines information between V1, V5 and the thalamus, two main techniques were used. V1 and V5 were derived from the functional localizer, using the individual thresholded activation in the ipsi- and contralesional hemisphere. The thalamus was extracted from the Destrieux atlas parcellation, output of the recon-all function of Freesurfer on the T1-weighted image (Yendiki et al., 2011). All masks were registered to the average b0 image using ANTs. The function tckedit (Tournier et al., 2019) from MRtrix was finally used to extract specific streamlines passing through either V1 and V5, V1 and the thalamus or V5 and the thalamus. The sum of the weights or the average FA along these tracts were used as indicators of cross-sectional area and integrity respectively.

Transcranial Magnetic Stimulation combined with functional Magnetic Resonance Imaging

For combined TMS-fMRI images, two dedicated coil arrays were used (Navarro de Lara et al., 2017). This setup consisted of an ultra-slim 7-channel receive-only coil array, which was

placed between the subject's head and the TMS coil (MRi-B91, MagVenture, Farum, Denmark) and connected to a MagPro XP stimulator (MagVenture, Farum, Denmark). A second, receive-only MR coil was positioned over Cz in the EEG 10-20 system to allow a full coverage of the participant's brain (Figure 5.4).

An event-related design was used to map the effect of TMS bursts composed of three pulses at alpha (10Hz) frequency. Three conditions were pseudorandomized and counterbalanced across the run: high-intensity TMS (*HighTMS),* low-intensity TMS *(LowTMS)* and no TMS *(noTMS),* with 25 repetitions of each condition with an inter-trial interval (ITI) of 6 seconds (covering 3 repetition times). The TMS intensity was set to ≈ 80% [range: 75 to 90%] maximal stimulator output (MSO) for the *HighTMS* condition, and ≈38 % [35 to 43%] MSO for the *LowTMS* condition. Intensity was individually adjusted prior the measurement to ensure phosphene sub-threshold stimulation and progressively increased until patients report pain or discomfort. The intensity was then chosen to get reliable BOLD signal while preserving participant's comfort. Participants were asked to look at a fixation cross throughout the acquisition, displayed in the middle of a 44cm x 27cm LCD monitor at a 2.5m distance via a mirror mounted on the head coil or on a frame on top of the TMS-fMRI setup. The duration of the *Rest TMS* sequence was 9 minutes. The TMS coil was individually placed to target the perilesional area using oil capsules placed on the TMS-MRI coil casing to monitor the coil position visible on a T2 image (see Supplementary Figure S5.4B for the TMS targeting of all patients).

The *TMS-fMRI* sequences were acquired with a GE-EPI sequence using the same parameters: 40 axial slices, slice thickness = 2.2 mm, in-plane resolution = 2.2 mm, TR = 2000 ms, TE = 30 ms, FOV = 242 mm, flip angle = 67°, GRAPPA = 2, Multiband Factor (MB) = 2. A gap was introduced between consecutive EPI volumes in order to guaranty artefact free MR images after TMS stimulation (Navarro de Lara et al., 2015). A single repetition time (TR=2000 ms) was therefore composed of 40 slices acquired during 1430 ms followed by a gap of 570 ms before the next volume acquisition. The synchronization of TMS pulse was carried out with an in-house script using Matlab (R2019).

Static field mapping was also performed with the TMS-MRI coils using the same double-echo spoiled gradient echo sequence (TR = 652 ms, TE = 4.92 and 7.38 ms, slice thickness: 2.2 mm, in-plane resolution = 2.2 mm, flip angle = 60°) that generates two magnitude images and one image representing the phase difference between the two echoes.

The same preprocessing steps than the ones described above were applied to the fMRI data expect that two additional coregistration steps were included. A first co-registration was performed between the mean realigned and slice timing corrected image and the SSFP sequence acquired with the same MR coil (and thus the same spatial coverage). The resulting, co-registered image was once more co-registered to the SSFP sequence acquired with the MR coil integrated into the scanner (i.e., the body coil, thus preserving the contrast). The latter could then be easily co-registered to the high resolution T1 image acquired with the 64-channel head coil that covered the whole brain, and later transformed into standard MNI space using a segmentation-based normalization approach (Ashburner and Friston, 2005).

Univariate analyses were applied to the fMRI data. We defined a design matrix comprising three conditions (*HighTMS*, *LowTMS* and *noTMS*). T-contrasts for each TMS condition were established for all participants. In this study, we focused on the contrast *HighTMS* versus Low*TMS* using a paired-t-test at the group level. The statistical significance threshold was set to a height threshold of $p < 0.001$ uncorrected, at the voxel level and to that of $p < 0.05$ at the cluster level after false-discovery rate (FDR) correction. To explore inter-individual variability, mean beta values were extracted from individual ipsilesional V1 cluster.

Statistical analyses

To compare the EEG metrics (Phase-Amplitude Coupling, Granger Causality and Time-Frequency values) before and after the two interventions, we used cluster-based non-parametric permutation tests corrected for multiple comparisons.

To evaluate differences in threshold performance for the CDDI task between the two interventions and across days, a linear mixed model was built with the raw NDR threshold as dependent variable, Training day, tACS condition and Order as fixed effects, and random effects for Patients. Finally, an ANOVA was applied on the model's parameters. When only the two interventions were directly compared without fixed effect, a paired t-test was performed after ensuring normal distribution with a Shapiro-Wilk test. Non-parametric equivalents were used if needed. A probability of type I error of $P < 0.05$ was considered statistically significant.

Finally, to evaluate the value of a structural and a functional variable for predicting improvements in visual processing after Forward-tACS, we ran a backward regression model

(p to enter: 0.05, p to remove: 0.1). The change in NRD thresholds was the dependent variable and the predictors were extracted from the combined TMS-fMRI exam and from diffusion weighted imaging.

5.4 Results

16 patients were enrolled in this cross-over and double-blinded trial (Figure 5.2A), at least one week after stroke-induced occipital damage (verified using structural MRI), with reliable 30-2 Humphrey Visual Field (HVF) perimetry (<20% fixation losses, false-positive and false-negative errors). Patients' characteristics are presented in Table 5.1 (see Methods section). They underwent two blocks of 10 daily visual training sessions using a coarse direction discrimination and integration (CDDI) task (see Figure 5.2B for the time-course of one trial) combined with Forward-tACS (synchronized V1 Alpha-tACS with MT Gamma-tACS promoting bottom-up cross-frequency interactions) or Backward-tACS (synchronized V1 Gamma-tACS with MT Alpha-tACS promoting top-down cross-frequency interactions). Pre/Post measurements included EEG, functional and structural MRI and performance on the CDDI task, as well as dynamic and static visual field perimetry.

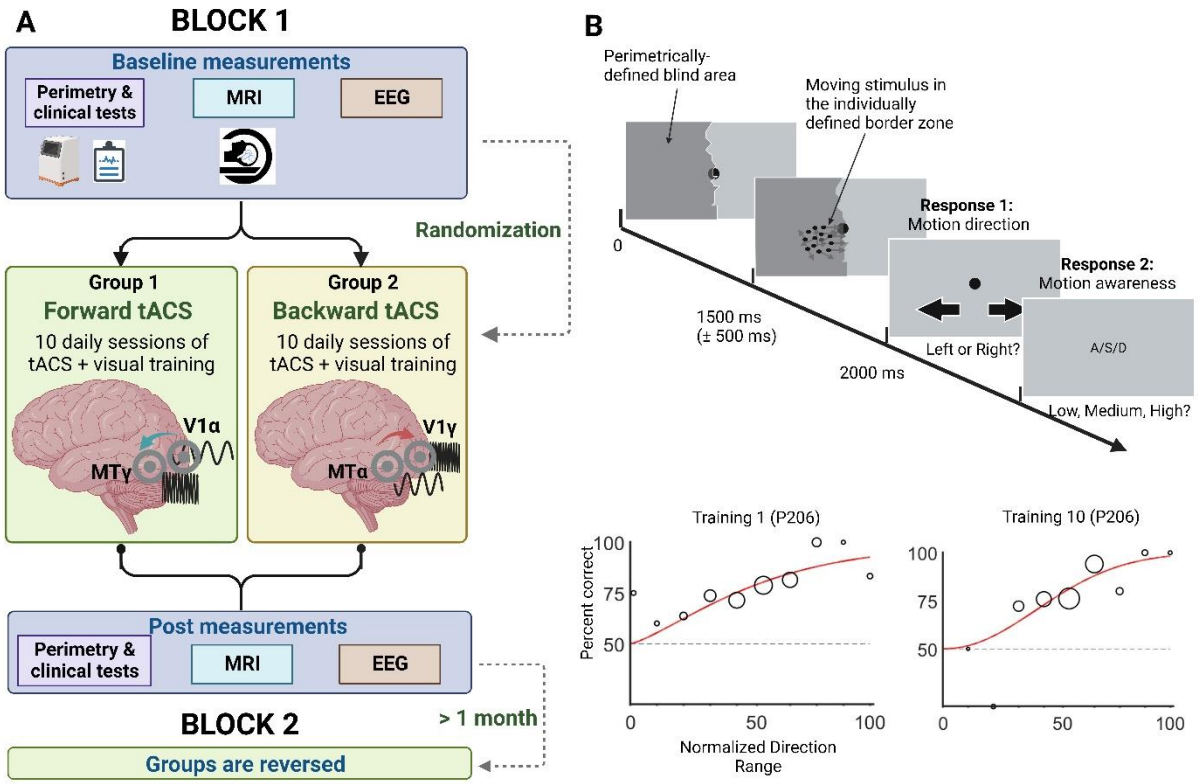

Figure 5.2: A: *Study flowchart. MRI: Magnetic Resonance Imaging, TMS: Transcranial Magnetic Stimulation, EEG: electroencephalography, tACS: transcranial Alternating Current Stimulation, V1: primary visual cortex; MT: motion-sensitive middle temporal cortex, α: Alpha tACS, γ: Gamma tACS;* ***B:*** *Trial sequence for the coarse direction discrimination and integration (CDDI) task, with stimulus location individualized for each patient.* ***C:*** *Bottom plots show the psychometric data Weibull fits (red lines) for patient P206 on Training Day 1 (NDR = 64%) and Training Day 10 (NDR = 55%). Individual trials are grouped into ten bins, with circle sizes scaling with the number of trials.*

Improved motion discrimination with Forward-tACS goes along with V1-MT cross-frequency synchrony

While receiving either Forward- or Backward-tACS, patients trained for 10 consecutive days at a 2-alternative, forced-choice, global CDDI task, as previously described (Huxlin et al., 2009a; Martin et al., 2010; Raffin et al., 2021; Saionz et al., 2020; Salamanca-Giron et al., 2021a). Patients were asked to discriminate the left–right direction of motion of random-dot stimuli individually located in their blind field. The trained location corresponded to each patient's visual field border (see Figure 5.1, Methods section). Patients' performance was close to chance level (54.3±4.2% correct) at the beginning of training. Importantly, performances at baseline did not differ between the Forward and Backward tACS group ($t_{(13)}$ = -1.07, p = 0.31).

Motion awareness was rated (low/medium/high) after each trial. Auditory feedback indicated whether the response was correct or incorrect. To measure changes in performance, we computed direction range thresholds by fitting a Weibull function to the percentage correct performance at each stimulus level and determining the stimulus value (i.e., direction range), resulting in 72% correct performance (see Figure 5.2C for an example of the Weibull fit). Direction range was then normalized by the maximum possible (360) to produce a Normalized Direction Range (NDR) whereby (0% = random motion, 100% = coherent motion) (Das et al., 2014) - see the Method section for more details.

Both tACS conditions led to improved NDR thresholds (-19% [SD = 26], one-sample t-test: $t(13) = -4.5$, $p < 0.001$ for Forward-tACS and -10.2±31%, one-sample t-test: $t(13) = -2.2$, $p = 0.05$ for Backward-tACS). The ANOVA testing the mixed linear model on the daily baseline-corrected NDR thresholds showed a significant *Training days* x *tACS condition* interaction ($F(9,196) = 2.5$, $p = 0.01$). This reflected a dissociation between the two learning curves, observable from training day 6, with Forward-tACS showing larger improvements in motion direction discrimination. There was a significant effect of *Training days* ($F_{(9, 27)} = 7.14$, $p < 0.001$) but no effect of *Order* nor *tACS condition* ($p > 0.05$). No difference in motion awareness and response times were observed between the two interventions (Supplementary Figure S5.1).

Given that our training task relied on motion processing, we measured pre/post changes in kinetic visual field maps. These visual field maps are extracted from kinetic Humphrey perimetry using moving stimuli of various sizes and light intensities along a vector, from a blind region to a seen region (Rowe et al., 2019). Results revealed that Forward-tACS significantly improved kinetic visual field boundaries compared to Backward-tACS (Forward-tACS: +698.3±921.8 deg^2, Backward-tACS (+121.9±805.3 deg^2, paired-t-test: $t(12) = -2.24$, $p = 0.045$) (Figure 5.3B for the group results and pre/post kinetic visual field maps from one example patient). In most patients, the extension corresponded to the trained area (see Supplementary Figure S5.2 for all kinetic visual field maps). Baseline maps were not different in the two groups ($t(12) = -0.42$, $p = 0.68$, paired t-test)

Under the hypothesis that Forward-tACS would specifically modulate the bottom-up V1 $\alpha_{\text{-phase}}$-MT $\gamma_{\text{-amp.}}$ Phase-Amplitude Coupling (PAC), we compared the maximal PAC values in the time domain during motion processing before and after Forward-tACS and Backward-tACS (Figure 5.3C upper panels, the associated comodulograms are provided in the bottom

panels). This analysis revealed an early increase in V1 $\alpha_{\text{-phase}}$-MT $\gamma_{\text{-amp.}}$ PAC around 100 ms post stimulus onset for Forward-tACS. This was followed by a significant decrease around 300 ms post stimulus onset. Interestingly, this pattern of early enhanced bottom-up PAC was already present after only one session of Forward-tACS (see supplementary Figure S5.3). The reversed direction, V1 $\gamma_{\text{-amp.}}$-MT $\alpha_{\text{-phase}}$ PAC, showed a significant increase in a late time window around 300 ms post stimulus onset. None of the two PAC showed significant changes after Backward-tACS. Note that the time-frequency content of motion processing showed stronger alpha synchronization on the EEG sources signals after Forward-tACS compared to Backward-tACS (Figure 5.4B right panels).

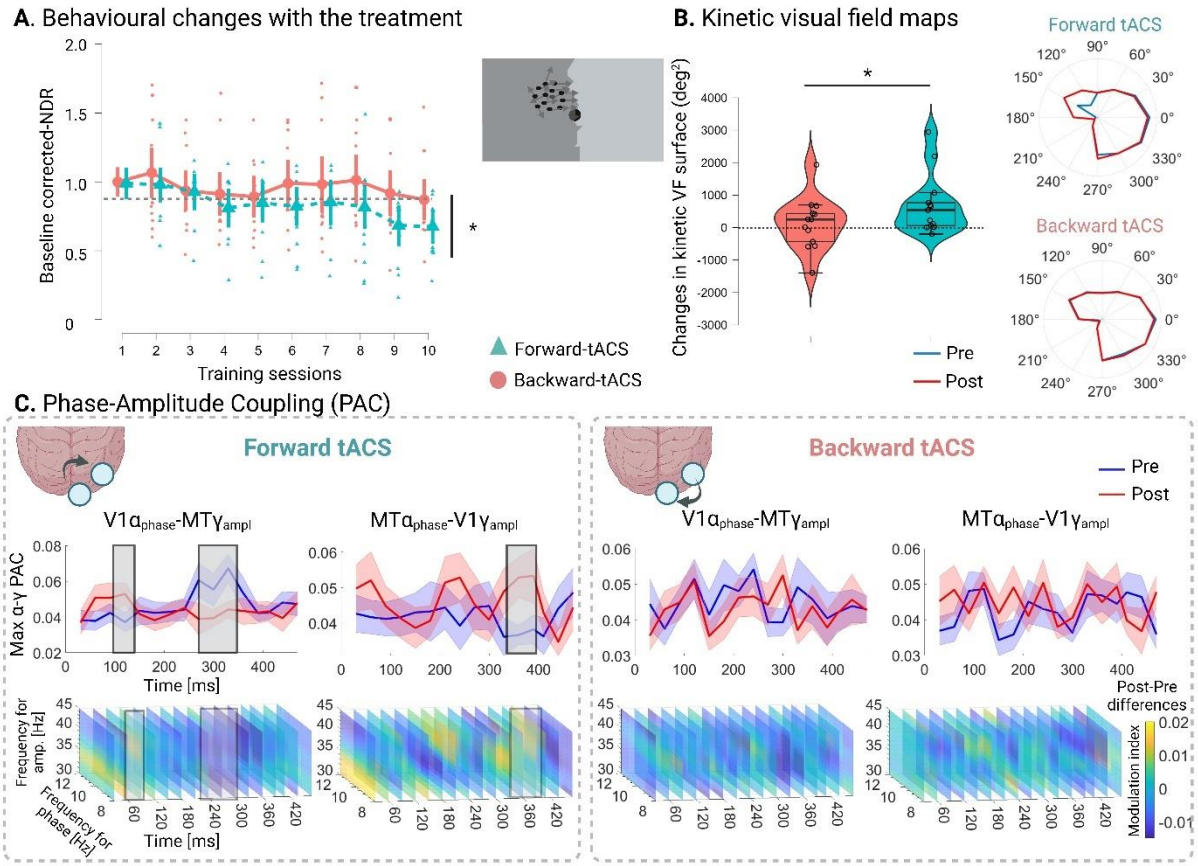

Figure 5.3: A: *Baseline-corrected behavioral performance at the training task (see methods) measured across the 10 daily sessions, for Forward-tACS and Backward-tACS;* ***B:*** *Group difference in kinetic visual field maps between Forward-tACS and Backward-tACS and kinetic visual field borders of an exemplary patient before/after Forward-tACS and Backward-tACS;* ***C:*** *Maximal Phase-Amplitude Coupling (PAC) between V1$\alpha_{\text{-phase}}$-MT$\gamma_{\text{-amplitude}}$ and the opposite V1$\gamma_{\text{-amplitude}}$-MT$\alpha_{\text{-phase}}$ for the two tACS group (upper row) and the associated comodulograms (bottom row). Significant differences in the PAC time-windows are indicated with grey rectangles.*

To further investigate how motion signals were differently processed after Forward-tACS and Backward-tACS, we compared fMRI activation patterns elicited by the same motion discrimination task. We designed a full factorial ANOVA with factors *Time* (Pre/Post) and *tACS condition* (Forward/Backward). This whole-brain analysis led to a significant effect of *Time* in V1. The extracted beta weights in V1 showed a BOLD increase after tACS in both conditions (Figure 5.4A). The *Time* x *tACS condition* interaction showed significant activity in the ipsilesional MT, bilateral frontal eyed field (FEF) and ipsilateral prefrontal cortex (MNI coordinates are reported in Supplementary Table 5.1). The beta-weights in the ipsilateral MT confirmed an increase after Forward-tACS and a decrease after Backward-tACS. Note that this contrast also led to a significant cluster in the ipsilesional lateral geniculate nucleus (LGN) at a more liberal threshold ($p<0.001$ uncorrected). Finally, we evaluated how the ipsilesional V1-MT coupling was influenced by other brain regions after the intervention using Physio-Physiological Interaction (PhPI) (Büchel and Friston, 1997). We found that the ipsilesional V1-MT functional connection was spatially less diffuse after Forward-tACS, potentially reflecting enhanced efficiency of the pathway, with less reliance on other neuronal resources. After Backward-tACS, we found a decreased modulatory effect of the contralesional V1 on the ipsilesional pathway (Figure 5.4B).

In addition, we compared the structural properties of the white matter fibers connecting ipsilesional V1 to MT using diffusion weighed imaging (DWI), positing they may underlie the changes in inter-areal communication reported above. We extracted the sum of the weights and fractional anisotropy (FA) of the relevant tracts connecting V1-MT bi-hemispherically, reflecting the importance of the bundles and the structural integrity of the tracts respectively. Although we observed a trend for an increase of bundles' density in the lesioned hemisphere after Forward-tACS compared to Backward-tACS, this was not significant (*tACS condition* x *Side* x*Time* interaction: $F_{(1,96)} = 1.9$, $p = 0.17$). The same observation was true for FA ($F_{(1,96)} = 1.10$, $p = 0.32$). FA showed a trend for an effect of *Side* reflecting the structural reorganization and loss of structural fibers occurring in the lesioned hemisphere (FA: $F(1,96) = 3.31$, $p = 0.07$).

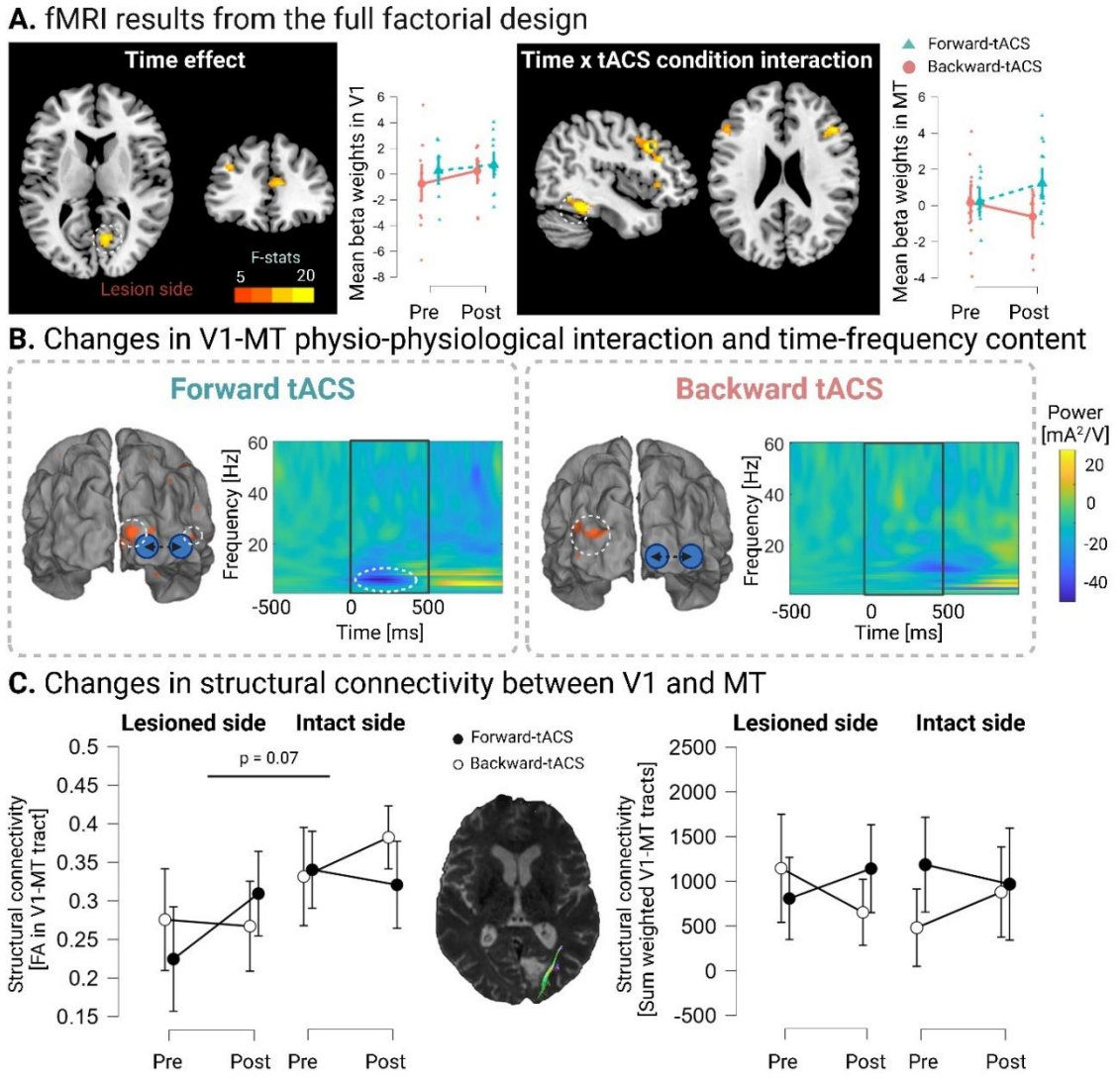

Figure 5.4A: *fMRI results from the full factorial design showing the main effect of Time (left panel) with the associated beta weights in V1 for the two tACS conditions and the Time by tACS condition interaction showing significant clusters in the ipsilesional MT, bilateral FEF and ipsilesional lateral prefrontal cortex, and the associated interaction in beta weights in the ipsilesional MT.* ***B:*** *Results of the PhPI analysis and the source-based time-frequency representation during motion processing for Forward-tACS (left panel) and Backward-tACS (right panel). PhPI results showing the Pre>Post contrast revealed a decreased coupling between ipsilesional V1-MT and ipsilesional clusters in V1 and MT for Forward-tACS, with contralesional clusters in the MT and MST regions for Backward-tACS. The other contrast Post>Pre did not reveal any significant cluster; Time-Frequency content shows stronger alpha desynchronization after Forward-tACS (Post>Pre difference);* ***C:*** *Changes in structural connectivity measured with Fractional Anisotropy (FA) (left side) and sum of the weighted V1-MT tracts (right side). No significant differences were found before/after any of the intervention.*

Baseline functional and structural predictors of Forward-tACS efficacy

We investigated whether individual functional or structural markers could predict the outcomes of Forward-tACS in these patients. In other words, we explored whether substantial residual fibers between V1 and MT or a functionally responsive ipsilesional primary visual cortex are a pre-requisite to achieve improvements. We extracted the fMRI-derived beta-weights in response to transcranial magnetic stimulation (TMS) applied to the ipsilesional V1 (see Methods section and Figure 5.5A.2 for the TMS-fMRI setup and Supplementary Figure S5.4 for all patient's individual TMS-fMRI setup). Group-wise fMRI activation revealed significant clusters in the perilesional V1 and remote clusters in the bilateral FEF and Cuneus (Figure 5.5A.1). To investigate a potential link between TMS induced BOLD activity and the individual changes in motion discrimination in the blind field, a covariate analysis was run. It showed a significant activation cluster in the ipsilesional V1 (Figure 5.5A.3). From the diffusion imaging data, we extracted the summed weights of the ipsilesional V1-MT tracts, reflecting the amount of residual structural fibers connecting the two regions (Figure 5.5B). A multiple regression model was built using functional and structural predictors measured prior the start of the intervention in order to explain the changes in motion perception: the lesion volume (mm^3), the beta weights in V1 induced by TMS over the perilesional V1 area and the sum of the weighted ipsilesional V1-MT tracts. The backward regression model was significant ($F(2,9) = 8.7$, $p = 0.013$) and explained a relevant amount of the variance ($R^2=0.72$). The beta weights in V1 and the summed weights of the V1-MT tracts were retained as significant predictors (V1 beta weight: $t(9) = -3.1$, $p = 0.02$, Sum: $t(9) = -3.3$, $p = 0.02$). Importantly, the two predictors were not correlated with each other ($r = 0.29$, $p = 0.41$). The lesion size did not contribute to behavioral changes. Figure 5.5C illustrates the relationship between the change in NDR thresholds and V1 beta weights (top panel) or the summed weights of the tracts (bottom panel).

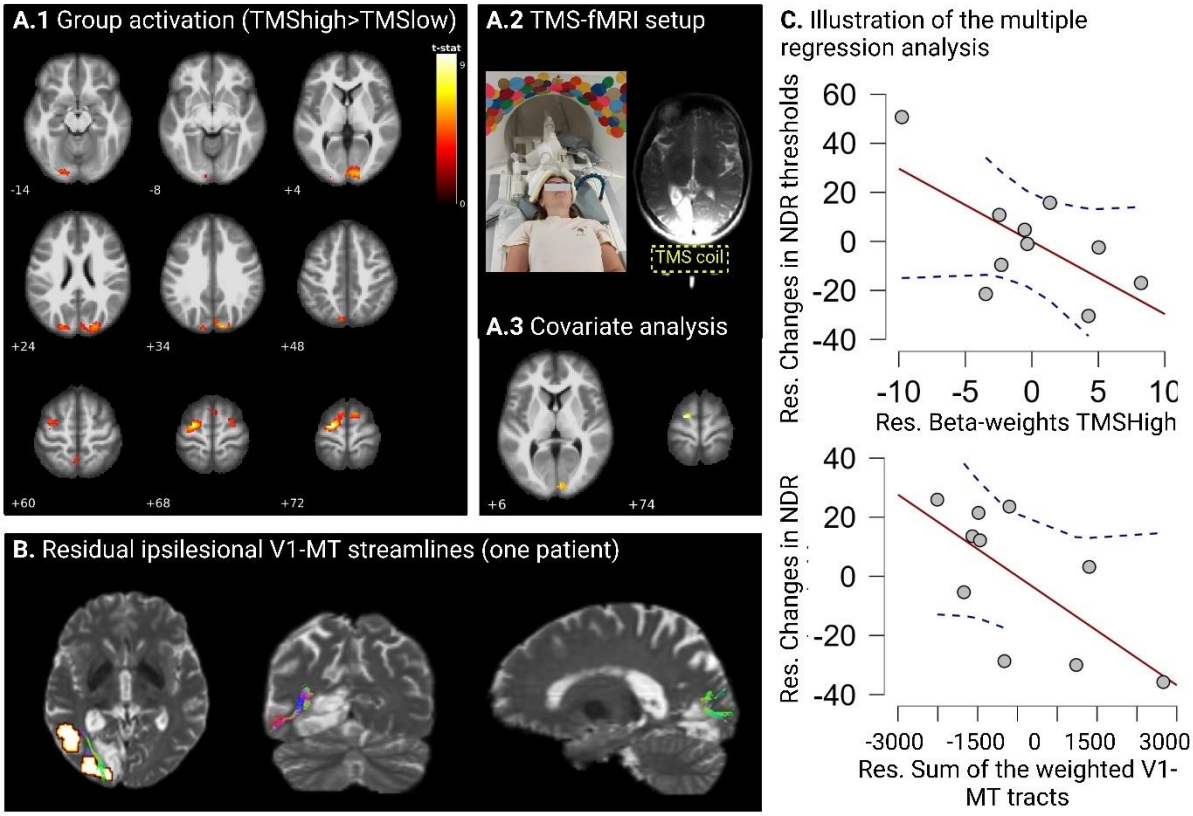

Figure 5.5: A1: *Whole group results of the one-sample t-test contrasting High-intensity TMS versus Low-intensity TMS;* ***A2:*** *TMS-fMRI setup with the coil positioning (right image);* ***A3:*** *Results of the covariate analysis showing the regions in the ipsilesional V1 and contralesional FEF that significantly increased with improved motion discrimination;* ***B****: one exemplary patients with residual V1-MT fibres in the ipsilesional hemisphere: C: Results of the multiple regression analysis showing the relationship between the residuals of the NDR changes with the residuals of the functional and structural predictors. Res.: Residuals, p < 0.001 uncorrected, at the voxel level and to that of p < 0.05 at the cluster level after false-discovery rate (FDR) correction.*

Static visual field maps

As a proof of principle that dual-site Forward-tACS combined with training not only enhances motion discrimination in the blind field but also static visual field recovery, we compared the composite visual field maps extracted from static Humphrey perimetry as previously described (Cavanaugh et al., 2017), before and after the intervention. While most of our patients had stable visual fields before starting the protocol, both tACS conditions led to substantial improvement, located close to where patients were training on the CDDI task (Figure 5.6, one sample t-test for Forward-tACS: $t_{(13)}$ = 4.33, p<0.001, for Backward tACS: $t_{(14)}$ = 6.14,

p<0.001). There was no significant difference between the two tACS conditions ($t_{(13)}$ = -0.382, p = 0.71, paired t-test).

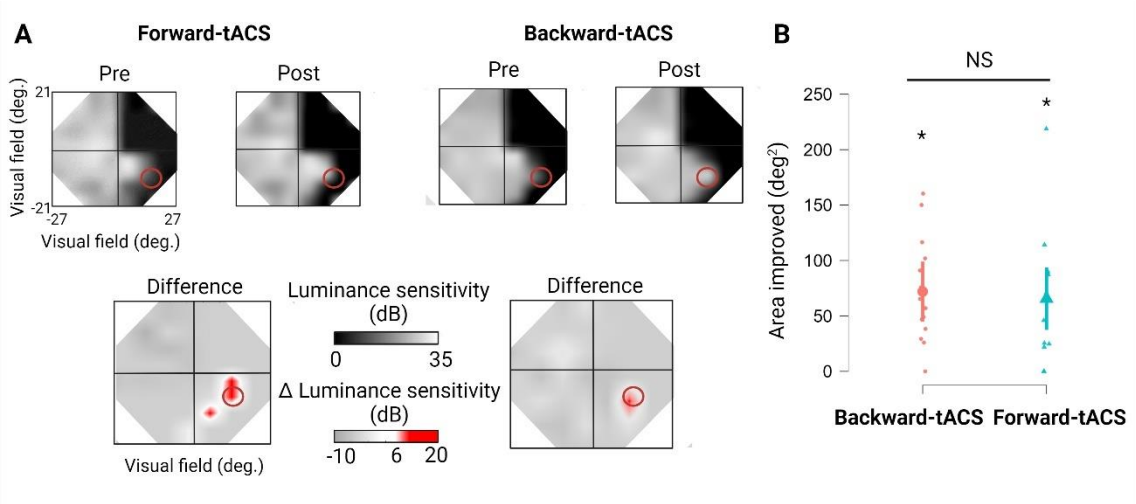

Figure 5.6: A*: Composite maps of the Humphrey visual fields pre and post Forward- and Backward-tACS (upper row) and plots of the area of the Humphrey visual fields that improve by >6 dB* (Cavanaugh and Huxlin, 2017) *after Forward-tACS and Backward-tACS (bottom row);* ***B:*** *Mean and individual data corresponding to the pre/post improvement in visual field. No significant differences were observed between the two interventions (paired t-test: P > 0.05). * indicates significant one-sample t-test in each tACS condition.*

5.5 Discussion

While non-invasive brain stimulation (NIBS) has been widely investigated in stroke patients for the recovery of motor functions, only a few clinical studies have applied brain stimulation to patients in conjunction with visual training (Battaglini et al., 2022; Herpich et al., 2019). Here, we developed a new interventional strategy based on co-entrainment of interregional oscillatory activity to reorchestrate feedforward and feedback interactions using multifocal, pathway-specific, physiology-inspired cross-frequency tACS to reduce visual impairment after an occipital stroke. Clinically relevant improvements were observed in a good part of our cohort, such as in patient P206, reporting being "*able to see the right arm of his wife when seated on the passenger seat, when she is driving. This was impossible before the protocol*".

This novel physiology-inspired approach uses a global motion training program recognized as promising in patients with chronic cortically-induced blindness although very intense and providing limited outcomes (Cavanaugh and Huxlin, 2017; Das et al., 2014; Huxlin et al., 2009a). Second, it builds on the recent evidence suggesting that vision deficits secondary to a stroke might not only be caused by the primary focal tissue damage, but also by a change in interregional communication or functional synchronization in underlying brain networks (Raffin et al., 2020; Siegel et al., 2008). Based on this pathophysiological concept, we investigated the effect of promoting forward (using Forward-tACS: α-tACS over V1 and ɣ-tACS over MT) compared to backward information flow (i.e., Backward-tACS: ɣ-TACS over V1 and α-tACS over MT) on motion discrimination learning and visual field recovery.

Pathway and directed effects of cross-frequency tACS

The proposed physiology-inspired cross-frequency tACS protocol is based on the extensive literature of animal model, humans, and computational modeling studies demonstrating that alpha-modulated gamma oscillations affect the probability of neurons in the visual system to respond to an incoming stimulus (Bahramisharif et al., 2013; Bonnefond and Jensen, 2015; Osipova et al., 2008; van Kerkoerle et al., 2014). In an inter-areal regional framework, the neuronal population that mediates alpha oscillations projects onto the population oscillating at a gamma frequency, producing an efficient inter-areal communication channel in the visual system (Bonnefond et al., 2017; Canolty and Knight, 2010; Osipova et al., 2008). In the present study, Forward-tACS, which was intended to enhance feedforward information flow, resulted in enhanced motion discrimination and integration learning compared to Backward-tACS in stroke patients with occipital cortex damage.

In line with the idea that Forward-tACS would act by restoring optimal inter-areal oscillatory interactions, the EEG-based phase-amplitude coupling (PAC) between V1 and MT showed phasic modulations during motion processing in both directions. More precisely, the bottom-up V1 $\alpha_{\text{-phase}}$-MT $ɣ_{\text{-amp.}}$ coupling significantly increased in the Forward-tACS group during the first 100ms of motion processing, suggesting enhanced early feedforward inputs to MT, followed by a significant decrease, probably preventing the system to saturate (Chacko et al., 2018). From a signal processing point of view, this PAC direction reflects bottom-up information flow. Hence, it is the coordinated activity of excitatory and inhibitory neuronal populations in the perilesional V1 area that influenced postsynaptic potentials at gamma

frequencies in neurons projecting to MT (Nandi et al., 2019) either directly or indirectly via V2 or V3. This suggests that the beneficial effects of Forward-tACS cannot solely be achieved by monofocal tACS over MT. Additionally, the late time window of motion processing was also associated with an increase in the opposite direction of PAC, reflecting backward inputs from MT to V1. All-in-all, Forward-tACS is likely to reactivate dynamical patterns of bi-directional V1-MT coupling, acting on the full feedforward-feedback motion processing loop, as also shown by the selective increase in BOLD activity during motion discrimination in MT. Mechanistically, the reactivation of the perilesional V1 neurons is interesting. Occipital alpha oscillations are crucial in motion discrimination learning and more generally in visual perceptual learning as reported in previous human EEG studies (Bays et al., 2015; Muller-Gass et al., 2017; Nikolaev et al., 2016) or in tactile perceptual learning (Brickwedde et al., 2019). Congruently, our results showed that training on a motion direction discrimination task was associated with increased BOLD activity in the ipsilesional V1. This is in line with past studies showing that visual training in cortically blind patients results in an enlargement of population receptive fields in the perilesional V1, and increases blind-field coverage in these patients (Barbot et al., 2021).

Previous visual re-learning studies suggest that patients might require several dozens of practice sessions over weeks and months before showing improvements in motion direction discrimination in their blind field (Cavanaugh et al., 2017; Huxlin et al., 2009a). In an attempt to overcome this limitation, Herpich and colleagues administered visual training coupled with transcranial random noise stimulation (tRNS) to HH patients and showed that this boosted the speed of visual motion discrimination learning in their blind fields (see Herpich et al., 2019). In the present study, 11 out of the 15 patients in the Forward-tACS condition showed meaningful improvements of direction range thresholds after only four sessions. Forward-tACS might allow patients to reach the outcomes reported by these past studies after months of training, in a much shorter period of time. Another important aspect to consider when referring to these earlier studies is the different study designs. Previous studies were home-based, enhancing patient compliance but with limited control on the exact setup (eye movements, level of attention etc.). In our proof-of-concept study, patients were training every day in the lab, with continuous eye tracking monitoring and feedback from a researcher.

Static perimetry is currently the most commonly used type of perimetry to assess visual field maps. With static perimetry, sensitivity thresholds are determined at different test locations. The thresholds are compared to the sensitivity thresholds of age-matched controls. Our results

revealed a mean increase of 62.9 deg^2 (for Forward-tACS) and 65.5 deg^2 (for Backward-tACS). These values are within the range of results obtained after months of training sessions reported in home-based studies (Barbot et al., 2021; Cavanaugh et al., 2017; Huxlin et al., 2009b). Improved motion direction discrimination and V1-MT oscillatory interactions after Forward-tACS did translate into an enlargement of visual field borders assessed with kinetic perimetry compared to Backward-tACS. These visual field maps are assessed with moving stimuli of various sizes and light intensities from a region of non-seeing to a region of seeing. They return contour lines or isopters with a very high spatial resolution, resulting in a map of visual field sensitivity (Weijland et al., 2004). Interestingly, in most of the patients (see supplementary Figure S5.2), the improvements were localized in the area that had been visually stimulated during the entire training protocol, confirming the retinotopic specificity of the training-induced improvements (Cavanaugh et al., 2017; Huxlin et al., 2009b).

Extending the capacity to detect motion in the blind field definitively has a positive and practical impact in patients' lives as acknowledged by the positive quotes from our patients. However, the limitations associated with this study should be considered. First, although similar to the sample sizes found in comparable studies (Barbot et al., 2021; Cavanaugh et al., 2015; Herpich et al., 2019), the limited sample size in this study prevents the results from being generalized to all cortically blind stroke survivors. Second, we did not measure long-term effects of the protocol. Therefore, it is unknown whether patients keep their visual improvements months after the end of the intervention. Third, while we controlled for the directionality of the oscillatory interactions, we did not include a sham tACS condition. Future studies with a pure sham intervention would help to disentangle the improvements explained by the visual training alone, the tACS intervention alone or by the interaction between the two.

Predictive values of residual V1 reactivity and V1-MT structural integrity

The multimodal evaluation battery performed before and after the intervention aimed at extracting predictors of Forward-tACS effects. Our initial hypothesis was that the residual V1 neurons spared by the lesion are critical for visual recovery. This was suggested in a study from Barbot and colleagues who measured retinotopic fMRI activity in cortically blind patients before and after 20.5 months of visual training on average (Barbot et al., 2021). They reported that spared V1 activity representing perimetrically blind areas before training was predictive of the amount of training-induced recovery of luminance detection sensitivity. To causally

probe the level of residual functions of perilesional V1 neurons in the present study, we used the unique opportunity of TMS-fMRI to measure the local response to TMS in the perilesional area prior to the intervention. We found that TMS-evoked activity was predictive of the changes induced by Forward-tACS in direction range thresholds in the blind field (there was no such association with Backward-tACS), suggesting that more functional surviving cortical tissue, the more likely a patient will benefit from Forward tACS.

Besides this functional metric, a strong predictor of Forward-tACS effects was the number of structural fibers connecting V1 to MT, as measured by the summed weights of the V1-MT tract. The relationship between structural markers and brain stimulation effects has been repeatedly shown in various contexts and networks (Kearney-Ramos et al., 2018; Khan et al., 2023; Momi et al., 2021; Muthuraman et al., 2017). Again, this finding provides another piece of evidence for target engagement, with Forward-tACS strongly relying on the cortical motion pathway. Finally, it is important to note that those two independent variables (no significant correlation between the functional and structural marker) need to be considered together to explain a sufficient amount of variance in the response to rehabilitation protocols that target a specific pathway or function.

5.6 Conclusions

The results provide first proof-of-concept evidence that orchestrated, pathway-specific, physiology-inspired tACS might be a novel treatment opportunity to improve post-stroke visual field recovery. The intervention relies on the hierarchical oscillatory interactions between visual cortical areas, which can be supported or restored with this physiologically-inspired protocol. The unique set of multimodal measurements confirmed the relevance of these oscillatory channels for visual learning in patients and showed reactivation of the ipsilesional V1-MT pathway.

Competing interests

The authors declare that they have no competing interests.

Funding

Funding was obtained from the Defitech Foundation (to FCH), Bertarelli Foundation (Catalyst BC77O7 to FCH & ER), by the Swiss National Science Foundation (PRIMA PR00P3_179867 to ER)

Acknowledgements

We would like to thank the EEG and neuromodulation facilities of the Human Neuroscience Platform of the Foundation Campus Biotech Geneva, for technical advice, and the Brain & Behavior Laboratory (BBL) facilities at the Centre Medical Universitaire (CMU) of Geneva.

5.7 Supplementary materials

Supplementary Tables

Regions	**F values**	**Z max**	**Cluster extent**	**MNI coordinates (x;y;z)**
Time effect (F test)				
R Primary Visual Cortex	13.4	3.35	31	4;-76;-3
R Med. Pre-Frontal Ctx.	12.7	3.26	19	3;46;3
L IFG	11.7	3.39	17	-29;46;28
Interaction Time X tACS cond.				
R MT	21.4	4.24	309	52;-56;-14
L Frontal Eye Field	17.56	3.85	44	46;22;34
R Frontal Eye Field	12.68	3.26	12	-38 ;12 ;46
R Prefrontal Ctx.	14.3	3.47	12	42 ;48 ;-8

Table S5.1*: Cluster information and MNI coordinates of the fMRI full factorial design analysis during motion discrimination*

Supplementary Figures

Figure S5.1: Motion awareness and response times

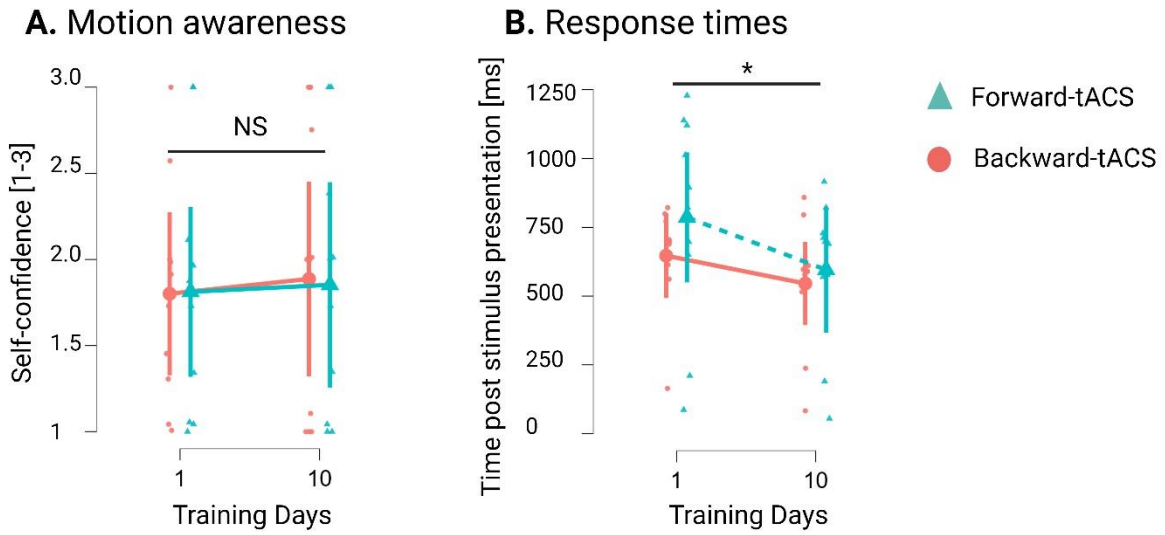

Figure S5.1: *Changes in motion awareness and response times after Forward-tACs (blue) and Backward-tACS (red). We also explored potential differences in motion awareness after the intervention, measured with a three items scale rating self-confidence on a trial-by-trial basis. Figure S5.1A shows the difference in motion awareness between Training 1 and Training 10, on correct trials for the two tACS conditions. Subjective awareness of the stimulus did not significantly change between the first and the last sessions for both groups (Time effect: $F(1,11) = 0.7$, $p = 0.43$). Note that some patients reported a clear sensation of motion (the left-or rightward for the CDDI task) while some appeared to predominantly rely on non-conscious motion processing. Additionally, reaction times of correct trials showed a common decrease after training (significant Time effect: $F(1,20) = 13.1$, $p = 0.002$) but no Time by tACS condition interaction ($F(1,18) = 1.3$, $p = 0.27$)(Figure S5.1B).*

Figure S5.2: Individual composite kinetic visual field maps before and after the interventions

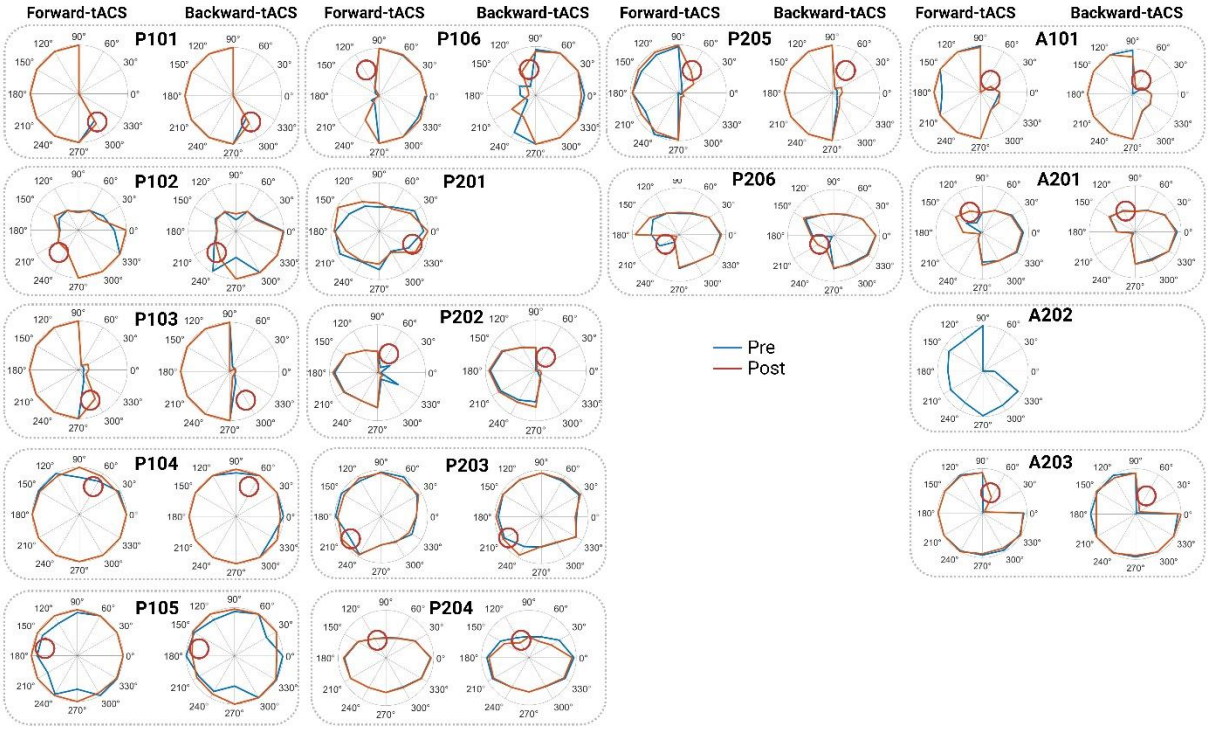

Figure S5.2: *Kinetic visual field maps before (blue contours) and after (red contours) Forwrad-tACS (left panel) and Backward-tACS (right panel) for all individual patients, with the individual location of the visual stimulus used during the visual training.*

Figure S5.3: Single session of cross-frequency tACS

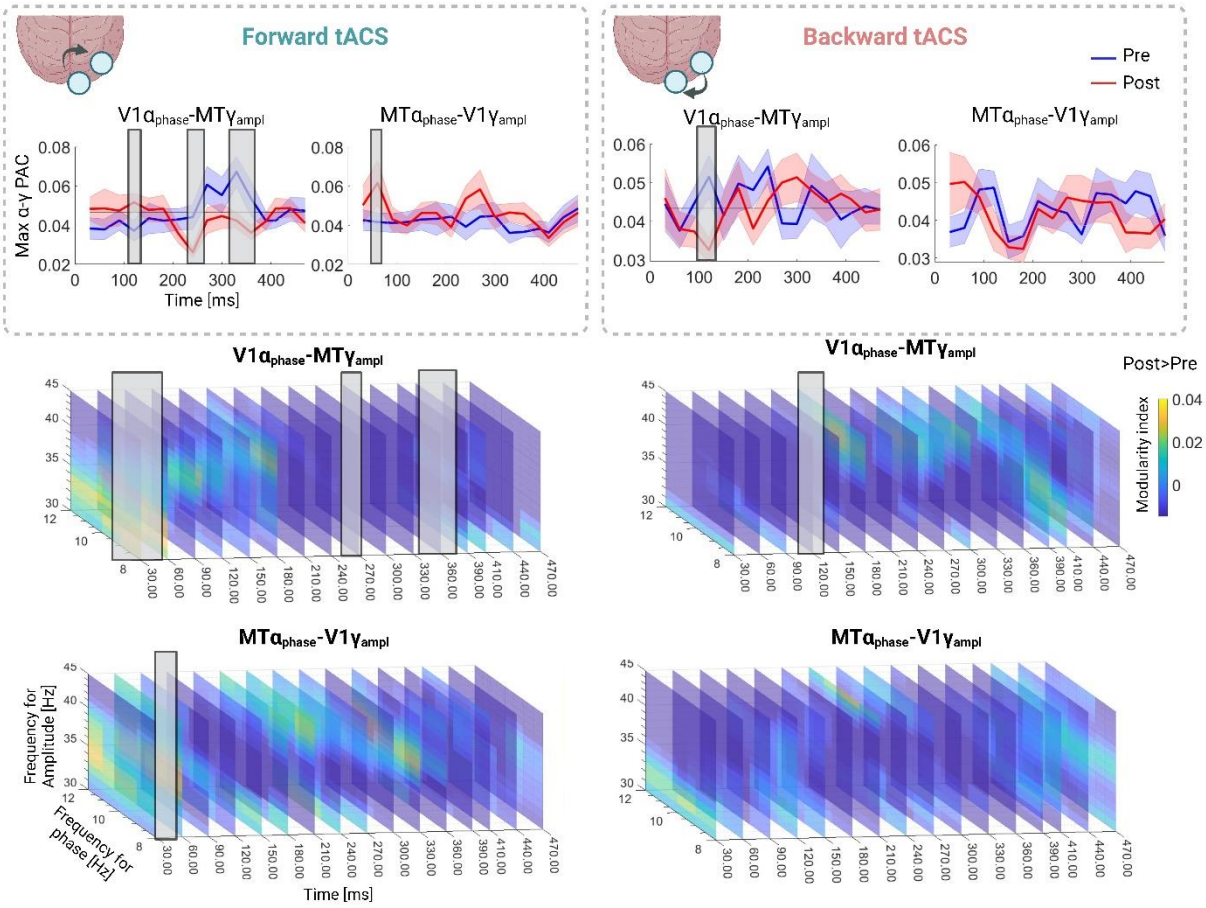

Figure S5.3: *Maximal Phase-Amplitude Coupling (PAC) between V1α-phase-MTγ-amplitude and the opposite V1γ-amplitude-MTα-phase after one session of Forward-tACS and Backward-tACS (upper row) and the associated comodulograms (bottom rows). Significant differences in the PAC time-windows are indicated with grey rectangles.*

Figure S5.4: TMS-fMRI setup all patients

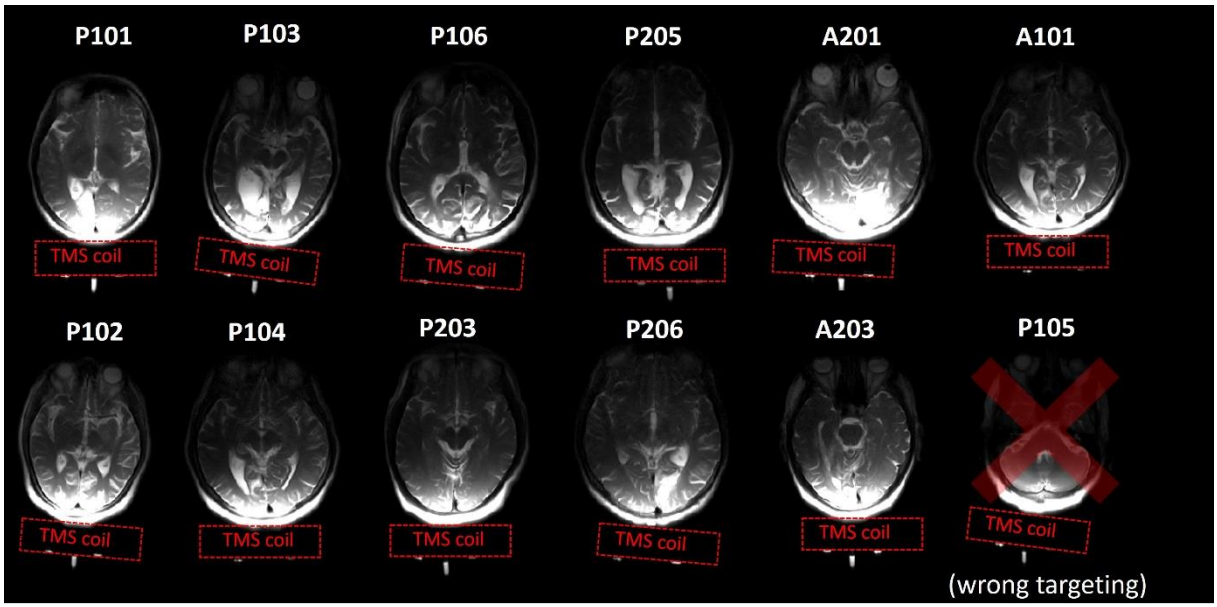

Figure S5.4: *Structural images based on t2 haste sequence displaying for all patients the TMS coil position targeting the perilesional area. Note that P105 was excluded from the analysis due to wrong targeting*

Chapter 6 - General Discussion

In the four experiments exposed in the previous chapters, we modulated using 2 different NIBS (ccPAS -Chapters 2 and 3- and cross-frequency bifocal tACS -Chapters 4 and 5-) neuronal activity along the motion discrimination pathway of healthy participants (Chapters 2 and 4) and stroke patients presenting homonymous visual field defects (Chapter 3, 4 and 5). We recorded EEG, sMRI, fMRI correlates as well as motion coherence discrimination performance and for patients, static and dynamic perimetries.

The overall aim of this thesis was threefold: 1) To obtain a better knowledge on the neurophysiological properties of the motion visual discrimination pathway V1-MT in humans; 2) To induce pathway-dependent plasticity within this pathway in healthy brains, either using STDP or cross-frequency oscillatory interactions, and measure the consequences on visual motion discrimination; and 3) assess the potential of these interventions in a clinical framework on brain-lesioned participants, either as biomarker of network integrity or for future therapeutic applications that would boost visual rehabilitation effects. Uncovering the plastic potential of the visual motion discrimination pathway, how it can be modulated by different non-invasive brain stimulation techniques and the effect of a tailored NIBS intervention on stroke hemianopic patients' visual recovery could represent a game changer for the development of future innovative visual rehabilitation therapies, and pave the way towards more personalized brain state-dependent protocols. In the next paragraph, I will summarize the main findings and discuss them in larger context. I will then specifically highlight some of the main insights brought by this PhD work. I will end this thesis proposing potential technological developments apt to further enhance the efficacy of the interventions.

6.1 Summary and interpretation of the results

In the first study (Chapter 2), we explored the effects of ccPAS between V1 and MT on motion direction discrimination performance in young, healthy participants. The hypothesis behind our approach was that enhancing the MT-to-V1 feedback (i.e., applying Backward ccPAS) strengthens global motion processing and awareness. Extending previous research by Romei *et al.*, (2016), our study confirmed that Backward ccPAS specifically enhances motion direction discrimination. Contrastingly, Forward ccPAS (the control condition, in which a first

TMS pulse was delivered over V1, followed by a second, 20ms later, over MT) did not change motion direction discrimination. Our findings are in line with previous anatomical studies that have explored the structural connections between V1 and higher-level extrastriate cortical areas. Notably, research by Sincich *et al.* (2004) and Xiao and Felleman, (2004) has shown that the projections from V1 to higher-order areas in the visual processing hierarchy, such as MT, do not express significant differentiation. This means that the outputs from V1 are relatively uniform and do not target preferentially specific subregions or neuron types in these higher extrastriate areas. As a result, the feedforward projections from V1 may not selectively enhance specific functions such as motion direction discrimination in the same way that feedback projections from MT to V1 do. Moreover, human and macaque findings show that feedforward connections from V1 predominantly consist of deper cortical neurons, which tend to project broadly across multiple areas (Nassi and Callaway, 2007). On the other hand, feedback connections, such as those from MT to V1, originate from more superficial cortical layers and are more targeted in their projections (Blasdel and Lund, 1983). This architectural difference in the cortical circuitry could explain why Forward ccPAS does not show the same enhancements in motion discrimination as Backward ccPAS, which is supposed to target the more specific and functionally distinct feedback pathways from MT. Interestingly, recent data have suggested that Hebbian activity-dependent plasticity protocols might go beyond synaptic changes but could also involve changes in white-matter fibers between V1 and MT (Lazari et al., 2022). This would need to be systematically measured.

Interestingly, Backward ccPAS further enhanced motion awareness, as measured with increased metacognitive confidence ratings. The interaction between perceptual learning and decision making has been thoroughly investigated by the ccPAS study of Di Luzio *et al.* (2022). Their findings demonstrate that enhancing V5/MT+-to-V1/V2 back-projections boosts motion sensitivity without impacting metacognition, whereas boosting IPS/LIP-to-V1/V2 back-projections increases metacognitive efficiency without affecting motion sensitivity, providing causal evidence of distinct networks for these cognitive processes. Our Granger Causality results showed indeed an increase in V1-to-IPS connectivity for both ccPAS conditions, hinting thus that strengthening the MT-V1 pathway might additionally support the neural mechanisms of metacognitive judgements in perceptual decision-making,

From the electrophysiological point of view, we observed that none of the ccPAS conditions induced local changes in EEG source level activity. However, significant changes in signal

propagation were detected using spectrally resolved Granger Causality. This method, combined with single pulse TMS stimulation over V1 and MT separately, allowed us to distinguish between direct output signal diffusion and re-entering signal transmission (Winkler et al., 2015). Notably, Backward-ccPAS significantly increased the re-entrant top-down MT-to-V1 connection in the Alpha range, correlating with enhanced motion direction discrimination. This finding highlights the efficacy of the Backward intervention in enhancing effective connectivity of the feedback projections, the ones thought to mediate motion discrimination abilities (Lamme et al., 1998; Pascual-Leone and Walsh, 2001; Silvanto et al., 2005b). Finally, spectral Granger Causality indicated increases in direct output connectivity after both ccPAS interventions from V1 to IPS and from V1 to MT in the Gamma band. These changes were not predictive of any behavioral improvement but might reflect an increase in bottom-up, exogenous attention associated with task exposure.

We then postulated that the acute reorganizational state of the visual system imposed by Backward-ccPAS could be exploited as a predictive metric for visual recovery in pathological conditions, such as in visual stroke patients. This measure would index to which extent residual pathways can be exploited for potential visual re-training protocols. This idea constitutes the rational of our second study.

In this subsequent study (Chapter 3), we investigated the possibility to artificially modulate MT-to-V1 connectivity in stroke patients presenting V1 lesions, with the goal of enhancing motion discrimination at the visual field's border. The study aimed to determine if the modulation of residual re-entrant MT-to-V1 fibers can improve motion discrimination ability also in a context in which the network is damaged. Furthermore, we wanted to assess whether structural connectivity or functional stimulation reactivity could predict a patient's response to ccPAS intervention.

We found that Backward-ccPAS in stroke patients led to significant improvements in motion discrimination at the group level, confirming that Hebbian plasticity principles apply even in lesioned brains. However, we observed notable inter-individual variability among patients, much higher than the one observed in the healthy cohort. To understand this variability, we compared spectral Granger Causality connectivity of the targeted pathway between patients who showed significant task improvement and those who didn't. Responders exhibited increased beta-band connectivity in the re-entrant top-down MT-V1 connections, highlighting the potential of beta oscillations as mediators and biomarkers of synaptic plasticity. The

modulation of beta oscillations in the V1-to-MT pathway appears to be crucial for top-down control of motion perception. This finding is consistent with literature suggesting beta-band's role also in cognitive and motor functions (Baker, 2007; Buschman and Miller, 2007; Engel and Fries, 2010; Richter et al., 2018). The shift observed from alpha to beta band oscillations in stroke patients could be linked to the reorganization of cerebral networks after a stroke, which impacts both alpha and beta oscillatory patterns (Ulanov and Shtyrov, 2022). Beta oscillations have a significant role in recovery following a stroke (Hordacre et al., 2020; Thibaut et al., 2017). Thibaut *et al.* (2017) discovered that an increase in high-beta power in the hemisphere affected by the stroke correlates with improved motor skills, suggesting that, at least in the motor domain, it would act as a compensatory mechanism for the imbalance in excitability caused by the lesion. Literature on non-human primates further suggests that beta-band influences from higher visual areas can modulate bottom-up gamma-band processes in V1 (Richter et al., 2018). Interestingly, behaviorally irrelevant increases in bottom-up connections were induced by Forward-ccPAS, a phenomenon also observed in healthy participants (Chapter 2).

Furthermore, Backward-ccPAS induced improvements in motion discrimination correlated with increased re-entrant MT-to-V1 beta inputs and with the residual V1-MT structural connectivity, estimated with diffusion-weighted imaging (DWI) and the fractional anisotropy (FA) values of the MT-V1 tract.

If ccPAS and TMS-EEG have been considered in this thesis as precious approaches to acquire insights on the neurophysiological properties of the intact/lesioned motion visual discrimination pathway, they have not been applied as potential rehabilitation techniques themselves. This for a handful of reasons. First, recent studies have shown promising results in improving visual field through intensive visual-attentional training, particularly within specifically defined blind spots or scotomas (Cavanaugh and Huxlin, 2017; Raninen et al., 2007; Sahraie et al., 2006). However, these training methods demand extensive time commitments from patients, often spanning months, and yield only a moderate level of improvement that is applicable to daily activities (Das et al., 2014; Huxlin et al., 2009b; Melnick et al., 2016). Our idea has been to integrate these methods with cutting-edge neurotechnology designed to re-establish neural connections within the brain's cortical visual motion pathway. Given the need for intensive daily visual training combined with NIBS, involving potentially in the future home-based rehabilitation setups, TMS instrumentation

nowadays does not represent the optimal fit for the role. Some of the reasons supporting this claim are the necessary need for a clinical environment and at least two experimenters, high costs, great complexity of the multimodal instrumentation in play and the high level of discomfort for the participant, who cannot move during the ccPAS delivery. Furthermore, and probably most importantly, our ccPAS protocol was not applied online, i.e., during the motion discrimination task. Therefore, its effects probably rather reflect the non-specific expression of a network's response, which might not be specifically and completely tuned to the neuronal populations involved in the task. Finally, there is so far, no report in the literature of long-term effects of daily ccPAS applications.

We thus decided to explore another mean of enhancing communication between V1 and MT, through the application of cross-frequency multisite tACS. This can be easily done in combination with motion direction discrimination behavioural task as a therapeutic approach for visual restoration.

In our third study (Chapter 4), we investigated the effects of a single session dual-site cross-frequency transcranial alternating current stimulation (tACS) on visual motion discrimination and integration tasks in two groups: young healthy individuals and hemianopic stroke patients. This stimulation protocol was designed to exogenously synchronize selective neural activity and prioritize information gating in the MT-V1 pathway. The tACS involved the application of individual alpha frequency signals in V1 and individual gamma signals in MT (V1α-MTγ, Forward-tACS), compared to the opposite electrode/frequency combination (V1γ-MTα, Backward-tACS) and compared to a sham condition for the healthy cohort. Our primary aim was to examine changes in cross-frequency inter-areal coupling between V1 and MT.

This study yielded two main findings: first, a single session of bifocal cross-frequency Forward tACS (V1α-MTγ) successfully modulated inter-areal synchronization in both healthy individuals and stroke patients, increasing early bottom-up coupling (V1pαMTaγ) in both cohorts. Second, these electrophysiological changes did not lead to significant behavioral improvements in motion discrimination tasks at the group level in either cohort.

Our findings reveal that Forward tACS influenced EEG-based PAC between the V1 and MT regions during motion processing in both healthy and patient groups. Particularly in patients, Forward tACS enabled remaining V1 neurons to synchronize with neuronal populations

oscillating in gamma in MT immediately after visual stimulus onset despite the reported diminished V1 alpha activity in patients (Allaman et al., 2021; Gallina et al., 2022).

Additionally, the reverse PAC pattern showed a late-stage reduction in healthy subjects and an early reduction in stroke patients. This suggests a late task-specific disconnection in healthy individuals, while in patients, it may indicate early adaptive reorganization in brain areas near the lesion, driven by preserved higher-order visual areas. Despite these neurophysiological findings, the study did not show corresponding behavioral improvements in visual motion discrimination tasks. This might suggest a more complex relationship between externally applied oscillatory activity and behaviorally relevant brain processing. Also, a single session may not effectively enhance motion discrimination abilities, as Forward tACS primarily influences the direct feedforward visual pathway, rather than the entire neural network, in such a short duration. This theory is backed by the previously cited researches highlighting the critical role of feedback from higher visual areas to the primary visual cortex (V1) in motion perception (Lamme et al., 1998; Pascual-Leone and Walsh, 2001; Silvanto et al., 2005b). Therefore, a protocol combining multiple days of cross-frequency tACS stimulation with targeted visual training for motion discrimination may be necessary to achieve observable behavioral progress.

For this reason, in our fourth and last study (Chapter 5), we developed a new treatment paradigm for stroke patients with cortically-induced blindness, the same cohort as study 2 and 3 (Chapter 3 and 4), combining multifocal cross-frequency transcranial alternating current stimulation (tACS) with 10-day long daily visual training. This approach aimed to enhance both feedforward and feedback neural transmissions by employing Forward-tACS (α-tACS over V1 and ɣ-tACS over MT) and Backward-tACS (ɣ-TACS over V1 and α-tACS over MT). The focus was on assessing the impact of these modalities on motion discrimination and visual field recovery.

In this 10-day daily training setup, Forward-tACS, designed to boost feedforward information flow, significantly managed to improve motion discrimination in patients. This improvement was defined by changes in EEG-based PAC between V1-α and MT-ɣ, indicating enhanced early feedforward inputs to MT. Furthermore, Forward-tACS facilitated the reactivation of bi-directional V1-MT coupling and resulted in increased BOLD activity in these areas during motion discrimination. Predictive factors for the effectiveness of Forward-tACS included

residual V1 reactivity as measured with online TMS-fMRI and the structural integrity of V1-MT connections.

A remarkable clinical finding was the enlargement of dynamic visual field borders in patients following Forward-tACS, as demonstrated by kinetic perimetry. This suggests that Forward-tACS can specifically improve motion processing and, very importantly, can lead to targeted visual field expansion. This represents our most relevant finding, since the effectiveness of cross-frequency bifocal tACS in rapidly boosting behavioral motion perception performance (effect comparable to literature in magnitude, but reached in a shorter time), which also translated in an enlargement of the dynamic visual field border, has not been reported in literature yet.

6.2 Enhancing long-term bottom-up information flow and promoting transient top-down inputs

One might wonder how two apparently opposite approaches and interventions such as Backward-ccPAS and Forward-tACS could have led to similar enhancing effects on motion discrimination ability. As first thing, it is important to clarify that "Backward" ccPAS and "Forward" tACS rely on completely different mechanisms. This ambiguous denomination does not necessarily mean that they are mutually exclusive, but instead, they could act in a complementary fashion. In this paragraph. I will argue that these two direction-dependent interventions probe distinct neuronal populations and have to be used in different context.

In the framework of the natural phase-amplitude coupling between alpha and gamma neuronal populations in the visual system, Forward-tACS cross-frequency protocol was tailored to exogenously mimic and synchronize selective neural activity. Because neural population generating low frequency activity are tough to project onto the high frequency population, by stimulating V1 in the alpha frequency band and MT in the gamma one, we primarily aimed to enhance bottom-up V1-to-MT information flow. This physiologically-inspired protocol successfully restored this neural coupling emerging during motion discrimination, which is necessary altered by the lesion. This was objectified by the specific improvement in motion detection.

In contrast, STDP is a form of plasticity induction requiring synchronized co-activity between MT and V1, which is unlikely to spontaneously occur in the same timeframe, in the everyday life. Importantly, time-dependent plasticity has been found to preferentially affect superficial fibers. In the visual system, bottom-up and top-down responses have been associated with distinct laminar profiles. Feedback connections have been found in more superficial layers of the visual cortex (Lawrence et al., 2019). This might explain why ccPAS mainly acted on the top-down connections. Interestingly, the effects were primarily driven by the enhancement of MT-to-V1 effective connectivity, in the alpha/low beta frequency range, which are highly dependent on the behavioral context (Richter et al., 2017). This context dependency might make ccPAS not a very well-suited approach for long term recovery, as it might be triggered by very specific visual states. Backward ccPAS increased motion perception but also metacognition of perceptual decision making, estimated through confidence rating assessment in healthy volunteers and in patients. This effect has been reported to be mediated by top-down attentional circuitry, partly mediated by the inferior parietal sulcus (IPS) as shown in our data and in previous studies (e.g., Di Luzio *et al.* 2022). This attentional effect might also explain the visual field increase induced by Backward-tACS.

Although the ccPAS and tACS studies were performed on the same stroke individuals, note that other factors might explain the discrepancies in the directionality effects of cf-tACS and ccPAS. Besides, the different plasticity mechanisms, the electrophysiological measures computed to quantify the inter-areal coupling changes (spectral GC vs PAC), the context in which brain stimulation was delivered (at rest for ccPAS vs during the behavioral task for tACS) and the context in which the measures (sGC and PAC) were extracted (probed by single pulse TMS at rest vs time-locked to the motion stimuli) need to be taken into account in order to build a comprehensive and fair comparison between the two interventions. Future studies should evaluate the potential of the two interventions in modulating V1-MT connectivity using exactly the same conditions and measures.

6.3 Structure-Function (de)coupling in visual recovery

In both groups of studies, specifically the ones targeting patients (Chapter 3 and 5) both structural and functional markers successfully predicted behavioral improvements but in an independent manner.

In Chapter 3, two key indicators, residual fractional anisotropy (FA) in the V1-MT pathway and changes in directed MT-to-V1 top-down connectivity, emerged as potential predictors for the effectiveness of the targeted intervention. In Chapter 5, through the use of a TMS-fMRI recording performed before the beginning of the tACS intervention, we reported that the initial response of perilesional V1 neurons to TMS could predict the success of Forward-tACS in improving motion discrimination in the blind field. Here again, the individual V1 to MT structural connectivity was also a significant predictor of improvements in motion discrimination.

In both cases, the structural and functional variables were not correlated with each other, indicating that they captured independent aspects of the individual potential to respond to brain stimulation. These findings align with existing research showing the importance of considering both structural and functional aspects in neural repair and rehabilitation (Preti and Van De Ville, 2019; Vázquez-Rodríguez et al., 2019).

Moreover, it is congruent with previous findings linking structural brain markers to non-invasive brain stimulation outcomes (Kearney-Ramos et al., 2018; Khan et al., 2023; Momi et al., 2021; Muthuraman et al., 2017; Quentin et al., 2015). Considering both functional reactivity and residual structural integrity of the lesioned system is crucial to explain and even anticipate the effect of a targeted intervention The fact that these two factors can co-exist independently from each other suggests the existence of different phenotypes of patients: individuals showing strong reliance on functional changes without necessarily having good or bad structural integrity or in contrast, individuals with few residual fibers and very resistant to functional changes and so on. The presence of these different phenotypes needs to be investigated in future studies. It could for instance discriminate between patients with good chance of long-term recovery versus patients with weak chances.

6.4 Future technological developments

Brain state dependency in non-invasive brain stimulation techniques refers to the idea that their effects can vary based on the functional state of the brain at the time of stimulation. This variability highlights the interaction between the induced stimulation and the ongoing neural activity, suggesting that the timing, nature, and outcomes of NIBS can be significantly

influenced by factors such as the phase of neuronal oscillations, levels of neurotransmitters, or the overall alertness of the individual (Thut et al., 2017).

For instance, research has shown that the outcomes of TMS can differ depending on whether the brain is in a state of rest or engaged in a task, indicating that the neural context plays a critical role in how the brain responds to stimulation (Miniussi et al., 2013; Silvanto et al., 2008). Similarly, the effectiveness of tES, like tDCS or tACS, can be modulated by the ongoing brain rhythms, which can be synchronized or desynchronized based on the frequency and timing of the stimulation (Antal et al., 2017; Thut and Miniussi, 2009).

In our lab, we previously demonstrated that short bursts of bifocal V1-MT tACS, time-locked to the presentation of a moving stimulus, might improve motion discrimination capacities of healthy subjects (Salamanca-Giron et al., in preparation). In the case of ccPAS, evidence in the motor and visual cortices suggest how ccPAS parameters, such as inter-stimulus timing (in the order of a few milliseconds) and directionality of the two pulses play a crucial role into enabling the occurrence of STDP by matching or not spontaneous inter-regional activity (Koch et al., 2013; Rizzo et al., 2009; Veniero et al., 2013). The influence and impact of ccPAS on MT-to-V1 projections, potentially mediated by STDP may undergo significant shifts depending on the state-dependent changes in neocortical excitability (Chao et al., 2015; Fehér et al., 2017; Koch et al., 2013). Consequently, to enhance the efficacy of Backward-ccPAS interventions, it could be advantageous to apply them within a framework that is sensitive to the state of neocortical excitability. In fact, the variability observed by stroke patients in response to Backward-ccPAS (Chapter 5) might be attributed not only to residual white matter tracts or the ability to alter effective connectivity but partially also to the variations in brain state during ccPAS paired pulses. Integrating EEG-based biomarkers into a phase-dependent system could continually optimize ccPAS, potentially enhancing its effectiveness, as highlighted by Wagner *et al.* (2016). One modifiable parameter that does not interfere with STDP induction timings is the repetition rate of TMS pulse pairs, traditionally set at 0.1 Hz. Research in the motor domain on state-dependent TMS, such as the work of Zrenner *et al.* (2016), has shown that stimulation during local alpha disinhibition leads to a stronger remote response in motor evoked potentials, emphasizing the influence of ongoing brain oscillations on stimulation effects. With this concept in mind, during my PhD I took part in the creation of an online EEG phase detection algorithm already tested on offline studies I co-authored in Bigoni *et al.* (2024). A possible effective way to combine the results coming from both ccPAS would be to align the first of the

two paired pulses of the Backward ccPAS on MT with the ongoing alpha phase over V1. Gamma oscillations will be incorporated into the phases of alpha oscillations, predominantly occurring during the maximal excitability phase of the alpha cycle. As the excitability phases of alpha oscillations are synchronized, gamma activity emanating from MT could have then the potential to substantially impact more consistently the neural activity in V1. Triggering STDP at the optimal alpha phase on MT could exploit cross-frequency inter-areal interactions and modulate more efficiently top-down MT-to-V1 backprojections or potentially even bottom-up V1-MT fibers. The current open-loop ccPAS systems do not consider the intra- and inter-individual differences in cortical excitability and connectivity, which can impact the intervention's outcome (Thabit et al., 2010). A state-dependent system, tailored to the brain's ongoing neural signature, could overcome these challenges, potentially leading to more effective clinical outcomes (Gilson et al., 2020).

Chapter 7 - General Conclusions

In addition to the fundamental knowledge on cortical motion processing provided by this Thesis, our work presents a promising new approach for rehabilitating visual impairments in stroke patients. First, from a clinical point of view, our results pave the way towards designing an MRI-ccPAS-TMSEEG protocol able to extract a multimodal biomarker of the visual system integrity in HH stroke patients. This biomarker could help in the stratification of the patients according to their "multimodal integrity index", in order to predict the effect of therapeutic NIBS protocols for motion perception rehabilitation, for instance. Secondly, improvement in motion perception and visual fields resembling the ones obtained after months of visual training alone (Cavanaugh et al., 2015; Das et al., 2014; Huxlin et al., 2009b) were obtained after only 10 days of daily visual training combined with tACS intervention. Forward-tACS, in particular, shows potential for rapidly improving motion discrimination and expanding visual fields, opening avenues for innovative cortical blindness rehabilitation strategies, with the potential to achieve faster and possibly better clinical outcomes. Future studies should include a bigger cohort, a longer period of daily training combined with bifocal cross-frequency tACS, potentially integrating further technological developments (i.e., state-dependent approaches), compared to a stimulation-less control condition to precisely control for non-stimulation related behavioral, electrophysiological and clinical changes.

I would like to informally conclude my dissertation with what I consider the greatest achievements of our work, reported directly through some of our patients' feedbacks:

«*I can now clearly see the left arm of my wife when she is driving*».

«*At halfway through the protocol, I suddenly realized that I could see the right knee of the person sitted in front of me in the train*».

«*My vision clearly improved. I have the feeling that I am more self-confident when walking in the street*».

Bibliography

Aaen-Stockdale, C., Thompson, B., Aaen-Stockdale, C., Thompson, B., 2012. Visual Motion: From Cortex to Percept, in: Visual Cortex - Current Status and Perspectives. IntechOpen. https://doi.org/10.5772/50402

Ajina, S., Pestilli, F., Rokem, A., Kennard, C., Bridge, H., 2015. Human blindsight is mediated by an intact geniculo-extrastriate pathway. eLife 4, e08935. https://doi.org/10.7554/eLife.08935

Alber, R., Moser, H., Gall, C., Sabel, B.A., 2017. Combined Transcranial Direct Current Stimulation and Vision Restoration Training in Subacute Stroke Rehabilitation: A Pilot Study. PM&R 9, 787–794. https://doi.org/10.1016/j.pmrj.2016.12.003

Albright, T.D., 1992. Form-Cue Invariant Motion Processing in Primate Visual Cortex. Science 255, 1141–1143. https://doi.org/10.1126/science.1546317

Albright, T.D., Desimone, R., Gross, C.G., 1984. Columnar organization of directionally selective cells in visual area MT of the macaque. J. Neurophysiol. 51, 16–31. https://doi.org/10.1152/jn.1984.51.1.16

Allaman, L., Mottaz, A., Guggisberg, A.G., 2021. Disrupted resting-state EEG alpha-band interactions as a novel marker for the severity of visual field deficits after brain lesion. Clin. Neurophysiol. Off. J. Int. Fed. Clin. Neurophysiol. 132, 2101–2109. https://doi.org/10.1016/j.clinph.2021.05.029

Allison, T., McCarthy, G., Wood, C.C., Williamson, P.D., Spencer, D.D., 1989. Human cortical potentials evoked by stimulation of the median nerve. II. Cytoarchitectonic areas generating long-latency activity. J. Neurophysiol. 62, 711–722. https://doi.org/10.1152/jn.1989.62.3.711

And, K. T. & Kolmel, H. W. Patterns of Recovery from Homonymous Hemianopia Subsequent to Infarction in the Distribution of the Posterior Cerebral Artery. *Neuro-Ophthalmol.* (1991) doi:10.3109/01658109109009640.

Anderson, J.C., Binzegger, T., Martin, K.A.C., Rockland, K.S., 1998. The Connection from Cortical Area V1 to V5: A Light and Electron Microscopic Study. J. Neurosci. 18, 10525–10540. https://doi.org/10.1523/JNEUROSCI.18-24-10525.1998

Andersson, J.L.R., Skare, S., Ashburner, J., 2003. How to correct susceptibility distortions in spin-echo echo-planar images: application to diffusion tensor imaging. NeuroImage 20, 870–888. https://doi.org/10.1016/S1053-8119(03)00336-7

Andersson, J.L.R., Sotiropoulos, S.N., 2016. An integrated approach to correction for off-resonance effects and subject movement in diffusion MR imaging. NeuroImage 125, 1063–1078. https://doi.org/10.1016/j.neuroimage.2015.10.019

Antal, A., Alekseichuk, I., Bikson, M., Brockmöller, J., Brunoni, A.R., Chen, R., Cohen, L.G., Dowthwaite, G., Ellrich, J., Flöel, A., Fregni, F., George, M.S., Hamilton, R., Haueisen, J., Herrmann, C.S., Hummel, F.C., Lefaucheur, J.P., Liebetanz, D., Loo, C.K., McCaig,

C.D., Miniussi, C., Miranda, P.C., Moliadze, V., Nitsche, M.A., Nowak, R., Padberg, F., Pascual-Leone, A., Poppendieck, W., Priori, A., Rossi, S., Rossini, P.M., Rothwell, J., Rueger, M.A., Ruffini, G., Schellhorn, K., Siebner, H.R., Ugawa, Y., Wexler, A., Ziemann, U., Hallett, M., Paulus, W., 2017. Low intensity transcranial electric stimulation: Safety, ethical, legal regulatory and application guidelines. Clin. Neurophysiol. Off. J. Int. Fed. Clin. Neurophysiol. 128, 1774–1809. https://doi.org/10.1016/j.clinph.2017.06.001

Antal, A., Kincses, T.Z., Nitsche, M.A., Bartfai, O., Paulus, W., 2004. Excitability changes induced in the human primary visual cortex by transcranial direct current stimulation: direct electrophysiological evidence. Invest. Ophthalmol. Vis. Sci. 45, 702–707.

Antal, A., Paulus, W., 2013. Transcranial alternating current stimulation (tACS). Front. Hum. Neurosci. 7. https://doi.org/10.3389/fnhum.2013.00317

Anwer, S., Waris, A., Gilani, S.O., Iqbal, J., Shaikh, N., Pujari, A.N., Niazi, I.K., 2022. Rehabilitation of Upper Limb Motor Impairment in Stroke: A Narrative Review on the Prevalence, Risk Factors, and Economic Statistics of Stroke and State of the Art Therapies. Healthc. Basel Switz. 10, 190. https://doi.org/10.3390/healthcare10020190

Apfelbaum, H., Peli, E., 2015. Tunnel Vision Prismatic Field Expansion: Challenges and Requirements. Transl. Vis. Sci. Technol. 4, 8. https://doi.org/10.1167/tvst.4.6.8

Apfelbaum, H.L., Ross, N.C., Bowers, A.R., Peli, E., 2013. Considering Apical Scotomas, Confusion, and Diplopia When Prescribing Prisms for Homonymous Hemianopia. Transl. Vis. Sci. Technol. 2, 2. https://doi.org/10.1167/tvst.2.4.2

Appelros, P., 2002. Stroke severity and outcome : in search of predictors using a population-based strategy. Institutionen för klinisk neurovetenskap, arbetsterapi och äldrevårdsforskning (NEUROTEC) / Department of Clinical Neuroscience, Occupational Therapy and Elderly Care Research (NEUROTEC).

Ashburner, J., Friston, K.J., 2005. Unified segmentation. NeuroImage 26, 839–851. https://doi.org/10.1016/j.neuroimage.2005.02.018

Ashida, H., Lingnau, A., Wall, M.B., Smith, A.T., 2007. fMRI Adaptation Reveals Separate Mechanisms for First-Order and Second-Order Motion. J. Neurophysiol. 97, 1319–1325. https://doi.org/10.1152/jn.00723.2006

Atapour, N., Worthy, K.H., Lui, L.L., Yu, H.-H., Rosa, M.G.P., 2017. Neuronal degeneration in the dorsal lateral geniculate nucleus following lesions of primary visual cortex: comparison of young adult and geriatric marmoset monkeys. Brain Struct. Funct. 222, 3283–3293. https://doi.org/10.1007/s00429-017-1404-4

Avants, B.B., Tustison, N., Johnson, H., n.d. Advanced Normalization Tools (ANTS).

Azouz, R., Gray, C.M., 2000. Dynamic spike threshold reveals a mechanism for synaptic coincidence detection in cortical neurons in vivo. Proc. Natl. Acad. Sci. U. S. A. 97, 8110–8115. https://doi.org/10.1073/pnas.130200797

Azzopardi, P., Fallah, M., Gross, C.G., Rodman, H.R., 2003. Response latencies of neurons in visual areas MT and MST of monkeys with striate cortex lesions. Neuropsychologia,

The Neuropsychology of Motion Perception 41, 1738–1756. https://doi.org/10.1016/S0028-3932(03)00176-3

Bahramisharif, A., van Gerven, M.A.J., Aarnoutse, E.J., Mercier, M.R., Schwartz, T.H., Foxe, J.J., Ramsey, N.F., Jensen, O., 2013. Propagating Neocortical Gamma Bursts Are Coordinated by Traveling Alpha Waves. J. Neurosci. 33, 18849–18854. https://doi.org/10.1523/JNEUROSCI.2455-13.2013

Bair, W., Zohary, E. & Newsome, W. T. Correlated firing in macaque visual area MT: time scales and relationship to behavior. *J. Neurosci. Off. J. Soc. Neurosci.* 21, 1676–1697 (2001).

Baker, S.N., 2007. Oscillatory interactions between sensorimotor cortex and the periphery. Curr. Opin. Neurobiol., Motor systems / Neurobiology of behaviour 17, 649–655. https://doi.org/10.1016/j.conb.2008.01.007

Barbot, A., Das, A., Melnick, M.D., Cavanaugh, M.R., Merriam, E.P., Heeger, D.J., Huxlin, K.R., 2021. Spared perilesional V1 activity underlies training-induced recovery of luminance detection sensitivity in cortically-blind patients. Nat. Commun. 12, 6102. https://doi.org/10.1038/s41467-021-26345-1

Barbur, J.L., Watson, J.D., Frackowiak, R.S., Zeki, S., 1993. Conscious visual perception without V1. Brain J. Neurol. 116 (Pt 6), 1293–1302. https://doi.org/10.1093/brain/116.6.1293

Barmashenko, G., Eysel, U.T., Mittmann, T., 2003. Changes in intracellular calcium transients and LTP in the surround of visual cortex lesions in rats. Brain Res. 990, 120–128. https://doi.org/10.1016/S0006-8993(03)03447-4

Barnes, S.J., Franzoni, E., Jacobsen, R.I., Erdelyi, F., Szabo, G., Clopath, C., Keller, G.B., Keck, T., 2017. Deprivation-Induced Homeostatic Spine Scaling In Vivo Is Localized to Dendritic Branches that Have Undergone Recent Spine Loss. Neuron 96, 871-882.e5. https://doi.org/10.1016/j.neuron.2017.09.052

Bastos, A.M., Vezoli, J., Bosman, C.A., Schoffelen, J.-M., Oostenveld, R., Dowdall, J.R., De Weerd, P., Kennedy, H., Fries, P., 2015. Visual areas exert feedforward and feedback influences through distinct frequency channels. Neuron 85, 390–401. https://doi.org/10.1016/j.neuron.2014.12.018

Battaglini, L., Di Ponzio, M., Ghiani, A., Mena, F., Santacesaria, P., Casco, C., 2022. Vision recovery with perceptual learning and non-invasive brain stimulation: Experimental set-ups and recent results, a review of the literature. Restor. Neurol. Neurosci. 40, 137–168. https://doi.org/10.3233/RNN-221261

Battaglini, L., Mena, F., Ghiani, A., Casco, C., Melcher, D., Ronconi, L., 2020. The Effect of Alpha tACS on the Temporal Resolution of Visual Perception. Front. Psychol. 11. https://doi.org/10.3389/fpsyg.2020.01765

Bauer, M.S., Damschroder, L., Hagedorn, H., Smith, J., Kilbourne, A.M., 2015. An introduction to implementation science for the non-specialist. BMC Psychol. 3, 32. https://doi.org/10.1186/s40359-015-0089-9

Baumann, T.P., Spear, P.D., 1977. Role of the lateral suprasylvian visual area in behavioral recovery from effects of visual cortex damage in cats. Brain Res. 138, 445–468. https://doi.org/10.1016/0006-8993(77)90683-7

Bays, B.C., Visscher, K.M., Le Dantec, C.C., Seitz, A.R., 2015. Alpha-band EEG activity in perceptual learning. J. Vis. 15. https://doi.org/10.1167/15.10.7

Bender, M., Romei, V., Sauseng, P., 2019. Slow Theta tACS of the Right Parietal Cortex Enhances Contralateral Visual Working Memory Capacity. Brain Topogr. 32, 477–481. https://doi.org/10.1007/s10548-019-00702-2

Bergmann, T.O., Karabanov, A., Hartwigsen, G., Thielscher, A., Siebner, H.R., 2016. Combining non-invasive transcranial brain stimulation with neuroimaging and electrophysiology: Current approaches and future perspectives. NeuroImage 140, 4–19. https://doi.org/10.1016/j.neuroimage.2016.02.012

Bergsma, D.P., Elshout, J.A., van der Wildt, G.J., van den Berg, A.V., 2012. Transfer effects of training-induced visual field recovery in patients with chronic stroke. Top. Stroke Rehabil. 19, 212–225. https://doi.org/10.1310/tsr1903-212

Bergsma, D.P., van der Wildt, G., 2010. Visual training of cerebral blindness patients gradually enlarges the visual field. Br. J. Ophthalmol. 94, 88–96. https://doi.org/10.1136/bjo.2008.154336

Bergsma, D.P., Van der Wildt, G.J., 2008. Properties of the regained visual field after visual detection training of hemianopsia patients. Restor. Neurol. Neurosci. 26, 365–375.

Bevilacqua, M., Huxlin, K.R., Hummel, F.C., Raffin, E., 2023. Pathway and directional specificity of Hebbian plasticity in the cortical visual motion processing network. iScience 26, 107064. https://doi.org/10.1016/j.isci.2023.107064

Bigoni, C., Pagnamenta, S., Cadic-Melchior, A., Bevilacqua, M., Harquel, S., Raffin, E., Hummel, F.C., 2024. MEP and TEP features variability: is it just the brain-state? J. Neural Eng. https://doi.org/10.1088/1741-2552/ad1dc2

Bikson, M., Brunoni, A.R., Charvet, L.E., Clark, V.P., Cohen, L.G., Deng, Z.-D., Dmochowski, J., Edwards, D.J., Frohlich, F., Kappenman, E.S., Lim, K.O., Loo, C., Mantovani, A., McMullen, D.P., Parra, L.C., Pearson, M., Richardson, J.D., Rumsey, J.M., Sehatpour, P., Sommers, D., Unal, G., Wassermann, E.M., Woods, A.J., Lisanby, S.H., 2018. Rigor and reproducibility in research with transcranial electrical stimulation: An NIMH-sponsored workshop. Brain Stimulat. 11, 465–480. https://doi.org/10.1016/j.brs.2017.12.008

Blakemore, C., Campbell, F.W., 1969. On the existence of neurones in the human visual system selectively sensitive to the orientation and size of retinal images. J. Physiol. 203, 237–260. https://doi.org/10.1113/jphysiol.1969.sp008862

Blasdel, G.G., Lund, J.S., 1983. Termination of afferent axons in macaque striate cortex. J. Neurosci. Off. J. Soc. Neurosci. 3, 1389–1413.

Bliem, B., Müller-Dahlhaus, J.F.M., Dinse, H.R., Ziemann, U., 2008. Homeostatic metaplasticity in the human somatosensory cortex. J. Cogn. Neurosci. 20, 1517–1528. https://doi.org/10.1162/jocn.2008.20106

Bolognini, N., Rasi, F., Coccia, M., Làdavas, E., 2005. Visual search improvement in hemianopic patients after audio-visual stimulation. Brain J. Neurol. 128, 2830–2842. https://doi.org/10.1093/brain/awh656

Bonder, T., Gopher, D., 2019. The Effect of Confidence Rating on a Primary Visual Task. Front. Psychol. 0. https://doi.org/10.3389/fpsyg.2019.02674

Bonnefond, M., Jensen, O., 2015. Gamma Activity Coupled to Alpha Phase as a Mechanism for Top-Down Controlled Gating. PLOS ONE 10, e0128667. https://doi.org/10.1371/journal.pone.0128667

Bonnefond, M., Kastner, S., Jensen, O., 2017. Communication between Brain Areas Based on Nested Oscillations. eNeuro 4. https://doi.org/10.1523/ENEURO.0153-16.2017

Bosman, C. A. *et al.* Attentional stimulus selection through selective synchronization between monkey visual areas. *Neuron* 75, 875–888 (2012).

Bourgeois, A., Chica, A.B., Valero-Cabré, A., Bartolomeo, P., 2013. Cortical control of Inhibition of Return: exploring the causal contributions of the left parietal cortex. Cortex J. Devoted Study Nerv. Syst. Behav. 49, 2927–2934. https://doi.org/10.1016/j.cortex.2013.08.004

Bowers, A.R., Keeney, K., Peli, E., 2014. Randomized crossover clinical trial of real and sham peripheral prism glasses for hemianopia. JAMA Ophthalmol. 132, 214–222. https://doi.org/10.1001/jamaophthalmol.2013.5636

Breitmeyer, B.G., Kafalıgönül, H., Öğmen, H., Mardon, L., Todd, S., Ziegler, R., 2006. Meta- and paracontrast reveal differences between contour- and brightness-processing mechanisms. Vision Res. 46, 2645–2658. https://doi.org/10.1016/j.visres.2005.10.020

Bressler, S.L., 1996. Interareal synchronization in the visual cortex. Behav. Brain Res., Advances in Understanding Visual Cortex Function 76, 37–49. https://doi.org/10.1016/0166-4328(95)00187-5

Bressler, S.L., Tang, W., Sylvester, C.M., Shulman, G.L., Corbetta, M., 2008. Top-Down Control of Human Visual Cortex by Frontal and Parietal Cortex in Anticipatory Visual Spatial Attention. J. Neurosci. 28, 10056–10061. https://doi.org/10.1523/JNEUROSCI.1776-08.2008

Brickwedde, M., Krüger, M.C., Dinse, H.R., 2019. Somatosensory alpha oscillations gate perceptual learning efficiency. Nat. Commun. 10, 1–9. https://doi.org/10.1038/s41467-018-08012-0

Bridge, H., Thomas, O., Jbabdi, S., Cowey, A., 2008. Changes in connectivity after visual cortical brain damage underlie altered visual function. Brain J. Neurol. 131, 1433–1444. https://doi.org/10.1093/brain/awn063

Briggs, F., 2020. Role of Feedback Connections in Central Visual Processing. Annu. Rev. Vis. Sci. 6, 313–334. https://doi.org/10.1146/annurev-vision-121219-081716

Brignani, D., Ruzzoli, M., Mauri, P., Miniussi, C., 2013. Is Transcranial Alternating Current Stimulation Effective in Modulating Brain Oscillations? PLOS ONE 8, e56589. https://doi.org/10.1371/journal.pone.0056589

Britten, K.H., Newsome, W.T., Shadlen, M.N., Celebrini, S., Movshon, J.A., 1996. A relationship between behavioral choice and the visual responses of neurons in macaque MT. Vis. Neurosci. 13, 87–100. https://doi.org/10.1017/S095252380000715X

Buch, E.R., Johnen, V.M., Nelissen, N., O'Shea, J., Rushworth, M.F.S., 2011. Noninvasive Associative Plasticity Induction in a Corticocortical Pathway of the Human Brain. J. Neurosci. 31, 17669–17679. https://doi.org/10.1523/JNEUROSCI.1513-11.2011

Büchel, C., Friston, K.J., 1997. Modulation of connectivity in visual pathways by attention: cortical interactions evaluated with structural equation modelling and fMRI. Cereb. Cortex N. Y. N 1991 7, 768–778. https://doi.org/10.1093/cercor/7.8.768

Budd, J.M., 1998. Extrastriate feedback to primary visual cortex in primates: a quantitative analysis of connectivity. Proc. R. Soc. B Biol. Sci. 265, 1037–1044.

Bullier, J., 2003. Cortical connections and functional interactions between visual cortical areas, in: Fahle, M., Greenlee, M. (Eds.), The Neuropsychology of Vision. Oxford University Press, p. 0. https://doi.org/10.1093/acprof:oso/9780198505822.003.0002

Buma, F., Kwakkel, G., Ramsey, N., 2013. Understanding upper limb recovery after stroke. Restor. Neurol. Neurosci. 31, 707–722. https://doi.org/10.3233/RNN-130332

Buschman, T.J., Miller, E.K., 2007. Top-down versus bottom-up control of attention in the prefrontal and posterior parietal cortices. Science 315, 1860–1862. https://doi.org/10.1126/science.1138071

Buxbaum, L.J., Ferraro, M.K., Veramonti, T., Farne, A., Whyte, J., Ladavas, E., Frassinetti, F., Coslett, H.B., 2004. Hemispatial neglect. Neurology 62, 749–756. https://doi.org/10.1212/01.WNL.0000113730.73031.F4

Buzsáki, G., 2006. Rhythms of the brain. Oxford University Press, Oxford ; New York.

Buzsáki, G., Draguhn, A., 2004. Neuronal oscillations in cortical networks. Science 304, 1926–1929. https://doi.org/10.1126/science.1099745

Buzsáki, G., Wang, X.-J., 2012. Mechanisms of gamma oscillations. Annu. Rev. Neurosci. 35, 203–225. https://doi.org/10.1146/annurev-neuro-062111-150444

Cabral-Calderin, Y., Wilke, M., 2020. Probing the Link Between Perception and Oscillations: Lessons from Transcranial Alternating Current Stimulation. The Neuroscientist 26, 57–73. https://doi.org/10.1177/1073858419828646

Canolty, R.T., Edwards, E., Dalal, S.S., Soltani, M., Nagarajan, S.S., Kirsch, H.E., Berger, M.S., Barbaro, N.M., Knight, R.T., 2006. High Gamma Power Is Phase-Locked to

Theta Oscillations in Human Neocortex. Science 313, 1626–1628. https://doi.org/10.1126/science.1128115

Canolty, R.T., Knight, R.T., 2010. The functional role of cross-frequency coupling. Trends Cogn. Sci. 14, 506–515. https://doi.org/10.1016/j.tics.2010.09.001

Capilla, A., Schoffelen, J.-M., Paterson, G., Thut, G., Gross, J., 2014. Dissociated α-Band Modulations in the Dorsal and Ventral Visual Pathways in Visuospatial Attention and Perception. Cereb. Cortex N. Y. NY 24, 550–561. https://doi.org/10.1093/cercor/bhs343

Caporale, N., Dan, Y., 2008. Spike Timing–Dependent Plasticity: A Hebbian Learning Rule. Annu. Rev. Neurosci. 31, 25–46. https://doi.org/10.1146/annurev.neuro.31.060407.125639

Carson, R., Kennedy, N., 2013. Modulation of human corticospinal excitability by paired associative stimulation. Front. Hum. Neurosci. 7.

Carter, A.R., Astafiev, S.V., Lang, C.E., Connor, L.T., Rengachary, J., Strube, M.J., Pope, D.L.W., Shulman, G.L., Corbetta, M., 2010. Resting interhemispheric functional magnetic resonance imaging connectivity predicts performance after stroke. Ann. Neurol. 67, 365–375. https://doi.org/10.1002/ana.21905

Casarotto, S., Fecchio, M., Rosanova, M., Varone, G., D'Ambrosio, S., Sarasso, S., Pigorini, A., Russo, S., Comanducci, A., Ilmoniemi, R.J., Massimini, M., 2022. The rt-TEP tool: real-time visualization of TMS-Evoked Potentials to maximize cortical activation and minimize artifacts. J. Neurosci. Methods 370, 109486. https://doi.org/10.1016/j.jneumeth.2022.109486

Castellano, M., Ibanez-Soria, D., Kroupi, E., Acedo, J., Campolo, M., Martinez, X., Soria-Frisch, A., Valls-Sole, J., Verma, A., Ruffini, G., 2017. Occipital tACS bursts during a visual task impact ongoing neural oscillation power, coherence and LZW complexity. bioRxiv 198788. https://doi.org/10.1101/198788

Catani, M., Jones, D.K., Donato, R., 2003. Occipito-temporal connections in the human brain. Brain 2093–2107. https://doi.org/10.1093/brain/awg203

Cavanagh, P., Mather, G., 1989. Motion: the long and short of it. Spat. Vis. 4, 103–129. https://doi.org/10.1163/156856889x00077

Cavanaugh, M.R., Barbot, A., Carrasco, M., Huxlin, K.R., 2017. Feature-based attention potentiates recovery of fine direction discrimination in cortically blind patients. Neuropsychologia. https://doi.org/10.1016/j.neuropsychologia.2017.12.010

Cavanaugh, M.R., Huxlin, K.R., 2017. Visual discrimination training improves Humphrey perimetry in chronic cortically induced blindness. Neurology 88, 1856–1864. https://doi.org/10.1212/WNL.0000000000003921

Cavanaugh, M.R., Zhang, R., Melnick, M.D., Das, A., Roberts, M., Tadin, D., Carrasco, M., Huxlin, K.R., 2015. Visual recovery in cortical blindness is limited by high internal noise. J. Vis. 15, 9. https://doi.org/10.1167/15.10.9

Chacko, R.V., Kim, B., Jung, S.W., Daitch, A.L., Roland, J.L., Metcalf, N.V., Corbetta, M., Shulman, G.L., Leuthardt, E.C., 2018. Distinct phase-amplitude couplings distinguish cognitive processes in human attention. NeuroImage 175, 111–121. https://doi.org/10.1016/j.neuroimage.2018.03.003

Chanes, L., Chica, A.B., Quentin, R., Valero-Cabré, A., 2012. Manipulation of Pre-Target Activity on the Right Frontal Eye Field Enhances Conscious Visual Perception in Humans. PLOS ONE 7, e36232. https://doi.org/10.1371/journal.pone.0036232

Chanes, L., Quentin, R., Tallon-Baudry, C., Valero-Cabré, A., 2013. Causal Frequency-Specific Contributions of Frontal Spatiotemporal Patterns Induced by Non-Invasive Neurostimulation to Human Visual Performance. J. Neurosci. 33, 5000–5005. https://doi.org/10.1523/JNEUROSCI.4401-12.2013

Chanes, L., Quentin, R., Vernet, M., Valero-Cabré, A., 2015. Arrhythmic activity in the left frontal eye field facilitates conscious visual perception in humans. Cortex J. Devoted Study Nerv. Syst. Behav. 71, 240–247. https://doi.org/10.1016/j.cortex.2015.05.016

Chao, C.-C., Karabanov, A.N., Paine, R., Carolina de Campos, A., Kukke, S.N., Wu, T., Wang, H., Hallett, M., 2015. Induction of Motor Associative Plasticity in the Posterior Parietal Cortex-Primary Motor Network. Cereb. Cortex 25, 365–373. https://doi.org/10.1093/cercor/bht230

Chen, C.S., Lee, A.W., Clarke, G., Hayes, A., George, S., Vincent, R., Thompson, A., Centrella, L., Johnson, K., Daly, A., Crotty, M., 2009. Vision-related quality of life in patients with complete homonymous hemianopia post stroke. Top. Stroke Rehabil. 16, 445–453. https://doi.org/10.1310/tsr1606-445

Chey, J., Grossberg, S., Mingolla, E., 1998. Neural dynamics of motion processing and speed discrimination. Vision Res. 38, 2769–2786. https://doi.org/10.1016/S0042-6989(97)00372-6

Chiappini, E., Silvanto, J., Hibbard, P.B., Avenanti, A., Romei, V., 2018. Strengthening functionally specific neural pathways with transcranial brain stimulation. Curr. Biol. 28, R735–R736. https://doi.org/10.1016/j.cub.2018.05.083

Chica, A.B., Bartolomeo, P., Valero-Cabré, A., 2011. Dorsal and Ventral Parietal Contributions to Spatial Orienting in the Human Brain. J. Neurosci. 31, 8143–8149. https://doi.org/10.1523/JNEUROSCI.5463-10.2010

Chicharro, D., 2011. On the spectral formulation of Granger causality. Biol. Cybern. 105, 331–347. https://doi.org/10.1007/s00422-011-0469-z

Childers, D.G., Perry, N.W., 1971. Alpha-like activity in vision. Brain Res. 25, 1–20. https://doi.org/10.1016/0006-8993(71)90563-4

Christiansen, C.M.C., Morten H., 2002. Sequential Learning by Touch, Vision, and Audition, in: Proceedings of the Twenty-Fourth Annual Conference of the Cognitive Science Society. Routledge.

Chubb, C., Sperling, G., 1989. Two motion perception mechanisms revealed through distance-driven reversal of apparent motion. Proc. Natl. Acad. Sci. U. S. A. 86, 2985–2989.

Colby, C.L., Goldberg, M.E., 1999. Space and attention in parietal cortex. Annu. Rev. Neurosci. 22, 319–349. https://doi.org/10.1146/annurev.neuro.22.1.319

Colgin, L.L., Denninger, T., Fyhn, M., Hafting, T., Bonnevie, T., Jensen, O., Moser, M.-B., Moser, E.I., 2009. Frequency of gamma oscillations routes flow of information in the hippocampus. Nature 462, 353–357. https://doi.org/10.1038/nature08573

Collins, F.S., Varmus, H., 2015. A new initiative on precision medicine. N. Engl. J. Med. 372, 793–795. https://doi.org/10.1056/NEJMp1500523

Cowey, A., Alexander, I., Stoerig, P., 2008. A blindsight conundrum: How to respond when there is no correct response. Neuropsychologia, Consciousness and Perception: Insights and Hindsights 46, 870–878. https://doi.org/10.1016/j.neuropsychologia.2007.11.031

Cowey, A., Walsh, V., 2001. Chapter 26 Tickling the brain: studying visual sensation, perception and cognition by transcranial magnetic stimulation, in: Progress in Brain Research. Elsevier, pp. 411–425. https://doi.org/10.1016/S0079-6123(01)34027-X

Cowey, A., Walsh, V., 2000. Magnetically induced phosphenes in sighted, blind and blindsighted observers. NeuroReport 11, 5.

Cramer, S.C., 2008. Repairing the human brain after stroke: I. Mechanisms of spontaneous recovery. Ann. Neurol. 63, 272–287. https://doi.org/10.1002/ana.21393

Darian-Smith, C., Gilbert, C.D., 1994. Axonal sprouting accompanies functional reorganization in adult cat striate cortex. Nature 368, 737–740. https://doi.org/10.1038/368737a0

Das, A., DeMagistris, M., Huxlin, K.R., 2012. Different Properties of Visual Relearning after Damage to Early Versus Higher-Level Visual Cortical Areas. J. Neurosci. 32, 5414–5425. https://doi.org/10.1523/JNEUROSCI.0316-12.2012

Das, A., Tadin, D., Huxlin, K.R., 2014. Beyond blindsight: properties of visual relearning in cortically blind fields. J. Neurosci. Off. J. Soc. Neurosci. 34, 11652–11664. https://doi.org/10.1523/JNEUROSCI.1076-14.2014

de Haan, G.A., Heutink, J., Melis-Dankers, B.J.M., Brouwer, W.H., Tucha, O., 2015. Difficulties in Daily Life Reported by Patients With Homonymous Visual Field Defects. J. Neuroophthalmol. 35, 259. https://doi.org/10.1097/WNO.0000000000000244

DeAngelis, G.C., Freeman, R.D., Ohzawa, I., 1994. Length and width tuning of neurons in the cat's primary visual cortex. J. Neurophysiol. 71, 347–374. https://doi.org/10.1152/jn.1994.71.1.347

DeAngelis, G.C., Ohzawa, I., Freeman, R.D., 1995. Receptive-field dynamics in the central visual pathways. Trends Neurosci. 18, 451–458. https://doi.org/10.1016/0166-2236(95)94496-r

Delorme, A., Makeig, S., 2004. EEGLAB: an open source toolbox for analysis of single-trial EEG dynamics including independent component analysis. J. Neurosci. Methods 134, 9–21. https://doi.org/10.1016/j.jneumeth.2003.10.009

Desimone, R., Albright, T.D., Gross, C.G., Bruce, C., 1984. Stimulus-selective properties of inferior temporal neurons in the macaque. J. Neurosci. Off. J. Soc. Neurosci. 4, 2051–2062. https://doi.org/10.1523/JNEUROSCI.04-08-02051.1984

Desimone, R., U., L.G., 1989. Neural Mechanisms of Visual Processing in Monkeys, in: Handbook of Neuropsychology. Elsevier Science, New York, pp. 267–299.

Di, X., Biswal, B.B., 2013. Modulatory Interactions of Resting-State Brain Functional Connectivity. PloS one 8, e71163. https://doi.org/10.1371/journal.pone.0071163

Di Lazzaro, V., Rothwell, J., Capogna, M., 2018. Noninvasive Stimulation of the Human Brain: Activation of Multiple Cortical Circuits. The Neuroscientist 24, 246–260. https://doi.org/10.1177/1073858417717660

Di Luzio, P., Tarasi, L., Silvanto, J., Avenanti, A., Romei, V., 2022. Human perceptual and metacognitive decision-making rely on distinct brain networks. PLOS Biol. 20, e3001750. https://doi.org/10.1371/journal.pbio.3001750

Dundon, N.M., Bertini, C., Làdavas, E., Sabel, B.A., Gall, C., 2015. Visual rehabilitation: visual scanning, multisensory stimulation and vision restoration trainings. Front. Behav. Neurosci. 9, 144157. https://doi.org/10.3389/fnbeh.2015.00192

Eckhorn, R., Bauer, R., Jordan, W., Brosch, M., Kruse, W., Munk, M., Reitboeck, H.J., 1988. Coherent oscillations: A mechanism of feature linking in the visual cortex? Biol. Cybern. 60, 121–130. https://doi.org/10.1007/BF00202899

Ekstrom, L.B., Roelfsema, P.R., Arsenault, J.T., Bonmassar, G., Vanduffel, W., 2008. Bottom-Up Dependent Gating of Frontal Signals in Early Visual Cortex. Science 321, 414–417. https://doi.org/10.1126/science.1153276

Ellison, A., Battelli, L., Cowey, A., Walsh, V., 2003. The effect of expectation on facilitation of colour/form conjunction tasks by TMS over area V5. Neuropsychologia 41, 1794–1801. https://doi.org/10.1016/S0028-3932(03)00180-5

Elshout, J.A., van Asten, F., Hoyng, C.B., Bergsma, D.P., van den Berg, A.V., 2016. Visual Rehabilitation in Chronic Cerebral Blindness: A Randomized Controlled Crossover Study. Front. Neurol. 7.

Engel, A.K., Fries, P., 2010. Beta-band oscillations--signalling the status quo? Curr. Opin. Neurobiol. 20, 156–165. https://doi.org/10.1016/j.conb.2010.02.015

Engel, A.K., Roelfsema, P.R., Fries, P., Brecht, M., Singer, W., 1997. Role of the temporal domain for response selection and perceptual binding. Cereb. Cortex N. Y. N 1991 7, 571–582. https://doi.org/10.1093/cercor/7.6.571

Fahrenthold, B.K., Cavanaugh, M.R., Jang, S., Murphy, A.J., Ajina, S., Bridge, H., Huxlin, K.R., 2021. Optic Tract Shrinkage Limits Visual Restoration After Occipital Stroke. Stroke 52, 3642–3650. https://doi.org/10.1161/STROKEAHA.121.034738

Fehér, K.D., Nakataki, M., Morishima, Y., 2017. Phase-Dependent Modulation of Signal Transmission in Cortical Networks through tACS-Induced Neural Oscillations. Front. Hum. Neurosci. 11, 471. https://doi.org/10.3389/fnhum.2017.00471

Feigin, V.L., Brainin, M., Norrving, B., Martins, S., Sacco, R.L., Hacke, W., Fisher, M., Pandian, J., Lindsay, P., 2022. World Stroke Organization (WSO): Global Stroke Fact Sheet 2022. Int. J. Stroke Off. J. Int. Stroke Soc. 17, 18–29. https://doi.org/10.1177/17474930211065917

Felleman, D.J., Van Essen, D.C., 1991. Distributed hierarchical processing in the primate cerebral cortex. Cereb. Cortex N. Y. N 1991 1, 1–47. https://doi.org/10.1093/cercor/1.1.1

Felleman, D.J., Van Essen, D.C., 1987. Receptive field properties of neurons in area V3 of macaque monkey extrastriate cortex. J. Neurophysiol. 57, 889–920. https://doi.org/10.1152/jn.1987.57.4.889

Fiori, F., Chiappini, E., Avenanti, A., 2018. Enhanced action performance following TMS manipulation of associative plasticity in ventral premotor-motor pathway. NeuroImage 183, 847–858. https://doi.org/10.1016/j.neuroimage.2018.09.002

Fischl, B., 2012. FreeSurfer. NeuroImage, 20 YEARS OF fMRI 62, 774–781. https://doi.org/10.1016/j.neuroimage.2012.01.021

Fischman, M.W., Meikle, T.H., 1965. Visual intensity discrimination in cats after serial tectal and cortical lesions. J. Comp. Physiol. Psychol. 59, 193–201. https://doi.org/10.1037/h0021811

Foster, J.J., Awh, E., 2019. The role of alpha oscillations in spatial attention: Limited evidence for a suppression account. Curr. Opin. Psychol. 29, 34–40. https://doi.org/10.1016/j.copsyc.2018.11.001

Franciotti, R., Falasca, N., 2018. The reliability of conditional Granger causality analysis in the time domain. https://doi.org/10.7287/peerj.preprints.26703

Fries, P., 2015. Rhythms for Cognition: Communication through Coherence. Neuron 88, 220–235. https://doi.org/10.1016/j.neuron.2015.09.034

Fries, P., 2009. Neuronal Gamma-Band Synchronization as a Fundamental Process in Cortical Computation. Annu. Rev. Neurosci. 32, 209–224. https://doi.org/10.1146/annurev.neuro.051508.135603

Fries, P., 2005. A mechanism for cognitive dynamics: neuronal communication through neuronal coherence. Trends Cogn. Sci. 9, 474–480. https://doi.org/10.1016/j.tics.2005.08.011

Fries, P., Reynolds, J.H., Rorie, A.E., Desimone, R., 2001. Modulation of Oscillatory Neuronal Synchronization by Selective Visual Attention. Science 291, 1560–1563. https://doi.org/10.1126/science.1055465

Friston, K.J., Buechel, C., Fink, G.R., Morris, J., Rolls, E., Dolan, R.J., 1997. Psychophysiological and modulatory interactions in neuroimaging. Neuroimage 6, 218–229. https://doi.org/10.1006/nimg.1997.0291

Friston, K.J., Stephan, K.E., Montague, R., Dolan, R.J., 2014. Computational psychiatry: the brain as a phantastic organ. Lancet Psychiatry 1, 148–158. https://doi.org/10.1016/S2215-0366(14)70275-5

Gallina, J., Pietrelli, M., Zanon, M., Bertini, C., 2022. Hemispheric differences in altered reactivity of brain oscillations at rest after posterior lesions. Brain Struct. Funct. 227, 709–723. https://doi.org/10.1007/s00429-021-02279-8

Gamberini, M., Bakola, S., Passarelli, L., Burman, K.J., Rosa, M.G.P., Fattori, P., Galletti, C., 2016. Thalamic projections to visual and visuomotor areas (V6 and V6A) in the Rostral Bank of the parieto-occipital sulcus of the Macaque. Brain Struct. Funct. 221, 1573–1589. https://doi.org/10.1007/s00429-015-0990-2

Gavaret, M., Ayache, S.S., Mylius, V., Mhalla, A., Chalah, M.A., Lefaucheur, J.-P., 2018. A reappraisal of pain-paired associative stimulation suggesting motor inhibition at spinal level. Neurophysiol. Clin. 48, 295–302. https://doi.org/10.1016/j.neucli.2018.04.003

GBD 2019 Stroke Collaborators, 2021. Global, regional, and national burden of stroke and its risk factors, 1990-2019: a systematic analysis for the Global Burden of Disease Study 2019. Lancet Neurol. 20, 795–820. https://doi.org/10.1016/S1474-4422(21)00252-0

Geesaman, B.J., Born, R.T., Andersen, R.A., Tootell, R.B., 1997. Maps of complex motion selectivity in the superior temporal cortex of the alert macaque monkey: a double-label 2-deoxyglucose study. Cereb. Cortex N. Y. N 1991 7, 749–757. https://doi.org/10.1093/cercor/7.8.749

Gerwig, M., Kastrup, O., Meyer, B.-U., Niehaus, L., 2003. Evaluation of cortical excitability by motor and phosphene thresholds in transcranial magnetic stimulation. J. Neurol. Sci. 215, 75–78. https://doi.org/10.1016/S0022-510X(03)00228-4

Gibson, E.J., 1963. Perceptual Learning. Annu. Rev. Psychol. 14, 29–56. https://doi.org/10.1146/annurev.ps.14.020163.000333

Gibson, J.J., 1950. The perception of the visual world, The perception of the visual world. Houghton Mifflin, Oxford, England.

Gielen, S., Krupa, M., Zeitler, M., 2010. Gamma oscillations as a mechanism for selective information transmission. Biol. Cybern. 103, 151–165. https://doi.org/10.1007/s00422-010-0390-x

Gilbert, C.D., Li, W., 2013. Top-down influences on visual processing. Nat. Rev. Neurosci. 14. https://doi.org/10.1038/nrn3476

Gilson, L., Ellokor, S., Lehmann, U., Brady, L., 2020. Organizational change and everyday health system resilience: Lessons from Cape Town, South Africa. Soc. Sci. Med. 1982 266, 113407. https://doi.org/10.1016/j.socscimed.2020.113407

Gizzi, M.S., Katz, E., Schumer, R.A., Movshon, J.A., 1990. Selectivity for orientation and direction of motion of single neurons in cat striate and extrastriate visual cortex. J. Neurophysiol. 63, 1529–1543. https://doi.org/10.1152/jn.1990.63.6.1529

Goetz, S.M., Deng, Z.-D., 2017. The development and modelling of devices and paradigms for transcranial magnetic stimulation. Int. Rev. Psychiatry 29, 115–145. https://doi.org/10.1080/09540261.2017.1305949

Gold, J.I., Shadlen, M.N., 2007. The Neural Basis of Decision Making. Annu. Rev. Neurosci. 30, 535–574. https://doi.org/10.1146/annurev.neuro.29.051605.113038

Goodale, M.A., Milner, A.D., 1992. Separate visual pathways for perception and action. Trends Neurosci. 15, 20–25. https://doi.org/10.1016/0166-2236(92)90344-8

Goodale, M.A., Milner, A.D., Jakobson, L.S., Carey, D.P., 1991. A neurological dissociation between perceiving objects and grasping them. Nature 349, 154–156. https://doi.org/10.1038/349154a0

Goodwin, D., 2014. Homonymous hemianopia: challenges and solutions. Clin. Ophthalmol. 1919. https://doi.org/10.2147/OPTH.S59452

Gorgoni, M., Ferlazzo, F., D'Atri, A., Lauri, G., Ferrara, M., Rossini, P.M., Gennaro, L.D., 2015. The assessment of somatosensory cortex plasticity during sleep deprivation by paired associative stimulation. Arch. Ital. Biol. 153, 110–123. https://doi.org/10.4449/aib.v153i2-3.3943

Gramfort, A., Luessi, M., Larson, E., Engemann, D., Strohmeier, D., Brodbeck, C., Goj, R., Jas, M., Brooks, T., Parkkonen, L., Hämäläinen, M., 2013. MEG and EEG data analysis with MNE-Python. Front. Neurosci. 7.

Gramfort, A., Papadopoulo, T., Olivi, E., Clerc, M., 2010. OpenMEEG: opensource software for quasistatic bioelectromagnetics. Biomed. Eng. Online 9, 45. https://doi.org/10.1186/1475-925X-9-45

Gray, C.M., König, P., Engel, A.K., Singer, W., 1989. Oscillatory responses in cat visual cortex exhibit inter-columnar synchronization which reflects global stimulus properties. Nature 338, 334–337. https://doi.org/10.1038/338334a0

Gray, C.M., Singer, W., 1989. Stimulus-specific neuronal oscillations in orientation columns of cat visual cortex. Proc. Natl. Acad. Sci. 86, 1698–1702. https://doi.org/10.1073/pnas.86.5.1698

Grefkes, C., Fink, G.R., 2005. REVIEW: The functional organization of the intraparietal sulcus in humans and monkeys. J. Anat. 207, 3–17. https://doi.org/10.1111/j.1469-7580.2005.00426.x

Grothe, I., Neitzel, S.D., Mandon, S., Kreiter, A.K., 2012. Switching Neuronal Inputs by Differential Modulations of Gamma-Band Phase-Coherence. J. Neurosci. 32, 16172–16180. https://doi.org/10.1523/JNEUROSCI.0890-12.2012

Grunda, T., Marsalek, P., Sykorova, P., 2013. Homonymous hemianopia and related visual defects: Restoration of vision after a stroke. Acta Neurobiol. Exp. (Warsz.) 73, 13.

Guggisberg, A.G., Koch, P.J., Hummel, F.C., Buetefisch, C.M., 2019. Brain networks and their relevance for stroke rehabilitation. Clin. Neurophysiol. 130, 1098–1124. https://doi.org/10.1016/j.clinph.2019.04.004

Guidali, G., Roncoroni, C., Bolognini, N., 2021. Paired associative stimulations: Novel tools for interacting with sensory and motor cortical plasticity. Behav. Brain Res. 414, 113484. https://doi.org/10.1016/j.bbr.2021.113484

Guzzetta, A., D'acunto, G., Rose, S., Tinelli, F., Boyd, R., Cioni, G., 2010. Plasticity of the visual system after early brain damage. Dev. Med. Child Neurol. 52, 891–900. https://doi.org/10.1111/j.1469-8749.2010.03710.x

Haegens, S., Osipova, D., Oostenveld, R., Jensen, O., 2010. Somatosensory working memory performance in humans depends on both engagement and disengagement of regions in a distributed network. Hum. Brain Mapp. 31, 26–35. https://doi.org/10.1002/hbm.20842

Hagan, M.A., Chaplin, T.A., Huxlin, K.R., Rosa, M.G.P., Lui, L.L., 2020. Altered Sensitivity to Motion of Area MT Neurons Following Long-Term V1 Lesions. Cereb. Cortex N. Y. NY 30, 451–464. https://doi.org/10.1093/cercor/bhz096

Hagen, M.C., Franzén, O., McGlone, F., Essick, G., Dancer, C., Pardo, J.V., 2002. Tactile motion activates the human middle temporal/V5 (MT/V5) complex. Eur. J. Neurosci. 16, 957–964. https://doi.org/10.1046/j.1460-9568.2002.02139.x

Han, B., Zhang, Y., Shen, L., Mo, L., Chen, Q., 2023. Task demands modulate pre-stimulus alpha frequency and sensory template during bistable apparent motion perception. Cereb. Cortex 33, 1679–1692. https://doi.org/10.1093/cercor/bhac165

Händel, B., Lutzenberger, W., Thier, P., Haarmeier, T., 2007. Opposite Dependencies on Visual Motion Coherence in Human Area MT+ and Early Visual Cortex. Cereb. Cortex 17, 1542–1549. https://doi.org/10.1093/cercor/bhl063

Hanslmayr, S., Staudigl, T., Fellner, M.-C., 2012. Oscillatory power decreases and long-term memory: the information via desynchronization hypothesis. Front. Hum. Neurosci. 6.

He, Q., Zhu, X., Fang, F., 2023. Enhancing visual perceptual learning using transcranial electrical stimulation: Transcranial alternating current stimulation outperforms both transcranial direct current and random noise stimulation. J. Vis. 23, 2. https://doi.org/10.1167/jov.23.14.2

Helfrich, R.F., Knepper, H., Nolte, G., Strüber, D., Rach, S., Herrmann, C.S., Schneider, T.R., Engel, A.K., 2014. Selective modulation of interhemispheric functional connectivity by HD-tACS shapes perception. PLoS Biol. 12, e1002031. https://doi.org/10.1371/journal.pbio.1002031

Hepworth, L., Rowe, F., Walker, M., Rockliffe, J., Noonan, C., Howard, C., Currie, J., 2015. Post-stroke visual impairment: a systematic literature review of types and recovery of visual conditions. Ophthalmol. Res. Int. J. 5. https://doi.org/10.9734/OR/2016/21767

Hernandez-Pavon, J.C., Veniero, D., Bergmann, T.O., Belardinelli, P., Bortoletto, M., Casarotto, S., Casula, E.P., Farzan, F., Fecchio, M., Julkunen, P., Kallioniemi, E.,

Lioumis, P., Metsomaa, J., Miniussi, C., Mutanen, T.P., Rocchi, L., Rogasch, N.C., Shafi, M.M., Siebner, H.R., Thut, G., Zrenner, C., Ziemann, U., Ilmoniemi, R.J., 2023. TMS combined with EEG: Recommendations and open issues for data collection and analysis. Brain Stimulat. 16, 567–593. https://doi.org/10.1016/j.brs.2023.02.009

Héroux, M.E., Loo, C.K., Taylor, J.L., Gandevia, S.C., 2017. Questionable science and reproducibility in electrical brain stimulation research. PLOS ONE 12, e0175635. https://doi.org/10.1371/journal.pone.0175635

Herpich, F., Melnick, M.D., Agosta, S., Huxlin, K.R., Tadin, D., Battelli, L., 2019. Boosting Learning Efficacy with Noninvasive Brain Stimulation in Intact and Brain-Damaged Humans. J. Neurosci. Off. J. Soc. Neurosci. 39, 5551–5561. https://doi.org/10.1523/JNEUROSCI.3248-18.2019

Hinds, O., Polimeni, J.R., Rajendran, N., Balasubramanian, M., Amunts, K., Zilles, K., Schwartz, E.L., Fischl, B., Triantafyllou, C., 2009. Locating the functional and anatomical boundaries of human primary visual cortex. NeuroImage 46, 915–922. https://doi.org/10.1016/j.neuroimage.2009.03.036

Holmes, G., 1918. DISTURBANCES OF VISUAL ORIENTATION. Br. J. Ophtalmol. 2, 506–516.

Hordacre, B., Goldsworthy, M.R., Welsby, E., Graetz, L., Ballinger, S., Hillier, S., 2020. Resting State Functional Connectivity Is Associated With Motor Pathway Integrity and Upper-Limb Behavior in Chronic Stroke. Neurorehabil. Neural Repair 34, 547–557. https://doi.org/10.1177/1545968320921824

Horton, J.C., 2005. Disappointing results from Nova Vision's visual restoration therapy. Br. J. Ophthalmol. 89, 1–2. https://doi.org/10.1136/bjo.2004.058214

Howard, C., Rowe, F.J., 2018. Adaptation to poststroke visual field loss: A systematic review. Brain Behav. 8, e01041. https://doi.org/10.1002/brb3.1041

Hsu, T.-Y., Chen, J.-T., Tseng, P., Wang, C.-A., 2021. Role of the frontal eye field in human microsaccade responses: A TMS study. Biol. Psychol. 165, 108202. https://doi.org/10.1016/j.biopsycho.2021.108202

Hubel, D.H., Wiesel, T.N., 1968. Receptive fields and functional architecture of monkey striate cortex. J. Physiol. 195, 215–243. https://doi.org/10.1113/jphysiol.1968.sp008455

Hubel, D.H., Wiesel, T.N., 1962. Receptive fields, binocular interaction and functional architecture in the cat's visual cortex. J. Physiol. 160, 106–154. https://doi.org/10.1113/jphysiol.1962.sp006837

Huk, A.C., Katz, L.N., Yates, J.L., 2017. The Role of the Lateral Intraparietal Area in (the Study of) Decision Making. Annu. Rev. Neurosci. 40, 349–372. https://doi.org/10.1146/annurev-neuro-072116-031508

Hummel, F., Gerloff, C., 2005. Larger Interregional Synchrony is Associated with Greater Behavioral Success in a Complex Sensory Integration Task in Humans. Cereb. Cortex 15, 670–678. https://doi.org/10.1093/cercor/bhh170

Hupé, J.M., James, A.C., Girard, P., Lomber, S.G., Payne, B.R., Bullier, J., 2001. Feedback connections act on the early part of the responses in monkey visual cortex. J. Neurophysiol. 85, 134–145. https://doi.org/10.1152/jn.2001.85.1.134

Huxlin, K.R., 2008. Perceptual plasticity in damaged adult visual systems. Vision Res., Vision Research Reviews 48, 2154–2166. https://doi.org/10.1016/j.visres.2008.05.022

Huxlin, K.R., 2004. Training-induced Recovery of Visual Motion Perception after Extrastriate Cortical Damage in the Adult Cat. Cereb. Cortex 14, 81–90. https://doi.org/10.1093/cercor/bhg106

Huxlin, K.R., Hayhoe, M.M., Pelz, J.B., 2009a. Systems and methods for improving visual discrimination. US7549743B2.

Huxlin, K.R., Martin, T., Kelly, K., Riley, M., Friedman, D.I., Burgin, W.S., Hayhoe, M., 2009b. Perceptual Relearning of Complex Visual Motion after V1 Damage in Humans. J. Neurosci. 29, 3981–3991. https://doi.org/10.1523/JNEUROSCI.4882-08.2009

Ilg, U.J., 2008. The role of areas MT and MST in coding of visual motion underlying the execution of smooth pursuit. Vision Res. 48, 2062–2069. https://doi.org/10.1016/j.visres.2008.04.015

Jackson, A., Mavoori, J., Fetz, E.E., 2006. Long-term motor cortex plasticity induced by an electronic neural implant 444, 5.

Jacobson, S.G., Eames, R.A., McDonald, W.I., 1979. Optic nerve fibre lesions in adult cats: Pattern of recovery of spatial vision. Exp. Brain Res. 36. https://doi.org/10.1007/BF00238518

Jacques, C., Jonas, J., Colnat-Coulbois, S., Maillard, L., Rossion, B., 2022. Low and high frequency intracranial neural signals match in the human associative cortex. eLife 11, e76544. https://doi.org/10.7554/eLife.76544

Jenkinson, M., Beckmann, C.F., Behrens, T.E.J., Woolrich, M.W., Smith, S.M., 2012. FSL. NeuroImage 62, 782–790. https://doi.org/10.1016/j.neuroimage.2011.09.015

Jensen, O., Mazaheri, A., 2010. Shaping Functional Architecture by Oscillatory Alpha Activity: Gating by Inhibition. Front. Hum. Neurosci. 4. https://doi.org/10.3389/fnhum.2010.00186

Kaas, J.H., Lyon, D.C., 2007. Pulvinar contributions to the dorsal and ventral streams of visual processing in primates. Brain Res. Rev. 55, 285–296. https://doi.org/10.1016/j.brainresrev.2007.02.008

Kafaligonul, H., Breitmeyer, B.G., Öğmen, H., 2015. Feedforward and feedback processes in vision. Front. Psychol. 6. https://doi.org/10.3389/fpsyg.2015.00279

Kandel, E., 2014. Visual Processing and Action, in: Principles of Neural Science. McGraw-Hill Education, New York, NY.

Kar, K., Krekelberg, B., 2014. Transcranial Alternating Current Stimulation Attenuates Visual Motion Adaptation. J. Neurosci. 34, 7334–7340. https://doi.org/10.1523/JNEUROSCI.5248-13.2014

Karabanov, A., Thielscher, A., Siebner, H.R., 2016. Transcranial brain stimulation: closing the loop between brain and stimulation. Curr. Opin. Neurol. 29, 397–404. https://doi.org/10.1097/WCO.0000000000000342

Kasten, E., Bunzenthal, U., Sabel, B.A., 2006. Visual field recovery after vision restoration therapy (VRT) is independent of eye movements: An eye tracker study. Behav. Brain Res. 175, 18–26. https://doi.org/10.1016/j.bbr.2006.07.024

Kearney-Ramos, T., Lench, D., Hoffman, M., Correia, B., Dowdle, L., Hanlon, C., 2018. Gray and white matter integrity influence TMS signal propagation: A multimodal evaluation in cocaine-dependent individuals. Sci. Rep. 8. https://doi.org/10.1038/s41598-018-21634-0

Keil, A., Sabatinelli, D., Ding, M., Lang, P.J., Ihssen, N., Heim, S., 2009. Re-entrant projections modulate visual cortex in affective perception: Evidence from Granger causality analysis. Hum. Brain Mapp. 30, 532–540. https://doi.org/10.1002/hbm.20521

Khan, A., Mosbacher, J.A., Vogel, S.E., Binder, M., Wehovz, M., Moshammer, A., Halverscheid, S., Pustelnik, K., Nitsche, M.A., Tong, R.K.-Y., Grabner, R.H., 2023. Modulation of resting-state networks following repetitive transcranial alternating current stimulation of the dorsolateral prefrontal cortex. Brain Struct. Funct. 228, 1643–1655. https://doi.org/10.1007/s00429-023-02667-2

Kim, S.Y., Kim, E.-K., Song, H., Cheon, J.-E., Kim, B.N., Kim, H.-S., Shin, S.H., 2023. Association of Brain Microstructure and Functional Connectivity With Cognitive Outcomes and Postnatal Growth Among Early School–Aged Children Born With Extremely Low Birth Weight. JAMA Netw. Open 6, e230198. https://doi.org/10.1001/jamanetworkopen.2023.0198

Kim, U.S., Mahroo, O.A., Mollon, J.D., Yu-Wai-Man, P., 2021. Retinal Ganglion Cells—Diversity of Cell Types and Clinical Relevance. Front. Neurol. 12, 661938. https://doi.org/10.3389/fneur.2021.661938

King, A.J., 1993. Multisensory Integration: The Merging of the Senses. Barry E. Stein and M. Alex Meredith. MIT Press, Cambridge, MA, 1993. xvi, 211 pp., illus. $42.50 or £38.25. Cognitive Neuroscience Series. Science 261, 928–929. https://doi.org/10.1126/science.261.5123.928

Klinge, C., Eippert, F., Röder, B., Büchel, C., 2010. Corticocortical Connections Mediate Primary Visual Cortex Responses to Auditory Stimulation in the Blind. J. Neurosci. 30, 12798–12805. https://doi.org/10.1523/JNEUROSCI.2384-10.2010

Klöppel, S., Lauer, E., Peter, J., Minkova, L., Nissen, C., Normann, C., Reis, J., Mainberger, F., Bach, M., Lahr, J., 2015. LTP-like plasticity in the visual system and in the motor system appear related in young and healthy subjects. Front. Hum. Neurosci. 9. https://doi.org/10.3389/fnhum.2015.00506

Klüver, H., 1941. Visual Functions After Removal of the Occipital Lobes. J. Psychol. 11, 23–45. https://doi.org/10.1080/00223980.1941.9917017

Klüver, H., 1937. Certain Effects of Lesions of the Occipital Lobes in Macaques. J. Psychol. 4, 383–401. https://doi.org/10.1080/00223980.1937.9917546

Koch, G., 2020. Cortico-cortical connectivity: the road from basic neurophysiological interactions to therapeutic applications. Exp. Brain Res. 238, 1677–1684. https://doi.org/10.1007/s00221-020-05844-5

Koch, G., Ponzo, V., Di Lorenzo, F., Caltagirone, C., Veniero, D., 2013. Hebbian and Anti-Hebbian Spike-Timing-Dependent Plasticity of Human Cortico-Cortical Connections. J. Neurosci. 33, 9725–9733. https://doi.org/10.1523/JNEUROSCI.4988-12.2013

Kolb, H., 2003. How the Retina Works: Much of the construction of an image takes place in the retina itself through the use of specialized neural circuits. Am. Sci. 91, 28–35.

Kraft, A., Roehmel, J., Olma, M.C., Schmidt, S., Irlbacher, K., Brandt, S.A., 2010. Transcranial direct current stimulation aVects visual perception measured by threshold perimetry. Exp Brain Res 8.

Kravitz, D.J., Saleem, K.S., Baker, C.I., Mishkin, M., 2011. A new neural framework for visuospatial processing. Nat. Rev. Neurosci. 12, 217–230. https://doi.org/10.1038/nrn3008

Krit, M., Gaudoin, O., Remy, E., 2021. Goodness-of-fit tests for the Weibull and extreme value distributions: A review and comparative study. Commun. Stat. - Simul. Comput. 50, 1888–1911. https://doi.org/10.1080/03610918.2019.1594292

Krug, K., Cicmil, N., Parker, A.J., Cumming, B.G., 2013. A Causal Role for V5/MT Neurons Coding Motion-Disparity Conjunctions in Resolving Perceptual Ambiguity. Curr. Biol. 23, 1454–1459. https://doi.org/10.1016/j.cub.2013.06.023

Kuriakose, D., Xiao, Z., 2020. Pathophysiology and Treatment of Stroke: Present Status and Future Perspectives. Int. J. Mol. Sci. 21, 7609. https://doi.org/10.3390/ijms21207609

Kveraga, K., Ghuman, A.S., Bar, M., 2007. Top-down predictions in the cognitive brain. Brain Cogn. 65, 145–168. https://doi.org/10.1016/j.bandc.2007.06.007

Laczó, B., Antal, A., Niebergall, R., Treue, S., Paulus, W., 2012. Transcranial alternating stimulation in a high gamma frequency range applied over V1 improves contrast perception but does not modulate spatial attention. Brain Stimulat. 5, 484–491. https://doi.org/10.1016/j.brs.2011.08.008

Lagae, L., Raiguel, S., Orban, G.A., 1993. Speed and direction selectivity of macaque middle temporal neurons. J. Neurophysiol. 69, 19–39. https://doi.org/10.1152/jn.1993.69.1.19

Lage-Castellanos, Agustín, Martínez-Montes, E., Hernández-Cabrera, J.A., Galán, L., 2009. False discovery rate and permutation test: An evaluation in ERP data analysis 12.

Lage-Castellanos, Alejandro, Pagnani, A., Weigt, M., 2009. Statistical mechanics of sparse generalization and graphical model selection. J. Stat. Mech. Theory Exp. 2009, P10009. https://doi.org/10.1088/1742-5468/2009/10/P10009

Lamme, V.A., Supèr, H., Spekreijse, H., 1998. Feedforward, horizontal, and feedback processing in the visual cortex. Curr. Opin. Neurobiol. 8, 529–535. https://doi.org/10.1016/S0959-4388(98)80042-1

Lamme, V.A.F., Roelfsema, P.R., 2000. The distinct modes of vision offered by feedforward and recurrent processing. Trends Neurosci. 23, 571–579. https://doi.org/10.1016/S0166-2236(00)01657-X

Lawrence, S.J., Norris, D.G., de Lange, F.P., 2019. Dissociable laminar profiles of concurrent bottom-up and top-down modulation in the human visual cortex. eLife 8, e44422. https://doi.org/10.7554/eLife.44422

Laycock, R., Crewther, D.P., Fitzgerald, P.B., Crewther, S.G., 2007. Evidence for Fast Signals and Later Processing in Human V1/V2 and V5/MT+: A TMS Study of Motion Perception. J. Neurophysiol. 98, 1253–1262. https://doi.org/10.1152/jn.00416.2007

Lazari, A., Salvan, P., Cottaar, M., Papp, D., Rushworth, M.F.S., Johansen-Berg, H., 2022. Hebbian activity-dependent plasticity in white matter. Cell Rep. 39, 110951. https://doi.org/10.1016/j.celrep.2022.110951

Ledgeway, T., Smith, A.T., 1994. Evidence for separate motion-detecting mechanisms for first- and second-order motion in human vision. Vision Res. 34, 2727–2740. https://doi.org/10.1016/0042-6989(94)90229-1

Liu, NJ, V., Galetta, SL, 2001. Retrochiasmal disorders, in: Neuro-Ophthalmology: Diagnosis and Management. Philadelphia, p. 296.

Livingstone, M.S., Hubel, D.H., 1984. Specificity of intrinsic connections in primate primary visual cortex. J. Neurosci. Off. J. Soc. Neurosci. 4, 2830–2835.

Llinás, R., Yarom, Y., 1986. Oscillatory properties of guinea-pig inferior olivary neurones and their pharmacological modulation: an in vitro study. J. Physiol. 376, 163–182. https://doi.org/10.1113/jphysiol.1986.sp016147

Lobier, M., Palva, J.M., Palva, S., 2018. High-alpha band synchronization across frontal, parietal and visual cortex mediates behavioral and neuronal effects of visuospatial attention. NeuroImage 165, 222–237. https://doi.org/10.1016/j.neuroimage.2017.10.044

López-Alonso, V., Cheeran, B., Río-Rodríguez, D., Fernández-Del-Olmo, M., 2014. Inter-individual variability in response to non-invasive brain stimulation paradigms. Brain Stimulat. 7, 372–380. https://doi.org/10.1016/j.brs.2014.02.004

Ma, X., Tang, L., Chen, X., Zeng, L., 2021. Periphery kinetic perimetry: clinically feasible to complement central static perimetry. BMC Ophthalmol. 21, 343. https://doi.org/10.1186/s12886-021-02056-5

Magee, J.C., 1997. A Synaptically Controlled, Associative Signal for Hebbian Plasticity in Hippocampal Neurons. Science 275, 209–213. https://doi.org/10.1126/science.275.5297.209

Maniglia, M., Cottereau, B.R., Soler, V., Trotter, Y., 2016. Rehabilitation Approaches in Macular Degeneration Patients. Front. Syst. Neurosci. 10. https://doi.org/10.3389/fnsys.2016.00107

Marcar, V.L., Cowey, A., 1992. The Effect of Removing Superior Temporal Cortical Motion Areas in the Macaque Monkey: II. Motion Discrimination Using Random Dot Displays. Eur. J. Neurosci. 4, 1228–1238. https://doi.org/10.1111/j.1460-9568.1992.tb00148.x

Mareschal, I., Baker, C.L., 1998. Temporal and spatial response to second-order stimuli in cat area 18. J. Neurophysiol. 80, 2811–2823. https://doi.org/10.1152/jn.1998.80.6.2811

Martin, T., Das, A., Huxlin, K., 2009. Visual motion retraining of a cortically-blind field increases BOLD responses in peri-lesional cortex and MT+ - a case study. J. Vis. 9, 666. https://doi.org/10.1167/9.8.666

Martin, T., Huxlin, K.R., Kavcic, V., 2010. Motion-onset visual evoked potentials predict performance during a global direction discrimination task. Neuropsychologia 48, 3563–3572. https://doi.org/10.1016/j.neuropsychologia.2010.08.005

Martinez-Cancino, R., Heng, J., Delorme, A., Kreutz-Delgado, K., Sotero, R.C., Makeig, S., 2019. Measuring transient phase-amplitude coupling using local mutual information. NeuroImage 185, 361–378. https://doi.org/10.1016/j.neuroimage.2018.10.034

Matteo, B.M., Viganò, B., Cerri, C.G., Meroni, R., Cornaggia, C.M., Perin, C., 2017. Transcranial direct current stimulation (tDCS) combined with blindsight rehabilitation for the treatment of homonymous hemianopia: a report of two-cases. J. Phys. Ther. Sci. 29, 1700–1705. https://doi.org/10.1589/jpts.29.1700

Maunsell, H.R., Van, C., 1983. THE CONNECTIONS OF THE MIDDLE TEMPORAL VISUAL AREA (MT) AND THEIR RELATIONSHIP TO A CORTICAL HIERARCHY IN THE MACAQUE MONKEY. J. Neurosci. 3, 24.

Maunsell, J.H., Van Essen, D.C., 1983. Functional properties of neurons in middle temporal visual area of the macaque monkey. I. Selectivity for stimulus direction, speed, and orientation. J. Neurophysiol. 49, 1127–1147. https://doi.org/10.1152/jn.1983.49.5.1127

Melnick, M.D., Tadin, D., Huxlin, K.R., 2016. Relearning to See in Cortical Blindness. Neurosci. Rev. J. Bringing Neurobiol. Neurol. Psychiatry 22, 199–212. https://doi.org/10.1177/1073858415621035

Merabet, L., Desautels, A., Minville, K., Casanova, C., 1998. Motion integration in a thalamic visual nucleus. Nature 396, 265–268. https://doi.org/10.1038/24382

Merabet, L., Minville, K., Ptito, M., Casanova, C., 2000. Responses of neurons in the cat posteromedial lateral suprasylvian cortex to moving texture patterns. Neuroscience 97, 611–623. https://doi.org/10.1016/s0306-4522(00)00056-7

Michalareas, G., Vezoli, J., van Pelt, S., Schoffelen, J.-M., Kennedy, H., Fries, P., 2016. Alpha-beta and gamma rhythms subserve feedback and feedforward influences among human visual cortical areas. Neuron 89, 384–397. https://doi.org/10.1016/j.neuron.2015.12.018

Mikami, A., Newsome, W.T., Wurtz, R.H., 1986. Motion selectivity in macaque visual cortex. I. Mechanisms of direction and speed selectivity in extrastriate area MT. J. Neurophysiol. 55, 1308–1327. https://doi.org/10.1152/jn.1986.55.6.1308

Milner, A.D., Goodale, M.A., 2008. Two visual systems re-viewed. Neuropsychologia 46, 774–785. https://doi.org/10.1016/j.neuropsychologia.2007.10.005

Miniussi, C., Harris, J.A., Ruzzoli, M., 2013. Modelling non-invasive brain stimulation in cognitive neuroscience. Neurosci. Biobehav. Rev. 37, 1702–1712. https://doi.org/10.1016/j.neubiorev.2013.06.014

Mishkin, M., Ungerleider, L.G., 1982. Contribution of striate inputs to the visuospatial functions of parieto-preoccipital cortex in monkeys. Behav. Brain Res. 6, 57–77. https://doi.org/10.1016/0166-4328(82)90081-X

Mittmann, T., Eysel, U.T., 2001. Increased synaptic plasticity in the surround of visual cortex lesions in rats. NeuroReport 12, 3341.

Momi, D., Ozdemir, R.A., Tadayon, E., Boucher, P., Shafi, M.M., Pascual-Leone, A., Santarnecchi, E., 2021. Network-level macroscale structural connectivity predicts propagation of transcranial magnetic stimulation. NeuroImage 229, 117698. https://doi.org/10.1016/j.neuroimage.2020.117698

Movshon, J.A., Newsome, W.T., 1996. Visual Response Properties of Striate Cortical Neurons Projecting to Area MT in Macaque Monkeys. J. Neurosci. 16, 7733–7741. https://doi.org/10.1523/JNEUROSCI.16-23-07733.1996

Muckli, L., Petro, L.S., 2013. Network interactions: non-geniculate input to V1. Curr. Opin. Neurobiol., Macrocircuits 23, 195–201. https://doi.org/10.1016/j.conb.2013.01.020

Muller-Gass, A., Duncan, M., Campbell, K., 2017. Brain states predict individual differences in perceptual learning. Personal. Individ. Differ., Robert Stelmack: Differential Psychophysiology 118, 29–38. https://doi.org/10.1016/j.paid.2017.03.066

Muthuraman, M., Deuschl, G., Koirala, N., Riedel, C., Volkmann, J., Groppa, S., 2017. Effects of DBS in parkinsonian patients depend on the structural integrity of frontal cortex. Sci. Rep. 7, 43571. https://doi.org/10.1038/srep43571

Nandi, B., Swiatek, P., Kocsis, B., Ding, M., 2019. Inferring the direction of rhythmic neural transmission via inter-regional phase-amplitude coupling (ir-PAC). Sci. Rep. 9, 6933. https://doi.org/10.1038/s41598-019-43272-w

Nassi, J.J., Callaway, E.M., 2007. Specialized Circuits from Primary Visual Cortex to V2 and Area MT. Neuron 55, 799–808. https://doi.org/10.1016/j.neuron.2007.07.037

Navarro de Lara, L.I., Tik, M., Woletz, M., Frass-Kriegl, R., Moser, E., Laistler, E., Windischberger, C., 2017. High-sensitivity TMS/fMRI of the Human Motor Cortex

Using a Dedicated Multichannel MR Coil. NeuroImage 150, 262–269. https://doi.org/10.1016/j.neuroimage.2017.02.062

Navarro de Lara, L.I., Windischberger, C., Kuehne, A., Woletz, M., Sieg, J., Bestmann, S., Weiskopf, N., Strasser, B., Moser, E., Laistler, E., 2015. A novel coil array for combined TMS/fMRI experiments at 3 T. Magn. Reson. Med. 74, 1492–1501. https://doi.org/10.1002/mrm.25535

Newsome, W., Pare, E., 1988. A selective impairment of motion perception following lesions of the middle temporal visual area (MT). J. Neurosci. 8, 2201–2211. https://doi.org/10.1523/JNEUROSCI.08-06-02201.1988

Nikolaev, A.R., Gepshtein, S., van Leeuwen, C., 2016. Intermittent regime of brain activity at the early, bias-guided stage of perceptual learning. J. Vis. 16, 11. https://doi.org/10.1167/16.14.11

Nishida, S., Ledgeway, T., Edwards, M., 1997. Dual multiple-scale processing for motion in the human visual System. Vision Res. 37, 2685–2698. https://doi.org/10.1016/S0042-6989(97)00092-8

Nowak, L.G., Bullier, J., 1997. The Timing of Information Transfer in the Visual System., in: Extrastriate Cortex in Primates., Cerebral Cortex. Springer, Boston, MA.

Nys, G.M.S., van Zandvoort, M.J.E., de Kort, P.L.M., Jansen, B.P.W., de Haan, E.H.F., Kappelle, L.J., 2007. Cognitive disorders in acute stroke: prevalence and clinical determinants. Cerebrovasc. Dis. Basel Switz. 23, 408–416. https://doi.org/10.1159/000101464

Olma, M.C., Dargie, R.A., Behrens, J.R., Kraft, A., Irlbacher, K., Fahle, M., Brandt, S.A., 2013. Long-Term Effects of Serial Anodal tDCS on Motion Perception in Subjects with Occipital Stroke Measured in the Unaffected Visual Hemifield. Front. Hum. Neurosci. 7. https://doi.org/10.3389/fnhum.2013.00314

O'Neill, E.C., Connell, P.P., O'Connor, J.C., Brady, J., Reid, I., Logan, P., 2011. Prism therapy and visual rehabilitation in homonymous visual field loss. Optom. Vis. Sci. Off. Publ. Am. Acad. Optom. 88, 263–268. https://doi.org/10.1097/OPX.0b013e318205a3b8

Osipova, D., Hermes, D., Jensen, O., 2008. Gamma Power Is Phase-Locked to Posterior Alpha Activity. PLOS ONE 3, e3990. https://doi.org/10.1371/journal.pone.0003990

Palmer, S.M., Rosa, M.G.P., 2006. A distinct anatomical network of cortical areas for analysis of motion in far peripheral vision. Eur. J. Neurosci. 24, 2389–2405. https://doi.org/10.1111/j.1460-9568.2006.05113.x

Palva, S., Kulashekhar, S., Hämäläinen, M., Palva, J.M., 2011. Localization of Cortical Phase and Amplitude Dynamics during Visual Working Memory Encoding and Retention. J. Neurosci. 31, 5013–5025. https://doi.org/10.1523/JNEUROSCI.5592-10.2011

Palva, S., Monto, S., Palva, J.M., 2010. Graph properties of synchronized cortical networks during visual working memory maintenance. NeuroImage 49, 3257–3268. https://doi.org/10.1016/j.neuroimage.2009.11.031

Palva, S., Palva, J.M., 2011. Functional Roles of Alpha-Band Phase Synchronization in Local and Large-Scale Cortical Networks. Front. Psychol. 2.

Palva, S., Palva, J.M., 2007. New vistas for α-frequency band oscillations. Trends Neurosci. 30, 150–158. https://doi.org/10.1016/j.tins.2007.02.001

Pan, H., Zhang, S., Pan, D., Ye, Z., Yu, H., Ding, J., Wang, Q., Sun, Q., Hua, T., 2021. Characterization of Feedback Neurons in the High-Level Visual Cortical Areas That Project Directly to the Primary Visual Cortex in the Cat. Front. Neuroanat. 14.

Papageorgiou, D., Papanikolaou, A., Smirnakis, S., 2014. A Systematic Approach to Visual System Rehabilitation — Population Receptive Field Analysis and Real-time Functional Magnetic Resonance Imaging Neurofeedback Methods. Adv. Brain Neuroimaging Top. Health Dis. - Methods Appl. https://doi.org/10.5772/58258

Papageorgiou, E., Hardiess, G., Schaeffel, F., Wiethoelter, H., Karnath, H.-O., Mallot, H., Schoenfisch, B., Schiefer, U., 2007. Assessment of vision-related quality of life in patients with homonymous visual field defects. Graefes Arch. Clin. Exp. Ophthalmol. Albrecht Von Graefes Arch. Klin. Exp. Ophthalmol. 245, 1749–1758. https://doi.org/10.1007/s00417-007-0644-z

Pascual-Leone, A., Walsh, V., 2001. Fast Backprojections from the Motion to the Primary Visual Area Necessary for Visual Awareness. Science 292, 510–512. https://doi.org/10.1126/science.1057099

Pasternak, T., Merigan, W.H., 1994. Motion Perception following Lesions of the Superior Temporal Sulcus in the Monkey. Cereb. Cortex 4, 247–259. https://doi.org/10.1093/cercor/4.3.247

Pasternak, T., Tadin, D., 2020. Linking Neuronal Direction Selectivity to Perceptual Decisions About Visual Motion. Annu. Rev. Vis. Sci. 6, 335–362. https://doi.org/10.1146/annurev-vision-121219-081816

Peli, E., Apfelbaum, H., Berson, E.L., Goldstein, R.B., 2016. The risk of pedestrian collisions with peripheral visual field loss. J. Vis. 16, 5. https://doi.org/10.1167/16.15.5

Pellicciari, M.C., Miniussi, C., Rossini, P.M., De Gennaro, L., 2009. Increased cortical plasticity in the elderly: changes in the somatosensory cortex after paired associative stimulation. Neuroscience 163, 266–276. https://doi.org/10.1016/j.neuroscience.2009.06.013

Perez, C., Chokron, S., 2014. Rehabilitation of homonymous hemianopia: insight into blindsight. Front. Integr. Neurosci. 8. https://doi.org/10.3389/fnint.2014.00082

Perrone, J.A., Thiele, A., 2001. Speed skills: measuring the visual speed analyzing properties of primate MT neurons. Nat. Neurosci. 4, 526–532. https://doi.org/10.1038/87480

Pichiorri, F., Petti, M., Caschera, S., Astolfi, L., Cincotti, F., Mattia, D., 2018. An EEG index of sensorimotor interhemispheric coupling after unilateral stroke: clinical and neurophysiological study. Eur. J. Neurosci. 47, 158–163. https://doi.org/10.1111/ejn.13797

Pitzalis, S., Sereno, M.I., Committeri, G., Fattori, P., Galati, G., Patria, F., Galletti, C., 2010. Human V6: The Medial Motion Area. Cereb. Cortex 20, 411–424. https://doi.org/10.1093/cercor/bhp112

Plow, E.B., Obretenova, S.N., Halko, M.A., Kenkel, S., Jackson, M.L., Pascual-Leone, A., Merabet, L.B., 2011. Combining Visual Rehabilitative Training and Noninvasive Brain Stimulation to Enhance Visual Function in Patients With Hemianopia: A Comparative Case Study. PM&R 3, 825–835. https://doi.org/10.1016/j.pmrj.2011.05.026

Poggel, D.A., Kasten, E., Sabel, B.A., 2004. Attentional cueing improves vision restoration therapy in patients with visual field defects. Neurology 63, 2069–2076. https://doi.org/10.1212/01.wnl.0000145773.26378.e5

Polanía, R., Nitsche, M.A., Korman, C., Batsikadze, G., Paulus, W., 2012. The importance of timing in segregated theta phase-coupling for cognitive performance. Curr. Biol. CB 22, 1314–1318. https://doi.org/10.1016/j.cub.2012.05.021

Pöppel, E., Held, R., Frost, D., 1973. Residual Visual Function After Brain Wounds Involving the Central Visual Pathways in Man. Nature 243, 295–6. https://doi.org/10.1038/243295a0

Pötter-Nerger, M., Fischer, S., Mastroeni, C., Groppa, S., Deuschl, G., Volkmann, J., Quartarone, A., Münchau, A., Siebner, H.R., 2009. Inducing homeostatic-like plasticity in human motor cortex through converging corticocortical inputs. J. Neurophysiol. 102, 3180–3190. https://doi.org/10.1152/jn.91046.2008

Preti, M.G., Van De Ville, D., 2019. Decoupling of brain function from structure reveals regional behavioral specialization in humans. Nat. Commun. 10, 4747. https://doi.org/10.1038/s41467-019-12765-7

Price, T.D., Khan, R., 2017. Evolution of Visual Processing in the Human Retina. Trends Ecol. Evol. 32, 810–813. https://doi.org/10.1016/j.tree.2017.09.001

Quartarone, A., Rizzo, V., Bagnato, S., Morgante, F., Sant'Angelo, A., Girlanda, P., Roman Siebner, H., 2006. Rapid-rate paired associative stimulation of the median nerve and motor cortex can produce long-lasting changes in motor cortical excitability in humans: Repetitive paired associative stimulation of human motor cortex. J. Physiol. 575, 657–670. https://doi.org/10.1113/jphysiol.2006.114025

Quentin, R., Chanes, L., Vernet, M., Valero-Cabré, A., 2015a. Fronto-Parietal Anatomical Connections Influence the Modulation of Conscious Visual Perception by High-Beta Frontal Oscillatory Activity. Cereb. Cortex N. Y. N 1991 25, 2095–2101. https://doi.org/10.1093/cercor/bhu014

Raffin, E., Salamanca-Giron, R.F., Hummel, F.C., 2020. Perspectives: Hemianopia—Toward Novel Treatment Options Based on Oscillatory Activity? Neurorehabil. Neural Repair 34, 13–25. https://doi.org/10.1177/1545968319893286

Raffin, E., Witon, A., Salamanca-Giron, R.F., Huxlin, K.R., Hummel, F.C., 2021. Functional Segregation within the Dorsal Frontoparietal Network: A Multimodal Dynamic Causal Modeling Study. Cereb. Cortex N. Y. N 1991 bhab409. https://doi.org/10.1093/cercor/bhab409

Ramsey, L.E., Siegel, J.S., Lang, C.E., Strube, M., Shulman, G.L., Corbetta, M., 2017. Behavioural clusters and predictors of performance during recovery from stroke. Nat. Hum. Behav. 1, 0038. https://doi.org/10.1038/s41562-016-0038

Raninen, A., Vanni, S., Hyvärinen, L., Näsänen, R., 2007. Temporal sensitivity in a hemianopic visual field can be improved by long-term training using flicker stimulation. J. Neurol. Neurosurg. Psychiatry 78, 66–73. https://doi.org/10.1136/jnnp.2006.099366

Rathore, S.S., Hinn, A.R., Cooper, L.S., Tyroler, H.A., Rosamond, W.D., 2002. Characterization of incident stroke signs and symptoms: findings from the atherosclerosis risk in communities study. Stroke 33, 2718–2721. https://doi.org/10.1161/01.str.0000035286.87503.31

Reijmer, Y.D., Freeze, W.M., Leemans, A., Biessels, G.J., 2013. The Effect of Lacunar Infarcts on White Matter Tract Integrity. Stroke 44, 2019–2021. https://doi.org/10.1161/STROKEAHA.113.001321

Reijmer, Y.D., Schultz, A.P., Leemans, A., O'Sullivan, M.J., Gurol, M.E., Sperling, R., Greenberg, S.M., Viswanathan, A., Hedden, T., 2015. Decoupling of structural and functional brain connectivity in older adults with white matter hyperintensities. NeuroImage 117, 222–229. https://doi.org/10.1016/j.neuroimage.2015.05.054

Reinhard, J., Schreiber, A., Schiefer, U., Kasten, E., Sabel, B.A., Kenkel, S., Vonthein, R., Trauzettel-Klosinski, S., 2005. Does visual restitution training change absolute homonymous visual field defects? A fundus controlled study. Br. J. Ophthalmol. 89, 30–35. https://doi.org/10.1136/bjo.2003.040543

Reuter, M., Schmansky, N. J., Rosas, H. D. & Fischl, B. Within-subject template estimation for unbiased longitudinal image analysis. *NeuroImage* 61, 1402–1418 (2012).

Reynolds, J.H., Desimone, R., 2003. Interacting roles of attention and visual salience in V4. Neuron 37, 853–863. https://doi.org/10.1016/s0896-6273(03)00097-7

Richter, C.G., Coppola, R., Bressler, S.L., 2018. Top-down beta oscillatory signaling conveys behavioral context in early visual cortex. Sci. Rep. 8, 6991. https://doi.org/10.1038/s41598-018-25267-1

Richter, C.G., Thompson, W.H., Bosman, C.A., Fries, P., 2017. Top-down beta enhances bottom-up gamma. J. Neurosci. 3771–16. https://doi.org/10.1523/JNEUROSCI.3771-16.2017

Riddoch, G., 1917. Dissociation of visual perceptions due to occipital injuries, with especial reference to appreciation of movement. Brain J. Neurol. 40, 15–57. https://doi.org/10.1093/brain/40.1.15

Rizzo, V., Siebner, H.S., Morgante, F., Mastroeni, C., Girlanda, P., Quartarone, A., 2009. Paired Associative Stimulation of Left and Right Human Motor Cortex Shapes Interhemispheric Motor Inhibition based on a Hebbian Mechanism. Cereb. Cortex 19, 907–915. https://doi.org/10.1093/cercor/bhn144

Ro, T., Rafal, R., 2006. Visual restoration in cortical blindness: insights from natural and TMS-induced blindsight. Neuropsychol. Rehabil. 16, 377–396. https://doi.org/10.1080/09602010500435989

Rockland, K., 2015. Axons and Brain Architecture. Academic Press.

Roder, H., 1931. Amplitude, Phase, and Frequency Modulation. Proc. Inst. Radio Eng. 19, 2145–2176. https://doi.org/10.1109/JRPROC.1931.222283

Rodieck, R.W., 1965. Quantitative analysis of cat retinal ganglion cell response to visual stimuli. Vision Res. 5, 583–601. https://doi.org/10.1016/0042-6989(65)90033-7

Rodman, H.R., Albright, T.D., 1987. Coding of visual stimulus velocity in area MT of the macaque. Vision Res. 27, 2035–2048. https://doi.org/10.1016/0042-6989(87)90118-0

Rodman, H.R., Gross, C.G., Albright, T.D., 1989. Afferent basis of visual response properties in area MT of the macaque. I. Effects of striate cortex removal. J. Neurosci. 9, 2033–2050.

Rogasch, N.C., Sullivan, C., Thomson, R.H., Rose, N.S., Bailey, N.W., Fitzgerald, P.B., Farzan, F., Hernandez-Pavon, J.C., 2017. Analysing concurrent transcranial magnetic stimulation and electroencephalographic data: A review and introduction to the open-source TESA software. NeuroImage 147, 934–951. https://doi.org/10.1016/j.neuroimage.2016.10.031

Romei, V., Chiappini, E., Hibbard, P.B., Avenanti, A., 2016. Empowering Reentrant Projections from V5 to V1 Boosts Sensitivity to Motion. Curr. Biol. CB 26, 2155–2160. https://doi.org/10.1016/j.cub.2016.06.009

Ronconi, L., Melcher, D., Junghöfer, M., Wolters, C.H., Busch, N.A., 2020. Testing the effect of tACS over parietal cortex in modulating endogenous alpha rhythm and temporal integration windows in visual perception. Eur. J. Neurosci. https://doi.org/10.1111/ejn.15017

Rosa, M.G.P., Tweedale, R., Elston, G.N., 2000. Visual Responses of Neurons in the Middle Temporal Area of New World Monkeys after Lesions of Striate Cortex. J. Neurosci. 20, 5552–5563. https://doi.org/10.1523/JNEUROSCI.20-14-05552.2000

Rossi, S., Antal, A., Bestmann, S., Bikson, M., Brewer, C., Brockmöller, J., Carpenter, L.L., Cincotta, M., Chen, R., Daskalakis, J.D., Di Lazzaro, V., Fox, M.D., George, M.S., Gilbert, D., Kimiskidis, V.K., Koch, G., Ilmoniemi, R.J., Lefaucheur, J.P., Leocani, L., Lisanby, S.H., Miniussi, C., Padberg, F., Pascual-Leone, A., Paulus, W., Peterchev, A.V., Quartarone, A., Rotenberg, A., Rothwell, J., Rossini, P.M., Santarnecchi, E., Shafi, M.M., Siebner, H.R., Ugawa, Y., Wassermann, E.M., Zangen, A., Ziemann, U., Hallett, M., 2021. Safety and recommendations for TMS use in healthy subjects and patient populations, with updates on training, ethical and regulatory issues: Expert Guidelines. Clin. Neurophysiol. 132, 269–306. https://doi.org/10.1016/j.clinph.2020.10.003

Rowe, F.J., 2017. Stroke survivors' views and experiences on impact of visual impairment. Brain Behav. 7. https://doi.org/10.1002/brb3.778

Rowe, F.J., Hepworth, L.R., Hanna, K.L., Mistry, M., Noonan, C.P., 2019. Accuracy of kinetic perimetry assessment with the Humphrey 850; an exploratory comparative study. Eye 33, 1952–1960. https://doi.org/10.1038/s41433-019-0520-1

Rowe, F.J., Hepworth, L.R., Howard, C., Hanna, K.L., Currie, J., 2022. Impact of visual impairment following stroke (IVIS study): a prospective clinical profile of central and peripheral visual deficits, eye movement abnormalities and visual perceptual deficits. Disabil. Rehabil. 44, 3139–3153. https://doi.org/10.1080/09638288.2020.1859631

Rowe, F.J., Wright, D., Brand, D., Jackson, C., Harrison, S., Maan, T., Scott, C., Vogwell, L., Peel, S., Akerman, N., Dodridge, C., Howard, C., Shipman, T., Sperring, U., MacDiarmid, S., Freeman, C., 2013. A Prospective Profile of Visual Field Loss following Stroke: Prevalence, Type, Rehabilitation, and Outcome. BioMed Res. Int. 2013, 1–12. https://doi.org/10.1155/2013/719096

Rudolph, K., 1999. Transient and Permanent Deficits in Motion Perception after Lesions of Cortical Areas MT and MST in the Macaque Monkey. Cereb. Cortex 9, 90–100. https://doi.org/10.1093/cercor/9.1.90

Ruzzoli, M., Marzi, C.A., Miniussi, C., 2010. The Neural Mechanisms of the Effects of Transcranial Magnetic Stimulation on Perception. J. Neurophysiol. 103, 2982–2989. https://doi.org/10.1152/jn.01096.2009

Saalmann, Y. B., Pigarev, I. N. & Vidyasagar, T. R. Neural mechanisms of visual attention: how top-down feedback highlights relevant locations. *Science* 316, 1612–1615 (2007).

Sabel, B.A., Kasten, E., 2000. Restoration of vision by training of residual functions. Curr. Opin. Ophthalmol. 11, 430–436. https://doi.org/10.1097/00055735-200012000-00008

Sabel, B.A., Thut, G., Haueisen, J., Henrich-Noack, P., Herrmann, C.S., Hunold, A., Kammer, T., Matteo, B., Sergeeva, E.G., Waleszczyk, W., Antal, A., 2020. Vision modulation, plasticity and restoration using non-invasive brain stimulation – An IFCN-sponsored review. Clin. Neurophysiol. 131, 887–911. https://doi.org/10.1016/j.clinph.2020.01.008

Sack, A.T., Kohler, A., Bestmann, S., Linden, D.E.J., Dechent, P., Goebel, R., Baudewig, J., 2007. Imaging the brain activity changes underlying impaired visuospatial judgments: simultaneous FMRI, TMS, and behavioral studies. Cereb. Cortex N. Y. N 1991 17, 2841–2852. https://doi.org/10.1093/cercor/bhm013

Sagi, D., 2011. Perceptual learning in Vision Research. Vision Res. 51, 1552–1566. https://doi.org/10.1016/j.visres.2010.10.019

Sahraie, A., Cederblad, A.M.H., Kenkel, S., Romano, J.G., 2020. Efficacy and predictors of recovery of function after eye movement training in 296 hemianopic patients. Cortex 125, 149–160. https://doi.org/10.1016/j.cortex.2019.12.005

Sahraie, A., Trevethan, C.T., MacLeod, M.J., Murray, A.D., Olson, J.A., Weiskrantz, L., 2006. Increased sensitivity after repeated stimulation of residual spatial channels in blindsight. Proc. Natl. Acad. Sci. 103, 14971–14976. https://doi.org/10.1073/pnas.0607073103

Saionz, E.L., Tadin, D., Melnick, M.D., Huxlin, K.R., 2020. Functional preservation and enhanced capacity for visual restoration in subacute occipital stroke. Brain. https://doi.org/10.1093/brain/awaa128

Salamanca-Giron, R.F., Raffin, E., Zandvliet, S.B., Seeber, M., Michel, C.M., Sauseng, P., Huxlin, K.R., Hummel, F.C., 2021. Enhancing visual motion discrimination by desynchronizing bifocal oscillatory activity. NeuroImage 240, 118299. https://doi.org/10.1016/j.neuroimage.2021.118299

Salazar, R.F., Dotson, N.M., Bressler, S.L., Gray, C.M., 2012. Content-Specific Fronto-Parietal Synchronization During Visual Working Memory. Science 338, 1097–1100. https://doi.org/10.1126/science.1224000

Salin, P.A., Bullier, J., 1995. Corticocortical connections in the visual system: structure and function. Physiol. Rev. 75, 107–154. https://doi.org/10.1152/physrev.1995.75.1.107

Salinas, E., Sejnowski, T.J., 2001. Correlated neuronal activity and the flow of neural information. Nat. Rev. Neurosci. 2, 539–550. https://doi.org/10.1038/35086012

Sand, K.M., Midelfart, A., Thomassen, L., Melms, A., Wilhelm, H., Hoff, J.M., 2013. Visual impairment in stroke patients – a review. Acta Neurol. Scand. 127, 52–56. https://doi.org/10.1111/ane.12050

Sand, K.M., Thomassen, L., Næss, H., Rødahl, E., Hoff, J.M., 2012. Diagnosis and Rehabilitation of Visual Field Defects in Stroke Patients: A Retrospective Audit. Cerebrovasc. Dis. Extra 2, 17–23. https://doi.org/10.1159/000337016

Sanders, M.D., Warrington, ElizabethK., Marshall, J., Wieskrantz, L., 1974. "BLINDSIGHT": VISION IN A FIELD DEFECT. The Lancet 303, 707–708. https://doi.org/10.1016/S0140-6736(74)92907-9

Saproo, S., Serences, J.T., 2014. Attention Improves Transfer of Motion Information between V1 and MT. J. Neurosci. 34, 3586–3596. https://doi.org/10.1523/JNEUROSCI.3484-13.2014

Schmid, M.C., Schmiedt, J.T., Peters, A.J., Saunders, R.C., Maier, A., Leopold, D.A., 2013. Motion-Sensitive Responses in Visual Area V4 in the Absence of Primary Visual Cortex. J. Neurosci. 33, 18740–18745. https://doi.org/10.1523/JNEUROSCI.3923-13.2013

Schmolesky, M.T., Wang, Y., Hanes, D.P., Thompson, K.G., Leutgeb, S., Schall, J.D., Leventhal, A.G., 1998. Signal Timing Across the Macaque Visual System. J. Neurophysiol. 79, 3272–3278. https://doi.org/10.1152/jn.1998.79.6.3272

Seghier, M.L., Lazeyras, F., Zimine, S., Saudan-Frei, S., Safran, A.B., Huppi, P.S., 2005. Visual recovery after perinatal stroke evidenced by functional and diffusion MRI: case report. BMC Neurol. 5, 17. https://doi.org/10.1186/1471-2377-5-17

Seymour, R.A., Rippon, G., Kessler, K., 2017. The Detection of Phase Amplitude Coupling during Sensory Processing. Front. Neurosci. 11.

Shipp, S., Zeki, S., 1985. Segregation of pathways leading from area V2 to areas V 4 and V5 of macaque monkey visual cortex. Nature 315, 3.

Siebenhühner, F., Wang, S.H., Palva, J.M., Palva, S., 2016. Cross-frequency synchronization connects networks of fast and slow oscillations during visual working memory maintenance. eLife 5, e13451. https://doi.org/10.7554/eLife.13451

Siegel, M., Donner, T.H., Engel, A.K., 2012. Spectral fingerprints of large-scale neuronal interactions. Nat. Rev. Neurosci. 13, 121–134. https://doi.org/10.1038/nrn3137

Siegel, M., Donner, T.H., Oostenveld, R., Fries, P., Engel, A.K., 2008. Neuronal synchronization along the dorsal visual pathway reflects the focus of spatial attention. Neuron 60, 709–719. https://doi.org/10.1016/j.neuron.2008.09.010

Silvanto, J., 2015. Why is "blindsight" blind? A new perspective on primary visual cortex, recurrent activity and visual awareness. Conscious. Cogn. 32, 15–32. https://doi.org/10.1016/j.concog.2014.08.001

Silvanto, J., Cowey, A., Lavie, N., Walsh, V., 2005a. Striate cortex (V1) activity gates awareness of motion. Nat. Neurosci. 8, 143–144. https://doi.org/10.1038/nn1379

Silvanto, J., Lavie, N., Walsh, V., 2005b. Double dissociation of V1 and V5/MT activity in visual awareness. Cereb. Cortex N. Y. N 1991 15, 1736–1741. https://doi.org/10.1093/cercor/bhi050

Silvanto, J., Muggleton, N., Lavie, N., Walsh, V., 2009. The Perceptual and Functional Consequences of Parietal Top-Down Modulation on the Visual Cortex. Cereb. Cortex 19, 327–330. https://doi.org/10.1093/cercor/bhn091

Silvanto, J., Muggleton, N., Walsh, V., 2008. State-dependency in brain stimulation studies of perception and cognition. Trends Cogn. Sci. 12, 447–454. https://doi.org/10.1016/j.tics.2008.09.004

Simoncelli, E.P., Heeger, D.J., 1998. A model of neuronal responses in visual area MT. Vision Res. 38, 743–761. https://doi.org/10.1016/S0042-6989(97)00183-1

Sincich, L.C., Park, K.F., Wohlgemuth, M.J., Horton, J.C., 2004. Bypassing V1: a direct geniculate input to area MT. Nat. Neurosci. 7, 1123–1128. https://doi.org/10.1038/nn1318

Singer, W., 2018. Neuronal oscillations: unavoidable and useful? Eur. J. Neurosci. 48, 2389–2398. https://doi.org/10.1111/ejn.13796

Singer, W., 1999. Neuronal Synchrony: A Versatile Code for the Definition of Relations? Neuron 24, 49–65. https://doi.org/10.1016/S0896-6273(00)80821-1

Singer, W., Gray, C.M., 1995. Visual Feature Integration and the Temporal Correlation Hypothesis. Annu. Rev. Neurosci. 18, 555–586. https://doi.org/10.1146/annurev.ne.18.030195.003011

Sjöström, P.J., Rancz, E.A., Roth, A., Häusser, M., 2008. Dendritic excitability and synaptic plasticity. Physiol. Rev. 88, 769–840. https://doi.org/10.1152/physrev.00016.2007

Smith, A.T., Greenlee, M.W., Singh, K.D., Kraemer, F.M., Hennig, J., 1998. The Processing of First- and Second-Order Motion in Human Visual Cortex Assessed by Functional Magnetic Resonance Imaging (fMRI). J. Neurosci. 18, 3816–3830. https://doi.org/10.1523/JNEUROSCI.18-10-03816.1998

Smith, R.E., Tournier, J.-D., Calamante, F., Connelly, A., 2015. SIFT2: Enabling dense quantitative assessment of brain white matter connectivity using streamlines tractography. NeuroImage 119, 338–351. https://doi.org/10.1016/j.neuroimage.2015.06.092

Smith, S.M., Jenkinson, M., Woolrich, M.W., Beckmann, C.F., Behrens, T.E.J., Johansen-Berg, H., Bannister, P.R., De Luca, M., Drobnjak, I., Flitney, D.E., Niazy, R.K., Saunders, J., Vickers, J., Zhang, Y., De Stefano, N., Brady, J.M., Matthews, P.M., 2004. Advances in functional and structural MR image analysis and implementation as FSL. NeuroImage 23 Suppl 1, S208-219. https://doi.org/10.1016/j.neuroimage.2004.07.051

Snyder, A.C., Foxe, J.J., 2010. Anticipatory attentional suppression of visual features indexed by oscillatory alpha-band power increases: a high-density electrical mapping study. J. Neurosci. Off. J. Soc. Neurosci. 30, 4024–4032. https://doi.org/10.1523/JNEUROSCI.5684-09.2010

Soto-Faraco, S., Väljamäe, A., 2012. Multisensory Interactions during Motion Perception: From Basic Principles to Media Applications, in: Murray, M.M., Wallace, M.T. (Eds.), The Neural Bases of Multisensory Processes, Frontiers in Neuroscience. CRC Press/Taylor & Francis, Boca Raton (FL).

Spaak, E., Bonnefond, M., Maier, A., Leopold, D.A., Jensen, O., 2012. Layer-Specific Entrainment of Gamma-Band Neural Activity by the Alpha Rhythm in Monkey Visual Cortex. Curr. Biol. 22, 2313–2318. https://doi.org/10.1016/j.cub.2012.10.020

Spampinato, D.A., Block, H.J., Celnik, P.A., 2017. Cerebellar–M1 Connectivity Changes Associated with Motor Learning Are Somatotopic Specific. J. Neurosci. 37, 2377–2386. https://doi.org/10.1523/JNEUROSCI.2511-16.2017

Stefan, K., 2000. Induction of plasticity in the human motor cortex by paired associative stimulation. Brain 123, 572–584. https://doi.org/10.1093/brain/123.3.572

Stein, B.E., Stanford, T.R., 2008. Multisensory integration: current issues from the perspective of the single neuron. Nat. Rev. Neurosci. 9, 255–266. https://doi.org/10.1038/nrn2331

Stein, A. von, Chiang, C., König, P., 2000. Top-down processing mediated by interareal synchronization. Proc. Natl. Acad. Sci. 97, 14748–14753. https://doi.org/10.1073/pnas.97.26.14748

Stepniewska, I., Qi, H.-X., Kaas, J.H., 2000. Projections of the superior colliculus to subdivisions of the inferior pulvinar in New World and Old World monkeys. Vis. Neurosci. 17, 529–549. https://doi.org/10.1017/S0952523800174048

Stonkus, R., Braun, V., Kerlin, J.R., Volberg, G., Hanslmayr, S., 2016. Probing the causal role of prestimulus interregional synchrony for perceptual integration via tACS. Sci. Rep. 6, 32065. https://doi.org/10.1038/srep32065

Suppa, A., Biasiotta, A., Belvisi, D., Marsili, L., La Cesa, S., Truini, A., Cruccu, G., Berardelli, A., 2013. Heat-Evoked Experimental Pain Induces Long-Term Potentiation-Like Plasticity in Human Primary Motor Cortex. Cereb. Cortex 23, 1942–1951. https://doi.org/10.1093/cercor/bhs182

Suppa, A., Li Voti, P., Rocchi, L., Papazachariadis, O., Berardelli, A., 2015. Early Visuomotor Integration Processes Induce LTP/LTD-Like Plasticity in the Human Motor Cortex. Cereb. Cortex 25, 703–712. https://doi.org/10.1093/cercor/bht264

Suppa, A., Quartarone, A., Siebner, H., Chen, R., Di Lazzaro, V., Del Giudice, P., Paulus, W., Rothwell, J.C., Ziemann, U., Classen, J., 2017. The associative brain at work: Evidence from paired associative stimulation studies in humans. Clin. Neurophysiol. 128, 2140–2164. https://doi.org/10.1016/j.clinph.2017.08.003

Tadel, F., Baillet, S., Mosher, J.C., Pantazis, D., Leahy, R.M., 2011. Brainstorm: A User-Friendly Application for MEG/EEG Analysis. Comput. Intell. Neurosci. 2011, 1–13. https://doi.org/10.1155/2011/879716

Tamura, Y., Ueki, Y., Lin, P., Vorbach, S., Mima, T., Kakigi, R., Hallett, M., 2009. Disordered plasticity in the primary somatosensory cortex in focal hand dystonia. Brain 132, 749–755. https://doi.org/10.1093/brain/awn348

Thabit, M.N., Ueki, Y., Koganemaru, S., Fawi, G., Fukuyama, H., Mima, T., 2010. Movement-Related Cortical Stimulation Can Induce Human Motor Plasticity. J. Neurosci. 30, 11529–11536. https://doi.org/10.1523/JNEUROSCI.1829-10.2010

Thibaut, A., Simis, M., Battistella, L.R., Fanciullacci, C., Bertolucci, F., Huerta-Gutierrez, R., Chisari, C., Fregni, F., 2017. Using Brain Oscillations and Corticospinal Excitability to Understand and Predict Post-Stroke Motor Function. Front. Neurol. 8.

Thomas Yeo, B.T., Krienen, F.M., Sepulcre, J., Sabuncu, M.R., Lashkari, D., Hollinshead, M., Roffman, J.L., Smoller, J.W., Zöllei, L., Polimeni, J.R., Fischl, B., Liu, H., Buckner, R.L., 2011. The organization of the human cerebral cortex estimated by intrinsic functional connectivity. J. Neurophysiol. 106, 1125–1165. https://doi.org/10.1152/jn.00338.2011

Thompson, B., Deblieck, C., Wu, A., Iacoboni, M., Liu, Z., 2016. Psychophysical and rTMS evidence for the presence of motion opponency in human V5. Brain Stimulat. 9, 876–881. https://doi.org/10.1016/j.brs.2016.05.012

Thut, G., Bergmann, T.O., Fröhlich, F., Soekadar, S.R., Brittain, J.-S., Valero-Cabré, A., Sack, A., Miniussi, C., Antal, A., Siebner, H.R., Ziemann, U., Herrmann, C.S., 2017. Guiding transcranial brain stimulation by EEG/MEG to interact with ongoing brain activity and associated functions: A position paper. Clin. Neurophysiol. Off. J. Int. Fed. Clin. Neurophysiol. 128, 843–857. https://doi.org/10.1016/j.clinph.2017.01.003

Thut, G., Miniussi, C., 2009. New insights into rhythmic brain activity from TMS-EEG studies. Trends Cogn. Sci. 13, 182–189. https://doi.org/10.1016/j.tics.2009.01.004

Thut, G., Schyns, P., Gross, J., 2011. Entrainment of Perceptually Relevant Brain Oscillations by Non-Invasive Rhythmic Stimulation of the Human Brain. Front. Psychol. 2.

Toft, P.B., Arkani-Hamed, J., Haggerty, S.E., 1990. The effects of serpentinization on density and magnetic susceptibility: a petrophysical model. Phys. Earth Planet. Inter. 65, 137–157. https://doi.org/10.1016/0031-9201(90)90082-9

Tononi, G., Sporns, O., Edelman, G.M., 1992. Reentry and the Problem of Integrating Multiple Cortical Areas: Simulation of Dynamic Integration in the Visual System. Cereb. Cortex 2, 310–335. https://doi.org/10.1093/cercor/2.4.310

Tournier, J.-D., 2019. Diffusion MRI in the brain – Theory and concepts. Prog. Nucl. Magn. Reson. Spectrosc. 112–113, 1–16. https://doi.org/10.1016/j.pnmrs.2019.03.001

Tournier, J.-D., Smith, R., Raffelt, D., Tabbara, R., Dhollander, T., Pietsch, M., Christiaens, D., Jeurissen, B., Yeh, C.-H., Connelly, A., 2019. MRtrix3: A fast, flexible and open software framework for medical image processing and visualisation. NeuroImage 202, 116137. https://doi.org/10.1016/j.neuroimage.2019.116137

Tsao, C.W., Aday, A.W., Almarzooq, Z.I., Anderson, C.A.M., Arora, P., Avery, C.L., Baker-Smith, C.M., Beaton, A.Z., Boehme, A.K., Buxton, A.E., Commodore-Mensah, Y., Elkind, M.S.V., Evenson, K.R., Eze-Nliam, C., Fugar, S., Generoso, G., Heard, D.G., Hiremath, S., Ho, J.E., Kalani, R., Kazi, D.S., Ko, D., Levine, D.A., Liu, J., Ma, J., Magnani, J.W., Michos, E.D., Mussolino, M.E., Navaneethan, S.D., Parikh, N.I., Poudel, R., Rezk-Hanna, M., Roth, G.A., Shah, N.S., St-Onge, M.-P., Thacker, E.L., Virani, S.S., Voeks, J.H., Wang, N.-Y., Wong, N.D., Wong, S.S., Yaffe, K., Martin, S.S., American Heart Association Council on Epidemiology and Prevention Statistics Committee and Stroke Statistics Subcommittee, 2023. Heart Disease and Stroke Statistics-2023 Update: A Report From the American Heart Association. Circulation 147, e93–e621. https://doi.org/10.1161/CIR.0000000000001123

Turrini, S., Fiori, F., Chiappini, E., Santarnecchi, E., Romei, V., Avenanti, A., 2022. Gradual enhancement of corticomotor excitability during cortico-cortical paired associative stimulation. Sci. Rep. 12, 14670. https://doi.org/10.1038/s41598-022-18774-9

Ulanov, M., Shtyrov, Y., 2022. Oscillatory beta/alpha band modulations: A potential biomarker of functional language and motor recovery in chronic stroke? Front. Hum. Neurosci. 16. https://doi.org/10.3389/fnhum.2022.940845

Ungewiss, J., Kübler, T., Sippel, K., Aehling, K., Heister, M., Rosenstiel, W., Kasneci, E., Papageorgiou, E., Simulator/On-road Study Group, 2018. Agreement of driving simulator and on-road driving performance in patients with binocular visual field loss. Graefes Arch. Clin. Exp. Ophthalmol. Albrecht Von Graefes Arch. Klin. Exp. Ophthalmol. 256, 2429–2435. https://doi.org/10.1007/s00417-018-4148-9

v. Monakow, C., 1895. Experimentelle und pathologisch-anatomische Untersuchungen über die Haubenregion, den Sehhügel und die Regio subthalamica, nebst Beiträgen zur Kenntniss früh erworbener Gross- und Kleinhirn-defecte. Arch. Für Psychiatr. Nervenkrankh. 27, 1–128. https://doi.org/10.1007/BF02076254

Valero-Cabré, A., Amengual, J.L., Stengel, C., Pascual-Leone, A., Coubard, O.A., 2017. Transcranial magnetic stimulation in basic and clinical neuroscience: A comprehensive review of fundamental principles and novel insights. Neurosci. Biobehav. Rev. 83, 381–404. https://doi.org/10.1016/j.neubiorev.2017.10.006

Van Essen, D.C., Gallant, J.L., 1994. Neural mechanisms of form and motion processing in the primate visual system. Neuron 13, 1–10. https://doi.org/10.1016/0896-6273(94)90455-3

van Kerkoerle, T., Self, M.W., Dagnino, B., Gariel-Mathis, M.-A., Poort, J., van der Togt, C., Roelfsema, P.R., 2014. Alpha and gamma oscillations characterize feedback and feedforward processing in monkey visual cortex. Proc. Natl. Acad. Sci. U. S. A. 111, 14332–14341. https://doi.org/10.1073/pnas.1402773111

Varela, F., Lachaux, J.-P., Rodriguez, E., Martinerie, J., 2001. The brainweb: Phase synchronization and large-scale integration. Nat. Rev. Neurosci. 2, 229–239. https://doi.org/10.1038/35067550

Varela, F.J., Toro, A., John, E.R., Schwartz, E.L., 1981. Perceptual framing and cortical alpha rhythm. Neuropsychologia 19, 675–686. https://doi.org/10.1016/0028-3932(81)90005-1

Vázquez-Rodríguez, B., Suárez, L.E., Markello, R.D., Shafiei, G., Paquola, C., Hagmann, P., van den Heuvel, M.P., Bernhardt, B.C., Spreng, R.N., Misic, B., 2019. Gradients of structure–function tethering across neocortex. Proc. Natl. Acad. Sci. 116, 21219–21227. https://doi.org/10.1073/pnas.1903403116

Veniero, D., Ponzo, V., Koch, G., 2013. Paired Associative Stimulation Enforces the Communication between Interconnected Areas. J. Neurosci. 33, 13773–13783. https://doi.org/10.1523/JNEUROSCI.1777-13.2013

Veraart, J., Novikov, D.S., Christiaens, D., Ades-Aron, B., Sijbers, J., Fieremans, E., 2016. Denoising of diffusion MRI using random matrix theory. NeuroImage 142, 394–406. https://doi.org/10.1016/j.neuroimage.2016.08.016

Vernet, M., Quentin, R., Chanes, L., Mitsumasu, A., Valero-Cabré, A., 2014. Frontal eye field, where art thou? Anatomy, function, and non-invasive manipulation of frontal regions involved in eye movements and associated cognitive operations. Front. Integr. Neurosci. 8.

Vernet, M., Stengel, C., Quentin, R., Amengual, J.L., Valero-Cabré, A., 2019. Entrainment of local synchrony reveals a causal role for high-beta right frontal oscillations in human visual consciousness. Sci. Rep. 9, 14510. https://doi.org/10.1038/s41598-019-49673-1

Véronneau-Troutman, S., 1978. Fresnel prisms and their effects on visual acuity and binocularity. Trans. Am. Ophthalmol. Soc. 76, 610–653.

Villeneuve, M.Y., Kupers, R., Gjedde, A., Ptito, M., Casanova, C., 2005. Pattern–motion selectivity in the human pulvinar. NeuroImage 28, 474–480. https://doi.org/10.1016/j.neuroimage.2005.06.015

von Stein, A., Sarnthein, J., 2000. Different frequencies for different scales of cortical integration: from local gamma to long range alpha/theta synchronization. Int. J. Psychophysiol. 38, 301–313. https://doi.org/10.1016/S0167-8760(00)00172-0

Vosskuhl, J., Strüber, D., Herrmann, C.S., 2018. Non-invasive Brain Stimulation: A Paradigm Shift in Understanding Brain Oscillations. Front. Hum. Neurosci. 12.

Voytek, B., Canolty, R., Shestyuk, A., Crone, N., Parvizi, J., Knight, R., 2010. Shifts in Gamma Phase–Amplitude Coupling Frequency from Theta to Alpha Over Posterior Cortex During Visual Tasks. Front. Hum. Neurosci. 4.

Wagner, J., Makeig, S., Gola, M., Neuper, C., Müller-Putz, G., 2016. Distinct β Band Oscillatory Networks Subserving Motor and Cognitive Control during Gait Adaptation. J. Neurosci. 36, 2212–2226. https://doi.org/10.1523/JNEUROSCI.3543-15.2016

Waldhauser, G.T., Johansson, M., Hanslmayr, S., 2012. Alpha/Beta Oscillations Indicate Inhibition of Interfering Visual Memories. J. Neurosci. 32, 1953–1961. https://doi.org/10.1523/JNEUROSCI.4201-11.2012

Wandell, B.A., Smirnakis, S.M., 2009. Plasticity and stability of visual field maps in adult primary visual cortex. Nat. Rev. Neurosci. 10, 873–884. https://doi.org/10.1038/nrn2741

Wang, L., Zhu, Z., Bastiaansen, M., 2012. Integration or Predictability? A Further Specification of the Functional Role of Gamma Oscillations in Language Comprehension. Front. Psychol. 3.

Wang, X.-J., 2010. Neurophysiological and Computational Principles of Cortical Rhythms in Cognition. Physiol. Rev. 90, 1195–1268. https://doi.org/10.1152/physrev.00035.2008

Warner, M.A., de la Plata, C.M., Spence, J., Wang, J.Y., Harper, C., Moore, C., Devous, M., Diaz-Arrastia, R., 2010. Assessing Spatial Relationships between Axonal Integrity, Regional Brain Volumes, and Neuropsychological Outcomes after Traumatic Axonal Injury. J. Neurotrauma 27, 2121–2130. https://doi.org/10.1089/neu.2010.1429

Waterston, M.L., Pack, C.C., 2010. Improved Discrimination of Visual Stimuli Following Repetitive Transcranial Magnetic Stimulation. PLOS ONE 5, e10354. https://doi.org/10.1371/journal.pone.0010354

Watson, J.D.G., Myers, R., Frackowiak, R.S.J., Hajnal, J.V., Woods, R.P., Mazziotta, J.C., Shipp, S., Zeki, S., 1993. Area V5 of the Human Brain: Evidence from a Combined Study Using Positron Emission Tomography and Magnetic Resonance Imaging. Cereb. Cortex 3, 79–94. https://doi.org/10.1093/cercor/3.2.79

Weerd, P., Sprague, J.M., Raiguel, S., Vandenbussche, E., Orban, G.A., 1993. Effects of Visual Cortex Lesions on Orientation Discrimination of Illusory Contours in the Cat. Eur. J. Neurosci. 5, 1695–1710. https://doi.org/10.1111/j.1460-9568.1993.tb00237.x

Weijland, A., Fankhauser, F., Bebie, H., Flammer, J., 2004. Automated perimetry : visual field digest.

Weiskrantz, L., 1996. Blindsight revisited. Curr. Opin. Neurobiol. 6, 215–220. https://doi.org/10.1016/s0959-4388(96)80075-4

Weller, R.E., Wall, J.T., Kaas, J.H., 1984. Cortical connections of the middle temporal visual area (MT) and the superior temporal cortex in owl monkeys. J. Comp. Neurol. 228, 81–104. https://doi.org/10.1002/cne.902280109

West, T.O., 2020. Measuring directed functional connectivity using non-parametric directionality analysis: Validation and comparison with non-parametric Granger Causality 19.

Weyand, T.G., 2016. The multifunctional lateral geniculate nucleus. Rev. Neurosci. 27, 135–157. https://doi.org/10.1515/revneuro-2015-0018

Wibral, M., Bledowski, C., Kohler, A., Singer, W., Muckli, L., 2009. The Timing of Feedback to Early Visual Cortex in the Perception of Long-Range Apparent Motion. Cereb. Cortex 19, 1567–1582. https://doi.org/10.1093/cercor/bhn192

Winkler, I., Haufe, S., Porbadnigk, A.K., Müller, K.-R., Dähne, S., 2015. Identifying Granger causal relationships between neural power dynamics and variables of interest. NeuroImage 111, 489–504. https://doi.org/10.1016/j.neuroimage.2014.12.059

Winstein, C.J., Stein, J., Arena, R., Bates, B., Cherney, L.R., Cramer, S.C., Deruyter, F., Eng, J.J., Fisher, B., Harvey, R.L., Lang, C.E., MacKay-Lyons, M., Ottenbacher, K.J., Pugh, S., Reeves, M.J., Richards, L.G., Stiers, W., Zorowitz, R.D., American Heart Association Stroke Council, Council on Cardiovascular and Stroke Nursing, Council on Clinical Cardiology, and Council on Quality of Care and Outcomes Research, 2016. Guidelines for Adult Stroke Rehabilitation and Recovery: A Guideline for Healthcare Professionals From the American Heart Association/American Stroke Association. Stroke 47, e98–e169. https://doi.org/10.1161/STR.0000000000000098

Wolters, A., Schmidt, A., Schramm, A., Zeller, D., Naumann, M., Kunesch, E., Benecke, R., Reiners, K., Classen, J., 2005. Timing-dependent plasticity in human primary somatosensory cortex. J. Physiol. 565, 1039–1052. https://doi.org/10.1113/jphysiol.2005.084954

Xiao, Y., Felleman, D.J., 2004. Projections from primary visual cortex to cytochrome oxidase thin stripes and interstripes of macaque visual area 2. Proc. Natl. Acad. Sci. 101, 7147–7151. https://doi.org/10.1073/pnas.0402052101

Xu, Y., 2007. The Role of the Superior Intraparietal Sulcus in Supporting Visual Short-Term Memory for Multifeature Objects. J. Neurosci. 27, 11676–11686. https://doi.org/10.1523/JNEUROSCI.3545-07.2007

Yamahachi, H., Marik, S.A., McManus, J.N.J., Denk, W., Gilbert, C.D., 2009. Rapid Axonal Sprouting and Pruning Accompany Functional Reorganization in Primary Visual Cortex. Neuron 64, 719–729. https://doi.org/10.1016/j.neuron.2009.11.026

Yendiki, A., Panneck, P., Srinivasan, P., Stevens, A., Zöllei, L., Augustinack, J., Wang, R., Salat, D., Ehrlich, S., Behrens, T., Jbabdi, S., Gollub, R., Fischl, B., 2011. Automated Probabilistic Reconstruction of White-Matter Pathways in Health and Disease Using an Atlas of the Underlying Anatomy. Front. Neuroinformatics 5, 23. https://doi.org/10.3389/fninf.2011.00023

Yu, H.-H., Atapour, N., Chaplin, T.A., Worthy, K.H., Rosa, M.G.P., 2018. Robust Visual Responses and Normal Retinotopy in Primate Lateral Geniculate Nucleus following Long-term Lesions of Striate Cortex. J. Neurosci. 38, 3955–3970. https://doi.org/10.1523/JNEUROSCI.0188-18.2018

Zhang, L.I., Tao, H.W., Holt, C.E., Harris, W.A., Poo, M., 1998. A critical window for cooperation and competition among developing retinotectal synapses. Nature 395, 37–44. https://doi.org/10.1038/25665

Zhang, X., Kedar, S., Lynn, M.J., Newman, N.J., Biousse, V., 2006. Natural history of homonymous hemianopia. Neurology 66, 901–905. https://doi.org/10.1212/01.wnl.0000203338.54323.22

Zhang, Y., Brady, M., Smith, S., 2001. Segmentation of brain MR images through a hidden Markov random field model and the expectation-maximization algorithm. IEEE Trans. Med. Imaging 20, 45–57. https://doi.org/10.1109/42.906424

Zihl, J., 2010. Rehabilitation of Visual Disorders After Brain Injury: 2nd Edition. Psychology Press.

ZIHL, J., VON CRAMON, D., MAI, N., 1983. SELECTIVE DISTURBANCE OF MOVEMENT VISION AFTER BILATERAL BRAIN DAMAGE. Brain 106, 313–340. https://doi.org/10.1093/brain/106.2.313

Zihl, J., Werth, R., 1984. Contributions to the study of “blindsight”--II. The role of specific practice for saccadic localization in patients with postgeniculate visual field defects. Neuropsychologia 22, 13–22. https://doi.org/10.1016/0028-3932(84)90003-4

Zrenner, C., Belardinelli, P., Müller-Dahlhaus, F., Ziemann, U., 2016. Closed-Loop Neuroscience and Non-Invasive Brain Stimulation: A Tale of Two Loops. Front. Cell. Neurosci. 10. https://doi.org/10.3389/fncel.2016.00092

Michele **Bevilacqua**

Contact

Avenue de Beaulieu, 1
Lausanne
1004
Switzerland

Phone: +41 787725253

Mail: mik.bevi@gmail.com

LinkedIn: Michele Bevilacqua
Skype: michele.bevilacqua10

Languages

Italian (Native)
English (Proficient)
French (C1)
Spanish (A2)

Certifications

Project Management:
PRINCE2
AgilePM
Clinical:
GCP (Good Clinical Practice)

Programming Skills

MATLAB
Python
C++
Git
LaTeX
Blender
Java

Others

Microsoft Office
iOS Environment

References available on request

- **Life science bioengineer** and **PhD candidate in Neuroscience and Neuroengineering**, working in the Neuro-X Laboratory of System and Translational Neuroscience at EPFL.
- Strong interest in innovation, in the biotech field and technological translation.
- My objective is **to give my personal contribution to the development and translation of innovative biotechnologies capable to revolutionize the actual panorama and enhance patients' quality of life**.

Education

2019-2024 — **Ph.D.** in **Neuroscience and Neuroengineering** — **EPFL**
Geneva, Switzerland
Non-Invasive Brain Stimulation combined with neuroimaging for stroke brain lesion recovery and personalized therapy

2015-2018 — **M.Sc.** in **Life Sciences and Technology** — **EPFL**
Lausanne, Switzerland
Orientation in Neuroengineering and Neurosciences

Minor in **Neuroprosthetics** — **EPFL**
Lausanne, Switzerland

2012-2015 — **B.Eng.** in **Bioengineering** — **Politecnico di Milano**
Milan, Italy

Work Experience

APR'19-DEC'23 — **PhD candidate in Neuroscience and Neuroengineering** — **EPFL - Campus Biotech, Geneva**
PhD project focused on systems and translational neuroscience.
- Targeting of neuroplasticity, functional reorganization and recovery in the visual system of subjects affected by focal brain lesions (stroke) and potentially other neurodegenerative diseases by the use of modern neuroimaging (EEG, MRI, fMRI), Non-Invasive Brain Stimulation (TMS, tUS, tDCS, tACS) and psychophysical and clinical evaluations.

JUL'17-OCT'17 — **Biosignal Engineering Internship** — **Mindmaze, Lausanne**
Internship on EEG BCI EMG
- 3-months internship in MindMaze, Swiss company specialized in Neuroengineering and Brain-Computer Interfaces applied to Virtual Reality environments for healthy subjects and stroke patients.
- Responsible of recording through EMG and EEG of muscular activity and neural evoked potentials during specific tasks in a VR environment.

Publications

MAY 2022 — **iScience**
First author
M. Bevilacqua, K.R. Huxlin, F. Hummel, E. Raffin, **"Pathway and directional specificity of Hebbian plasticity in the cortical visual motion processing network"**.
iScience, CellPress, 26, 7 (2023)

JAN 2024 — **Journal of Neural Engineering**
Coauthor
C. Bigoni, S.Pagnamenta, A. Cadic-Melchior, M. Bevilacqua, S. Harquel, E. Raffin and F. C. Hummel, **"MEP and TEP features variability: is it just the brain-state?"**.
Journal of Neural Engineering, 21 (2024)

MAR 2018 **Nature Communications**
Coauthor
L. Ferlauto, M. J. I. Airaghi Leccardi, N. A. L. Chenais, S. C. A. Gilliéron, P. Vagni, M. Bevilacqua, T. J. Wolfensberger, K. Sivula and D. Ghezzi, **"Design and validation of a foldable and photovoltaic wide-field epiretinal prosthesis"**.
Nature Communications 9, 992 (2018)

DEC 2019 **IEEE Open Journal of Engineering in Medicine and Biology**
First author
M. Bevilacqua, S. Perdikis, J.del R. Millàn, **"On Error-Related Potentials During Sensorimotor-Based Brain-Computer Interface: Explorations With a Pseudo-Online Brain-Controlled Speller"**.
IEEE Open Journal of Engineering in Medicine and Biology 1, 17-22 (2019)

Academic Experience

OCT'17-APR'18 **Brain sources of error-related potentials for neural control of robotic arm** **INE - TU Graz**
6 Months Master Project at INE in Graz (Austria)
- EEG data processing, analysis and EEG source localization mapping of different brain potentials studied in BCI.
- Definition of a new experimental protocol, data acquisition, processing, analysis and scientific presentation of novel results.

Skills

Project Management – Literature Review – Data Analysis – Oral Presentation – Written Presentation – Biosignal Acquisition – Signal Processing – Statistical analysis – Programming in Python – Programming in MATLAB
Critical Thinking – Self-Learning – Teamwork – Proactive Attitude – Ability to integrate academia, industry and business knowledge – Versatility

Other passions and activities

2019-2021 **Member of "EPFL Innovation Forum"** **Lausanne, Switzerland**
Event and Conference Organizer

2016 **Member participant of "MUN EPFL", Model United Nations** **Lausanne, Switzerland**

2013-2015 **Member of contemporary theatre troupe "Teatro Magro"** **Mantova, Italy**

2013 **Founding Member of "L'Officina"** **Mantova, Italy**
Recording studios and practice room

2012 **National finalist of the International Championship of Mathematical Games** **Milan, Italy**

Interests

Life Sciences Innovation – Clinical Translation – Neurodegenerative Diseases – Brain-Computer Interfaces – Cricular Economy – Virtual Reality – Artificial Intelligence